Variability of Elemental Abundances in the Local Neighborhood and its Effect on Planetary Systems

by

Michael Pagano

A Dissertation Presented in Partial Fulfillment
of the Requirement for the Degree
Doctor of Philosophy

Approved April 2014 by the
Graduate Supervisory Committee:

Patrick Young, Chair
Sang-Heon Shim
Jennifer Patience
Steven Desch
Ariel Anbar

ARIZONA STATE UNIVERSITY

May 2014

ABSTRACT

As the detection of planets become commonplace around our neighboring stars, scientists can now begin exploring their possible properties and habitability. Using statistical analysis I determine a true range of elemental compositions amongst local stars and how this variation could affect possible planetary systems. Through calculating and analyzing the variation in elemental abundances of nearby stars, the actual range in stellar abundances can be determined using statistical methods. This research emphasizes the diversity of stellar elemental abundances and how that could affect the environment from which planets form. An intrinsic variation has been found to exist for almost all of the elements studied by most abundance-finding groups.

Specifically, this research determines abundances for a set of 458 F, G, and K stars from spectroscopic planet hunting surveys for 27 elements, including: C, O, Na, Mg, Al, Si, S, Ca, Sc, Ti, V, Cr, Mn, Fe, Co, Ni, Cu, Zn, Y, Zr, Mo, Ba, La, Ce, Nd, Eu, and Hf. Abundances of the elements in many known exosolar planet host stars are calculated for the purpose investigating new ways to visualize how stellar abundances could affect planetary systems, planetary formation, and mineralogy. I explore the Mg/Si and C/O ratios as well as place these abundances on ternary diagrams with Fe.

Lastly, I emphasize the unusual stellar abundance of τ Ceti. τ Ceti is measured to have 5 planets of Super-Earth masses orbiting in near habitable zone distances. Spectroscopic analysis finds that the Mg/Si ratio is extremely high (~ 2) for this star, which could lead to alterations in planetary properties. τ Ceti's low metallicity and oxygen abundance account for a change in the location of the traditional habitable zone, which helps clarify a new definition of habitable planets.

DEDICATION

I dedicate this to those who have stood by me and helped me through this process.

.

.

.

To my family for always being there for me, for all the phone calls and all the times I said "I'll be done when I'm done"

.

.

.

To Liz, my moonlight, for finding a way to get through all this craziness and keep me sane.

.

.

.

To all my friends who have made my graduate life amazing.

"For small creatures such as we, the vastness is bearable only through love"

⌣ Carl Sagan

ACKNOWLEDGMENTS

I would like to thank my advisor, Patrick Young, who took me in when I was lost at the start of my graduate career and made me feel like I truly belonged here. I hope this project has not only taken myself, but also my advisor, into new directions of exploration. To my committee: Steve Desch, Ariel Anbar, Jenny Patience, and Dan Shim. All of you have helped shape my understanding of science and how to stay open to advise from any field. Through mixing all your specialties we can start to understand so much more about the universe around us. I would like to thank Paul Butler and the Carnegie Institute of Washington for allowing me to use their spectra and teaching me how to reduce them. Thanks to Eric Bubar and Jade Bond who really taught me how to measure, understand, and interpret stellar abundances.

I'm extremely grateful for Natalie Hinkel (Mew! Mew! Mew!), who started off as a friend and quickly became my most important colleague (and I hope we will always remain both). Your help during this last year has really kept me calm and made a lot of this possible. Thanks to Priya Challa and Joshua Gonzalez, whose help was instrumental in getting my abundance code standardized and working. They both have a good future ahead of them. Thank you to Nahks Tr'Ehnl for being such a great office-mate and really making me think about the connections between art and sceince. It was lonely in that office without you.

Thank you to all of the Follow the Elements teams. I enjoyed every meeting and every new piece of information I learned about topics I never would have considered. I still look forward to the meeting when I get asked if I have abundances for a certain element (Phosphorus) and I actually have them to show. I've learned a lot from working with that group.

I don't know where I'd be without Caren Burgermeister, whose friendship and support can get me through anything. Thank you Erinne Blakeman for all your help and

friendship. Thanks to my roommates over the years, especially Drew, Caleb and Jean-François. For all my friends, which is a list too long to write here, and for that I am blessed.

I would like to acknowledges support from the Follow the Elements" grant through the NASA Astrobiology Institute and Ariel Anbar (08-NAI5-0018), and from GPSA for multiple travel grants to present my material at conferences.

TABLE OF CONTENTS

CHAPTER Page

CHAPTER Page

LIST OF TABLES

LIST OF FIGURES

Figure Page

Figure Page

Chapter 1

INTRODUCTION

One of the fundamental goals of astronomy is the eventual discovery of life on a planet outside of our solar system. The *Kepler* mission was launched in 2009 with an explicit goal of finding an earth-sized planet in the classical habitable zone (HZ) of its host star (Borucki et al., 2010). At the time of this writing, approximately 1800 extrasolar planets have been discovered. Statistical analysis has predicted that one in five sun-like stars and half of all M dwarfs have an Earth-sized planet orbiting within their HZ (Petigura et al., 2013; Gaidos, 2013; Dressing & Charbonneau, 2013).

For astronomers hoping to find inhabited planets (meaning supporting any sort of life, not necessarily someone staring back at us), this introduces the novel problem of having *too many* candidates. Direct observation of an Earth-sized planet in the HZ of a sun-like star is an exceedingly difficult prospect due to the intrinsic faintness of the planet and the problem of separating its signal from the vastly brighter nearby star. Obtaining spectra of significant quality to detect chemical compounds in the planet's atmosphere that are produced by biological processes will likely require a large-scale space mission. Even then, such a project will only be able to observe a small number of stars, perhaps $\sim$100 over the mission lifetime (e.g. Turbull, 2012). Such an outlay of capital and human workload demands a very careful selection of targets for observation.

Current astrophysical research into the habitability of exoplanets has a strong focus on the concept of a habitable zone, which is classically defined as the range of distances from a star within which a planet can maintain liquid water on its surface. The location of the HZ is determined primarily by the host stars luminosity and secondarily by its spectral characteristics coupled to a planetary atmosphere calculation. Given

assumptions about the nature of the atmosphere, it is possible to predict the temperature on the planetary surface and therefore the possibility for stable liquid water (Kasting, Whitmire, & Reynolds, 1993; Kopparapu et al., 2013a). It is now commonplace to announce the discovery of a planet within the HZ, based upon comparing the planet's orbit to the present-day location of the HZ as predicted from the relatively easily measured stellar parameters.

If we are to choose a very restricted target list from the apparently large fraction of stars with planets in the HZ, we clearly need more sophisticated criteria. It may be useful to introduce the concept of a "Detectability Index" (DI) in the form of a probability that a given planet will have observable evidence of life. The DI is based on three broad considerations. First, the planet must be able to sustain a biosphere. Second is the likelihood that biosignatures can persist at detectable levels and be distinguished from the products of abiotic processes. The third term incorporates the engineering limitations of the chosen method of detection. Based upon our experience of Earth, a terrestrial planet in the classical HZ provides favorable conditions for the first two requirements to be satisfied. Some inhabited planets will probably be unidentifiable until we are able to examine them from up close. An obvious example is Europa in our own solar system, which may support abiota in an ocean under its icy crust. The limited communication of the potentially life-sustaining region with the surface gives Europa a low DI because biosignatures will escape at low levels at best and will be destroyed rapidly by Jupiter's radiation environment. Conversely, the tenuous free O envelope around Europa owes its existence to that same radiation environment rather than oxygenic photosynthesis. More subtle effects may come into play that prevent detection even of surface biospheres on terrestrial planets. As examples, planets with a highly reducing bulk chemistry could conceivably fix free oxygen faster than photosynthesizing organisms could produce it, depriving us of one of the more "easy" to detect biosignatures. Such a planet might, on the

other hand, be able to sustain high levels of biogenic methane that could not be attributed to geological processes such as serpentinization. Such a planet would have a higher DI for a mission able to observe methane as well as oxygen.

Many of the terms that contribute to the habitability of an exoplanet and the detectability of life depend sensitively on chemical composition. The effects range from a marked influence on stellar evolution to the bulk physical structure of a planet to the rates of production and destruction of chemical compounds in the atmosphere by competing processes. Planets and their host stars form from the same nebular material. With the exception of a very late injection of material into a protoplanetary disk from a nearby supernova, we can be confident that both have the same starting composition. Accurately measuring stellar elemental abundances and being able to predict how they affect the star's evolution and the composition and behavior of its planets can provide a sophisticated characterization of an exoplanetary system. The estimate of the DI of a potential target can be greatly refined.

In this work I examine the range of variation in the compositions of nearby stars, present new abundance measurements for a large stellar sample, and discuss a range of planetary mineralogical properties that are allowed by the observed compositions. Finally, I present an example of chemical characterization of the τ Ceti system and how such an analysis can inform discussions of its planets' habitability.

1.1 The Solar Composition

As technologies and scientific thought advance, we must constantly update our previous knowledge so as to use the most accurate methods to investigate the world around us. However, not all astronomical quantities have exact values determined even after years of scrutiny. The solar chemical composition has become a standard by which we compare, not only other stars, but any other astronomical object we can measure

abundances for. This is not simply a sign of our vanity towards the star which our inhabited planet orbits, but a logical starting point as the Sun is by far the most well observed star. Hydrogen and helium account for 98.5% of the solar composition and heavier elements (referred to as metals by astronomers) make up 1.5% of the mass (Lodders et al., 2009). The most abundant metals (in astronomy this means anything besides H and He) in the Sun are O, C, Fe, Ne, Si, N, Mg, and S (in that order).

There are two distinct ways that solar astrophysicists determine the chemical abundances of our star. The first is the analysis of meteorites through mass spectroscopy in laboratories. This allows the direct measurements and abundance analysis of every element present and to very high precision. CI chondrites are the most pristine meteorites that we know to date, having been the least altered over the last 4.56 Gyr, and therefore are used to represent the presolar nebula from which the Sun itself formed. However, even though they have the least amount of alteration of any known meteorites, they still have a depletion in volatile elements such as hydrogen, helium, carbon, nitrogen, oxygen, and neon (Asplund et al., 2009) and therefore meteoritic compositions are more useful when used in conjunction with the second method of solar abundance determination, the analysis of the solar photosphere.

Unlike the accurate measurement of elemental abundances in meteorites, finding the composition of a star requires the use of multiple models, inferences, and deductions that naturally creates a much larger degree of uncertainty. The abundances of the elements are determined through analysis of the stellar spectrum and the absorption lines created by the presence of multiple ions. Through the use of solar atmosphere models, the measured absorption of continuum emission by spectral lines is converted to absolute numbers of atoms of a particular element. This process is model dependent. As a result, the mass fraction of elements heavier than hydrogen and helium deduced in this way has varied from $\sim$1.9% to $\sim$1.4% (Anders & Grevesse, 1989; Grevesse & Sauval, 1998; Grevesse et

al., 2007; Asplund et al., 2009; Lodders et al., 2009). Estimates of the total amount of heavy elements and oxygen in the Sun dropped sharply when 3D solar atmosphere models became available in the early years of this century. Motions and temperature variations caused by convection in the solar photosphere produce quite different absorption line profiles from 1D average atmospheres, especially for oxygen (Grevesse et al., 2007).

1.2 Stellar Abundances

Changing determinations aside, the composition of the Sun has generally been taken to be a good representation of the stars in the local neighborhood ($\sim$100 pc) with a similar level of chemical enrichment, including stars that could host exosolar planets (Twarog, 1980; Edvardsson et al., 1993; Woosley & Weaver, 1995). In many cases stellar abundances were (and still are) inferred by only measuring the Fe abundance and scaling all others according to solar ratios. As new techniques and surveys have improved our ability to accurately measure the compositions of large samples of other stars, we find that deviations from the elemental abundance ratios in the solar composition are present (Reddy et al., 2003; Valenti & Fischer, 2005; Bond et al., 2006; Gilli et al., 2006; Bond et al., 2008; Mishenina et al., 2008; Delgado Mena et al., 2010; Petigura & Marcy, 2011).

Similarly, stellar evolution models almost always take the solar abundances as their basic initial composition. Low metallicities may have an increase in alpha elements, those formed by nucleosynthetic addition of a helium atom, and first stars use a big bang composition, but otherwise different metallicities are scaled versions of solar. Stellar evolution and the determination of stellar parameters by comparing models to observations are sensitive to the assumed composition. This sensitivity arises primarily, but not entirely, from two composition-dependent effects: the equation of state and the radiation opacity (Rogers et al., 1996; Iglesias & Rogers, 1996; Rogers & Nayfonov, 2002; Däppen, 2011; Mussack & Däppen, 2011). The CNO elements, Ne, Si, Ti, and

Fe-peak elements are particularly important because of their relative abundance and number of electron transitions. Rearranging the proportions of different species at a constant metallicity can result in opacity changes of tens of percent. Variation of [O/Fe] of the order found in nearby stars, around 0.5 solar to 2 times solar(see Chapter 2), changes the main sequence lifetime of a $1M_{\odot}$star at solar [Fe/H] by $\sim$3Gy (Young et al., 2012). The stability of massive stars against catastrophic mass loss, the Cepheid pulsational instability, and the depth of the solar convection zone can all be strongly affected.

Fe has been used as both an indicator of stellar composition and as a normalization point for astronomical abundances due to the multitude of observable transitions in the optical spectrum and because of its relatively high abundance in stars. The Fe/H abundance ratio in a star is usually reported as the logarithm of the number ratio of these elements scaled to the ratio in the Sun, denoted [Fe/H] (Helfer et al., 1959). In other words, [X/H]=$\log(N(X)/N(H))_{star} - \log(N(X)/N(H))_{\odot}$ where $\log(N(H)) = 12$. We can discuss other elemental ratios normalized to the Sun in the same way. It is common to use the same notation to quantify elemental ratios relative to Fe, since Fe is most commonly measured. For an element X,
$[X/Fe] = \log[(X/H)_{star}/(X/H)_{\odot}] - \log[(Fe/H)_{star}/(Fe/H)_{\odot}]$. The term metallicity is often used to refer to the total amount of elements heavier than H and He in a star. In practice, metallicity and [Fe/H] are often used interchangeably because thousands of stars have measured [Fe/H], but many fewer have complete measurements for even the most abundant subset of elements.

Since the introduction of high-precision radial velocity surveys looking for extrasolar planets, there has been an influx of high resolution spectra that can be used to find elemental abundances of stars. The first extrasolar planets were discovered in the mid-1990s (Mayor & Queloz, 1995; Marcy & Butler, 1996) and since then, over 450 planets have been discovered using the radial velocity method. Following the discovery of

these extrasolar planets, it was observed that host stars on average have a higher metallicity than non-host stars (Gonzalez, 1997; Valenti & Fischer, 2005). With more and more planets being discovered, we can begin to look for more complex trends. It is important to thoroughly examine the host stars. The field of measuring stellar abundances is growing, but it can be difficult to compare results of multiple studies. Determinations of the abundance of an element for the same star by different research groups often differ by more than the quoted error bars (Hinkel, 2012).

1.3 Sources of Abundance Variations

H, He, and small amounts of Li, Be and B (one part in $\sim 10^9$ by mass) were all formed in the Big Bang and are considered primordial. Everything heavier accounted for 10^{-12} of the baryons in the universe (Steigman, 2012). The abundance of these heavier elements had increased by a factor of 10^{10} in the material from which the solar system formed, almost entirely through stellar nucleosynthesis.

There are several distinct sites of nucleosynthesis. One source is spallation, or modification of a nucleus through a collision with a high-energy cosmic ray. This is a significant production channel for a few isotopes of Li, Be, and B. In general, it is not a major source of elements (Arnett, 1996). Much more important are stellar nucleosynthesis sources involving interacting binary stars. Novae, thermonuclear explosions on the surface of white dwarfs accreting matter from a companion, create products of high-temperature hydrogen burning, including isotopes of Na, Mg, and Al. Type Ia supernovae (SNeIa) are the thermonuclear explosion and complete destruction of an interacting white dwarf. SNeIa produce alpha elements, so called because they can be produced by successive addition of alpha particles to atomic nuclei (C, O, Ne, Mg, Si, S, Ar, Ca, Ti, Cr, Mn, Fe, and Ni), and are the source of more than half of the iron in the Galactic disk. They also produce significant amounts of Si and Ca. Neutron star-neutron star mergers are predicted

to eject 10-3 $M_\odot$ of very high atomic number *r*-process (rapid neutron capture process) material (e.g. Goriely et al., 2011).

Single stars also contribute significantly to nucleosynthesis. In low- to intermediate-mass ($< 8M_\odot$) stars, deep convection dredges up material processed by nuclear burning during the stars lifetimes. This is the dominant source of C in the universe as well as *s*-process (slow neutron capture process) elements. The *s*-process is responsible for roughly half of the species between the iron peak and ^{209}Bi. All of these sources create elements only hundreds of millions of years after the progenitor stars form.

The timescale for nucleosynthesis in massive stars is much shorter, between a few and a few tens of million years. Stars above $\sim$25 $M_\odot$, depending on metallicity, lose their entire hydrogen envelopes to eruptive phases as luminous blue variables and continue losing substantial mass as Wolf-Rayet stars. Wolf-Rayets, which are basically bare stellar cores, have very strong winds, which may contain products of hydrogen burning (He with modified abundances of Na, Mg, Al), partial He burning (high C abundance), or complete He burning (O dominated with modified Ne abundances). Finally, stars above $\sim$8 $M_\odot$ can explode as core collapse supernovae (CCSNe), which are the primary production site of most elements between O and the Fe peak and a significant fraction of Fe. CCSNe eject many isotopes of elements with both even and odd proton numbers, for example P (SNeIa produce mainly even-Z elements). CCSNe also produce *r*-process elements, which are the remainder of the nuclei beyond the iron peak, including all nuclei heavier than ^{209}Bi.

The elemental abundances of a stellar system depend primarily on the composition of the molecular cloud from which it forms, which is primarily set by overall Galactic chemical evolution, or GCE (e.g. Tinsley, 1980; Timmes, Woosley, & Weaver, 1995; Schönrich & Binney, 2009). A molecular cloud may differ in its chemical composition from other molecular clouds, if it were to receive contributions in different proportions from the sources discussed above. It is also possible for stars within a cloud to differ

chemically, if parts of the cloud can be contaminated by the products of stellar nucleosynthesis during the few tens of Myr during which it is forming stars. Baring rare chance encounters with old stars formed far away in time and space, the only candidates for this pollution are self-enrichment by Wolf-Rayet winds and CCSNe, since their progenitors live only $\sim$3 to 20 Myr before ejecting elements. Isotopic evidence from meteorites for the presence of short-lived radioactive elements (SLRs) at high levels in the early solar system supply strong evidence for this scenario. SLRs such as ^{26}Al, ^{41}Ca, and ^{60}Fe have half-lives of order 10^6 years, and are present at levels well above those expected from GCE (Wadhwa et al., 2007; Huss et al., 2009). These isotopes had to have been produced nearby and contemporaneous with the solar system's formation. An injection of supernova material of $\sim 10^{-4}$ of the mass in the protoplanetary disk, less than few $\times 10^5$ yr before the formation of the first solids could explain these abundances (Wadhwa et al., 2007). Stable isotope anomalies in meteorites paint a similar picture. Young et al. (2009) showed that clumps from particular sites in the supernova explosion could deliver amounts of ^{26}Al at the levels necessary to match the meteoritic constraints. Ellinger, Young, & Desch (2010) argued that this injection could take place without wildly disturbing O isotope ratios, with $\sim$1% of the Solar Systems oxygen injected into the Suns molecular cloud after its composition was determined by GCE. Ellinger, Young, & Desch (2010) showed that creation of these clumps sampling distinct compositions within the supernova are a robust feature of CCSN explosions. Pan et al. (2012) further showed that such clumps can mix effectively with molecular cloud material and enrich it at significant levels.

The purpose of this dissertation is to show that a true range in elemental stellar abundances exist and that this variation of the chemical make-up of stars should influence the kind of planets around stars and their habitability. In Chapter 2 we discuss a statistical method used to understand the physical spread in elemental abundances, by analyzing

previous abundances finding surveys. In Chapter 3, we present the elemental abundances that we determined for 458 stars and any trends we find that are contrary to previous studies. In Chapter 4, we present the abundances results specifically for those stars with known exosolar planets as of this paper. As well, we look into the effect that extremes in certain elements and elemental ratios could possibly have on those planets around those stars. In Chapter 5, we examine the extreme case of τ Ceti and its large Mg/Si ratio. The results of the abundance determinations are listed in the Appendix for all non-host and planet host stars.

Chapter 2

ELEMENTAL ABUNDANCE VARIATIONS IN NEARBY STARS

2.1 Introduction

The composition of the Sun has generally been taken to be a representation of the stars in the local neighborhood ($\sim$ 100 pc) with a similar level of chemical enrichment, including stars that could host exosolar planets (Twarog, 1980; Edvardsson et al., 1993; Woosley & Weaver, 1995). As new techniques and surveys have improved our ability to accurately measure the compositions of large samples of other stars, we find that deviations from the solar composition are present (Reddy et al., 2003; Valenti & Fischer, 2005; Bond et al., 2006; Gilli et al., 2006; Bond et al., 2008; Mishenina et al., 2008; Delgado Mena et al., 2010; Petigura & Marcy, 2011).

Stellar evolution and the determination of stellar parameters by comparing models to observations are sensitive to the assumed composition. This sensitivity arises primarily, but not entirely, from two composition-dependent effects: the equation of state and the radiation opacity (Rogers et al., 1996; Iglesias & Rogers, 1996; Rogers & Nayfonov, 2002; Däppen, 2011; Mussack & Däppen, 2011). The CNO elements, Ne, Si, Ti, and Fe-peak elements are particularly important because of their relative abundance and number of electron transitions. Rearranging the proportions of different species at a constant metallicity can result in opacity changes of tens of percent, or 20% by including Ni and Cr (Iglesias & Rogers, 1996). The temperature ranges where these effects are particularly relevant affect, for example, the stability of massive stars against catastrophic mass loss, the Cepheid pulsational instability, and the depth of the solar convection zone. A newer study (Grevesse et al., 2007, henceforth GAS07) applies 3D hydrodynamic

models to line formation in the solar lower atmosphere and derives a much lower total metallicity of present day z=0.0126 vs. 0.0188 for their previous work (Grevesse & Sauval, 1998, henceforth GS98) and a higher O/Fe ratio. These values continue to be revised, with other groups (Lodders et al., 2009, henceforth LPG09) finding a primordial solar metallicity of z$\sim$0.0153. This discrepency had profound consequences for the standard solar model (Bahcall, Pinsonneault, & Basu, 2001), rendering it unable to match the solar convection zone depth determined by helioseismology. Reconciliation could involve the introduction of arbitrary abundance enhancements (particularly of Ne) or heretofore ignored hydrodynamic processes (Bahcall, Basu, & Serenelli, 2005; Bahcall et al., 2005; Lodders et al., 2009; Arnett, Meakin & Young, 2010; Antia & Basu, 2011). If variations of abundance of similar scales to those tested in experimental high energy density physics measurements of opacity or encountered in the revision of the solar abundances are found between compositions of other stars, updated stellar models are required (Iglesias & Rogers, 1996; Rogers & Iglesias, 1998). A variation of [O/Fe] of the order found herein changes the main sequence lifetime of a $1M_{\odot}$ star at solar [Fe/H] by $\sim$3Gy (Young et al., 2012).

To better examine the intrinsic variation in initial compositions of stars in the solar neighborhood, it is necessary to eliminate as many systematic variations and observational errors in the abundance data as possible. We require a uniform, high quality sample of stars with minimal modification of the initial abundance by stellar processes. We restrict our analysis to older (>3 Gyr) F, G and K main sequence stars because they can be considered close enough to Sun-like stars that we expect similar abundance ratios without complications from high magnetic activity, molecule formation in the stellar atmosphere, and very deep surface convection zones. The most significant processes in these stellar atmospheres should be gravitational settling and radiative diffusion. For solar-type stars, settling and diffusion produce a uniform depletion of elements up to the Fe peak of $\sim$

-0.03 dex at 3.7 Gyr (Michaud et al., 2004). Even more important than the nature of the sample, we must eliminate the large systematic differences that arise when comparing abundance determinations from multiple research groups. Determinations of a given elemental abundance in a single star can vary between surveys by more than the quoted error of either survey (Hinkel, 2012). Thus, combining multiple surveys does not produce a self-consistent assemblage. Instead, we perform independent analyses of several large surveys and compare our conclusions from each.

We focus on the surveys of Bond et al. (2006, 2008); Mishenina et al. (2008); González Hernández et al. (2010); Delgado Mena et al. (2010). These surveys find abundances for a large number of elements for a statistically robust number of stars.

The Bond et al. (2006, 2008) survey examined spectra from the Anglo-Australian Planet Search, which used the Anglo-Australian Telescope. They looked at a selection of nearby G dwarfs, encompassing 4820 to 8420 Å with a signal-to-noise ratio between 200 and 300 per spectral pixel at resolution $\lambda/\Delta\lambda \approx 80{,}000$. Bond et al. (2006) obtained equivalent width estimates via direct integration over the line to determine abundances for Fe, C, Na, Al, Si, Ca, Ti, and Ni. Bond et al. (2008) used Gaussian line-fits to the spectra to determine O, Mg, Cr, Y, Zr, Ba, Nd, and Eu abundances. The study used 145 stars, 29 of which have planets. Not all abundances were measured for each star. Abundances given in Bond et al. (2006, 2008) were combined to give the abundances for each star in the sample.

The Mishenina et al. (2008) survey used spectra from the 1.93 meter telescope at the Observatoire de Haute-Provence (France) with the echelle-spectograph ELODIE. The S/N of the spectra range from 130 to 230 with a resolving power of $\lambda/\Delta\lambda \approx 42{,}000$ in the region of 4400 to 6800 Å. They determined abundances for Fe, Li, O, Na, Mg, Al, Si, Ca, Sc, Ti, V, Cr, Co, Ni, and Zn for 131 F and G stars. They fit the equivalent widths with Gaussian lines using the software package DECH20 (Galazutdinov, 1992).

González Hernández et al. (2010) determined abundances for 7 solar twins and 95 solar analogs, 24 of which have known planets from the HARPS and UVES spectra, which had a spectral resolution of $\lambda/\Delta\lambda \approx 85{,}000$ and a signal-to-noise of 800 on average. They used the 3.6 m telescope equipped with HARPS at the Observatorio de La Silla in Chile, the 8.2 m Kueyen VLT (UT2) telescope equipped with UVES at the Observatorio Cerro, Paranal in Chile, and the 4.2 m WHT telescope equipped with UES at the Observatorio del Roque de los Muchachos in La Palma, Spain. They used the ARES code (Sousa et al., 2008) and Gaussian fits to calculate their equivalent widths, finding abundances for C, O, S, Na, Mg, Al, Si, Ca, Sc, Ti, V, Cr, Mn, Co, Ni, and Cu.

Delgado Mena et al. (2010) present abundances of Fe, Ni, C, O, Mg and Si for 61 planet host stars and 270 stars without detected planets. They use the HARPS GTO sample of high resolution, high S/N FGK stars observed by the CORALIE spectrograph at La Silla Observatory. Stellar parameters were taken from Sousa et al. (2008).

In addition we perform a more restricted analysis using the studies of Neves et al. (2009); Ramírez et al. (2007). Neves et al. (2009) looked at 12 elements for 451 stars from the HARPS GTO sample and the CORALIE spectrograph at La Silla Observatory. The spectra have a resolution of $\lambda/\Delta\lambda \approx 110{,}000$, with S/N ranging from 70 to 2000. Ramírez et al. (2007) only looked at oxygen for 523 stars, which were a conglomeration of spectra from many surveys with resolution varying from $\lambda/\Delta\lambda \approx 45{,}000$-$120{,}000$ and S/N of 100-600. The results of Ramírez et al. (2007) are used in discussion of O.

We use these uniform, high quality studies as the basis of our analysis, while focusing on the spread in abundance ratios at a given metallicity. We derive the mean abundances and the intrinsic variation of element to iron ratio as a function of iron enrichment. Ratios are given as $[X/Fe] = \log[(X/H)_{star} / (X/H)_{\odot}] - \log[(Fe/H)_{star}/ (Fe/H)_{\odot}]$. We also individually note stars that are $> 3\sigma$ or 5σ from the local mean in any ratio as outliers.

2.2 Abundance Analysis

In order to construct initial compositions for stellar and planet formation models representative of nearby stars we need to know not only the commonly measured [Fe/H], but also the mass fraction of each element relative to solar. For this purpose we have made a linear fit to the data for each species as a function of [Fe/H] to determine the mean and the intrinsic variation in abundance ratios In this section we briefly discuss the fit to the observed stellar distributions, the method of determining variation in abundance ratios and its results, and compare our results with those of other literature sources where available. In general direct comparisons are limited by the small number of elements measured in other surveys, very heterogeneous stellar samples, or the study's treatment of errors in the abundance determination. We discuss the general results of these analyses and then examine each element in detail.

2.2.1 Intrinsic Variation

The principal purpose of this study is to quantify the level of variation in elemental abundance ratios at a given [Fe/H]. Disentangling the intrinsic scatter from the observational errors is not straightforward. To obtain the errors and spreads, we performed a χ^2 fit (Isobe et al., 1990), in which the total scatter is assumed to be the sum in quadrature of an observational uncertainty $u_{observational}$ and an intrinsic scatter, $u_{intrinsic}$. The goodness of fit parameter χ^2 of the observed points is

$$\chi^2_{reduced} = \frac{1}{n} \sum_{i=1}^{n} \frac{(X_i - \mu_i)^2}{{u_{obs}}^2 + {u_{intrinsic}}^2} \tag{2.1}$$

where n is the number of measured stars, X_i is the measured abundance ratio in star i, μ_i is the average of all X_i, and again u_{obs} is the observational uncertainty and $u_{intrinsic}$ represents the real, physical scatter in the abundance ratios. (A priori we do not expect a normal

distribution, so we do not use σ to represent the scatter in the denominator.) To measure X_i, we perform a linear fit to each study for [X/Fe] as a function of [Fe/H]. The correlations of individual elements with Fe abundance vary from study to study. For Bond et al. (2006, 2008) the correlation of most elements with Fe is weak, with correlation coefficients of $R^2 < 0.2$. The exceptions are Ti, with R^2 near 0.5, and Nd and Eu near 0.3 (see Table 2.2). The R^2 values for the González Hernández et al. (2010) fits are much stronger, with $R^2 > 0.3$ for 16 elements. The highest correlation is 0.91 for Mn, while Al, S, Sc, Cr, Y, Zr, and Ce are all under 0.1. The correlations with Fe in Mishenina et al. (2008) are also weak except for O, Mg, and Si, which have R^2 of 0.71, 0.43, and 0.27, with everything else having values under 0.1. All 5 elements for the Delgado Mena et al. (2010) study have a R^2 value between 0.3 and 0.5. Second-order fits do not significantly improve the reduced χ^2, and result in equal or reduced R^2 values, with R^2 being reduced by up to 0.417.

If there is a real intrinsic scatter in the stars, correctly estimated errors should not be able to account for all of the observed dispersion. For each element and for each star there is a quoted observational error u_{obs}, so all variables except $u_{intrinsic}$ are fixed. We vary the intrinsic scatter term until $\chi^2 = 1$ (De Silva et al., 2006; Stuart & Ord, 2009). If $\chi^2 > 1$ without a non-zero $u_{intrinsic}$ term, this would mean there is more dispersion in the data than can be accounted for by observational errors alone. For $\chi^2 \leqslant 1$, the spread for that element might be entirely explained by the observational error, although an intrinsic variation may yet exist at a small value hidden in generously estimated observed uncertainties. The inclusion of the intrinsic uncertainty term in this formulation also allows us to avoid unwanted emphasis on a few well-measured points.

These results are summarized in Table 2.1 for the surveys listed in Section 2.1. We discuss results for individual elements in Section 2.3. This formula relies heavily on observational errors given by each author. Of the studies included only Bond et al. (2006,

2008), González Hernández et al. (2010), Ramírez et al. (2007), and Neves et al. (2009) give elemental errors for individual stars. The other datasets only give the average error per element for the entire study. This lessens the robustness from this statistical method, as $u_{intrinsic}$ directly links observational error to spread on a star to star basis. Having an average error still allows for the calculation and comparison of $u_{intrinsic}$, but is less robust. Studies with larger observational errors, such as Delgado Mena et al. (2010), whose quoted observational errors would produce a dispersion higher than or equal to the measured standard deviation of each element, tend to not have a measurable $u_{intrinsic}$ value because their errors are overestimated. Most elements have a consistent relative $u_{intrinsic}$ across all studies, i.e. C, Si, Ca, and Cr have lower $u_{intrinsic}$ than other elements below the Fe peak in all cases. The relatively low $u_{intrinsic}$ found for C may be mostly due to the large observational errors in its measurement. Na has a relatively small $u_{intrinsic}$, but has more outliers at the supersolar metallicity end of the distribution in all studies that measure it. Few studies look at elements beyond the Fe peak. Where data is available, these heavier elements have a large spread. The $u_{intrinsic}$ derived from González Hernández et al. (2010) for heavy elements is low since they give an average observational error for the whole sample for O, Cu, Sr, Zr, Nd, and Eu, rather than an error for each star.

There is a marked variation in the intrinsic spread of abundances that appears to correlate with atomic number for the Bond et al. (2006, 2008) sample. C and Na have moderate spreads, which may be underestimated, as discussed above. For the rest of species measured with $Z < 14$ (which we will refer to as "light elements") and for Ti and the r- and s-process elements, the spread is quite large. Si, Ca, Cr, and Ni have smaller spreads, though the variation in every element except for Ca and Ni cannot be accounted for by observational error alone. For the González Hernández et al. (2010) sample, the intrinsic variations remain low and of similar magnitude throughout the entire periodic table, and the spreads in more elements are able to be explained through observational

errors. The elements with 0 $u_{intrinsic}$ are in the transition metals and s and r process elements. This is the only study that observed sulfur. Mishenina et al. (2008) yields large $u_{intrinsic}$ values for some lighter elements, but they do choose to use an average abundance error for all stars for a given element. Their average error for Al and Mg are relatively small, which increases the amount of scatter outside of error. The largest value is for Oxygen, which seems to be the most intrinsically variable element among most studies. Neves et al. (2009) has similar $u_{intrinsic}$ as the other studies, except for much more scatter in the transition metals Sc and V. Both gonz10, mish08 measure these elements with values of ≈ 0.03, and Mishenina et al. (2008) finds no intrinsic scatter for Sc. In contrast, Neves et al. (2009) finds a $u_{intrinsic}$ of 0.143 and 0.175 for Sc and V respectively.

The 3 $u_{intrinsic}$ variation can range up to a factor of order two above and below the mean for the five light elements. The large spread in O is not entirely unexpected. Most O is produced by core collapse supernovae (Arnett, 1996). Lifetimes of massive stars and the mixing of their ejecta into molecular cloud material are short compared to the Galactic rotation period and Galactic mixing timescale (Pan et al., 2012), so variations in [O/Fe] in different star formation regions at different times is possible and perhaps likely. After several Gy, the resulting stars are assumed to be kinematically mixed, so we would expect > 3 Gy old field stars near the sun to have a variety of compositions. Given that its high abundance causes it to play a very important role in stellar opacity and CNO cycle nucleosynthesis, stellar models with large variations in O abundances will show real significant impact on stellar evolution and observable quantities (Young et al., 2012).

Si, Ca, and Ni have smaller spreads of a factor of $\sim$1.0 - 1.2 about the mean. Ti abundances determined from two different ionization states (denoted TiI and TiII) give different absolute abundances and spreads, so the value of the intrinsic variation should merely be taken as large. The abundances of r and s-process elements vary up to a factor of almost 7 in each direction. There is a large variation about the mean as well as an

interesting number of far outliers among potential planet hosts in the solar neighborhood. Even for those elements with little to no statistically significant intrinsic scatter outside of the observational errors there are outliers.

Figure 2.1 is a visual representation of the intrinsic variation for 24 elements throughout 4 different studies. The y-axis is the average observational error for each element. citetmish08 provided this value for each element and did not give individual star observational errors. We calculated the value for the other surveys. For most elements the largest $u_{intrinsic}$ value for each element comes from the Neves et al. (2009) sample, which has by far the most number of stars in its study, with 451 compared to around 100 each for Bond et al. (2006); González Hernández et al. (2010); Mishenina et al. (2008). This is often the case even when their errors are larger than other studies.

2.3 Individual Elements

2.3.1 Carbon

The [C/Fe] ratio in halo and disk dwarfs has been long been observed to be roughly solar with a scatter of about 0.3 dex over the entire measurement range of -3.0 $\leqslant$ [Fe/H] $\leqslant$ 0.5 dex (Sneden, 1974; Bell & Branch, 1976; Clegg, 1977; Peterson & Sneden, 1978; Clegg, Tomkin & Lambert, 1981; Tomkin & Lambert, 1984; Laird, 1985; Tomkin, Sneden, & Lambert, 1986; Carbon et al., 1987), but this spread is found by combining surveys which may have systematic differences. A solar and relatively flat [C/Fe] ratio is interesting because carbon and iron are synthesized by very different processes at different stages in the Galaxy's evolution. Carbon is produced by the triple-alpha process during hydrostatic helium burning in massive, intermediate, and low mass stars. Iron on the other hand, is synthesized in explosive burning conditions by Type II and Type Ia supernovae. The relative contributions and evolutionary time scales for each of these origin sites of

carbon and/or iron are quite different.

Metal-poor massive star synthesis of primary carbon and iron are generally sufficient to explain the metal-poor halo dwarf observations, with small undulations due to mass and metallicity variations. Two competing sources come into play at [Fe/H] $\simeq$ -0.8 dex. Intermediate and low mass stars begin depositing large amounts of carbon but no iron, while Type Ia supernovae start injecting significant amounts of iron but no carbon. The interplay between these two sources, such that [C/Fe] $\simeq$ 0 dex, places tight constraints on chemical evolution models.

Of the studies we used for $u_{intrinsic}$ comparison, only Bond et al. (2006) and citetgonz10 measure carbon abundances. The calculated $u_{intrinsic}$ for each study are 0.017 and 0.043, respectively. González Hernández et al. (2010) have a larger $u_{intrinsic}$ than Bond et al. (2006), which is most likely due to their treatment of errors. Both show a relatively large spread throughout all metallicities (with no greater dispersion at any given [Fe/H]), with Bond et al. (2006) varying from [C/Fe] = -0.1 to 0.4 and González Hernández et al. (2010) from [C/Fe] = -0.2 to 0.2. However the errors for Bond et al. (2006) are much larger and vary more on a star to star basis; whereas González Hernández et al. (2010) often use an error of 0.07 for when there is only one line to fit for Carbon. Though this is a common practice in abundance error determination, it leads to less reliable $u_{intrinsic}$.

The Bond et al. (2006) data show [C/Fe] $\geqslant$ 0 at all [Fe/H], with a slight negative slope, while GCE surveys with wider samples show -0.3 $\leqslant$ [C/Fe] $\leqslant$ 0.3 dex. This offset arises from the significant departure of C/H in LPG09 from older solar values (Grevesse & Sauval, 1998, e.g.) used in previous surveys. Delgado Mena et al. (2010) has the most negative slope of the surveys considered here. González Hernández et al. (2010) have a much smaller spread of C and on the whole find significantly lower [C/Fe] than the other studies.

Reddy et al. (2003) had an almost identical trend to the Bond et al. (2006) data,

with a slightly negative slope going towards higher metallicities that evens off at around solar metallicity. The Reddy et al. (2003) data, however, only goes to [Fe/H]= 0.2, whereas the Bond et al. (2006) data go to [Fe/H]= 0.4. A newer study (Petigura & Marcy, 2011) published abundances for 941 similar FGK stars, for just O and C, and found similar trends in [C/Fe] vs. [Fe/H], with a downward trend. Their data, however, has a much steeper negative slope, and many more outliers.

2.3.2 Oxygen

We chose to plot the abundances for a single element, Oxygen, for the studies involved in the $u_{intrinsic}$ study. Figure 2.2 shows [O/Fe] vs. [Fe/H] for Bond et al. (2008); González Hernández et al. (2010); Mishenina et al. (2008); Ramírez et al. (2007). The best fit line is accurate for Oxygen, which has a very linear trend for all studies. The $u_intrinsic$ values have been plotted away from the best fit line to show how the variation of Oxygen, even though large, still includes some outliers. Mishenina et al. (2008) has a rather tight spread, but also the smallest $u_intrinsic$.

Oxygen has the highest average $u_{intrinsic}$ values for any element in this study, with 4 studies reporting O values and errors (Bond et al., 2008; González Hernández et al., 2010; Mishenina et al., 2008; Ramírez et al., 2007). Though there are difficulties in measuring O values as discussed below, determining $u_{intrinsic}$ within a self-consistent sample ameliorates most potential concerns. Even if there is a systematic difference in absolute abundance values between surveys, internal comparisons within a single survey are subject to the same biases. The highest value comes from Ramírez et al. (2007), whose data give a $u_{intrinsic}$ of 0.155 for their LTE analysis and 0.197 for their NLTE analysis, which should be the more accurate of the two. Bond et al. (2008) give a $u_{intrinsic}$ of 0.092. The smallest $u_{intrinsic}$ value is from González Hernández et al. (2010), with a value of 0.078. It should be noted that the González Hernández et al. (2010) oxygen abundances were found using the

6300 Å line, and the error was once again estimated to be 0.07 due to the use of only one line. Even finding oxygen this way, with a problematic line and no per star errors, gives a moderate $u_{intrinsic}$, confirming the existence of a real, large variation in oxygen amongst near-by stars. Mishenina et al. (2008) also used the 6300 Å line and got a $u_{intrinsic}$ of 0.153, similar to that of Ramírez et al. (2007).

Bond et al. (2008) has a negative trend from [Fe/H] = -0.5 to 0, which is consistent with other studies such as Edvardsson et al. (1993),Reddy et al. (2003), and Mishenina et al. (2008). Edvardsson et al. (1993) shows a flattening trend around [Fe/H] = 0. The Bond et al. (2008) abundances suggest a similar flattening near [Fe/H] = 0, but it is not statistically significant. Compared to two of the newer surveys, the Bond et al. (2008) abundances are in decent agreement with Delgado Mena et al. (2010), once again shifted slightly towards O enrichment. The solar analog study of González Hernández et al. (2010) shows a constant decrease with a larger negative slope across [Fe/H]=0, and no upturn in O as seen in some of the other studies. The trend in Petigura & Marcy (2011) also shows a much more significant decrease in [O/Fe] with metallicity, with over twice the negative slope for the overall trend as compared to Bond et al. (2008); Delgado Mena et al. (2010). Differences could be partially due to the difficulty in measuring O abundances and a discrepancy in measurements due to the 6300 Å forbidden line (Nissen, 2013). This line is strongly affected by a blended line of Ni I with strength $\sim$ 55% of the O I line in the sun. At higher metallicities or lower O/Fe-peak the contribution can be even larger. The [OI] line at 6363 Å has a small contribution from a CN line in cool stars (Caffau et al., 2013), but is generally considered more reliable than the 6300 Å line. The O I triplet at 7774Å is not affected by blends, but is sensitive to NLTE effects (Takeda, 2003; Ramírez et al., 2007; Fabbian et al., 2009). In our intrinsic variation analysis we can expect reliable results from the 6363 Å line and 7774 Å triplet.

Oxygen is the dominant element ejected by Type II supernovae. There is relatively

little contribution to its abundance from low mass stellar sources; the convective envelope of low mass stars near the base of the red giant branch do not reach down deep enough into material where significant ON processed material could be dredged-up to the surface (Iben, 1964; Leep & Wallerstein, 1981; Lambert & Ries, 1981; Iben & Renzini, 1983). Surface oxygen abundances should not be affected in G and K field dwarfs beyond gravitational settling, and may be valuable tools for analyzing *ab initio* oxygen abundances. Intermediate mass stars begin to dominate contributions to the interstellar medium later on, but because they produce very little oxygen and no iron the [O/Fe] ratio is not affected. Type Ia supernovae begin to inject large amounts of iron and negligible amounts of oxygen into the interstellar medium beyond about 1 Gyr, which causes the distinct downturn of [O/Fe] to the solar value. Determining the metallicity at which Type Ia supernovae begin to affect the [O/Fe] ratio is observationally very difficult, as the uncertainties in even the best of the observations is much larger than the size of the expected effect (e.g. Wallerstein (1994)).

2.3.3 Sodium, Magnesium, and Aluminum

Sodium, magnesium and aluminum are adjacent to each other in the periodic table and have large production factors in the ashes of hydrostatic carbon and neon burning. The α chain isotope ^{24}Mg has two stable neutron rich sisters, ^{25}Mg and ^{26}Mg, while sodium and aluminum have only one stable isotope, ^{23}Na and ^{27}Al, since even-A odd-Z isotopes are generally unstable (Arnett, 1996). All these elements can be readily observed in the spectra of dwarf stars.

Sodium

Sodium has a low $u_{intrinsic}$ through all of the studies, with a value of 0.06 or less and an average of 0.037. Mishenina et al. (2008) has the largest spread in Na at all metallicities,

but one of the smallest $u_{intrinsic}$ values. This is due to their relatively high average error (0.15 dex), which is significantly larger than the average error for Neves et al. (2009), which has the largest $u_{intrinsic}$ at 0.058 and an average Na error of 0.03, with errors as low as 0.01 on a star to star basis. These small errors come only from the difference in abundance values for different sodium lines measured.

Edvardsson et al. (1993) suggests the [Na/Fe] ratio is 0.1 ± 0.15 over the metallicity range -1.0 $\leqslant$ [Fe/H] $\leqslant$ 0.2 dex, with hints of an upwards trend for [Fe/H] $>$ 0.0 dex. Bond et al. (2006) generally agree with these trends, with a linear least squares fit suggesting a slight increase of [Na/Fe] with [Fe/H] over the the metallicity range -0.4 $\leqslant$ [Fe/H] $\leqslant$ 0.3 dex and an upward turn at about [Fe/H] = 0.1. However, there is a paucity of stars with [Na/Fe] $\approx$ 0 dex in the Bond et al. (2006) survey that do appear in the Edvardsson et al. (1993) survey. Mishenina et al. (2008) has the same trend, but with a mean that passes closer to the solar value at [Fe/H] = 0. Reddy et al. (2003) has a different trend, with a negative slope that evens out at around [Fe/H] = -0.3 and then stays flat, but their data show the sun at low values, similar to Bond et al. (2006). Valenti & Fischer (2005) shows a similar negative trend until about [Fe/H] = 0.1, where the slope flattens. This trend is also apparent in Takeda (2007); Neves et al. (2009); González Hernández et al. (2010), with the first two also having a small number of high metallicity stars that continue to follow the downward trend that flattens out at [Fe/H]$\sim$ 0.1 in the other studies.

The dominant source of sodium production is hydrostatic C and Ne burning in massive stars. For [Fe/H] $>$ -0.5 dex the chemical evolution curves suggest that there might be small additional sources of sodium. Standard paradigm Type Ia supernovae are not promising candidates. Massive stars that have lost only their hydrogen envelope may affect the ^{23}Na abundance through production of Na in high temperature hydrogen burning (Arnett, 1996). Synthesis of sodium in intermediate mass stars can also occur in the hydrogen burning shell through the neon-sodium cycle (Denisenkov & Denisenkova,

1990; Langer, Hoffman & Sneden, 1993). On longer time scales, reaction chains involving the more abundant ^{20}Ne also produce sodium. If the convective mixing time scale in these intermediate mass stars is small enough, then this sodium rich (but oxygen depleted) material can brought to the surface. Mass loss of the stellar envelopes would then enrich the interstellar medium. This process is supported by observations of intermediate mass field giants and globular cluster giants that appear to be sodium rich (Boyarchuk & Lyubimkov, 1985; Shetrone, 1996).

Magnesium

In the studies that measure magnesium (Bond et al., 2006; González Hernández et al., 2010; Mishenina et al., 2008; Neves et al., 2009), the $u_{intrinsic}$ values vary more than any sub-Fe peak elements except oxygen with its known measurement issues. González Hernández et al. (2010) has the lowest $u_{intrinsic}$, 0.026; however, they also have the lowest average $u_{intrinsic}$ across their entire sample, which is most likely due to generous error measurements. The Mishenina et al. (2008) study has largest value, 0.116. Their errors are well documented and small ($\sim$0.05). Generally the $u_{intrinsic}$ values are high for Mg, which confirms that there is a real spread in magnesium over the sample of nearby stars.

There appears to be little difference in the local behavior of [Mg/Fe] with larger GCE trends. The Edvardsson et al. (1993) survey suggests the [Mg/Fe] ratio starts at -0.5 dex at [Fe/H] = -1.0 dex and increases to near solar by [Fe/H] = 0.0 dex. Their data also suggest a slight upturn at high metallicities. Bond et al. (2006) shows a similar upturn after [Fe/H] = 0.0 dex, and has a similar average ratio. The trends in Reddy et al. (2003); Takeda (2007); Mishenina et al. (2008); Neves et al. (2009); González Hernández et al. (2010) are very similar, with the only difference being that the Reddy et al. (2003) data show a super solar [Mg/Fe] at [Fe/H] = 0. The trend from Delgado Mena et al. (2010) is almost identical, except that their data shows little spread around [Mg/H] = 0. ^{26}Mg can

be produced during He burning in both intermediate mass and massive stars, but ^{24}Mg is not created in large amounts until carbon burning. Core collapse supernovae are the primary sources of Mg (Limongi & Chieffi, 2006), although SNIa produce significant amounts, albeit at much lower [Mg/Fe] (Maeda et al., 2010).

Aluminum

The $u_{intrinsic}$ values range from 0.036 (González Hernández et al., 2010) to 0.112 (Mishenina et al., 2008). The $u_{intrinsic}$ in Al is one of the largest for any element below the Fe peak, similar to that of Mg, and signifies a substantial variation amongst the stars. The [Al/Fe] ratio is 0.0 $\pm$ 0.15 over the metallicity range -1.0 $\leqslant$ [Fe/H] $\leqslant$ 0.2 dex according to Edvardsson et al. (1993). Most of the dwarfs in the Bond et al. (2006) survey has [Al/Fe] $<$ 0.0 over the metallicity range -0.3 $\leqslant$ [Fe/H] $\leqslant$ 0.3 dex., with some evidence for an upturn in [Al/Fe] above [Fe/H] $>$ 0.0. (Reddy et al., 2003) shows a slight negative slope, as opposed to the other studies' slight positive slope, but does show evidence for the upturn at [Fe/H] = 0.2. However, they have few super solar metallicity stars. (Mishenina et al., 2008; Neves et al., 2009) both show a much larger spread, and a similar lower metallicity trend, but with no upturn at [Fe/H]= 0.2. Takeda (2007); González Hernández et al. (2010) also do not show as large an upturn at [Fe/H]. Al can be produced in high temperature H shell burning in both massive and intermediate mass stars by proton capture onto Mg. Observations of globular cluster red giants show an anti-correlation of Al and ^{24}Mg, indicating proton capture onto ^{24}Mg at $T \approx 7 \times 10^7$K. Primary production of Al is from C and Ne burning in massive stars (both quasi-static and explosive) (Arnett, 1996).

2.3.4 Silicon, Sulfur

Silicon shows a very tight trend throughout all metallicities, except for a few stars at the high end. The $u_{intrinsic}$ for silicon is therefore unsurprisingly low, with the largest

value being 0.062 (Mishenina et al., 2008), and most likely arises from the use of an average error versus observational errors on a start to star basis. Even though this value is low across all studies, a $u_{intrinsic}$ still exists indicating that the actual variation in silicon must be low since low observational errors lead to high $u_{intrinsic}$ values for more variable elements such as aluminum and magnesium. Most of the variation arises near the highest metallicity range, much like Na. The highest metallicities may represent stars formed from material polluted by massive stars without time for a concomitant contribution from low mass stellar sources, leading to a larger spread. Sulfur is represented by one study, González Hernández et al. (2010), which shows a pedestrian $u_{intrinsic} = 0.031$. It is difficult to measure S in the optical, and few stars are represented.

The Bond et al. (2006) results are in general agreement with galactic trends from (Timmes, Woosley, & Weaver, 1995), and are very similar to those in (Edvardsson et al., 1993), which has a similar metallicity range of -1.0 $\leqslant$ [Fe/H] $\leqslant$ 0.2. In other studies, however, (Mishenina et al., 2008; Prantzos, 2008; Takeda, 2007), the slope for silicon is slightly negative. The sun is generally placed at the bottom of the [Si/Fe] range of all studies. The data from Prantzos (2008) show only compositions of stars up until [Fe/H] = 0, so it is slightly difficult to do a complete comparison. The Reddy et al. (2003) show the start of an upturn at the high metallicity end of their distribution ([Fe/H]= 0.1). Valenti & Fischer (2005) show evidence for an upturn for a subset of stars at [Fe/H] = 0.1. The Bond et al. (2006) data also suggest an upturn beginning at the same metallicity. Delgado Mena et al. (2010) have the same trend, in the same [Si/Fe] range as the Bond et al. (2006) data, but without the upturn seen at higher metallicities. This upturn is seen in Neves et al. (2009) and slightly in González Hernández et al. (2010). In all cases the slopes are small. The abundance of [Si/Fe] stays relatively flat, until the far metal rich region, which is a good agreement with chemical evolution models where the silicon produced by massive stars is balanced by the iron produced from Type Ia supernovae in all but the most recent

and therefore typically high metallicity star formation (Timmes, Woosley, & Weaver, 1995; Timmes & Clayton, 1996). Sulfur is dominated by core collapse supernovae, as its production is favored in low entropy O burning, whereas Si is favored in explosive and NSE conditions (Arnett, 1996).

2.3.5 Calcium

The $u_{intrinsic}$ for calcium is very similar to that of silicon, ranging from 0.016 to 0.065. Like Si, Ca has the most variation at the high metallicity range. Interestingly, most of the variation comes from outliers that are extremely depleted in Ca.

Comparing the evolutionary trends of Timmes, Woosley, & Weaver (1995) to the Bond et al. (2006) data show agreement except at lower metallicities ([Fe/H] $\leqslant$ -0.2. At these lower metallicities, there are limited data points and they are of higher [Ca/Fe] value than the evolutionary trends. Typically [Ca/Fe] has been measured to be super-solar in metal-poor halo dwarfs ((Wallerstein, 1962; Edvardsson et al., 1993)). Mishenina et al. (2008) goes to a lower metallicity than Bond et al. (2006)([Fe/H] = -0.6) but does not show very much increase at these lower metallicities. Reddy et al. (2003) have similar trends to Edvardsson et al. (1993) at low metallicity, but at higher [Fe/H] all of these studies agree well. Calcium is produced primarily in core collapse supernovae, with an additional component from Type Ia events (Arnett, 1996).

2.3.6 Titanium

The $u_{intrinsic}$ for Titanium ranges from 0.024 to 0.099, where the largest value is from the Neves et al. (2009) study, which has the largest sample of stars. On a whole, Neves et al. (2009) has the largest $u_{intrinsic}$ values, a good sign that the more stars included in the statistical sample the more the intrinsic variation can be seen.

Chemical evolution models (Timmes, Woosley, & Weaver, 1995) are known to fit

observations of titanium abundance poorly, and this remains true with the Bond et al. (2006) data. The Bond et al. (2006) data match well with previous studies (Edvardsson et al., 1993; Reddy et al., 2003), except that it has a larger negative slope from [Fe/H] = -0.4 to -0.1. [Ti/Fe] is difficult to interpret, since trends from measurements relying on TiI and TiII have differing slopes and normalizations. Observations of titanium show many features consistent with other α-elements, since titanium is produced in deep layers of massive stars (Timmes, Woosley, & Weaver, 1995). Ti production is suppressed relative to Ca in NSE and α-rich freeze-out near a lepton fraction of $Y_e = 0.5$, since the N=Z isotope ^{44}Ti is unstable and decays to ^{44}Ca (Magkotsios et al., 2010). Production is therefore concentrated in the deep mantles of core collapse SNe with little contribution from SNeIa.

2.3.7 Chromium, Scandium, Vanadium, Manganese

The $u_{intrinsic}$ values for chromium are mostly very low or non-existent, making it very similar to silicon. This continues a trend observed for the other intermediate mass alpha elements with the exception of S and Ti, which is difficult to measure. Cr, unlike most of those elements, has a very consistent spread at all metallicities, and does not appears to become more variable with higher iron content. The only studies with a significant $u_{intrinsic}$ are Bond et al. (2006) (0.019) and Mishenina et al. (2008) (0.063), which uses averaged uncertainties for every element. Scandium shows significant variations in two studies, with $u_{intrinsic} \sim 0.143$ for Neves et al. (2009) and a small value of 0.031 in González Hernández et al. (2010). Vanadium shows variation ranging from 0.035 (González Hernández et al., 2010) to a very large value of 0.175 in Neves et al. (2009). Manganese displays a very consistent $u_{intrinsic}$ of 0.065 and 0.083 in Neves et al. (2009); González Hernández et al. (2010). These transition metals seem to have an increase in intrinsic variation when looking at a larger statistical sample such as Neves et al. (2009).

Not as many studies observe Cr abundances at such high metallicities as the Bond

et al. (2006) data, but those that do (Gratton & Sneden, 1991; Mishenina et al., 2008; Takeda, 2007; Neves et al., 2009) are in agreement with a relatively flat trend, except for a very slight upturn near the greater metallicities. Gilli et al. (2006) shows a very flat trend with very little to no scatter, however their results are on a whole about 0.05 dex higher, with a much more dramatic positive trend. The fit of solar abundances for most of the Cr isotopes can be explained through the inclusion of nucleosynthesis through core collapse and Type Ia supernova. Cr is formed with odd-Z elements Sc, V, and Mn under QSE and high entropy NSE conditions.

2.3.8 Nickel and Cobalt

Nickel displays a very small or zero $u_{intrinsic}$ across all studies, with a maximum of 0.029 in González Hernández et al. (2010). Even for the large sample set of Neves et al. (2009) the variation in nickel is minimal at 0.022, with only Cr having less variation for that study. This is perhaps not surprising, as Ni is co-produced with Fe by explosive burning of material with $Y_e < 0.5$. Interestingly, Co has a measurable $u_{intrinsic}$ in all four surveys that report Co abundances. The values $0.051 < u_{intrinsic} < 0.08$ are larger than any found for Ni, possibly indicating the importance of the weak s-process in Co production.

Nickel is the second most abundant element in the iron group. It has fewer spectral lines (Timmes, Woosley, & Weaver, 1995), but still enough to give robust results, with papers such as Gilli et al. (2006) finding over 100 stars in the solar neighborhood with good Ni measurements. The ISM-normalized chemical evolution model of Timmes, Woosley, & Weaver (1995) fits the general trends of the surveys well. The studies of Bond et al. (2006); Gilli et al. (2006); Mishenina et al. (2008); Neves et al. (2009); González Hernández et al. (2010), agree well. Edvardsson et al. (1993) shows a similar upward trend.

2.3.9 s and r process

The final elements in this study are those that are heavier than iron and formed via either slow (s-process) or rapid (r-process) neutron capture, where these refer to the rate of neutron captures with respect to the β-decay rate. In the rapid neutron capture case the neutron capture occurs before β-decay, allowing very n-rich isotopes to be produced and thereby allowing nucleosynthesis to extend pass the stability gap at atomic number $A = 209$. In the slow process case, β-decay can occur before another neutron is captured, preventing the creation of nuclides more than one decay away from a stable isotope. The r-process is produced in core collapse supernovae and neutron star mergers. Massive stars also contribute to the weak s-process for atomic numbers $A < 40$ (Arnett, 1996; Maeda et al., 2010). Virtually all of the s-process with $A > 40$ is produced in intermediate mass AGB stars.

The elements Zn, Sr, Y, Zr, Ba, and Ce measured in these surveys are primarily s-process products. Neodymium is roughly equally produced by the s- and r- processes (Arlandini, C. et al., 1999). The only r-process dominated element is Eu. With the exception of Zn, a weak s-process element, only Bond et al. (2008); González Hernández et al. (2010) report abundances for these elements. We should expect Ba, Ce, and s-process Nd to dominate over Sr, Y, and Zr at low [Fe/H] where there is less competition for neutrons among seed nuclei, but this effect is difficult to discern above [Fe/H] $\sim$ -0.5, which is a lower metallicity than commonly encountered in these surveys. Overall there is a decrease in [X/Fe] with [Fe/H] observed in Bond et al. (2008); González Hernández et al. (2010), in agreement with previous surveys. The elements with a large r-process contribution, Nd and Eu, have stronger negative trends. We would expect this behavior for elements produced primarily in massive stars as they are diluted by late contributions of Fe by SNeIa.

The values of $u_{intrinsic}$ for Zn are very close (0.032, 0.034) for González Hernández et al. (2010); Mishenina et al. (2008). The $u_{intrinsic}$ values for Y are also close (0.032, 0.048). For heavier elements the work of González Hernández et al. (2010) tends to yield smaller $u_{intrinsic}$ than Bond et al. (2008) where both provide a measurement. Both studies have large values for Ba (0.117, 0.087), which tends to have smaller observational errors. Bond et al. (2008) find very large $u_{intrinsic} = 0.135$ for Eu and $u_{intrinsic} = 0.113$ for Zr. The much smaller $u_{intrinsic}$ found by González Hernández et al. (2010) are most likely a result of their different treatment of observational uncertainty in elements with abundances derived from a single weak line.

2.3.10 Outlier Stars

We denote any star that is outside of three sigma for any abundance as an outlier. Table 2.3 shows the abundances for elements lighter than and including Ni for all the outliers for four studies(Bond et al., 2006, 2008; González Hernández et al., 2010; Mishenina et al., 2008; Delgado Mena et al., 2010). In this table the enhancement is given relative to the average abundance at the stellar [Fe/H] given by the fits in Table 2.2. These exceptional stars are worth our attention as they or their planets may exhibit special properties or may preserve evidence of individual enrichment events. In general, stars that are outliers in one or more abundance ratios tend to have very high or very low metallicity compared to the rest of the sample. This is the main reason why the Bond et al. (2006, 2008) sample has a larger number of outliers than the others. It has more extreme metallicity stars. Two of the stars (HD 199288 and HD 136352) have proper motions significantly higher than the rest of the sample, and could be representatives of kinematically, and therefore potentially chemically, distinct populations (the thick disk or halo). These stars have [Fe/H] of -0.54 and -0.31. One of the outliers (HD 23079) has a planet, evidence for planets forming in conditions that are mineralogically quite unlike the

solar nebula. Interestingly, all of the elements up to the Fe peak are represented by outliers.

2.4 Conclusions

The surveys discussed herein independently provide abundances for uniform samples of dwarfs with small observational errors for a large number of elements. Unfortunately, results from individual surveys cannot be combined, as there are commonly large systematic differences between abundances determined by different research groups for a given star. These stars are unlikely to have their original compositions perturbed by self enrichment or preferential depletion of some species by dust or molecule formation, problems that occur for lower mass and evolved stars. These stars are subject to gravitational settling and radiative levitation, but the effects are nearly uniform across elements. As such, this sample should provide as accurate a reflection of the range of primordial compositions of stars in the solar neighborhood as we can expect to find. These stars not only represent a more uniform sample than large scale Galactic abundance surveys, they are drawn from the stars that will be the target of extensive astrobiological exploration over the coming decades. Understanding the elemental composition of these stars can have a direct bearing on how such searches are conducted.

The most striking fact about the local abundances is the intrinsic variation in the lighter elements. The factor of two variations in species below the iron peak will have substantial effects in at least two areas. First is the mineralogy of planetary systems. The equilibrium distribution of different mineral species in primitive solids in a protoplanetary disk depends upon the relative abundances of mineral forming species. An extreme example is HD136352, where [C/Fe] is enriched by 0.448 dex. There are many stars and even planetary systems that seem to have significantly different compositions than solar. This could mean that planets will form with unusual elemental compositions that could

alter how we imagine other worlds. The C/O ratio controls the distribution of Si among carbide and oxide species, while Mg/Si gives information about the silicate mineralogy (Bond et al., 2010a,b). Bond et al. (Bond et al., 2010a,b) carried out simulations of planet formation where the chemical composition of the protoplanetary cloud was taken as an input parameter, showing that for C/O values > 0.8, condensation pathways can change dramatically. This leads to carbon-dominated rocky planets rather than the silicate-dominated composition found in the Solar Systems four inner rocky planets (the solar C/O value is 0.54; (Lodders et al., 2009). Terrestrial planets were found to form in all the simulations with a wide variety of chemical compositions – and these planets might be very different from the Earth. Two ratios deserve special consideration. High C/O ratios (> 1) can potentially produce planetary compositions dominated by SiC and graphite (Bond et al., 2010a,b). A more subtle but potentially important ratio is that of Mg/Si. A planet forming from material enriched in Mg/Si would possibly have planetary composition and dynamics substantially different from Earth, even if the planet has a similar mass. A much higher Mg/Si would shift the olivine/pyroxene ratio in the mantle. Such a ferropericlase-dominated mantle would have significantly lower viscosity and a different melting behavior (Ammann et al., 2011; de Koker et al., 2013). Both of these properties determine mantle dynamics, with potential application to plate tectonics.

The variations can also have measurable effects on the stellar evolution. It turns out that the sun does not fall exactly at the mean abundance of solar neighborhood dwarfs. The sun is not hugely variant compared to its neighbors, but it does represent tens of percent for some light elements. Abundant moderate Z elements, in particular O and Ne, are significant contributors to the Rosseland mean opacities under stellar conditions. It will be necessary to run suites of stellar models with variant abundances to establish the effect on the evolution and observable quantities. Determinations of internal mixing for massive stars based on surface abundances, and mixing and stellar age determinations

based on color and luminosity would have to be revised if there is a primordial compositional variation of tens of percent. Nucleosynthetic yields may also change to some extent. Taking the solar composition as the standard for stellar evolution calculations is unavoidable for many species that are difficult to measure in stellar spectra, but it is not ideal. Using the measured mean composition trends from a sample such as this one with ancillary models reflecting the spread in variable species would be an instructive approach for population synthesis, for example. Young et al. (2012) show that the main sequence lifetimes of solar mass stars at [Fe/H] = 0 with the extremes of [O/Fe] found here have lifetimes ranging from 9 to 12 Gyr.

The variation in trends fitted to different abundance studies shows the importance of star selection and abundance finding methods. González Hernández et al. (2010) looked at solar twins, and therefore their stellar abundances should be preferential towards solar metallicity stars. As a result, the intercepts for their trends are all relatively solar. The majority of intercepts are between -0.04 and 0.04, with the largest being only -0.05. All of these studies concentrated on looking at stars with planets, which includes a high metallicity bias. The fact that different studies have such variation in intercepts is a result of different solar normalization. Bond et al. (2006, 2008) uses Grevesse & Sauval (1998), while González Hernández et al. (2010); Mishenina et al. (2008); Delgado Mena et al. (2010) all use their own differential analysis, which makes it hard to compare their solar values. The difference in slops could be a cause of the stellar selection, with only Si having drastic change in slopes. Although this shows the difficulty in comparing these studies, the intrinsic spread in each set still helps show that variation in elemental abundances exist outside of these comparison issues.

Larger samples of stars with high quality spectra need to be gathered and analyzed in a uniform manner to follow up the preliminary conclusions of this work. From the theoretical side, new stellar models with a wider variety of compositions must be

produced to ascertain the full impact of compositional variation for both field stars and enriched cluster stars. Recent collaborations have shown that stellar abundance techniques require improvement to allow studies by different groups to used in combination. Doing an analysis such as $u_{intrinsic}$ on individual groups work has validity, but there are discrepancies when trying to compare actual values of the same star by two different groups (Hinkel, 2012). Ongoing work shows that differences in line lists, oscillator strengths, stellar atmosphere code, stellar parameter calculation, and solar normalization can lead to substantial difference is measured abundances (Hinkel & Pagano, in prep).

Table 2.1: Intrinsic variation of abundance ratios for different abundance finding groups. Value is for [X/Fe].

Element	Intrinsic Variation				
	Bond06&08	Gonz10	Mish08	Neves09	Ramirez07
C	0.017	0.043			
O	0.092	0.078	0.153		0.155(L) and 0.197(N)
Na	0.036	0.042	0.013	0.058	
Mg	0.068	0.026	0.116	0.069	
Al	0.047	0.036	0.112	0.101	
Si	0.014	0.018	0.062	0.038	
S		0.031			
Ca	0.016	0.032	0.065	0.050	
Sc		0.031	0	0.143	
Ti	0.026	0.024	0.061	0.099	
V		0.035	0.037	0.175	
Cr	0.019	0	0.063	0	
Mn		0.083		0.065	
Co		0.051	0.080	0.072	
Ni	0	0.029	0	0.022	
Cu		0			
Zn		0.032	0.034		
Sr		0.020			
Y	0.032	0.048			
Zr	0.113	0			
Ba	0.117	0.083			
Ce		0.033			
Nd	0.033	0			
Eu	0.135	0			

Table 2.2: Statistics for abundance finding studies of Bond et al. (2006, 2008); González Hernández et al. (2010); Mishenina et al. (2008); Delgado Mena et al. (2010).

Element	Slope				Intercept				R^2			
	Bond	GH	Mish	DM	Bond	GH	Mish	DM	Bond	GH	Mish	DM
C	-0.11	-0.147		-0.252	0.09	-0.026		0.004	0.03	0.295		0.359
O	-0.17	-0.389	-0.910	-0.381	0.01	-0.006	-0.055	-0.024	0.08	0.550	0.709	0.429
S		-0.007				-0.053				0.001		
Na	0.25	0.172	0.217		0.09	0.007	0.026		0.21	0.346	0.062	
Mg	-0.26	-0.125	-0.483	-0.23	-0.03	0.024	-0.018	0.005	0.19	0.216	0.433	0.489
Al	0.09	0.003	-0.012		-0.08	0.028	0.109		0.03	0.000	0.000	
Si	0.11	-0.062	-0.238	-0.126	0.11	0.016	0.079	0.025	0.11	0.276	0.266	0.368
Ca	-0.14	-0.179	-0.046		0.02	0.028	0.025		0.08	0.691	0.006	
Sc		0.045	-0.145			0.047	0.071			0.044	0.062	
Ti	-0.4	-0.099	-0.073		0.04	0.031	0.061		0.45	0.345	0.021	
V		0.159	0.072			0.016	0.020			0.452	0.031	
Cr	0.05	-0.006	0.018		0.04	0.003	0.081		0.02	0.013	0.001	
Mn		0.453				-0.036				0.906		
Co		0.224	-0.034			0.012	0.062			0.606	0.003	
Ni	0.15	0.154	0.019	1.065	0.01	-0.006	0.031	0.008	0.13	0.762	0.003	0.986
Cu		0.094				0.018				0.223		
Zn		-0.100	-0.127			0.014	-0.051			0.109	0.043	
Sr		0.181				-0.023				0.231		
Y	-0.15	-0.020			-0.1	-0.001			0.08	0.005		
Zr	-0.31	-0.079			0.02	0.025			0.14	0.078		
Ba	-0.2	-0.298			-0.05	0.028			0.05	0.376		
Ce		0.046				0.041				0.028		
Nd	-0.47	-0.170			0.04	-0.046			0.27	0.366		
Eu	-0.53	-0.189			-0.12	0.045			0.31	0.349		

Table 2.3: Table of outlier stars for the surveys of Bond et al. (2006, 2008); González Hernández et al. (2010); Mishenina et al. (2008); Delgado Mena et al. (2010).

Bond (2006, 2008)				
Star	Fe/H	Element	3 or 5 sigma	Var. From Avg.
22104	0.2	Ni	3	0.18
23079(host)	-0.15	Cr	5	0.25
31827	0.25	Al	3	0.31
		Si	3	0.04
33811	0.2	Ca	3	-0.31
39213	0.25	Na	3	0.16
42902	0.22	Ni	3	-0.21
53705	-0.18	O	5	0.56
80635	0.23	O	3	0.36
		Al	3	0.37
		Ni	3	0.14
136352	-0.26	C	3	0.33
158738	0	Na	3	-0.32
192865	0.02	Ni	3	-0.27
193193	-0.04	Ca	5	-0.67
199288	-0.49	Al	5	0.49
208998	-0.29	Mg	3	0.43
		O	3	0.32
212708	0.18	Ni	3	-0.3
Gonzalez Hernandez 2010				
Star	Fe/H	Element	3 or 5 sigma	Var. From Avg.
11505	-0.22	Al	3	0.15
		Si	3	0.08
		Sc	3	0.13
		Ti	3	0.12
117207	0.24	Cr	3	0.04
Mishenina 2008				
Star	Fe/H	Element	3 or 5 sigma	Var. From Avg.
45088	-0.21	V	3	0.22
64468	0	Cr	3	0.28
201091	-0.03	Ca	3	0.31
		V	3	0.22
220221	0.16	Cr	3	0.27
Delgado-Mena 2010				
Star	Fe/H	Element	3 or 5 sigma	Var. From Avg.
207583	0.01	O	3	0.56

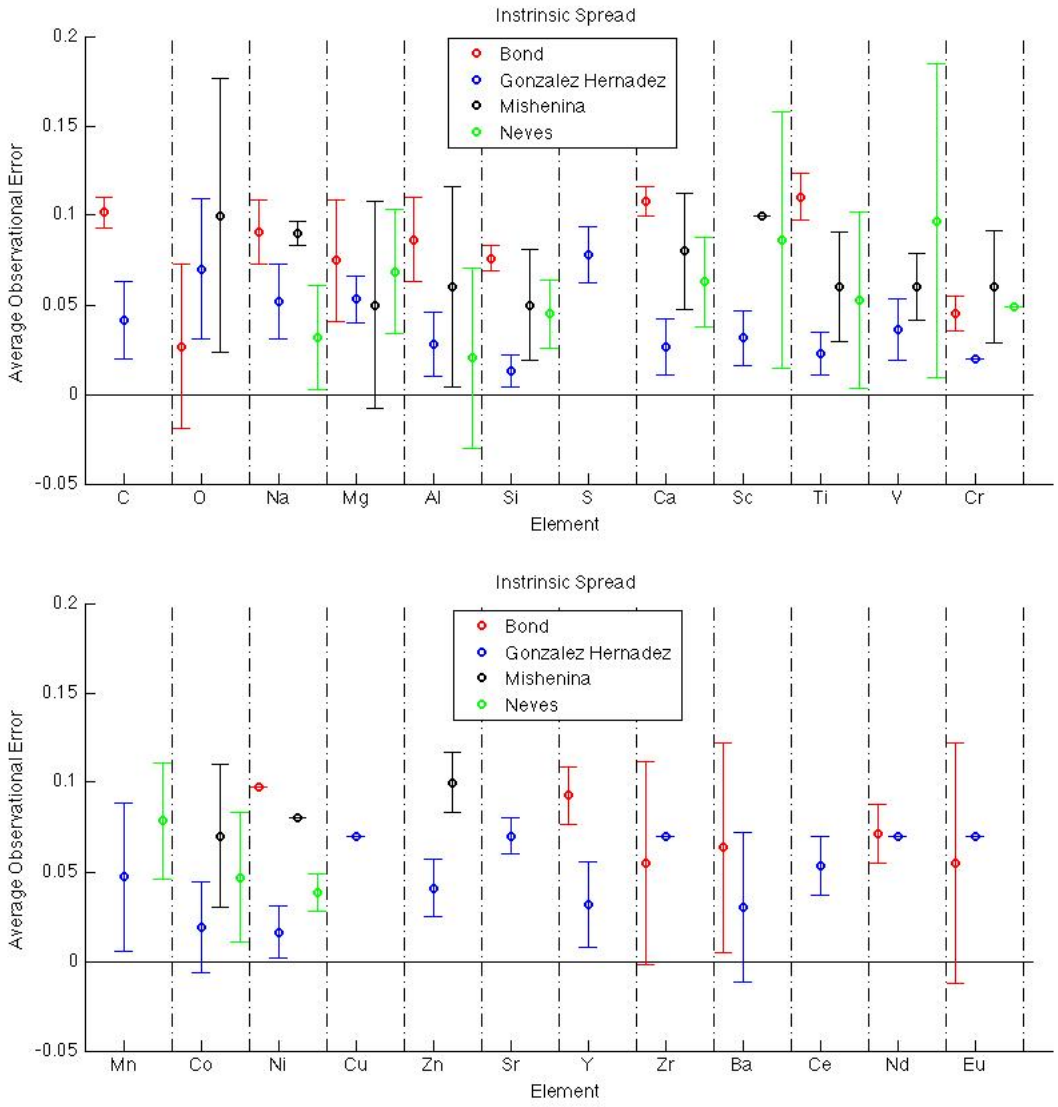

Figure 2.1: Intrinsic Variation for the studies of Bond et al. (2006, 2008); Mishenina et al. (2008); González Hernández et al. (2010); Neves et al. (2009).

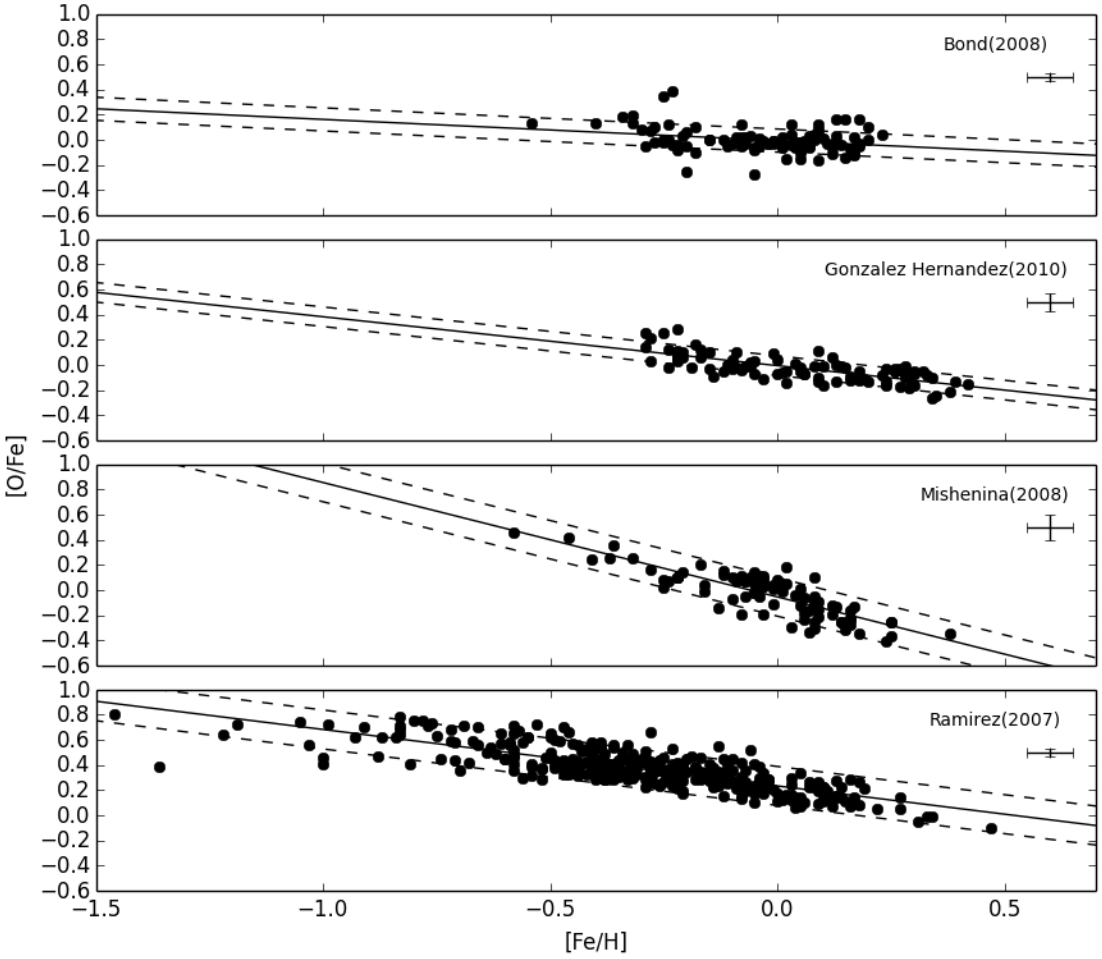

Figure 2.2: Plot of [O/Fe] vs. [Fe/H] for the studies of Bond et al. (2008); González Hernández et al. (2010); Mishenina et al. (2008); Ramírez et al. (2007)(top to bottom). The solid line represents the linear best fit and the dotted lines are the $u_{intrinsic}$ values away from the best fit line.

Chapter 3

ABUNDANCES OF NEARBY STARS

3.1 Stellar Data

3.1.1 Target Stars and Observations

The stellar spectra for this study were taken by Paul Butler and his team from the Carnegie Institute of Washington and were given to Arizona State University for elemental abundance analysis. The spectra were observed through the Magellan Planet Search Program between December 2002 and July 2009. Data was taken using the MIKE echelle spectrograph (Bernstein et al. 2003) on the 6.5 m Magellan II telescope. The spectra have a resolution of R$\sim$50,000 in the wavelength range 4700 Å to 7100 Å. The spectra have a range of signal to noise from 7 to 800, depending on the quality of the original spectra, with an average of 200. Only the red chip data was used for abundance determination. Wavelength calibration was carried out by iodine absorption cell (Marcy and Butler 1992). Only F, G, and K stars were observed in this survey. Of the 456 spectra obtained, only 24 stars with known planets had their abundances determined. These planet hosts will be discussed separately in the following chapter. The spectra were wavelength calibrated in IDL and combined using the *odcombine* function of IRAF. They were velocity shifted using the 6750.15 Å Fe I line and the *dopcor* function and continuum normalized using *continuum*.

3.1.2 Abundance Analysis

These stars were run through a pipeline developed for this project to obtain stellar parameters and elemental abundances using a differential local thermodynamic

equilibrium (LTE) analysis. The pipeline takes all of the stars from reduced but uncalibrated spectra all the way through the abundance finding process, starting with wavelength calibration in IDL and combining all of the orders into a single FITS file. The pipeline uses the 'abfind' function of the 2002 version of the spectral analysis program MOOG (Sneden, 1973), with a grid of model atmospheres that is created by the program mspawn from ATLAS9 model atmospheres (Kurucz, 1993). Given the wavelength range of the spectra, this pipeline can measure up to 27 different elements, including iron, which is measured in the parameter determination. The equivalent widths were measured automatically using the ARES program (Sousa et al., 2007), which automatically measures individual equivalent widths of spectral lines. Given a 1D spectrum, the ARES program will fit a continuum and fit a gaussian to the spectral line if it can be found within the resolution of the options file. The abundance of each element is normalized to the solar values by differential comparison to a high resolution solar spectrum. This was done on a line by line basis, with each measured line compared to the same line in the solar spectrum. The unnormalized results are given in Table A.7 for the purposes of absolute elemental ratio comparisons. These unnormalized values are taken before comparing to the solar spectrum and represent absolute abundances, or the amount of atoms compared to H. In Table A.7, the absolute values are secondarily normalized to 10^6 Si atoms for comparison with geophysical abundances. These absolute abundances can later be normalized to literature solar values for comparisons with other studies. Within the abundance determination literature, there is a discrepancy in oxygen abundances that is known to arise from differences in LTE vs. non-LTE analyses. To account for this, the absolute O abundances have been corrected by forcing the values derived from the average solar spectrum to agree with Asplund et al. (2009) The corrected abundances are used for comparisons as well as re-normalizing the stellar line abundances. The atomic parameters, line wavelengths (λ), excitation energy of the lowest excited state (ξ_1), and oscillator

strength (log(gf)) of each line were collected for different elements from five sources(Reddy et al., 2003; Feltzig & Gustafsson, 1998; Bubar & King, 2010; Bond et al., 2006; De Silva et al., 2006) to include the largest variety of elements. Table A.1 gives our complete line list with these quantities and their sources. The ARES program was run multiple times on three control stars to ensure the most accurate line list and parameter selections. These control stars had their equivalent widths measured manually through the IRAF function *splot* after they were continuum normalized. The reduction in line list and selection of ARES parameters led to under 10% change in stellar parameters in these stars. The final chosen parameters adopted in ARES were: smoother = 4, space = 1.0, rejt = 0.995, lineresol = 0.05, and miniline = 0.7, where the smoother is a boxcar smoother, space is the wavelength interval around the line where the computation will be conducted, rejt controls the local continuum, linesol is the minimum distance between lines to differentiate them, and miniline is the minimum equivalent width value to be calculated(Sousa et al., 2007).

3.1.3 Stellar Parameters

Spectroscopic stellar parameters were determined using balance constraints of the abundances derived from neutral (Fe I) and ionized (Fe II) iron. The iron line list was reduced down to 71 lines as an increase in the number of iron lines lead to no decrease in the abundance errors. A trial analysis was performed with three abbreviated line lists from literature sources consisting of 28 (Bond et al., 2006), 35 (Reddy et al., 2003), and 108 (Bubar & King, 2010) lines. A fourth line list was varied to try and determine if using more Fe lines had a large effect on stellar parameters. Each analysis used the same equivalent widths, line centers, and atomic constants for the lines common to all lists. When the Fe I line list had over 70 lines, the values did not change outside of the uncertainties, but at lower numbers the addition of Fe I lines could change the parameters

significantly. The stellar parameters were calculated using an iterative script that started at solar values (effective temperature T_{eff} = 5777 K, surface gravity $\log(g)$ = 4.44, microturbulent velocity ξ = 1 km/s, and [Fe/H] = 0) in the ATLAS9 model atmosphere grid. The stellar T_{eff} and ξ were determined through balancing the reduced equivalent widths and excitation potentials for Fe I lines. First the temperatures from the input model atmospheres were adjusted by 10 K intervals until there was no correlation between the normalized line by line abundances and the excitation potential of each individual Fe I line. Afterwards, ξ was adjusted in 0.01 km/s intervals until there was no correlation with reduced equivalent widths and the line by line abundances. After, every adjustment in ξ the temperature was recalculated so that both correlations were constantly removed. This process yielded an [Fe/H] for the Fe I lines. The [Fe/H] from Fe II is primarily influenced by the stellar surface gravity and was forced to match the [Fe/H] from Fe I lines by adjusting the surface gravity in 0.01 dex intervals until the mean abundance of Fe I lines matches that of Fe II lines. The final stellar parameters (T_{spec}, ξ, $\log(g)$, and [Fe/H]) are shown in Table A.2. Uncertainties in temperature were determined by adjusting the temperature solution until the correlation between the abundances and excitation potential reached a 1σ linear correlation coefficient for the given number of lines. This was done by slowly increasing the temperature until there was a linear 1σ deviation from the calculated value. The same 1σ approach was used for the ξ uncertainty but with the abundances versus reduced equivalent widths. The errors for [Fe/H] were determined by using a standard deviation of all the line abundances for Fe I, combined with the change resulting from varying the T_{spec} and ξ by their 1σ uncertainties. Table A.2 lists all of the stellar parameters for the stars in this study, with the planet host stars being covered in the next chapter.

3.1.4 Abundance Determination

This study looks at all possible elements in the observed wavelength range. Abundances are differential with respect to the Sun and are presented in standard bracket notation, defined in Chapter 1, where $\log(N(H)) = 12$. Due to the use of various different determinations of the absolute solar abundances in use (for example Grevesse & Sauval, 1998; Asplund et al., 2009; Lodders et al., 2009), it is important to provide unnormalized abundances. This is especially helpful when examining elemental ratios. Since the spectra obtained did not include the O I triplet located between 7771 Å and 7775 Å, only the 6363 Å and 6156 Å lines were used, since a discrepancy in measurements using the 6300Å forbidden line due to blending with a nearby Ni I line has been noted (Nissen, 2013). Oxygen abundances are the most variable amongst abundance finding groups and remain controversial, with different spectral lines giving O values for the same stars of up to 1 dex difference(Israelian et al., 2003). Uncertainties for each element were determined by the standard deviation of the abundances given for each line for that given element. Any abundance that was determined through the use of only one line has an error assumed to be that of [Fe/H] uncertainty and is marked with an asterisk.

3.2 Results

Table A.4 gives the abundances of all the elements for the entire study. These are listed as [X/H] for each element, and can easily be converted to [X/Fe] by subtracting the log values of [X/H] and [Fe/H]. Figures 3.1- 3.11 show [X/H] vs. [Fe/H] (left) and [X/Fe] vs. [Fe/H] (right) for the full sample (green) and the known planet hosts (red). The [X/Fe] vs. [Fe/H] distributions are plotted with a linear fit, the slope, y-intercept, and R^2 value of which are given in Table 3.1 for 24 elements. The slopes and intercepts of the linear fit for the data were found with the same method used in Chapter 2. This table also gives the

average $[X/Fe]_{avg}$ standard deviation, and $u_{intrinsic}$ for each element in the sample.

This survey probes lower metallicity regimes than most similar abundance surveys, which typically stop at [Fe/H]$\sim$ -0.2. For a few elements, notably Si, S, Na, and Al, there appears to be a slight upturn in the slope at these low metallicities. The small number of points in the -0.6<[Fe/H]<-0.2 range do not significantly affect the overall slope, but when more data are available in this region a piecewise or higher order fit may be warranted. The trend lines show similar behavior to at least one other study (Mishenina et al., 2008; Bond et al., 2006; Delgado Mena et al., 2010; González Hernández et al., 2010; Neves et al., 2009), with the exceptions of Al and Si. The trends for those elements are far more negative then the other studies, due to the population of high [X/Fe] stars at lower metallicities. However, no two studies have great agreement. This may well be a result of the difficulty in measuring elemental abundances. There is also a possible selection effect in studies specifically looking for solar analogs (Delgado Mena et al., 2010; González Hernández et al., 2010).

Carbon shows a slightly increasing but relatively flat trend of [C/Fe], in keeping with the other surveys and GCE models discussed in Chapter 2. Smaller studies unpopulated at low [Fe/H] tend to have slightly negative trends (Bond et al., 2006; González Hernández et al., 2010; Delgado Mena et al., 2010). The Sun lies slightly above the median value of the sample, in agreement with other studies and predictions of the [Fe/H] at which SNeIa start injecting Fe without a corresponding addition of C (Tomkin & Lambert, 1984). The distribution is fairly uniform, with the exception of two planet hosts. Both have very similar values, with extremely low [C/Fe]$\sim$ -0.6 at a high [Fe/H]$\sim$0.2.

Oxygen shows a downward trend as expected, though some studies show a much sharper drop off of [O/Fe] as [Fe/H] increases (Mishenina et al., 2008). The Sun lies nearly 0.2 dex below the trend of [O/Fe], and below almost all of the sample in [O/H]. The two lowest metallicity stars with O values happen to be planet hosts.

[Na/Fe] often shows a complicated trend in other studies from between [Fe/H] $\simeq$ -0.4 and [Fe/H] $\simeq$ 0.4, with a downward trend until -0.2 and a gradual increase at larger [Fe/H]. Given the distribution of stars in [Fe/H] in this study, the change in slope appears to be present, but too few points are available at low [Fe/H] to measure a slope at this end. A population of stars with systematically higher values of [Na/H] at a given [Fe/H] appears to parallel the overall trend. The Sun lies close to the trend. [Mg/Fe] has a decreasing trend throughout the metallicity range. It has the most negative slope of all the α elements. Outliers at high [Mg/Fe] are all planet hosts. The solar value lies slightly below the trend. [Al/Fe] has a large scatter which is not seen in the smaller studies Bond et al. (2006); González Hernández et al. (2010); Mishenina et al. (2008) but is comparable to Neves et al. (2009). Its trend is similar to that of the α elements, with a decrease until [Fe/H] $\simeq$ 0.1, and then an upturn afterwards. There is a great deal of scatter in stars with large [Al/Fe] at solar metallicities. The sun has a slightly higher [Al/Fe] than the overall trend. A hint of the parallel higher trend seen in Na may be present.

[Si/Fe] shows a downward trend from [Fe/H] $\simeq$-0.6 to [Fe/H] $\simeq$ 0.1, then levels off towards higher [Fe/H]. This supports other studies that claim two distinct populations at higher and lower metallicities for Si (Neves et al., 2009). The average [Si/Fe] values varies between groups, with this study falling with those studies that find lower overall values for this plateau (Bond et al., 2006; González Hernández et al., 2010). The trend falls significantly below the solar value. The few points at [Fe/H]$<$ -0.4 almost all have very high [Si/Fe]. [S/Fe] has a slight upward slope. The scatter to low [S/Fe] is substantially larger than that to higher values at [Fe/H]$>$ -0.2, but all of the lower metallicity stars lie above the trend. It is difficult to compare to other studies due to the paucity of S measurements in the literature. The trend is slightly lower than solar. [Ca/Fe] shows the same negative trend as Mg, with a slightly smaller slope. As with the other α elements, most stars with [Fe/H]$<$ -0.2 lie above the fitted trend. There is more scatter

towards higher values of [Ca/Fe]; stars with low values clump more tightly towards the trend. The Sun lies almost exactly on the trend line.

For the representative *s*- and *r*-process elements, Ba has a small scatter and is biased to low [Ba/Fe] at [Fe/H]< -0.2. The trend is strongly negative. [Eu/Fe] has a greater scatter than other studies, but a similar trend and $u_{intrinsic}$ to Bond et al. (2008). [Eu/Fe] has a striking scatter to low values of [Eu/Fe] at [Fe/H]> -0.2.

The biggest variety in abundances is for V, which ranges from [V/Fe] of 1.17 to -0.55. This is a factor of 50 difference between the most V enriched star and the least. This is not uncommon as Neves et al. (2009), whose study looked at a similar number of stars (451 FGK stars), found a large scatter, with an increase in [V/H] at supersolar metallicities. They included a cutoff for V at stars with T<5300 K, because they saw a trend with T_{eff} that was attributed to blending effects in cooler stars. This reduced the scatter, but not entirely.

3.2.1 Comparison to Planet Hosts

For the elements C, O, S, and Ba, the planet hosts are evenly, or close to evenly, distributed above and below the best fit trend line. As discussed above, however, two of the hosts are the largest outliers in [C/Fe] for the entire sample, with very low [C/Fe]. For a few elements the hosts are biased toward higher [X/Fe] than the rest of the sample. Al, Ca, Ni, and Mg all have 20 stars above the trend line as compared to only 3 below. Na has 19 above the trend line and 4 below. It is not surprising that Al, Mg, and Na are all similar as they are produced by similar processes as described in Chapter 2. Silicon has one host on the trend line, with 18 above and 4 below. Europium is the only element strongly biased toward low values. Several of the hosts are in the tail of very low [Eu/Fe] stars at high metallicity. With 6 above and 15 below, O also appears biased, but small number statistics make this marginal. Barium and Eu are considered as representative *s*- and

r-process elements. Other elements beyond the Fe peak are not considered separately here due to their low abundances.

3.2.2 Intrinsic Variation

Table 3.1 shows the $u_{intrinsic}$ values for certain elements in this study to match those discussed in Chapter 2. The $u_{intrinsic}$ values most closely match Neves et al. (2009), which is the only other study that looks at a larger sample size. Given the range of variation between those studies, none of the abundant elements in this sample are exceptional. Unsurprisingly, considering the results of Chapter 2, all the elements below Si have large values of $u_{intrinsic}$. Sodium and Al have somewhat larger values than those studies, some of which may be due to large scatter at low [Fe/H] not probed by other samples. Sulfur has a large $u_{intrinsic}$=0.14 Given that this study has substantially increased the number of stars in the literature with S measurements, this value should at present be taken as the standard. Silicon has no measurable $u_{intrinsic}$ for this sample, in agreement with small to zero values for other studies. Nickel also correlates closely with Fe. The largest $u_{intrinsic}$ is found for V. There is a substantial range of $u_{intrinsic}$ in the other studies that measure V. This study does not remove stars with T<5300K as in Neves et al. (2009). Doing so may decrease $u_{intrinsic}$ significantly, as unidentified line blending would increase the observational uncertainty. The $u_{intrinsic}$ for Mn is larger than for other studies as well. With the exception of Ba, all of the elements measured above the Fe peak have moderately large $u_{intrinsic}$. Interestingly, most are of the same order as for elements lighter than Si. Common species are subject to the same level of variation as trace elements.

The $u_{intrinsic}$ values are reliant on the observational errors, with those elements having large average errors registering small to no $u_{intrinsic}$. It is important to develop a standard method for abundance errors, as well as to find methods to reduce the uncertainties, to try and deduce what real variation exists in elemental abundance ratios.

Table 3.1: Table of statistics

Element	$[X/Fe]_{avg}$	StdDev	$u_{intrinsic}$	Slope	Intercept	R^2
C	-0.07	0.17	0.14	0.028	-0.074	0.001
O	0.14	0.15	0.14	-0.163	0.174	0.019
Na	-0.05	0.13	0.15	-0.017	-0.048	0.000
Mg	-0.03	0.14	0.1	-0.458	0.046	0.270
Al	-0.06	0.18	0.17	-0.192	-0.035	0.033
Si	-0.12	0.06	0	-0.190	-0.097	0.279
S	-0.1	0.17	0.14	0.041	-0.102	0.002
Ca	-0.04	0.18	0.04	-0.359	0.012	0.112
Sc	-0.05	0.12	0.1	-0.177	-0.021	0.062
Ti				-0.349	0.083	0.038
V	0.06	0.35	0.32	-0.133	0.078	0.004
Cr	-0.08	0.11	0.05	-0.077	-0.070	0.014
Mn	0.05	0.35	0.26	0.506	-0.020	0.058
Co				0.037	-0.056	0.001
Ni	-0.06	0.13	0	-0.077	-0.046	0.010
Cu	-0.06	0.17	0.13	0.088	-0.070	0.008
Y	-0.05	0.14	0.12	-0.223	-0.017	0.065
Zr	0.02	0.23	0.21	-0.321	0.062	0.054
Ba	-0.2	0.15	0.05	-0.644	-0.111	0.516
Ce				0.086	0.160	0.001
Nd	0	0.16	0.12	-0.609	0.082	0.412
Eu	0.16	0.18	0.16	-0.449	0.226	0.165

However, it is evident that there is a real spread, and even for an element like Si, whose stellar abundances seem to correlate closely with Fe abundance in a star, there should still exist enough stars with unique [Si/Fe] ratios to observe true diversity.

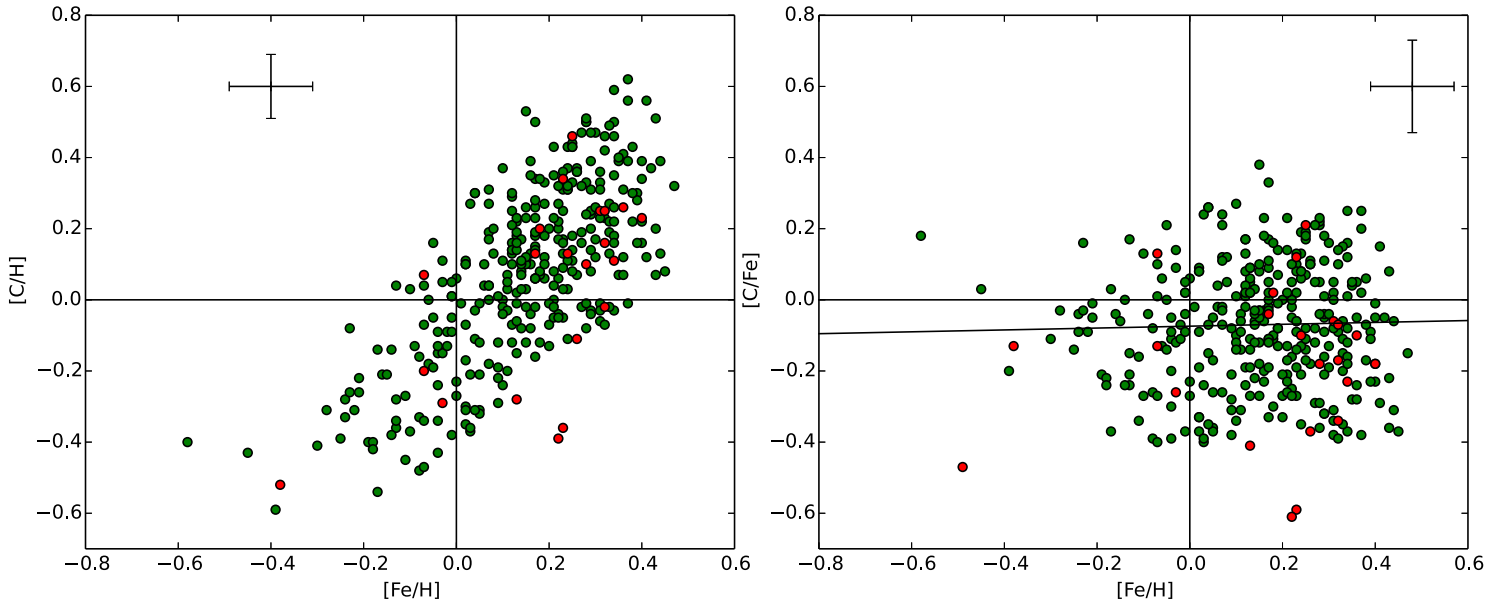

Figure 3.1: Left: Carbon to hydrogen ratio with respect to solar, [C/H], as a function of [Fe/H]. Red data points are exosolar planet host stars. Right: Carbon to iron ratio with respect to solar, [C/Fe] as a function of [Fe/H]. The solid line is a least-squared linear fit to the entire distribution.

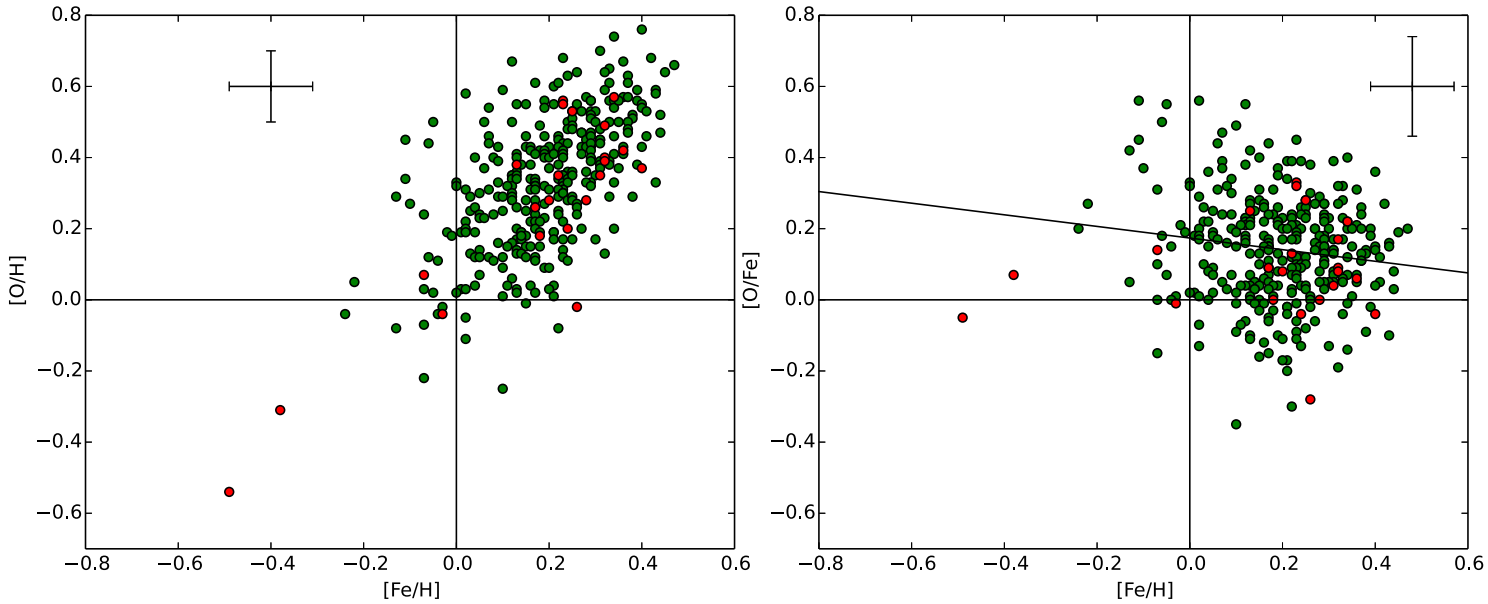

Figure 3.2: Left: Oxygen to hydrogen ratio with respect to solar, [O/H], as a function of [Fe/H]. Red data points are exosolar planet host stars. Right: Oxygen to iron ratio with respect to solar, [O/Fe] as a function of [Fe/H]. The solid line is a least-squared linear fit to the entire distribution.

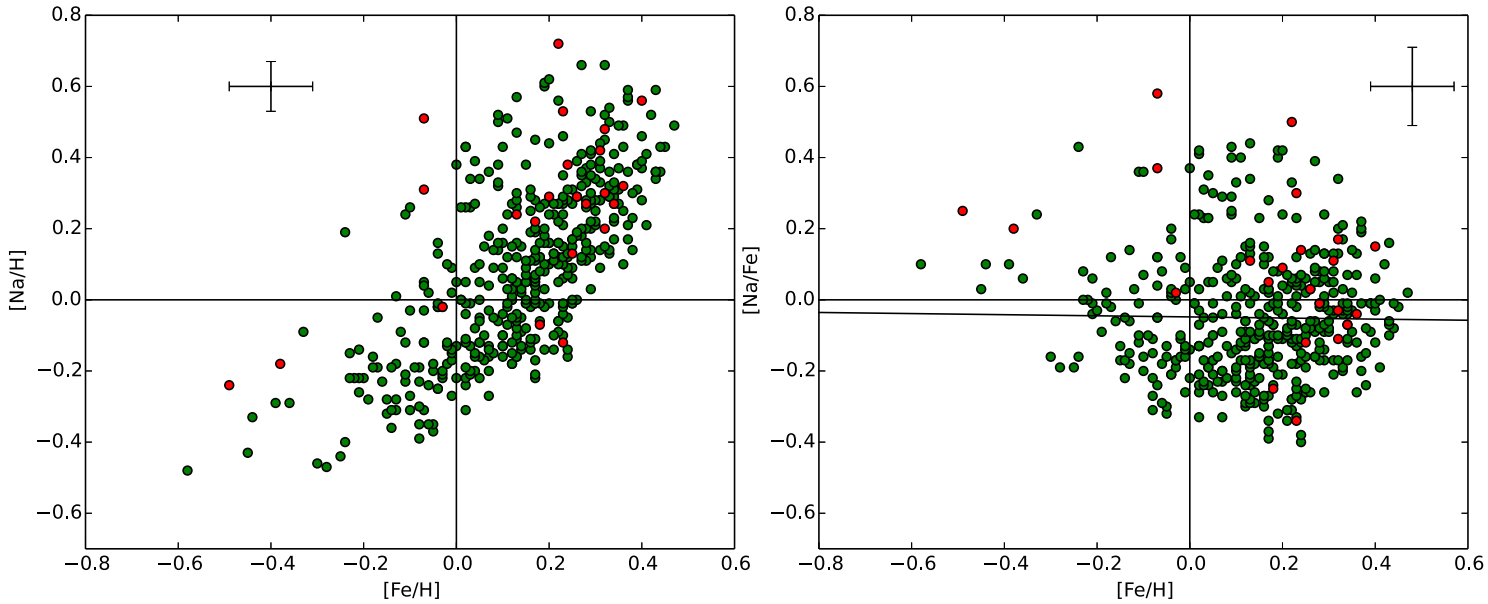

Figure 3.3: Left: Sodium to hydrogen ratio with respect to solar, [Na/H], as a function of [Fe/H]. Red data points are exosolar planet host stars. Right: Sodium to iron ratio with respect to solar, [Na/Fe] as a function of [Fe/H]. The solid line is a least-squared linear fit to the entire distribution.

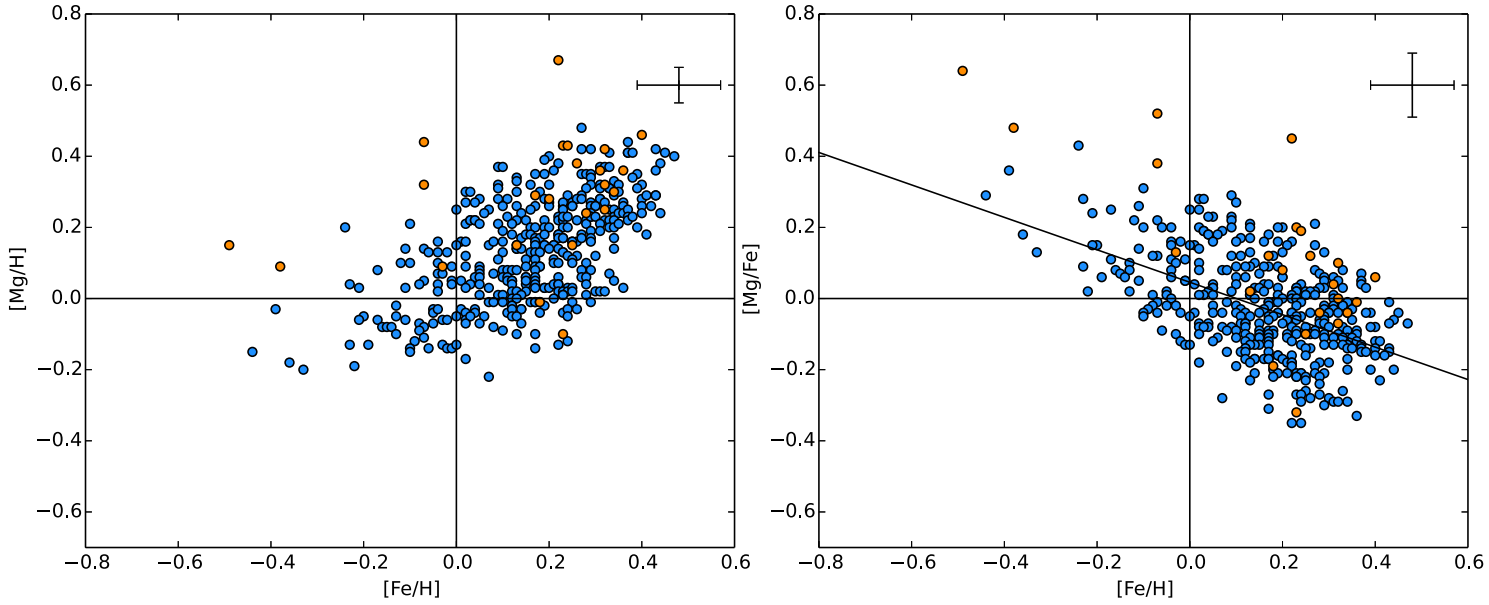

Figure 3.4: Left: Magnesium to hydrogen ratio with respect to solar, [Mg/H], as a function of [Fe/H]. Red data points are exosolar planet host stars. Right: Magnesium to iron ratio with respect to solar, [Mg/Fe] as a function of [Fe/H]. The solid line is a least-squared linear fit to the entire distribution.

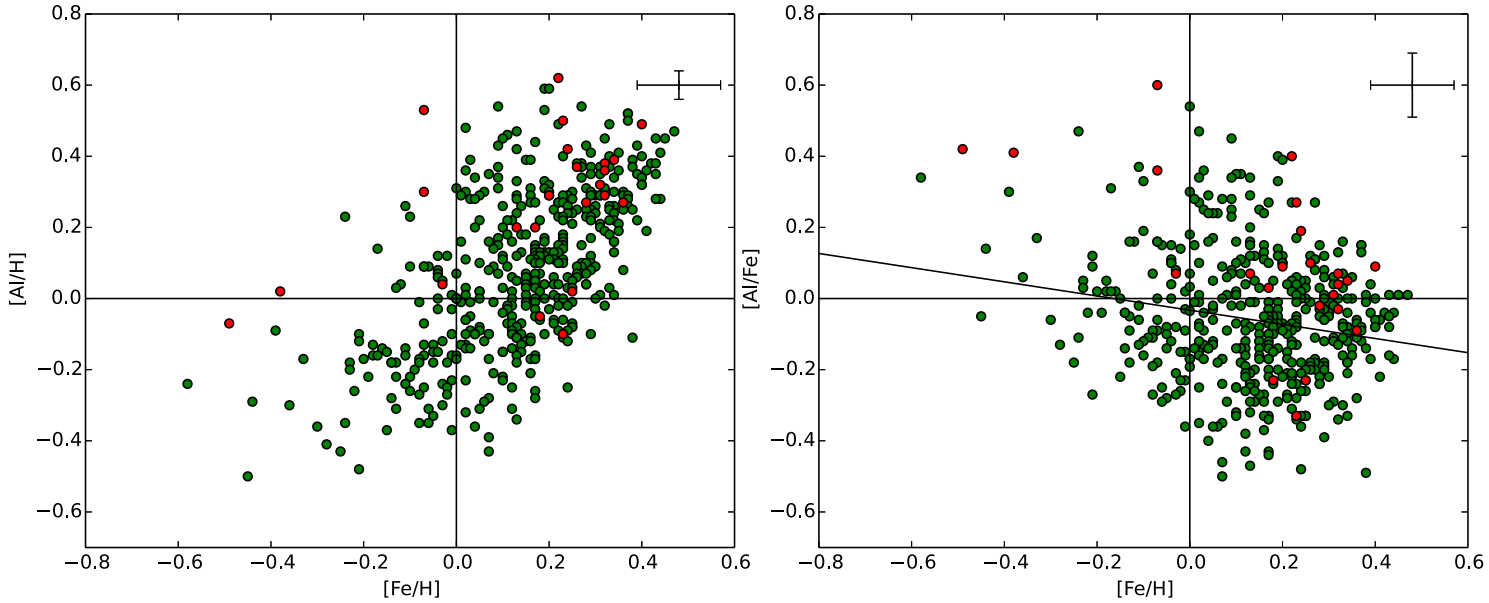

Figure 3.5: Left: Aluminum to hydrogen ratio with respect to solar, [Al/H], as a function of [Fe/H]. Red data points are exosolar planet host stars. Right: Aluminum to iron ratio with respect to solar, [Al/Fe] as a function of [Fe/H]. The solid line is a least-squared linear fit to the entire distribution.

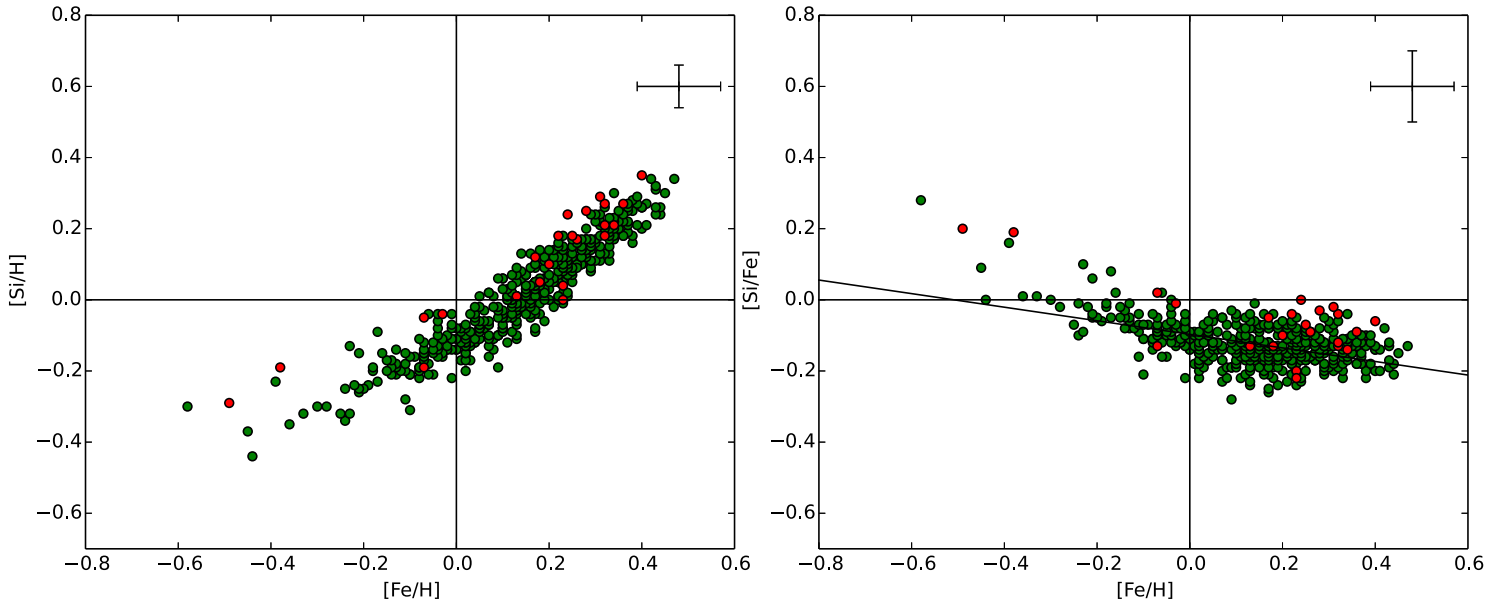

Figure 3.6: Left: Silicon to hydrogen ratio with respect to solar, [Si/H], as a function of [Fe/H]. Red data points are exosolar planet host stars. Right: Silicon to iron ratio with respect to solar, [Si/Fe] as a function of [Fe/H]. The solid line is a least-squared linear fit to the entire distribution.

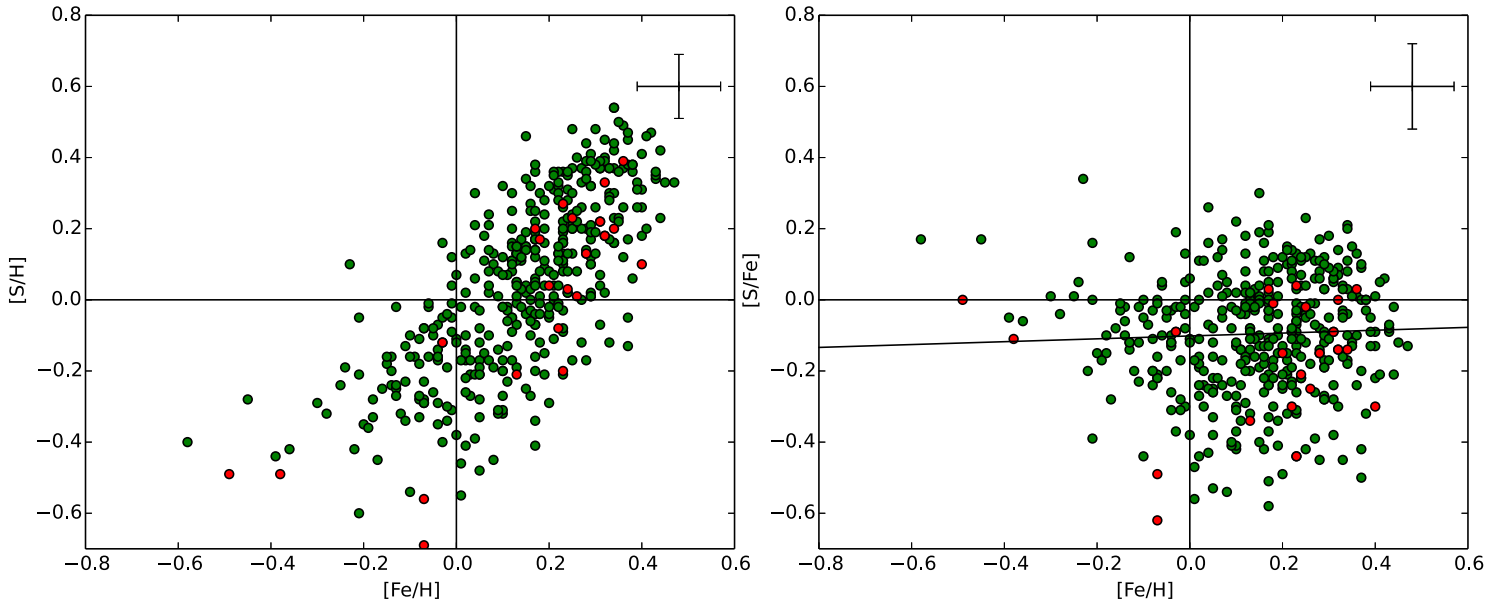

Figure 3.7: Left: Sulfur to hydrogen ratio with respect to solar, [S/H], as a function of [Fe/H]. Red data points are exosolar planet host stars. Right: Sulfur to iron ratio with respect to solar, [S/Fe] as a function of [Fe/H]. The solid line is a least-squared linear fit to the entire distribution.

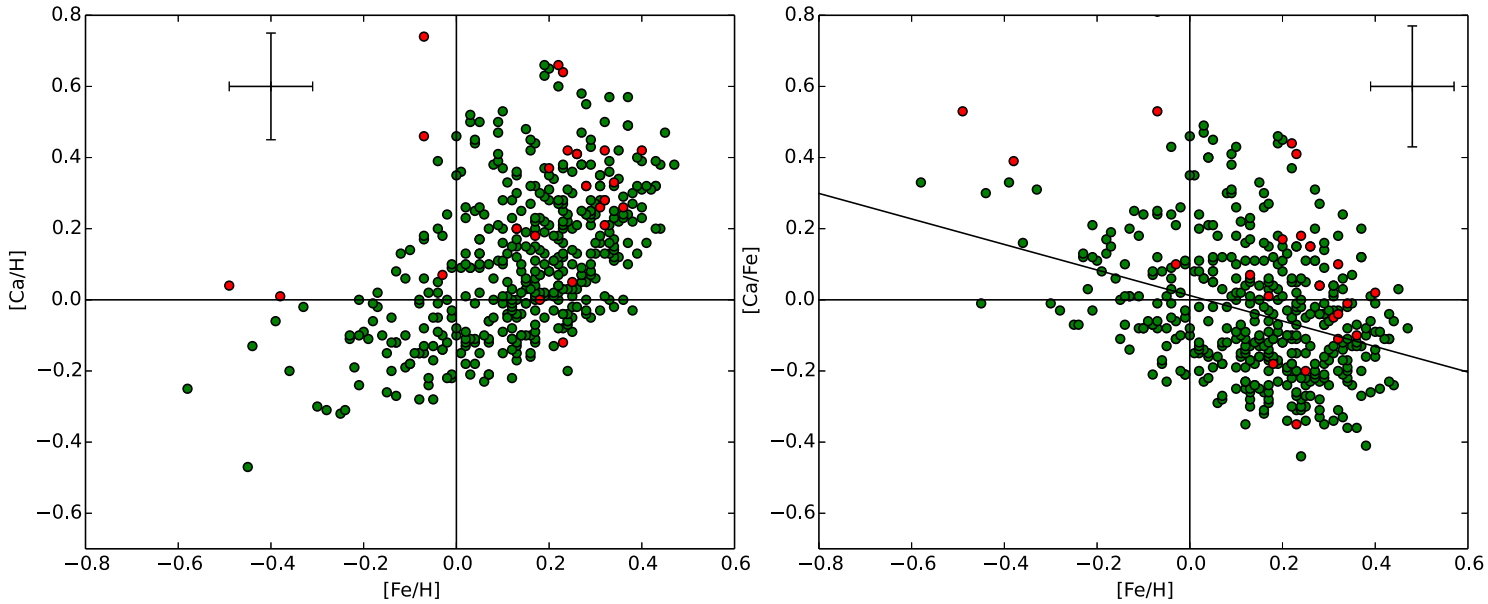

Figure 3.8: Left: Calcium to hydrogen ratio with respect to solar, [Ca/H], as a function of [Fe/H]. Red data points are exosolar planet host stars. Right: Calcium to iron ratio with respect to solar, [Ca/Fe] as a function of [Fe/H]. The solid line is a least-squared linear fit to the entire distribution.

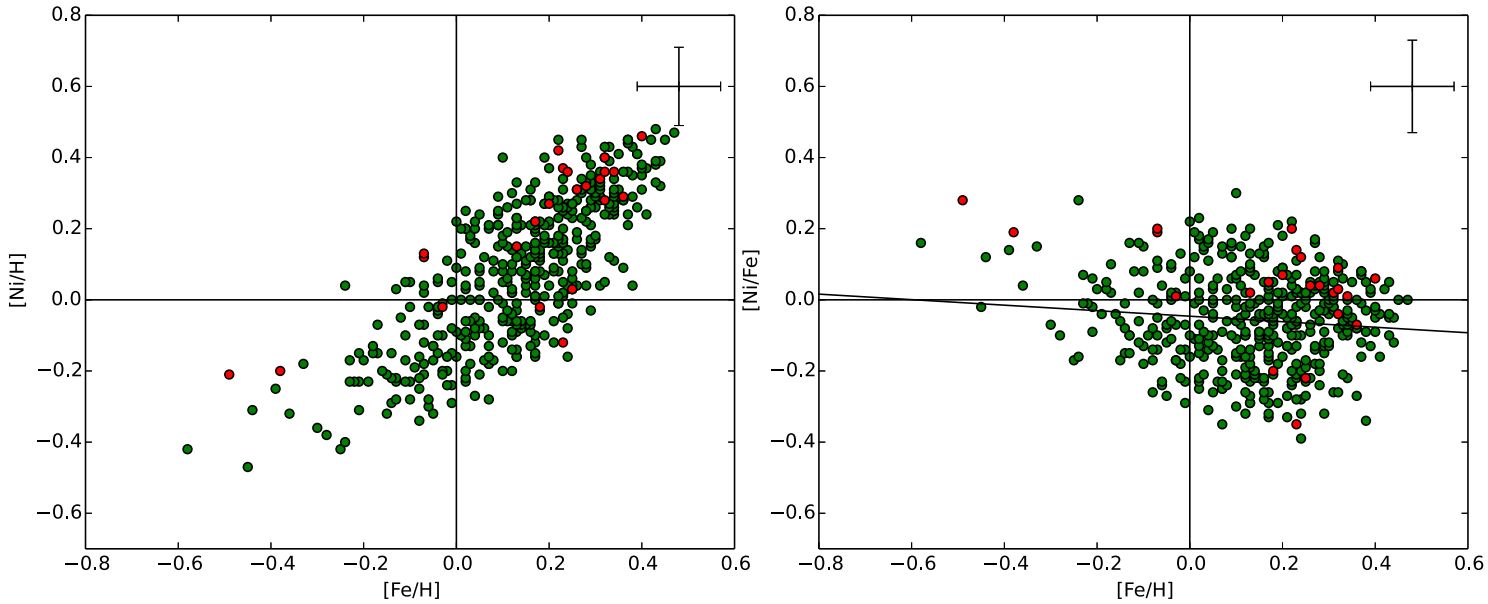

Figure 3.9: Left: Nickel to hydrogen ratio with respect to solar, [Ni/H], as a function of [Fe/H]. Red data points are exosolar planet host stars. Right: Nickel to iron ratio with respect to solar, [Ni/Fe] as a function of [Fe/H]. The solid line is a least-squared linear fit to the entire distribution.

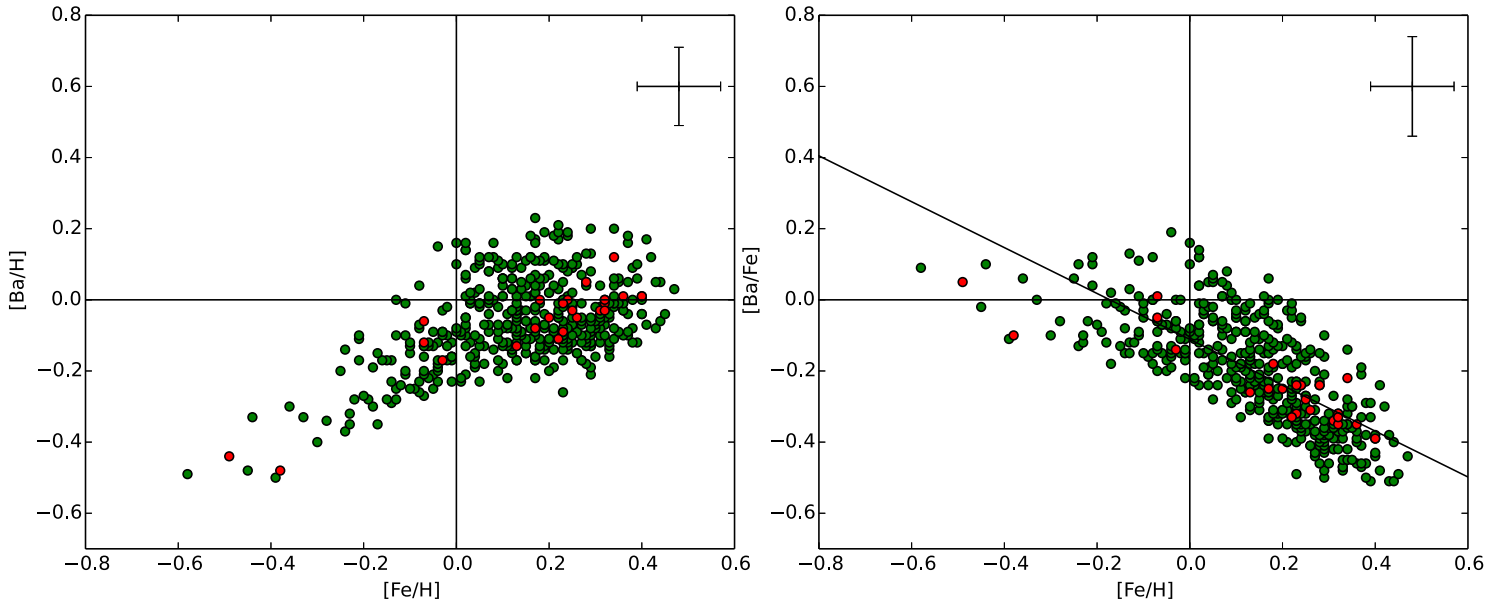

Figure 3.10: Left: Barium to hydrogen ratio with respect to solar, [Ba/H], as a function of [Fe/H]. Red data points are exosolar planet host stars. Right: Barium to iron ratio with respect to solar, [Ba/Fe] as a function of [Fe/H]. The solid line is a least-squared linear fit to the entire distribution.

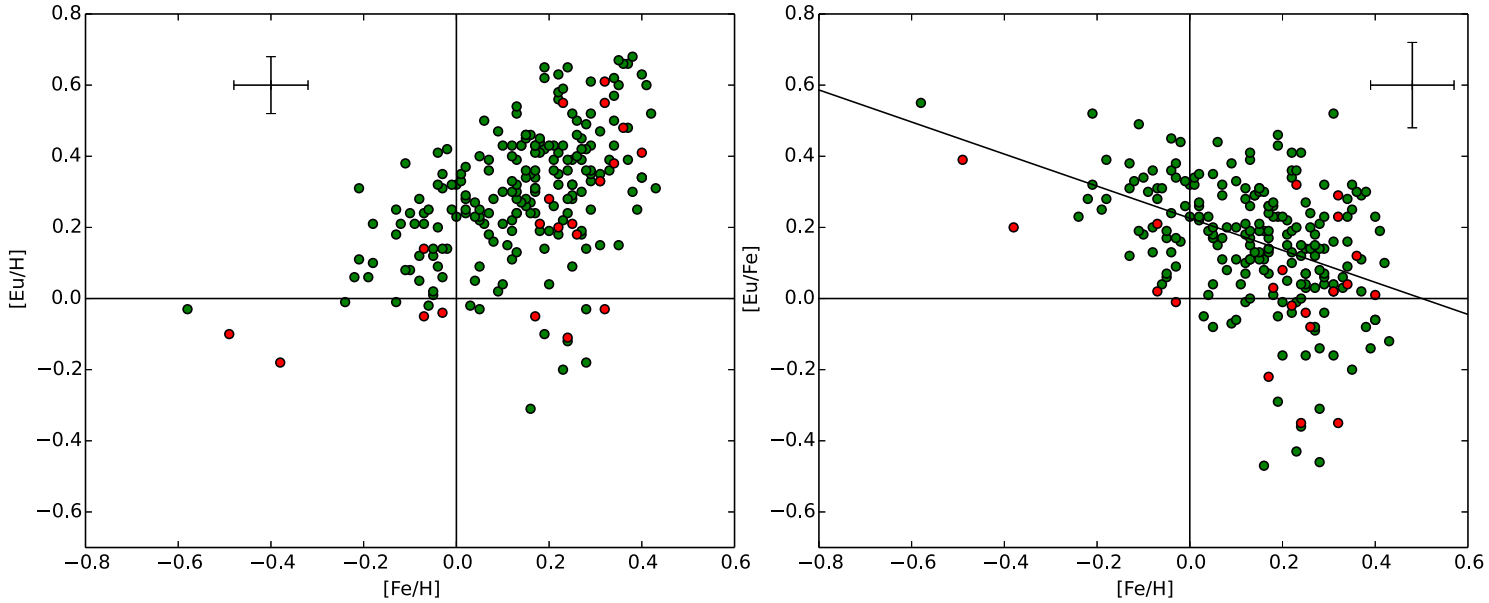

Figure 3.11: Left: Europium to hydrogen ratio with respect to solar, [Eu/H], as a function of [Fe/H]. Red data points are exosolar planet host stars. Right: Europium to iron ratio with respect to solar, [Eu/Fe] as a function of [Fe/H]. The solid line is a least-squared linear fit to the entire distribution.

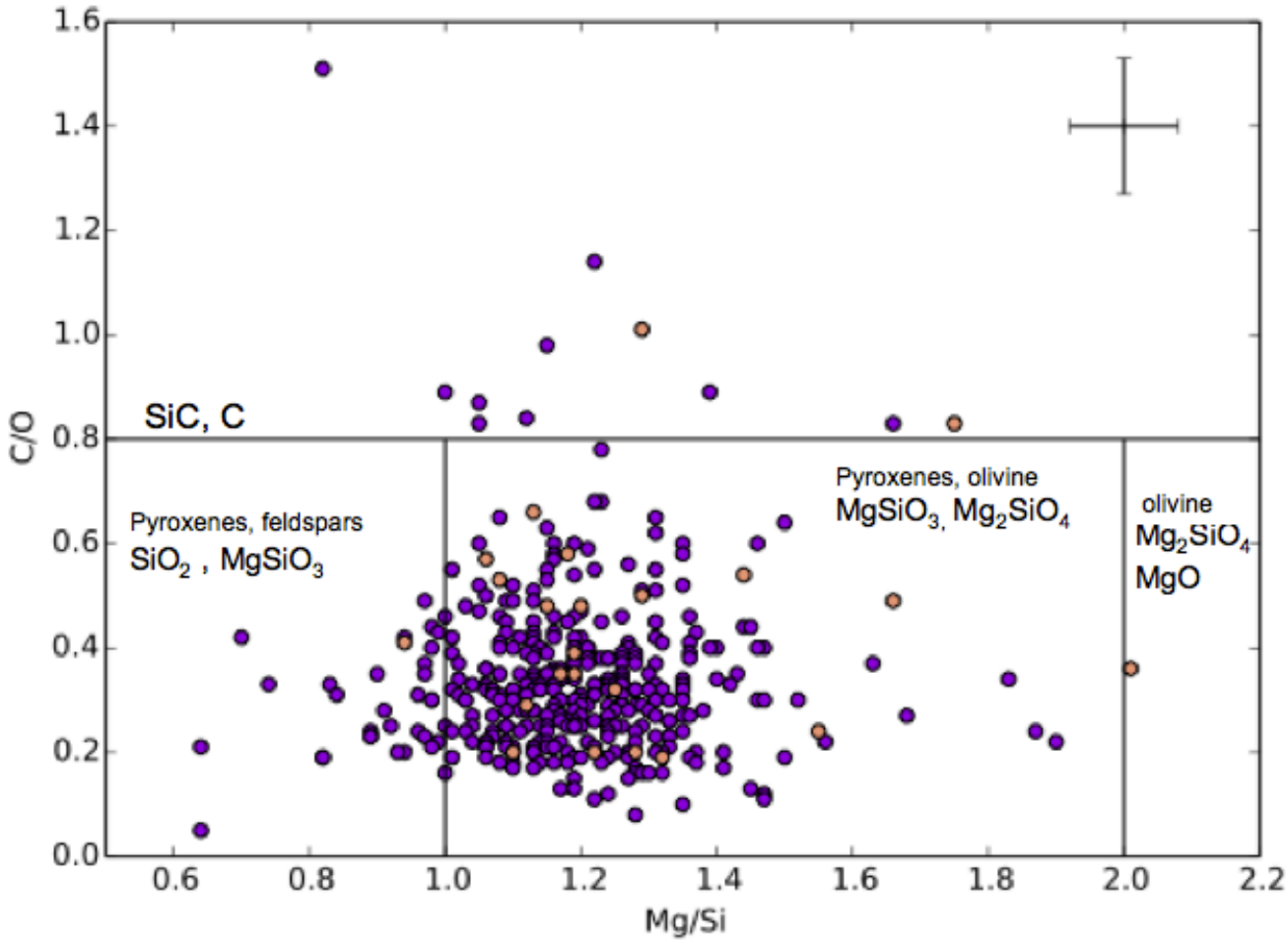

Figure 3.12: Mg/Si vs. C/O ratios for stars in this study. Planet hosts are in orange. Divisions between dominant rock forming minerals from Bond et al. (2010b); Delgado Mena et al. (2010).

Chapter 4

ABUNDANCES OF PLANET HOSTS

4.1 Stellar Data

4.1.1 Target Stars and Observations

The stellar spectra for this study were taken by Paul Butler and his team from the Carnegie Institute of Washington and were given to Arizona State University for elemental abundance analysis. The spectra were observed through the Magellan Planet Search Program between December 2002 and July 2009. They used the MIKE echelle spectrograph (Bernstein et al. 2003) on the 6.5 m Magellan II telescope. The spectra have a resolution of R$\sim$50,000 in the wavelength range 4700 Å to 7100 Å. Only the red chip data was used for abundance determination. Wavelength calibration was carried out by iodine absorption cell (Marcy and Butler 1992). Only F, G and K stars were observed in this survey. Of the 458 spectra with determined abundances, only 24 stars have currently known exoplanets. These planet hosts were determined by cross-referencing the full list of stars in the sample with the Extrasolar Planets Encyclopedia catalogue[1].

4.1.2 Abundance Analysis

These stars were run through the pipeline explained in the previous chapter to obtain stellar parameters and elemental abundances using a differential local thermodynamic equilibrium (LTE) analysis. We take all of the stars from reduced but uncalibrated spectra all the way through the abundance finding process, starting with wavelength calibration in IDL and combining all of the orders into a single FITS file. The

[1] www.exoplanet.eu

pipeline uses the 'abfind' function of the 2002 version of the spectral analysis program MOOG (Sneden, 1973), with a grid of model atmospheres that is created by the program mspawn through ATLAS9 (Kurucz, 1993). With the wavelength range of the spectra, this pipeline can measure up to 27 different elements, including iron, which is measured in the parameter determination. Equivalent widths were measured by hand, using the 'splot' function of IRAF and fit with gaussians. The atomic parameters, line wavelengths (λ), excitation energy of the lower energy level ($xi1$), and oscillator strength (log(gf)) of each line were collected for different elements from five sources (Reddy et al., 2003; Feltzig & Gustafsson, 1998; Bubar & King, 2010; Bond et al., 2006; De Silva et al., 2006) to include the largest variety of elements. Table A.1 gives our complete line list with these quantities and their sources. Spectroscopic stellar parameters were determined using balance constraints of the abundances derived from neutral (Fe I) and ionized (Fe II) iron. This process is described in Chapter 3, along with the abundance determination.

4.2 Results

Table A.8 gives the stellar parameters for the planet host stars, Table A.9 gives the [X/H] abundances and Table A.13 gives the absolute abundances normalized to 10^6 Si. Abundance trends for the full sample are discussed in Chapter 3. Here we focus on the planet hosts and elements that are important for planet formation and evolution. We find two hosts with very low metallicity, HD10700 ([Fe/H] = -0.49 ± 0.08) and HD111232 ([Fe/H] = -0.38 ± 0.07). Most of the stars are significantly supersolar, with [Fe/H] up to 0.4.

The ratios C/O and Mg/Si have been identified as important to planetary properties. In addition, ratios of combinations of Fe, Ca, Si, Mg, and Al can affect mineralogy on a more subtle level. Since Bond et al. (2010b) calculated C/O ratios and modeled planetary bulk chemistry for non-solar abundance ratios, a few other studies have attempted larger

C/O ratio abundance determinations. Delgado Mena et al. (2010) found abundances for C, O, Mg, and Si for 370 FGK stars from the HARPS planet-search sample and Petigura & Marcy (2011) for 941 F, G, and K stars from the California Planet Survey sample. Both included planet host stars and stars that did not have confirmed planets. Delgado Mena et al. (2010) find 34% of their stars have a C/O ratio > 0.8, and Bond et al. (2010b) find nearly half of their stars are over the theoretical threshold identified by Bond et al. (2010b) between silicate and carbide-dominated planets. These surveys found average C/O ratios significantly higher than that of the sun, 0.55 (Asplund et al., 2009). However, Fortney (2012) questions this high percentage of C/O stellar abundances, arguing for a true measured fraction of C/O > 0.8 in 10-15% of stars and 1-5% having C/O >1. This implies that carbide planets should be rarer than these few studies suggest for solar-type stars. They show that as the C/O ratio increases, so do the average errors, culminating in error bars for the C/O ratio of 0.23 dex for C/O of 1. Petigura & Marcy (2011) finds C/O > 0.8 in only 4.8% of their sample, which is in better agreement with Fortney (2012).

In this sample of planet hosts, we find the mean C/O ratio to be 0.44, which is lower than that for the sun. Only one star, HD143361, has a C/O ratio over 1. HD142022 is the only other star over 0.8. This makes 2 out of 24 stars with measurable C and O abundances exceeding the 0.8 suggestion for carbide planets. That is 4% over C/O = 1 and 9% over C/O = 0.8. However, this sample of planet hosts may be too small to do an effective analysis and using the full dataset gives more useful statistics. The full dataset from Chapter 3 has 376 stars with measurable C and O abundances. The mean C/O ratio is even lower than that for planet hosts, at 0.36, with 6 stars over 1 and 13 over 0.8. This gives 1.6% of stars with a C/O ratio over 1 and 4% over 0.8. The latter value is low compared to most other studies and the estimate by Fortney (2012), but in good agreement with Petigura & Marcy (2011).

The full dataset has 449 stars with abundances of Mg and Si. This study finds a

mean Mg/Si ratio of 1.22, which is above the solar value, and only slightly below the mean found by Bond et al. (2010b) of 1.32. Delgado Mena et al. (2010) found 56% of their planetary host stars to have Mg/Si < 1, as opposed to only one star out of 24, or 4.3%, in our planet host study and 7% of our full study. We find one star (τ Ceti, [Fe/H]=-0.49$\pm$0.08) with Mg/Si > 2. No other study found any stars in the Mg/Si > 2 regime. We will discuss this star in detail in Chapter 5. The second highest Mg/Si in our planet host sample is 1.75 for HD137388, which has an [Fe/H] = 0.22$\pm$0.08 and a C/O ratio of 0.83, making it possibly a reduced carbide planet with excess Mg. In contrast, τ Ceti has C/O = 0.36, putting it below average for C/O.

4.3 Exoplanetary Mineralogy

Although planet formation simulations involving planetary orbital evolution and accretion are required to get more accurate ratios for possible planetary systems(Carter-Bond et al., 2012), using stellar abundances to try and predict extreme planetary conditions is a solid starting point Delgado Mena et al. (2010). The mantle and core compositions of exoplanets should be variable as a result of extreme variations of major rock-forming elements. Extreme elemental planetary compositions should affect how a planet transports energy from its interior to its surface, the size and composition of its core, and the rheology of both mantle and crustal rocks. These factors in turn relate to the presence and behavior of plate tectonics, volcanism, volatile cycles, and magnetic fields. As an example, Earth's mantle has been vigorously convecting over its lifetime, but the mantle of a planet with greater viscosity and thermal conductivity could more efficiently transport energy through conduction, and these are functions of mineral structure of the mantle(Unterborn et al., 2013). Figure 4.1 shows the current standard diagnostic for assessing possible bulk mineralogy of planets, which simultaneously considers the Mg/Si and C/O ratios.

C, O, Mg, and Si play an important role in determining the mineralogical properties of extrasolar terrestrial planets. We will discuss these elements with respect to each other and to Fe. When dealing with these ratios, it is important to note that they refer to elemental atom number ratios, not solar normalized logarithmic ratios such as discussed previously and shown in Table A.13.

The C/O ratio plays a large part in controlling the distribution of Si throughout the planet. This will determine if a planet would be considered an Earth-like silicate planet or a carbon-dominated carbide planet. As discussed in Bond et al. (2010b), if the C/O ratio is greater than 0.8 (at a pressure in the protoplanetary disk of 10^{-4} bar), Si will condense in solid form primarily as SiC and other carbide phases such as TiC. C will also be present in pure element phases such as graphite. The material for terrestrial planet formation is mostly in the innermost disk, where these C-rich materials would be found, while further from the host star there would still be metallic Fe and Mg silicates such as olivine(Mg_2SiO_4) and pyroxene($MgSiO_3$). For systems with C/O $<$0.8, silicate would be present in rock-forming minerals as SiO_4^{4-} and SiO_2. (Sen et al. (2013) suggested that substitution of C for O in SiC may be far more energetically favored at high pressures than substitution of C for Si. This may lead to the formation of SiO_xC_{4-x} type materials in carbon-rich planets. It is unclear, however, if such phases can be stable under highly reducing conditions.) SiC has dramatically different material properties from silicates at low pressure, though little experimental data is available at the high temperature-pressure conditions of planetary materials. It is believed that SiC has no significant phase transitions up to 90 GPa (Yoshida et al., 1993), in contrast to silica (Stishov & Popova, 1961; Grocholski et al., 2013). At 1 bar, SiC has a factor of 3 times smaller thermal expansivity and 400 times greater thermal conductivity. If these differences persist at high pressures, SiC-rich minerals will gain much less buoyancy when heated and will transfer much more energy through conduction. Even in silicate-dominated planets the C/O ratio

will determine the redox conditions of the planet.

For a silicate-dominated planet, the mineral makeup is determined by the Mg/Si ratio. Our sun lies in the region: $1 < \mathrm{Mg/Si} < 2$, with a value of 1.05(Asplund et al., 2009). In this region, the planet would have predominately olivine and pyroxene, with planets similar to Earth and be dominated by O, Fe, Mg, Si and to a lesser extent Ca and Al(Delgado Mena et al., 2010). For Mg/Si ratio < 1, the Mg in planets is expected to be in pyroxene and its high pressure polymorphs. Solids in the protoplanetary disk would be dominated by pyroxene and metallic Fe, without much olivine present. Any available excess Si would most likely form other silicates such as feldspars or even free silica, SiO_2 (Hirose et al., 2005; Ricolleau et al., 2008). For the Mg/Si > 2 range, for which we find only one star, Tau Ceti, to be further explored in the next chapter, all the Si is almost entirely in olivine, with the excess Mg available to form MgO and MgS. Such a large amount of MgO could drastically affect planetary processes. At high T,P, pyroxene ($MgSiO_3$) changes phase to stishovite SiO_2 plus spinel Mg_2SiO_4. Forsterite olivine Mg_2SiO_4 decomposes into perovskite ($MgSiO_3$) and ferropericlase (MgO). Ferropericlase may exist at much shallower depths than in Earth's mantle. A ferropericlase-dominated mantle , where the grains are mechanically interconnected, would have significantly lower viscosity, by about two orders of magnitude and a different melting behavior (Ammann et al., 2011; de Koker et al., 2013). Lower viscosity should lead to more vigorous mantle convection. Different melting properties will influence differentiation as well as near surface behaviors connected to volcanism, crust and lithosphere formation, and lithospheric dynamics.

Figure 4.2 shows a ternary diagram with Mg, Si, and Fe for the full sample from Chapter 3 and the known planet hosts. This diagram uses the unnormalized abundances and normalizes them such that the sum of the elements adds up to 1. This plot allows us not only to see the areas in which olivine and MgO or pyroxene dominate, but also allows

us to visualize where the iron abundance falls with respect to these elements. It is important to note that these shaded regions are not areas in which these minerals are solely found, but loose indicators for when they would start to dominate the mineralogy. Stars closer to the Fe corner of the plot may host planets with bigger Fe cores. The bulk of the planet hosts from this study have higher Mg/Si than the Sun, but almost all lie within the region expected to have a mixed olivine and pyroxene composition. Only one star is in the near complete olivine region, and one from this study in the pyroxene region. The Sun lies in the middle of the distribution on the Fe axis. Earth's mantle is depleted in Fe due to differentiation. As can been seen from comparing the bulk earth values from McDonough & Sun (1995) and the bulk mantle or pyrolite model, even though the Fe content drastically drops, as can be expected as the core contains most of the Earth's iron, the Mg/Si ratio stays relatively the same. There is a slight increase in Mg when looking at just the mantle, and this could be due to Si accounting for 4.23 to 8.2% of the core(Allegre et al., 1995; Ringwood, 1966). Since the Sun and the Earth have very similar compositions on this ternary plot, exosolar planets that have similar redox states as the Earth could expect a similar trend in mantle to core distribution of Mg/Si.

Figure 4.3 shows a ternary diagram for the full sample and planet hosts with C, O and Fe. The trend of decreasing C/O with decreasing Fe is consistent with galactic chemical evolution (GCE) trends (Timmes, Woosley, & Weaver, 1995), with a classic α-element behavior for O and late contributions to Fe and C from Type Ia supernovae and Asymptotic Giant Branch stars, respectively. The redox balance of the planet, controlled by C/O, will affect the alloying of light elements in the core and therefore its size and chemical and physical properties. If the C/O ratio of the star and planet were more reducing, with a higher C/O value than the Earth, the planet could have less iron in the mantle and less Si in the core, resulting in a more Fe and Si-rich mantle. This means that carbide planets, such as those theorized in Madhusudhan et al. (2012) could also have

smaller core sizes.

4.4 Conclusions

Detailed modeling on a planet to planet basis around individual stars is required to understand the true effect stellar abundance variation can have on exoplanets, but the more easily measured stellar abundances can be used to identify planets that are likely to have exotic compositions. Stellar compositions can also be used as primordial conditions for models of planet formation that can provide better estimates for exoplanet composition and structure. This paper presents the results of a new abundance survey for known planet hosts. The survey covers nearly a factor of eight in [Fe/H], giving us a glimse of the makeup of known planet hosts beyond the usual high metallicity bias. There is a trend for higher metallicity stars to have a higher C/O, as might be expected from GCE models, but there is a large amount of variation even in this small sample. The percentage of high C/O stars that might host carbide planets is lower than expected based on other surveys. In fact, only 4 of 24 stars are near or above the solar C/O. The chemistry of a large fraction of exoplanets may turn out to be substantially more oxidizing than Earth's.

The survey contains one planet each in the olivine and pyroxene dominated Mg/Si regimes. There does not appear to be a strong correlation with metallicity, with relatively low and high values of Mg/Si at both metallicity extremes. Earth lies below the bulk of the stars, at the lower end of the mixed olivine/pyroxene domain. Planets with exotic silicate mineralogy therefore appear to be rare but present. Even in a small number of known planet hosts we find examples of extreme abundance ratios that influence planetary mineralogy. These exotic ratios occur at a wide range of metallicities, and different ratios are not strongly correlated with each other. It is therefore not possible to generalize the composition of stars and their planets from measurement of a limited set of elements. A comprehensive abundance analysis of any system of interest is called for. Given the

possible effects of extreme compositions on planetary interior dynamics, these special cases are worth searching out. Trying to deduce planetary properties can be a tricky ordeal, however, there is much to learn from stellar spectroscopy and exploring the unknown territory of non-Earth-centric planetary mineralogy.

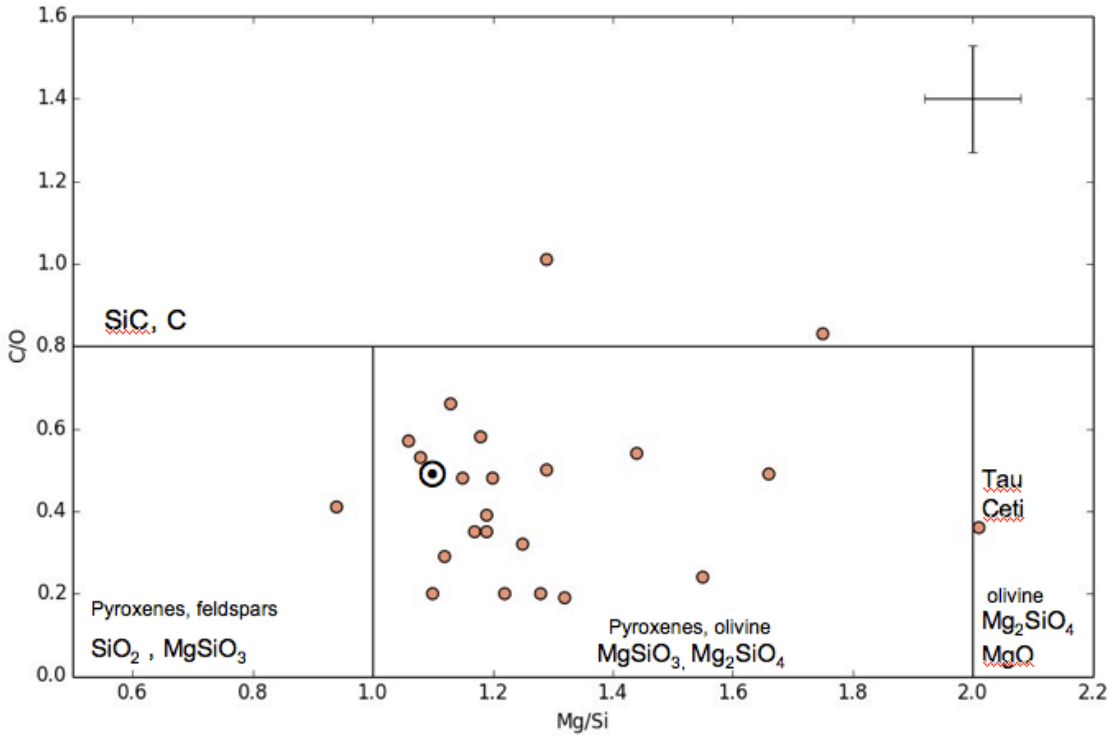

Figure 4.1: Mg/Si vs. C/O ratios for 24 planet hosts and the sun. Solar value is from Asplund et al. (2009). Average errors in upper right corner. Divisions between dominant rock forming minerals from Bond et al. (2010b); Delgado Mena et al. (2010). Planets are blue data points, and Earth mantle (pyrolite) and bulk Earth values are from McDonough & Sun (1995)

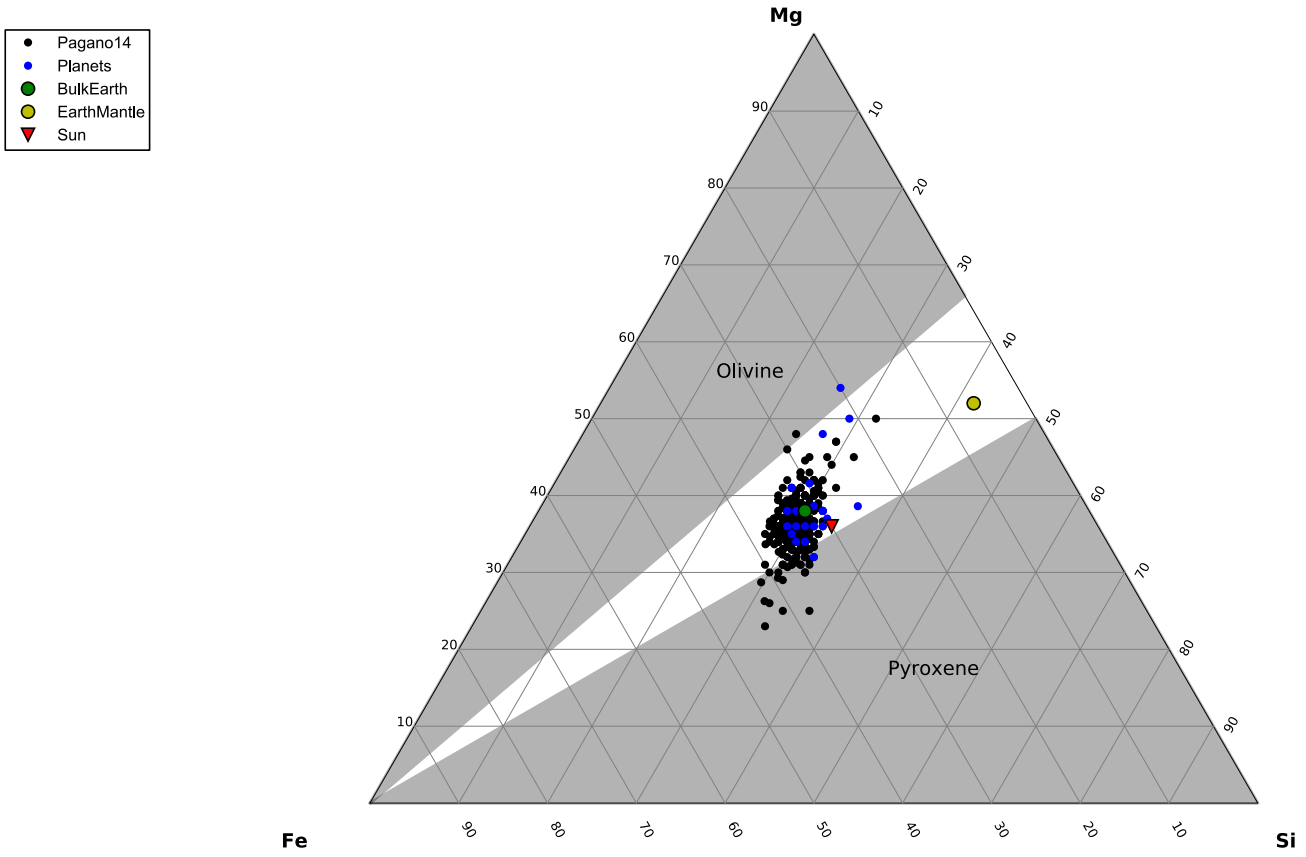

Figure 4.2: Ternary plot for Mg, Si and Fe. All abundances are unnormalized to the sun and normalized to each other so that Mg + Si + Fe = 1. Solar value is from Asplund et al. (2009) and olivine and pyroxene boundaries are from Bond et al. (2010b) Planets are blue data points.

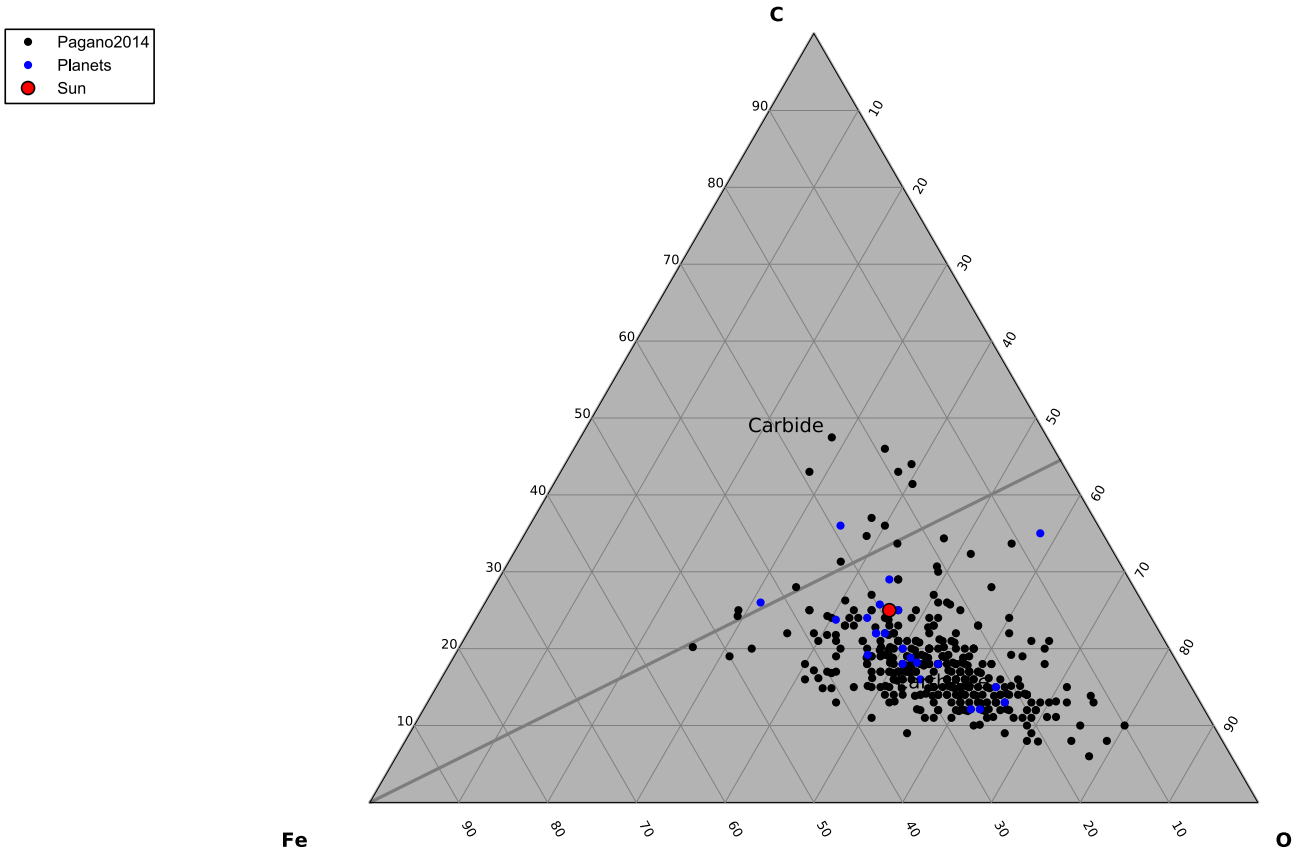

Figure 4.3: Ternary plot for C, O and Fe. All abundances are unnormalized to the sun and normalized to each other so that C + O + 10*Fe = 1. Solar value is from Asplund et al. (2009) and carbide vs. silicate line is from Bond et al. (2010b).

Chapter 5

THE EXTREME EXAMPLE OF TAU CETI

With the number of exosolar planets increasing exponentially, we are starting to believe that Earth-sized planets in their host star's habitable zone (HZ, (e.g. Kasting, Whitmire, & Reynolds, 1993; Kopparapu et al., 2013a)) should be numerous and detectable as our technology increases (Marcy et al., 2000; Gaidos, 2013; Dressing & Charbonneau, 2013; Kasting et al., 2013; Batalha et al., 2013; Petigura et al., 2013). In two decades we have progressed from having no candidate planets to having too many to practically search for detectable biosignatures. A more nuanced analysis than the location of a planet relative to the instantaneous HZ is necessary to choose among candidates. One way of conceptualizing this process is through a detectability index (DI) that accounts for the ability of a planet to host life, its ability to maintain biosignatures at a detectable level, and the observational techniques that determine what qualifies as a detectable level. The first two terms depend upon the characteristics of the host star, for example the luminosity, which determines the position of the classical HZ, and its time evolution. The majority of orbits that spend time in the habitable zone do so in the second half of a star's life. The first two terms are also determined by the characteristics of the individual planets, for example atmospheric composition and geological activity. Different atmospheres will produce different greenhouse effects, changing the position of the habitable zone boundaries. More rapid geochemical cycling may prevent biosignatures from building up to a measurable level. These factors are interdependent. Earth's biosphere took ~ 2 Gy to produce potentially detectable changes in the amount of non-equilibrium species in the atmosphere. Hence a planet that entered the HZ only a few hundred million years ago as the star gradually increased in luminosity may well be habitable and even inhabited, but

not detectable. Both the stellar and planetary properties that determine habitability and detectability for terrestrial planets depend fundamentally on chemical composition.

The determination of elemental abundances has led to the knowledge that every star has its own unique fingerprint. Variations on element to element scales exist between all stars for every element. As a community, we have begun the exploration of extreme cases, especially for the significant rock- forming elements Mg, Si, O and C (Delgado Mena et al., 2010; Bond et al., 2010b; Unterborn et al., 2013). Although stellar abundances do not correlate directly with planetary abundances, terrestrial planet simulations have been used to try and estimate the final planetary compositions (O'Brien et al., 2006; Bond et al., 2010b).

Bond et al. (2010b) found that substantial stellar enrichments could lead to planets with compositions enhanced relative to Fe in particular elements, especially for the 4 major rock-forming minerals we are considering. This diversity in bulk compositions could lead to variance in planetary mantles and core compositions of terrestrial planets (Elkins-Tanton & Seager, 2008). Since the stellar enrichments are likely primordial, it should lead to planets forming from the same enriched material Santos et al. (2001, 2003); Valenti & Fischer (2005); Bond et al. (2006). Recently there have been many discoveries and theories about carbon-rich systems (Bond et al., 2010b; **?**; **?**), with Bond et al. (2010b) finding 21 of their 60 stars having C/O ratio above 0.80, believed to be a threshold for carbon and carbide dominated planets, as opposed to solar system-like silicate dominated planets. On the other hand, there are few observations of stars with extreme Mg/Si abundances, with only a handful of stars over Mg/Si$>$1.9, and the only star over 1.9 in the Bond et al. (2010b) simulations is HD177830 (Mg/Si of 1.93). When Bond et al. (2010b) simulated planets from this initial composition, they ended up with an olivine-rich planet outside of 0.3 AU, with up to 22% wt Mg and a Mg/Si ratio of 1.71, much greater than that of Earth.

The star τ Ceti is of long-standing scientific and popular interest as a nearby (3.65 pc) reasonably sun-like G8 dwarf. The recent discovery of planet candidates around Tau Ceti (Tuomi et al., 2013) gives us an example of a nearby planetary system around a sun-like star with relatively small planets, though still on the order of Super-Earths. Two of these planets, Tau Ceti e and f, could be in a theoretical HZ. These planets were listed in a press release from the Planetary Habitability Lab at the University of Puerto Rico at Arecibo among the "nine planets most likely to host alien life". These planets are estimated to have masses of 4.29 ± 2.00 and $6.67 \pm 3.50 M_{\oplus}$ (Tuomi et al., 2013). A high profile and potentially promising system such as τ Ceti warrants a careful analysis.

In this study we evaluate properties of the system that could affect habitability and the DI from a chemical perspective, contributing to a complete and accurate characterization of the system. Section 5.1 describes new observations from the MIKE spectrograph on Magellan used to derive abundances for 23 elements. Section 5.2 discusses the possible effects of τ Ceti's Mg-rich composition on the internal dynamics and structure of terrestrial planets. New stellar models and HZ predictions using the newly determined abundances are presented in Section 5.3. The possible implications for the habitability of τ Ceti e and f are discussed in Section 5.4.

5.1 Abundance Determinations

5.1.1 Observations

The stellar spectra for Tau Ceti was taken by Paul Butler from the Carnegie Institute of Washington and was given to Arizona State University for elemental abundance analysis. The spectra were observed through the Magellan Planet Search Program, which makes use of the MIKE echelle spectrograph (Bernstein et al. 2003) on the 6.5 m Magellan II telescope. The spectra have a resolution of R 50,000 in the wavelength range 4700 Åto 7100 Å.. Only the red chip data was used for abundance

determination. Wavelength calibration was carried out by iodine absorption cell (Marcy and Butler 1992). Only F, G and K stars were used in this survey. These stars were run manually or through a pipeline to obtain stellar parameters and elemental abundances. It takes all of these stars from uncalibrated spectra all the way through the abundance finding process, starting with wavelength calibration in IDL and combining all of the orders into a single FITS file. The pipeline uses the spectral analysis program MOOG (Sneden, 1973), with a model atmosphere that is created by the program mspawn through ATLAS9(Kurucz, 1993). With the wavelength range and limitations of the spectra, this pipeline can measure up to 27 different elements, including iron, which is measured in the parameter determination.

5.1.2 Abundances

We find the stellar $T_{eff} = 5433$K and log (g) = 4.55. τ Ceti is relatively metal-poor, with $[\mathrm{Fe/H}] = -0.49 \pm 0.08$. Table 5.1 gives abundances [X/H] relative to H. Values for the absolute number ratios C/O and Mg are also provided. These ratios are taken before normalizing to any solar spectrum, and therefore represent only the composition of the host star, and are not in the typical [X/H] format which includes solar normalization. Due to the low metallicity and the spectral range used, the C/O ratio has a fairly large uncertainty. Tau Ceti has Mg/Si = 2.01 $\pm$ 0.04, much higher than Earth $Mg/Si = 1.01$(Kargel & Lewis, 1993) and the sun $Mg/Si = 1.05$(Asplund et al., 2005). The absolute abundance of Mg is higher than the sun, despite the star's low metallicity. Ca is also supersolar. The [Al/Fe] is enhanced, but the absolute abundance is slightly less than solar. The r-process element Eu has an elevated [Eu/Fe]. The pattern of r-process elements in stars is remarkably consistent with the solar pattern, even in the known extremely metal poor (EMP) stars with r-process enhancements, which are assumed to have been enriched by few or one nucleosynthesis events (Roederer et al., 2009; Beers & Christlieb, 2005;

Barbuy et al., 2011, and references therein). The exceptions are ”actinide boost” EMP stars with even further enhanced abundances of the actinide elements, including U and Th (Honda et al., 2004; Lai et al., 2008; Hayek et al., 2009; Barbuy et al., 2011).

5.2 Internal Structure and Dynamics of Mg-rich Terrestrial Planets

The estimated sizes of the exoplanets around Tau Ceti span a considerable range. These planets range in mass from 2.0 to 6.6 $M_{\oplus}$. It is considered likely that they qualify as terrestrial planets, but it is uncertain without an estimate of bulk densities. The following analysis assumes that the planets are terrestrial Super-Earths or that smaller, undiscovered terrestrial planets are present. It also assumes that Mg/Si in terrestrial planets scales roughly with Mg/Si in the star. We know from the example of Earth that there is not a 1:1 correspondence between the abundance ratios of star and planet (see Section 5.1.2), but for our solar system at least, the numbers are similar, with the terrestrial value being higher than the solar. This work speculates on the effects of the extreme Mg/Si ratio observed in τ Ceti on terrestrial planets, but would benefit from tighter constraint on the planetary compositions. Such constraints are more likely to come from models of planet assembly from a protoplanetary disk of τ Ceti's primordial composition.

Though some work has been done into establishing how much of a connection there is between planetary composition and stellar spectroscopic data (Bond et al. 2009), the stellar abundances most likely represent primordial composition (Santos et al. 2001, 2003a, 2003b, 2005; Fischer & Valenti 2005; Bond et al. 2006) and the compositions of planets can be different due to various processes occurring during formation and evolution of planets. For example, the Mg/Si ratio of Earth's upper mantle is greater by $\sim$20% than that of Sun's photosphere. Because the impact of these processes on composition is not well known, we assume that the Mg/Si ratios of the mantles of terrestrial τ Ceti planets remain similar to that of the star. While solubility of Mg may be very small for the

Table 5.1: Abundances of Tau Ceti

	Value	$\pm$
Temp	5373	43
MtVel	1.08	0.18
log(g)	4.57	
$[Fe/H]$	-0.46	0.07
$[C/H]$	-0.96	0.19
$[O/H]$	-0.54	0.08
$[Na/H]$	-0.24	0.06
$[Mg/H]$	0.15	0.02
$[Al/H]$	-0.07	0.01
$[Si/H]$	-0.29	0.04
$[S/H]$	-0.49	0.11
$[Ca/H]$	0.04	0.10
$[Sc/H]$	-0.32	0.09
$[Ti/H]$	0.16	0.08
$[V/H]$	0.16	0.05
$[Cr/H]$	-0.33	0.22
$[Mn/H]$	-0.26	0.18
$[Co/H]$	-0.21	0.04
$[Ni/H]$	-0.21	0.12
$[Cu/H]$	-0.20	0.15
$[Zn/H]$	-0.83	*
$[Y/H]$	-0.26	0.30
$[Mo/H]$	-0.18	*
$[Ba/H]$	-0.44	0.02
$[La/H]$	-0.16	*
$[Ce/H]$	0.23	*
$[Nd/H]$	-0.03	0.38
$[Eu/H]$	-0.10	*
C/O	0.36	0.21
Mg/Si	2.01	0.05

metallic iron core and some amount of Si can exist as an impurity in the core, most Mg and Si may remain in the rocky mantle.

The mantles of planets with Mg/Si $\geqslant 2$, as observed for τ Ceti, will be almost entirely made of olivine, $(Mg,Fe)_2SiO_4$, with very little or no pyroxene, $(Mg,Fe)(Al,Si)O_3$. This is in sharp contrast with the mineralogy of Earth's mantle where the proportions of these two minerals are similar to each other. Furthermore, the Mg-rich mantle could even contain ferropericlase, (Mg,Fe)O, at shallow depths. Ferropericlase exists only in the lower mantle (700–3000 km depths) in Earth. If the Mg-rich terrestrial exoplanets have surface volcanism through (partial) melting of the deep mantle similar to Earth, such as some hot spots and mid oceanic ridges, the different Mg/Si ratio will result in very different magnitude of melting and the composition of melts. It is notable that some deep melting processes are believed to be responsible for the formation of the crust on Earth.

If the composition remains similar throughout the mantle, the deeper mantle may be composed mainly of Mg-silicate perovskite and ferropericlase, similar to the Earth. However, the content of ferropericlase may be comparable to that of Mg-silicate perovskite, $(Mg,Fe)(Al,Si)O_3$, unlike the Earth's lower mantle where Mg-silicate perovskite is dominant (70%). It has been predicted that Mg-silicate perovskite may breakdown into oxides (ferropericlase and silica) at 1 TPa (Umemoto et al., 2006). However, the known terrestrial planet candidates around τ Ceti may not have sufficient mass to reach this pressure. Therefore, except for the shallow depths (< 600 km), the mantles of these large terrestrial planet candidates should be composed mainly of the phases of the Earth's lower mantle (perovskite and ferropericlase) but with different proportions.

The increased amount of ferropericlase may have profound impact on the mantle dynamics. For the lower mantle, an increase in ferropericlase expected from the elevated Mg/Si ratio ($\simeq 2$) could decrease the viscosity of the lower mantle by two orders of

magnitude (Ammann et al., 2011). The severe decrease in the viscosity of the mantle could result in much more vigorous convection in the mantle, potentially affecting surface tectonics of the planet. In addition, τ Ceti's [Eu/Fe] =0.39, significantly higher than solar. The values of [U/Fe] and [Th/Fe] are likely to scale similarly (see Section 5.1.2). This enhancement suggests that there is significantly more potential for radioactive heating of the interior. The combination of enhanced heating and reduced mantle viscosity may well have an important impact on the level of geological activity on a planet 3Gy older than Earth. [1]

5.3 Habitable Zone

We evaluate the astrobiological potential of candidate exoplanets in the Tau Ceti system by investigating habitable zone (HZ) boundaries defined by theoretical stellar evolution tracks coupled with the radiative-convective atmospheric models of Kopparapu et al. (2013a,b). Evolutionary tracks were created with the TYCHO code (Young & Arnett, 2005). TYCHO is a 1D stellar evolution code with a hydrodynamic formulation of the stellar evolution equations. It uses OPAL opacities (Iglesias & Rogers, 1996; Alexander & Ferguson, 1994; Rogers & Nayfonov, 2002). The code uses a combined OPAL and Timmes equation of state (HELMHOLTZ) (Timmes & Arnett, 1999; Rogers & Nayfonov, 2002), gravitational settling (diffusion) (Thoul, Bahcall, & Loeb, 1994), general relativistic gravity, time lapse, and curvature, automatic rezoning, and an adaptable nuclear reaction network with a sparse solver. A 177 element network terminating at ^{74}Ge is used throughout the evolution. The network uses the latest REACLIB rates (Rauscher & Thielemann, 2000; Angulo et al., 1999; Iliadis et al., 2001; Wiescher et al., 2006), weak rates from Langanke & Martìnez-Pinedo (2000), and screening from Graboske et al. (1973). Neutrino cooling from plasma processes and the

[1] Section analysis and partial text by S-H. D. Shim

Urca process is included. Mass loss is included but is trivial for a $1M_{\odot}$ main sequence star. (Heightened early mass loss seen in some young stars (Wood et al., 2005) is not included. This may play a role in early habitable zone evolution and be relevant to the "faint young sun" paradox). It incorporates a description of turbulent convection (Meakin & Arnett, 2007; Arnett, Meakin, & Young, 2009; Arnett, Meakin & Young, 2010; Arnett & Meakin, 2011) which is based on three dimensional, well-resolved simulations of convection sandwiched between stable layers, which were analyzed in detail using a Reynolds decomposition into average and fluctuating quantities. It has no free parameters to adjust, unlike mixing-length theory (MLT). We used an initial mass of 0.784 $M_{\odot}$ (Tang & Gai, 2011). The initial composition has the elemental ratios derived in Section ?, scaled so that when diffusion is included the modeled surface composition matches the abundances at the best-fit model age. Tracks were computed to the end of its main sequence lifetime since it will be some time before the post-MS evolution becomes relevant. In order to find the best-fit age, we step through the evolutionary track and evaluate:

$$\chi^2 = \frac{(R_{mod}R_{obs})^2}{\sigma_R^2} + \frac{(L_{mod}L_{obs})^2}{\sigma_L^2} \tag{5.1}$$

where R_{mod} and R_{obs} are the model and observed radii, L_{mod} and L_{obs} are the model and observed luminosities, and σ_R and σ_L are the observational errors in radius and luminosity. The uncertainty in age is given by the ages at which the evolutionary track crosses the observational error box. The adopted radius is $0.7817R_{\odot}$, which is the mean of the interferometrically and asteroseismological radii ($0.773\pm0.024R_{\odot}$ and $0.07916\pm0.016R_{\odot}$, respectively) determined by (Tang & Gai, 2011). For our error in R we use the error of the interferometrically defined radius, which encompasses the range of uncertainty of the asteroseismological value. This provides us with a conservative estimate of the age uncertainty. We adopt $L = 0.504L_{\odot}$ (Teixiera, et al., 2009; Pijpers, 2003; Pijpers et al., 2003). Tang & Gai (2011) find $\log g \simeq 4.53$ using their

asteroseismological analysis, similar to our spectroscopically-determined $\log g = 4.51$. The age of the system from this analysis is $7.63^{+0.87}_{-1.5}$Gy.

In this work we evaluate the classical "liquid water" habitable zone around τ Ceti, where liquid water is stable at the planetary surface given reasonable assumptions about the planetary atmosphere. Luminosity of any given star changes over the course of its lifetime, and thus the boundaries of the continuously habitable zone would change accordingly. The stellar parameters of τ Ceti are relatively well determined, so we can predict the evolution of the star itself with a fair degree of confidence. From this simulation we can predict the location of the inner and outer edges of the habitable zone as a function of time, and ask the question of whether a planet would be in the habitable zone long enough to harbor potential life. Locations for the inner and outer edges of the habitable zone are calculated using the stellar luminosity and temperature parameterizations from Kopparapu et al. (2013a,b). Kopparapu et al. (2013a) provide updated 1-D radiative-convective climate models (originally from Kasting, Whitmire, & Reynolds (1993)) to obtain new estimates for habitable zone widths around F, G, K, and M-type stars. Their paper examines potential habitability in terms of stellar flux incident on a planet, as opposed to the equilibrium temperature. This removes the dependence on albedo, which varies depending upon the parent star's spectral type.

Rayleigh scattering by water vapor in the atmosphere of exoplanets with new scattering coefficients is included. The models assume Earth-mass planets with water- (corresponding to the inner HZ edge) or CO_2 (corresponding to the outer HZ edge) dominated atmosphere. Both inner and outer edge calculations are based on "inverse climate modeling" where the planetary surface temperature is specified, and the models are used to determine the solar flux needed to sustain that given temperature. They also find that near the inner edge of a habitable zone, there is no clear distinction between runaway greenhouse effects and water loss limits for stars with effective temperatures less

than 5000 K. One potential issue is that the τ Ceti planet candidates are all super-Earths. Models of planets with higher masses and earth and thicker atmospheres are discussed, but parameterizations are not provided. For the cases discussed the edge of the habitable zone moves by at most a few percent in radius, however, so for the present we adopt the Kopparapu et al. (2013a) parameterizations.

Figure 5.1 shows the inner and outer radii of the habitable zone for the cases in Table 3 of Kopparapu et al. (2013a,b). The orbits of the putative planets are indicated by the horizontal dashed lines. The vertical line is the best-fit age of the system at 7.63 Gy with the age uncertainty indicated by the gray box. The solid lines show the inner edge of the habitable zone for, in order of distance from the star, the Recent Venus, Runaway Greenhouse, and Moist Greenhouse cases. The outer edge is shown by the dotted lines for the Maximum Greenhouse and Early Mars cases. After the pre-main sequence the radii of the habitable zone limits increase monotonically with time as the stellar luminosity increases. The three inner candidates are well inside the habitable zone even for the most optimistic prediction. Candidates e and f are potentially interesting marginal cases. For the Recent Venus case (assuming that Venus moved out of its habitable zone 1 Gy ago) planet e is reaching the end of its habitable lifetime. At the best-fit age of τ Ceti it is right at the edge of the habitable zone. In a future of direct observations from space-based interferometers/occulters this world has the potential to place constraints on climate models. For the theoretically-motivated greenhouse cases candidate e is always interior to the habitable zone. Candidate f is potentially more promising, at least judging by the theoretical climate models. The outer edge of the habitable zone is approaching the position of planet f. Given the uncertainty in the stellar age, arising largely from the observational uncertainty in the star's luminosity, candidate f is between 0 and 1.5 Gy from entering the habitable zone defined by the Early Mars case (assuming mars was habitable 3.8 Gy ago). The range is extended by $\sim$1 Gy for the Maximum Greenhouse

case. Even in the most pessimistic case, the planet will have about 7 Gy of habitable lifetime until the end of the main sequence, plus additional time while the star traverses the subgiant branch. From a detectability standpoint, however, f is a poor candidate. At best, the planet has been in the HZ for $<<$1Gy under these assumptions. Cases similar to f where a planet enters the habitable zone in the latter part of the star's life are more common than planets that have been in the habitable zone since early times. The habitable zone becomes wider when the star's effective temperature decreases along the main sequence. This serves as a reminder that the present "habitability" of a planet does not necessarily indicate that it is a good candidate for detecting biosignatures. The temporal evolution of the system must be taken into account.

The general characteristics of the τ Ceti habitable zone are also interesting in the event that other planets, perhaps closer to the mass of Earth, are discovered. Table 5.2 summarizes the range of orbits with given durations of habitability, assuming a stellar age of 7.63 Gy. We find ranges for orbits that are continuously habitable for the entire main sequence, orbits that remain habitable for at least 4 Gy (the length of time required for metazoan life to develop on earth), and orbits that are currently habitable and have been so for at least 2 Gy. This last case reflects the approximate amount of time required for life to make potentially detectable changes in the composition of Earth's atmosphere (in particular the presence of free oxygen, methane, and nitrous oxide). Two cases are tabulated, a conservative case for the minimum size habitable zone using the Moist Greenhouse and Maximum Greenhouse prescriptions, and an optimistic case using the Recent Venus and Early Mars climate models. For the conservative case there are *no* continuously habitable orbits. In this dire situation the maximum duration of habitability is a mere 16 Gy. Orbits from 0.8 to 1.25 AU remain habitable for 10 Gy, as long as the main sequence lifetime of the sun. Of the known candidates, the best case for a planet which has detectable atmospheric signatures of an active biota is τ Ceti e. The most

Table 5.2: Habitable Zone Properties

	Conservative	Optimistic
	AU	
Currently Habitable	0.73 - 1.28	0.55 - 1.32
Continuously Habitable Range		0.84 - 1.1
4 Gy Habitable Range	0.67 - 1.52	0.5 - 1.6
Habitable $\leqslant -2$Gy to Present	0.73 - 1.18	0.55 - 1.25

favorable location for a hypothetical sixth planet that has developed atmospheric biosignatures is the 0.45 AU range between 0.73 and 1.18 AU.

5.4 Conclusions

The τ Ceti system has been the object of speculation about extraterrestrial life in both the popular imagination and the scientific literature for decades due to its proximity to Earth and the star's sun-like characteristics. The recent discovery of Super-Earth mass planet candidates has further increased interest in the system. Two of the candidates, τ Ceti e and f, are near the edges of the theoretical habitable zone. These worlds could potentially be high priority candidates for observations by a future direct detection mission looking for biosignatures. A more thorough analysis of the system is therefore warranted. We specifically examine the contributions of chemical composition to the likelihood of e and f being habitable and detectable.

Two main considerations turn out to be important for the case of τ Ceti. First, the star has a very high Mg/Si=2.01 and above solar Eu/Fe. The Mg/Si ratio is near the boundary at which a planetary mantle would be expected to transition from a mixed olivine/pyroxene mineralogy to a very olivine- dominated composition (with perovskite

and ferropericlase possibly dominating at depth). The viscosity of the mantle could be much lower than earth. Coupled with an enhanced abundance of actinide elements contributing to radiogenic heating of the interior, planets around τ Ceti may have much more vigorous and long-lived mantle convection, which would in turn affect the activity of surface processes and (bio)geochemical cycling. This could be an essential point when considering the habitability and detectability of a planet 7.6 Gy old. While this could benefit the habitability of τ Ceti's planets, it could interfere with the DI of a younger planet. Faster geochemical cycling could impede the buildup of biologically produced non-equilibrium chemical species in the planet's atmosphere. Time dependent analyses of planetary evolution are required.

Second, the time and composition dependent modeling of the star provides a better estimate of not only the planets' habitability potential now, but their habitability history. Given the HZ prediction used herein, planet e is very near the edge of the HZ for very optimistic assumptions. For more conservative cases it lies interior to the HZ at all times. Planet f highlights the time-dependent nature of detectability. The planet is near the edge of the predicted HZ. For the most optimistic case it has just entered, while for conservative cases it is still just outside. Even though it will likely see more than 7 Gy of continued habitability as the star ages, as far as we can trust existing climate models it has been in the HZ at most much less than 1 Gy. Earth required $\sim$2 Gy before the biota modified the atmosphere sufficiently to possibly detectable from another stellar system. Even if f's habitability potential is high, its detectability index is low.

In conclusion, the known candidate planets around τ Ceti are not as promising targets for finding life as they appear at first analysis. They do, however, show the power of full characterization of exoplanetary systems, in particular their chemical composition, for choosing targets for future missions to detect life.

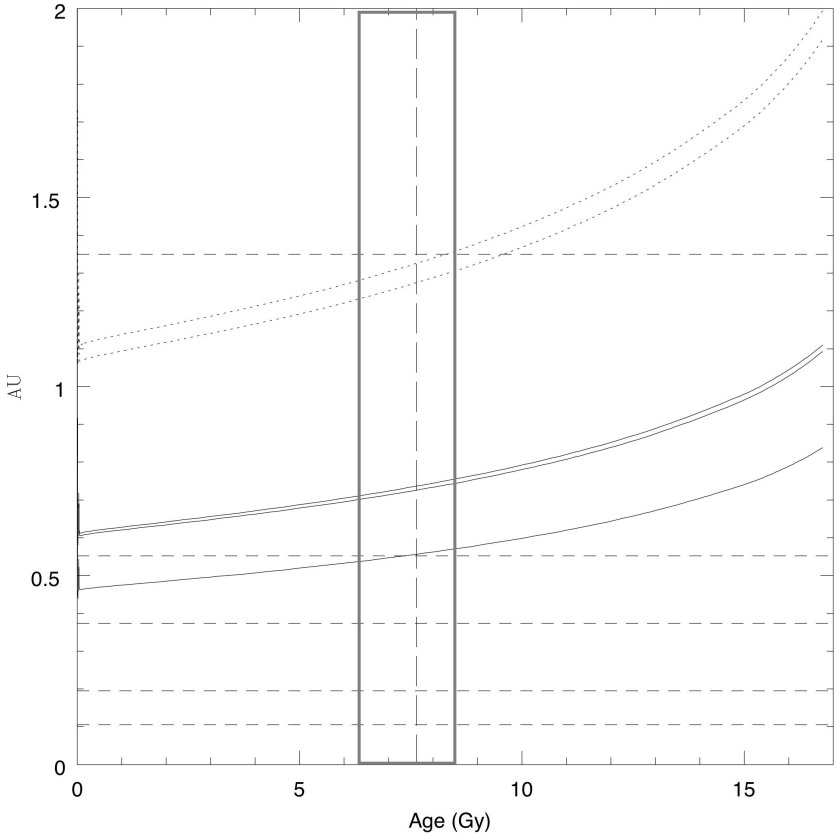

Figure 5.1: Inner and outer radii of the habitable zone of τ Ceti for the cases in Table 3 of Kopparapu et al. (2013a,b). Solid lines show the inner edge of the habitable zone for, in order of distance from the star, the Recent Venus, Runaway Greenhouse, and Moist Greenhouse cases. The outer edge is shown by the dotted lines for the Maximum Greenhouse and Early Mars cases. The orbits of the putative planets are indicated by the horizontal dashed lines. The vertical line is the best-fit age of the system at 7.63 Gy with the age uncertainty indicated by the gray box. Candidate e is at the edge of the habitable zone for the Recent Venus case, near the end of its potential habitability. Candidate f is near the outer edge of the calculated habitable zone. As the habitable zone moves outward as the stellar luminosity increases, this planet is likely to enter the habitable zone and spend at least 7 Gy inside.

Chapter 6

CONCLUSIONS

Part of the goal of observing stellar abundances and using them to theorize on exosolar planet compositions is to understand the habitability of our solar neighborhood. One way to do that is not only think about what is required of a planet for the survival of life, but also what detectables could lead us to believe that life exists on an exoplanet. In Chapter 1 we discussed the concept of the Detectability Index (DI) and how it could help us begin to narrow our search for life outside of our solar system. The best insight we have into the environment that could create new habitable planets is looking at the stars that those planets would be orbiting. My dissertation delved into how the chemical elements distribute themselves amongst our neighboring stars, and what affect those individual abundances could have on planetary systems.

The variability in stellar abundances has been shown in Chapter 2, including the idea that outliers could extend into unusual compositional territory. Chapter 3 presents a high precision, large, and comprehensive abundance survey for 458 planets. Chapter 4 discusses the 24 planet host stars in that study, and how varying the elemental ratios of C, O, Mg, Si, and Fe (and to a lesser extent Al and Ca) could create unusual planetary compositions. This shows that there is a treasure trove of possible planetary starting materials. This should lead us to fascinating new thought processes about how and what worlds outside of our solar system could exist. In Chapter 5, we looked at one specific example of an extreme compositional system, τ Ceti. The very high Mg/Si abundances of that star could prove to house strange and unthought of planets, whose mineralogy would greatly differ from Earth's. Although this makes τ Ceti extremely interesting and unique, it also means that it's habitability could suffer. Also, the habitable zone that help us

constrain the possibility for liquid water can be drastically altered by the stellar evolution of individual stars. The presence of abundant elements C and O will change the distance and lifetime of such habitable zones. A planet such as τ Ceti, whose distance from Earth and possible planetary configuration could lead us to put it on a list of possible planetary targets, becomes a far less tantalizing prospect when considering how short it could have a continuous habitable zone.

The planet itself forms from the same material and composition that we see in stars. This presolar disk composition would be the starting point for the formation of planets. Planetary properties are an important part of the survival of life on an exoplanet and can be roughly deduced from stellar elemental abundances. This includes the mineralogy of possible planets around unusual stars as discussed, but also the presence of radiogenic heating from elements such as Eu and Ba, which could act as proxies for important radioactive elements such as U and Th. The exoplanetary mineralogy could have an impact on crustal composition and strength, the vigor of convection in the planetary interior, tectonics, volcanism, and other geophysical properties of planets. As well, there are biological effects from possible combinations of planetary abundances such as nutrient availability. The planetary volatile content should be entirely derived from the starting materials at planetary formation. Not just from those volatiles available in protoplanetary phases, but also those volatiles that end up in comets. The volatile content of a planet could determine whether it has an atmosphere, ocean, or biogeochemical cycling such as the carbon silicate cycle.

Another key to the future of stellar abundances is developing better techniques to normalize the field. Currently, different groups us their own line lists, spectra synthesis program (such as MOOG) and calculate their errors in different ways. This leads to the inability to compare results of different groups. We are currently running an experiment to try and pinpoint the reason for spread amongst abundance finding groups, such as that

found in **?**. Having 4 separate abundances finding groups analyze the same data under different scenarios, such as using the same line list and stellar parameters, we will make assessments as to how to improve the reliability of the field amongst different groups (Hinkel & Pagano, in prep).

Although the wavelength ranged used in my study makes excellent use of the elemental lines available in the optical spectra, there are other important bioessential and major rock forming elements that are not being measured. Phosphorus, nitrogen, and potassium could be useful and important when trying to determine the habitability and possible planetary mineralogy of stellar systems. Very few stars have known phosphorus abundances, due to it's primary spectral lines occurring in the near infrared. Caffau et al. (2011) observed P in twenty stars using the CRIRIES spectrograph on the Very Large Telescope (VLT). The major P lines are between 10500 and 10820 Å and therefore outside of the optical spectrographs. ARIES and MAESTRO on the MMT in Arizona both do not cover wavelengths in the 10,000 Å but could be used for the potassium lines in the 7,600 Å range. However, both the P and K lines are very weak and would require stars with high metallicity (> 0) to try and measure the abundances of these elements.

Stellar abundances can also be used to understand the connection between binary stars and possible planets in their system. If the abundances of binary stars are similar, it could help us understand if they formed from the same material, as well how this could affect the condensation temperatures around these stars with respect to planetary formation (Liu et al., 2014; Teske et al., 2013). Using chemical abundances could help gain insight into planetary densities. As mentioned in the discussion of 4.2, the abundances of Mg, Si, and Fe could help give insight into the core size of a planet. When combined with planets of known radius and mass, the density of the planet can be combined with the stellar abundances to try to understand the mineralogical make-up of exoplanets.

From the statistics presented and the new abundances calculated, it should become

obvious that our sun, and Earth, are one of a kind. However, there should be enough stars that are close enough in elemental abundances to the sun that a planet could form the right distance away from its star and be considered Earth-like. Our attempts to discover and observe these similar planets should lead us to discover just as many unusual ones, with elemental ratios that create distinctly new planets. So we must keep our imaginations running and begin to leave our Solar System-centric norms behind and begin to explore the possibilities that the vast differences around us present.

REFERENCES

Alexander, D.R. and Ferguson, J.W. 1994, ApJ, 437, 879

Allegre, C.J., Poirier, J.P., Humler, E., Hofmann, A.W. 1995 , Earth and Planetary Science Letters 134, 515

Ammann, M. W., Brodholt, J. P., Dobson, D. P. 2011, E&PSL, 302, 393

Anders E., & Grevesse N. 1989. Geochim. Cosmochim. Acta 53:197214

Angulo, C., Arnould, M., Rayet, M., Descouvemont, P., Baye, D., Leclercq-Willain, C., Coc, A., Barhoumi, S., Aguer, P., Rolfs, C., Kunz, R., Hammer, J. W., Mayer, A., Paradellis, T., Kossionides, S., Chronidou, C., Spyrou, K., DeglInnocenti, S., Fiorentini, G., Ricci, B., Zavatarelli, S., Providencia, C., Wolters, H., Soares, J., Grama, C., Rahighi, J., Shotter, A., and Lamehi Rachti, M. 1999, Nucl. Phys. A, 656, 3

Antia, H.M. & Basu, S. 2011, JPhCS, 271, 2034

Arlandini, C., Käppeler, F., & Wisshak, K. 1999, ApJ, 525, 886

Arnett, David 1996, *Supernovae and Nucleosynthesis*, Princeton: Princeton University Press

Arnett, D., Meakin, C., & Young, P. 2010, ApJ, 710, 1619

Arnett, D., Meakin, C., and Young, P. A. 2009, ApJ, 690, 1715

Arnett, D. and Meakin, C. 2011, ApJ, 733, 78

Asplund, Martin, Grevesse, Nicolas, Sauval, A. Jacques, Scott, Pat 2009 Annual Reviews of Astronomy and Astrophysics, 47, 481:522

Asplund, M., Grevesse, N., & Sauval, A. J. 2005, in ASP Conf. Ser. 336, Cosmic Abundances as Records of Stellar Evolution and Nucleosynthesis, ed. T. G. Barnes, III & F. N. Bash (San Francisco, CA: ASP), 25

Bahcall, J.N., Pinsonneault, M.H., & Basu, S. 2001, ApJ, 555, 990

Bahcall, J.N., Basu, S., & Serenelli, A.M. 2005, ApJ, 631, 1281

Bahcall, J.N., Basu, S., Pinsonneault, M., & Serenelli, A.M. 2005, ApJ, 619, 1049

Barbuy, B. & Erdelyi-Mendes, M. 1989, A&A 214, 239

Barbuy, B. Spite, M. Hill, V. Primas, F. Plez, B. Cayrel, R. Spite, F. Wanajo, S. Siqueira Mello Jr., C. Andersen, J. Nordstrom, B. Beers, T. C. Bonifacio, P. Francois, P. and Molaro, P. 2011, A&A, 534, 60

Batalha et al. 2013, ApJS 204, 24B

Beers, T. C., & Christlieb, N. 2005, ARA&A, 43, 531

Bell, R.A., Branch, D., Upson, W.L., II. 1976, JQSRT, 16, 177

Bensby, T., Feltzing, S., Lundstrm, I., & Ilyin, I. 2005 A&A, 433, 185

Bond, J.C. et al. 2006, MNRAS, 370, 163

Bond, J.C. et al. 2008, ApJ, 682, 1234

Bond, J. C., Lauretta, D. S., OBrien, D. P 2010a, Icarus, 205, 321

Bond, J. C., OBrien, D. P., Lauretta, D. S. 2010b, ApJ, 715, 1050

Borucki, William J et al. 2010 ApJ 713, 126

Boyarchuk, A.A. & Lyubimkov, L.S. 1985, BCAO, 66, 119

Bubar, E. & King, J. 2010 AJ, 140, 293

Caffau, E., Ludwig, H.G., Malherbe, J.M., Bonifacio, P., Steffen, M., & Monaco, L. 2013 A&A, 554, 126

Caffau, E., Bonifacio, P., Faraggiana, R., & Steffen, M. 2011, arXiv:1107.2657v1

Carbon, D.F., Barbuy, B., Kraft, R.P., Friel, E.D., & Suntzeff, N.B. 1987, PASP, 99, 335

Carter-Bond, J.C., OBrien, D.P. & Raymond, S.N. 2012 Astrophys. J. 760:44.

Clegg, R.E.S. 1977, MNRAS, 181, 1C

Clegg, R.E.S., Tomkin, J., & Lambert, D.L. 1981, ApJ, 250, 262

Cuhna, K. & Lambert, D.L. 1992, ApJ, 399, 586.

Cuhna, K., Smith, V.V., & Lambert, D.L. 1998, ApJ, 493, 195.

Däppen, W. 2011 Contrib. Plasma Phys. 51, 328

De Silva, G. M. et al. 2006, ApJ, 151, 455

de Koker, N., Karki, B. B., Stixrude, L. 2013, E&PSL, 361, 58

Delgado Mena, E., Israelian, G., González Hernández, J.I., Bond, J.C., Santos, N.C., Udry, S., & Mayor, M. 2010, ApJ, 725, 2349

Denisenkov, P.A. & Denisenkova, S.N. 1990, SvAL, 16, 275

Dressing, C.D. & Charbonneau, D. 2013 ApJ 767, 95D

Edvardsson, B., Andersen, J., Gustafsson, B., Lambert, D.L., Nissen, P.E., & Tomkin, J. 1993, ApJ, 275, 101

Elkins-Tanton, L.T. & Seager, S. 2008, ApJ 688, 628

Ellinger, C., Young, P.A., Desch, S.J. 2010, ApJ, 725, 1495

Ellinger,CarolaI., Young,PatrickA., Fryer,ChristopherL., & Rockefeller,Gabriel 2012 ApJ 755:160-194.

Fabbian, D., Asplund, M., Barklem, P.S., Carlsson, M., & Kiselman, D. 2009 A&A, 500, 1221

Feltzing, S., & Gustafsson, B. 1998, A&AS, 129, 237

Fortney, J. J. 2012, Astrophys. J. Lett., 747, L27+

Gaidos, E. 2013, ApJ 770, 90G

Galazutdinov, G. A. 1992, Special Astrophysical Observatory preprint, 92, 2

Gilli, G. , Israelian, G., Ecuvillion, A. Santos, N.C., & Mayor, M. 2006 A&A 449, 723

Gonzalez, G. 1997, MNRAS, 285, 403

González Hernández, J.I., Israelian, G., Santos, N.C., Sousa, S., Delgado-Mena, E., Neves, V. & Udry, S. ApJ, 720, 1592

Goriely, S.; Chamel, N.; Janka, H.-T.; Pearson, J. M. 2011 A&A 531, 78

Graboske, H. C., Dewitt, H. E., Grossman, A. S., and Cooper, M. S. 1973, ApJ, 181, 457

Gratton, R.G. 1985, A&A, 148, 105G.

Gratton, R.G. & Ortolani, S. 1986, A&A, 169, 201

Gratton, R.G., & Sneden, C. 1988, A&A, 204,193

Gratton, R.G., & Sneden, C. 1991, A&A 241, 501

Grevesse, N., Asplund, M., & Sauval, A. J. 2007, Space Sci. Rev., 130, 105.

Grevesse, N., & Sauval, A. J. 1998, Space Sci. Rev., 85, 161.

Grocholski, B. Shim, S.-H. and Prakapenka. V.B. 2013, J.Geophys.Res., (unpublished data).

Hayek, W., Wiesendahl, U., Christlieb, N., et al. 2009, A&A, 504, 511

Helfer, H. L., Wallerstein, G., & Greenstein, J. L. 1959, ApJ, 129, 700

Hinkel, N. 2012, PhD Thesis

Hinkel, N. & Pagano, M.D. In prep.

Hirose, K., Takafuji, N., Sata, N., and Ohishi, Y. 2005, Earth Planet.Sc.Lett., 237:239251.

Honda, S., Aoki, W., Kajino, T., et al. 2004, ApJS, 152, 113

Huss, G. R., Meyer, B. S., Srinivasan, G., Goswami, J. N. & Sahijpal, S. 2009 Geochim. Cosmochim. Acta 73:4922-4945.

Iben, I. 1964, ApJ, 69, 545

Iben, I. & Renzini, A. 1983, ARA&A, 21, 271

Iglesias, C.A., & Rogers, F.J. 1996, ApJ, 464, 943.

Iliadis, C., D'Auria, J. M., Starrfield, S., Thompson, W. J., and Wiescher, M. 2001, ApJS, 134, 151

Isobe, Takashi, Feigelson, Eric D., Akritas, Michael G., & Babu, Gutti Jogesh 1990, ApJ, 364, 104

Israelian, G., Santos, N. C., Mayor, M., & Rebolo, R. 2003, A&A, 405, 753

Kargel, J. S., & Lewis, J. S. 1993, Icarus, 105, 1

Kasting, J.F., Kopparapu, R., Ramirrz, R.M., & Harman, C. 2013 arXiv:1312.1328

Kasting, J. F., Whitmire, D. P., and Reynolds, R. T. 1993, Icarus, 108, 108

Kopparapu, Ravi Kumar; Ramirez, Ramses; Kasting, James F.; Eymet, Vincent; Robinson, Tyler D.; Mahadevan, Suvrath; Terrien, Ryan C.; Domagal-Goldman, Shawn; Meadows, Victoria; Deshpande, Rohit 2013, ApJ, 765, 131

Kopparapu, Ravi Kumar; Ramirez, Ramses; Kasting, James F.; Eymet, Vincent; Robinson, Tyler D.; Mahadevan, Suvrath; Terrien, Ryan C.; Domagal-Goldman, Shawn; Meadows, Victoria; Deshpande, Rohit 2013, ApJ, 770, 82

Kurucz, R. 1993, ATLAS9 Stellar Atmosphere Programs and 2 kms?1 grid. Kurucz CD-ROM No. 13 (Cambridge, Mass.: Smithsonian Astrophysical Observatory), 13

Lai, D. K., Bolte, M., Johnson, J. A., et al. 2008, ApJ, 681, 1524

Laird, J.B. 1985, ApJ, 289, 556

Lambert, D.L. & Ries, L.M. 1981, ApJ, 248, 228

Langanke, K. and Martìnez-Pinedo, G. 2000, Nucl. Phys. A, 673, 481

Langer, G.E., Hoffman, R. & Sneden, C. 1993, PASP, 105, 301

Leep, E.M. & Wallerstein, G. 1981, MNRAS, 196, 543

Liu, F., Asplund, M., Ramirez, I., Yong, D., & Melendez, J. 2014, arXiv:1404.2112

Limongi, M., & Chieffi, A. 2006, ApJ, 647, 483

Lodders, K., Palme, H., & Gail, H. 2009, Landolt-Bornstein, New Series, Astronomy and Astrophysics. Berlin: Springer.

Maeda, K., Rpke, F. K., Fink, M., Hillebrandt, W., Travaglio, C., & Thielemann, F.-K. 2010, ApJ, 712, 624

Magkotsios, G., Timmes, F.X., Hungerford, A.L., Fryer, C.L., Young, P.A., & Wiescher, M. 2010, ApJS, 191, 66

Madhusudhan,N. Lee, K.K.M. andMousis, O. 2012 Astrophys.J.Lett., 759:L40.

Marcy G. W., Butler R. P., 1996, ApJ, 464, L147

Marcy, G., Butler, P. R., Fischer, D. A., & Vogt, S. S. 2000, in ASP Conf. Ser. 213, Bioastronomy 99, ed. G. Lemarchand & K. Meech (San Francisco, CA:ASP), 85

Mayor, M., & Queloz, D. 1995, Nature, 378, 355

McDonough, W. F., & Sun. 1995, Chemical Geology, 120, 223

Meakin, C. A. and Arnett, D. 2007, ApJ, 667, 448

Meléndez, J., Asplund, M., Gustafsson, B., & Yong, D. 2009 ApJ, 704, 66

Michaud, G., Richard, O., Richer, J., & Van den Berg, D. A. 2004, ApJ, 606, 452

Mishenina, T. V., Soubiran, C., Bienaymè, O., korotin, S. A., Belik, S.I., Usenko, I.A., and Kovtyukh, V.V. 2008, A&A, 489, 923

Mowlavi, N., Eggenberger, P., Meynet, G., Ekström, S., Georgy, C., Maeder, A., Charbonnel, C., & Eyer, L. 2012, A&A, 541A, 41

Mussack, K. & Däppen, W. 2011 ApJ, 729, 96

Neves, V., Santos, N.C., Sousa, S.G., Correia, A.C.M., & Israelian, G. 2009, A&A 497, 563

Nissen, P.E. 2013 A&A, 552, 73

OBrien, D. P., Morbidelli, A., & Levison, H. F. 2006, Icarus, 184, 39

Pan, L., Desch, S. J., Scannapieco, E. & Timmes, F. X. 2012 Ap.J. 756:102-122.

Peterson, R.C., Sneden, C. 1978, ApJ, 225, 913

Peterson, R.C. 1981, ApJ, 244, 989.

Peterson, R.C., Kurucz, R.L. & Carney, B.W. 1990, ApJ, 350, 173

Petigura, E.A. & Marcy, G.W. 2011, ApJ, 735, 41

Petigura, E.A, Howard, A.W. & Marcy, G.W. 2013 Proceedings of the National Academy of Sciences, 110, 48, pp. 19273-19278

Pijpers, F. P. 2003, A&A, 400, 241

Pijpers, F. P., Teixeira, T. C., Garcia, P. J., Cunha, M. S., Monteiro, M. J. P. F. G., & Christensen-Dalsgaard, J. 2003, A&A, 406, L15

Prantzos, N. 2008, Stellar Nucleosynthesis, EAS Publications Series Vol. 32, 311

Ramírez, I., Allende Prieto, C., & Lambert, D.L. 2007 A&A 465, 271

Rauscher, T. and Thielemann, F.-K. 2000, Atomic Data and Nuclear Data Tables 75, 1

Reddy, B. E., Tomkin, J., Lambert, D. L., & Allende Priesto, C. 2003 MNRAS 340, 304

Ricolleau, A.Fiquet, G. Addad, A. Menguy, N. Vanni, C. Perrillat, J.-P. ,Daniel, I.,Cardon, H.,and Guignot, N. 2008, Am.Mineral., 93:144153.

Ringwood, A.E. Advances in Earth Science., pp. 287-356, MIT Press, 1966.

Roederer, I. U., Kratz, K.L., Frebel, A., et al. 2009, ApJ, 698, 1963

Rogers, F.J., Swenson, F.J., & Iglesias, C.A. 1996, ApJ, 456, 902

Rogers, F.J. & Iglesias, C.A. 1998, SSR, 85, 61

Rogers, F.J. & Nayfonov, A. 2002, ApJ, 576, 1064

Santos, N. C., Israelian, G., & Mayor, M. 2001, A&A, 373, 1019

Santos, N. C., Israelian, G., Mayor, M., Rebolo, R., & Udry, S. 2003, A&A, 398, 363

Schönrich R., & Binney, J. 2009 MNRAS, 396:203-222.

Sen, S. Widgeon, S.J. Navrotsky, A. Mera, G., Tavakoli, A., Ionescu, E. and Riedelc, R. 2013 Proc Natl Acad Sci, 110(40): 15904

Shetrone, M.D. 1996, AJ, 112, 1517

Sneden, C. 1974, ApJ, 189, 493S

Sneden, C. A. 1973, PhD thesis, University of Texas, Austin, Texas

Sousa, S. G., Santos, N. C., Israelian, G., Mayor, M., & Monteiro, M. J. P. F. G. 2007, A&A, 469, 783

Sousa, S. G., Santos, N. C., Israelian, G., Mayor, M., & Monteiro, M. J. P. F. G. 2007, A&A, 469, 783

Soubrian, C. & Girard, P. 2005, A&A, 438, 139

Steigman G. 2012 arXiv.1208.0032

Stishov,S.M. & Popova, S.V. 1961, Geokhimiya, 10:837839.

Kendall's Advanced Theory of Statistics, Volume 1: Distribution Theory Stuart, Alan & Ord, Keith 2009, Wiley

Takeda, Y. 2007 PASJ 59, 335

Takeda, Y. 2003 A&A 402, 343T

Tang, Y. K. & Gai, N. 2011, A&A, 526, A35

Teixeira, T. C., Kjeldsen, H., Bedding, T. R., Bouchy, F., Christensen-Dalsgaard, J., Cunha, M. S., Dall, T., Frandsen, S., Karoff, C., Monteiro, M. J. P. F. G., & Pijpers, F. P. 2009, A&A, 494, 237

Teske, J., Schuler, S., Cunha, K., Smith, V., Griffith, C. 2013, arXiv:1304.0395

Thoul, A. A., Bahcall, J. N., and Loeb, A. 1994, ApJ, 421, 828

Timmes, F.X., Woosley, S.E., & Weaver, T.A. 1995, ApJS, 98, 617

Timmes, F.X. & Clayton, D.D. 1996, ApJ, 472, 723

Timmes, F. X. and Arnett, D. 1999, ApJS, 125, 277

Tinsley, B. M. 1980 Fund. Cos. Phys., 5:287-388.

Tomkin, J., Lambert, D.L. 1984, ApJ, 279, 220

Tomkin, J., Sneden, C., & Lambert, D.L. 1986, ApJ, 302, 415

Tuomi, M. et al. 2013, A&A, 551A, 79T

Turnbull, M. C.; Glassman, T.; Roberge, A.; Cash, W.; Noecker, C.; Lo, A.; Mason, B.; Oakley, P.; Bally, J. 2012, PASP 124, 418

Twarog, B.A. 1990. ApJ, 242, 242T

K. Umemoto, R. M. Wentzcovitch, and P. B. Allen 2006 Science, 311:983-986

Unterborn, C.T., Kabbes, J.E., Pigott, J., Reaman, D., Panero, W.R. 2013 ApJ, arXiv:1311.0024v3

Valenti, J.A. & Fischer, D.A. 2005, ApJS, 159, 141

Wadhwa, M., Amelin, Y., Davis, A. M., Lugmair, G. W., Meyer, B., Gounelle, M. & Desch, S. J. 2007. In Protostars and Planets V, Univ. Arizona Press, Tucson pp 835-848.

Wallerstein, G. 1962, ApJS, 6, 407.

Wallerstein, G. 1994, The Observatory, 114, 113

Wiescher, M., Azuma, R. E., Gasques, L., Görres, J., Pignatari, M., and Simpson, E. 2006, Memorie della Societa Astronomica Italiana 77, 910

Wood, B. E., Müller, H.-R., Zank, G. P., Linsky, J. L., and Redfield, S. 2005, ApJ, 628, 143

Woosley, S.E. & Weaver, T.A., 1995, ApJS, 101, 181

Yoshida, M.Onodera, A. Ueno, M. Takemura, K.& Shimomura, O.1993, Phys.Rev.B, 48:1058710590.

Young, P. A. & Arnett, D. 2005, ApJ, 618, 908

Young, P.A., Ellinger, C., Arnett, D., Fryer, C.L., Rockefeller, G. 2009, ApJ, 699, 938

Young, P. A., Liebst, K., Pagano, M. 2012, ApJ, 755, 31

APPENDIX A

TABLES

A.1 Line List

Table A.1: Line List. Reference: 1 (Bubar & King, 2010), 2 (Reddy et al., 2003), 3 (Feltzig & Gustafsson, 1998), 4 (Bond et al., 2006), 5 (De Silva et al., 2006)

Wavelength (Å)	Ion	χ_l (eV)	$\log(gf)$	Damping Constant	Solar EQW (mÅ)	Reference
5052.17	C I	7.68	-1.3	2.2	37.8	2
5380.34	C I	7.68	-1.61	2.2	21.9	2
6587.62	C I	8.54	-1	2.2	14	2
6156.8	O I	10.7	-0.43	2.2	4.1	3
6363.79	O I	0	-9.72	2.2	4.9	1
6154.23	Na I	2.1	-1.53	2.2	39.8	1
6160.75	Na I	2.1	-1.23	2.2	58.4	1
4730.04	Mg I	4.34	-2.39	2.2	76.8	2
5711.09	Mg I	4.35	-1.83	2.2	104.1	1
6318.72	Mg I	5.11	-1.99	2.2	39.8	2
6696.03	Al I	3.14	-1.58	2.2	38.1	3
6698.67	Al I	3.14	-1.95	2.2	21.9	1
5690.43	Si I	4.93	-1.77	2.2	52.6	5
5793.08	Si I	4.93	-2.06	2.2	44.9	2
6125.03	Si I	5.61	-1.51	2.2	33.8	2
6142.48	Si I	5.62	-1.54	2.2	36.8	3
6145.01	Si I	5.62	-1.36	2.2	40.3	1
6155.13	Si I	5.62	-0.78	2.2	81.4	1
6244.48	Si I	5.61	-1.36	2.2	48.4	2
6721.86	Si I	5.86	-0.94	2.2	49.1	2
6046.02	S I	7.87	-0.51	2.2	17.1	2
6757.17	S I	7.87	-0.31	2.2	17	2
5868.57	Ca I	2.93	-1.57	2.2	25.2	1
6161.3	Ca I	2.52	-1.27	2.2	59.8	1
6166.44	Ca I	2.52	-1.14	2.2	72.3	1
6169.04	Ca I	2.52	-0.79	2.2	104.1	1
6169.56	Ca I	2.53	-0.47	2.2	106.7	1
6455.6	Ca I	2.52	-1.5	2.2	58.7	1
6471.66	Ca I	2.53	-0.59	2.2	85.2	4
6499.65	Ca I	2.52	-0.59	2.2	79.8	1
6572.8	Ca I	0	-4.28	2.2	33.2	1
5318.36	Sc II	1.36	-2	2.2	13.2	2
6245.62	Sc II	1.51	-1.02	2.2	36.2	2
6604.6	Sc II	1.36	-1.3	2.2	37.1	2
5024.85	Ti I	0.82	-0.56	2.2	73.2	2
5113.45	Ti I	1.44	-0.73	2.2	27.6	2
5219.71	Ti I	0.02	-2.24	2.2	29.1	2
5866.46	Ti I	1.07	-0.76	2.2	48.7	2

Continued on next page

Table A.1 – *Continued from previous page*

Wavelength	Ion	χ_l	$\log(gf)$	Damping Constant	Solar EQW	Reference
5978.54	Ti I	1.87	-0.5	2.2	21.7	1
6064.63	Ti I	1.05	-1.94	2.2	10.1	1
6091.18	Ti I	2.27	-0.37	2.2	15.3	2
6126.22	Ti I	1.07	-1.43	2.2	23.2	1
6258.1	Ti I	1.44	-0.35	2.2	52.3	1
6261.1	Ti I	1.43	-0.48	2.2	46.8	1
6336.1	Ti I	1.44	-1.74	2.2	7.8	1
6491.56	Ti II	2.06	-1.79	2.2	36.8	1
6606.95	Ti II	2.06	-2.79	2.2	6.9	1
5727.06	V I	1.08	-0.01	2.2	39.6	2
6039.74	V I	1.06	-0.65	2.2	13.2	2
6090.22	V I	1.08	-0.06	2.2	34	2
6111.65	V I	1.04	-0.71	2.2	11.7	2
6251.83	V I	0.29	-1.34	2.2	16.1	2
5300.75	Cr I	0.98	-2.13	2.2	62.2	2
5304.18	Cr I	3.46	-0.69	2.2	20.1	3
5783.09	Cr I	3.32	-0.5	2.2	31.2	3
5783.89	Cr I	3.32	-0.29	2.2	45.8	2
5787.93	Cr I	3.32	-0.08	2.2	47.4	2
5305.87	Cr II	3.83	-1.97	2.2	26.7	2
5308.42	Cr II	4.07	-1.82	2.2	26.9	3
5394.67	Mn I	0	-3.5	2.2	81.1	2
5420.36	Mn I	2.14	-1.46	2.2	87.1	2
6013.53	Mn I	3.07	-0.25	2.2	78.7	1
6016.67	Mn I	3.08	-0.1	2.2	93.6	1
5247.06	Fe I	0.09	-4.94	2.3	67.6	2
5358.12	Fe I	3.3	-3.16	2.3	10.2	2
5412.79	Fe I	4.44	-1.71	2.3	20.1	2
5522.45	Fe I	4.21	-1.55	2.2	37.5	1
5539.28	Fe I	3.64	-2.66	2.2	17.4	1
5543.94	Fe I	4.22	-1.14	2.2	65.2	1
5546.5	Fe I	4.37	-1.31	2.2	51.2	1
5546.99	Fe I	4.22	-1.91	2.2	24.3	1
5560.21	Fe I	4.43	-1.19	2.2	52.1	1
5577.03	Fe I	5.03	-1.55	2.2	9.7	1
5579.34	Fe I	4.23	-2.4	2.2	10.3	1
5651.47	Fe I	4.47	-2	2.2	20.7	1
5652.32	Fe I	4.26	-1.95	2.2	23.2	1
5653.87	Fe I	4.39	-1.64	2.2	40	1
5667.52	Fe I	4.18	-1.58	2.2	51.8	1
5679.02	Fe I	4.65	-0.92	2.2	58.9	1
5731.76	Fe I	4.26	-1.3	2.2	57.2	1
5732.28	Fe I	4.99	-1.56	2.2	14.2	1
5741.85	Fe I	4.26	-1.85	2.2	34.7	1
5752.03	Fe I	4.55	-1.18	2.2	54.5	1

Continued on next page

Table A.1 – *Continued from previous page*

Wavelength	Ion	χ_l	$\log(gf)$	Damping Constant	Solar EQW	Reference
5775.08	Fe I	4.22	-1.3	2.2	53.6	1
5778.45	Fe I	2.59	-3.48	2.2	17.7	1
5784.66	Fe I	3.4	-2.53	2.3	27.8	2
5809.22	Fe I	3.88	-1.61	2.3	50.8	2
5852.23	Fe I	4.55	-1.17	2.3	41.1	2
5855.09	Fe I	4.61	-1.48	2.3	22.2	2
5856.1	Fe I	4.29	-1.56	2.3	33.7	2
5858.79	Fe I	4.22	-2.18	2.3	13	2
5902.47	Fe I	4.59	-1.81	2.2	10.3	1
5905.67	Fe I	4.65	-0.73	2.2	54.2	1
5927.79	Fe I	4.65	-1.09	2.2	41.8	1
5929.67	Fe I	4.55	-1.41	2.2	38.4	1
6005.54	Fe I	2.59	-3.6	2.2	21.2	1
6027.05	Fe I	4.08	-1.09	2.2	63.8	1
6079	Fe I	4.65	-1.12	2.2	42.9	1
6085.26	Fe I	2.76	-3.1	2.2	41.4	1
6105.13	Fe I	4.55	-2.05	2.2	13.2	1
6127.91	Fe I	4.14	-1.4	2.2	46.6	1
6151.62	Fe I	2.18	-3.3	2.2	47.4	1
6157.73	Fe I	4.08	-1.26	2.2	56.1	1
6159.37	Fe I	4.61	-1.97	2.2	11.9	1
6165.36	Fe I	4.14	-1.47	2.2	40.1	1
6180.21	Fe I	2.73	-2.78	2.2	55.1	4
6187.99	Fe I	3.94	-1.72	2.2	48.8	1
6220.78	Fe I	3.88	-2.46	2.2	18.7	1
6226.73	Fe I	3.88	-2.22	2.2	26.4	1
6229.23	Fe I	2.85	-2.97	2.2	33.9	3
6240.65	Fe I	2.22	-3.23	2.2	44.2	1
6271.28	Fe I	3.33	-2.72	2.2	27.8	1
6293.92	Fe I	4.83	-1.72	2.2	13.6	1
6380.74	Fe I	4.19	-1.38	2.2	46.9	1
6494.5	Fe I	4.73	-1.46	2.2	45.6	1
6498.95	Fe I	0.96	-4.7	2.2	42.6	1
6518.37	Fe I	2.83	-2.45	2.3	58.9	2
6581.21	Fe I	1.49	-4.68	2.2	20.5	1
6597.56	Fe I	4.79	-1.07	2.2	41.6	1
6608.02	Fe I	2.28	-4.03	2.2	16	1
6627.54	Fe I	4.55	-1.68	2.2	24.4	1
6703.57	Fe I	2.76	-3.16	2.2	41.2	1
6705.1	Fe I	4.61	-1.39	2.2	44	1
6710.32	Fe I	1.49	-4.88	2.2	14.1	1
6713.75	Fe I	4.79	-1.52	2.2	17.4	1
6715.38	Fe I	4.61	-1.64	2.2	25	1
6716.22	Fe I	4.58	-1.92	2.2	15.9	1
6725.35	Fe I	4.1	-2.3	2.2	15.8	1

Continued on next page

Table A.1 – *Continued from previous page*

Wavelength	Ion	χ_l	$\log(gf)$	Damping Constant	Solar EQW	Reference
6726.67	Fe I	4.61	-1.13	2.2	47.5	1
6733.15	Fe I	4.64	-1.58	2.2	24.1	1
6739.52	Fe I	1.56	-4.79	2.2	13	1
6752.72	Fe I	4.64	-1.3	2.2	37.3	1
6786.86	Fe I	4.19	-2.07	2.2	23.4	1
6837.01	Fe I	4.59	-1.69	2.3	18.3	2
6857.25	Fe I	4.08	-2.04	2.3	23.4	2
5234.62	Fe II	3.22	-2.22	9.9	83.5	2
5425.26	Fe II	3.2	-3.16	9.9	42.5	2
5991.38	Fe II	3.15	-3.55	2.2	29	1
6084.11	Fe II	3.2	-3.8	2.2	20.2	1
6147.74	Fe II	3.89	-2.83	2.2	72	1
6149.25	Fe II	3.89	-2.88	2.2	34.4	1
6238.39	Fe II	3.89	-2.75	2.2	47.7	1
6247.56	Fe II	3.89	-2.44	2.2	51.9	1
6369.46	Fe II	2.89	-4.23	2.2	16.6	1
6416.92	Fe II	3.89	-2.88	2.2	37.6	1
6432.68	Fe II	2.89	-3.52	9.9	41.7	2
6442.95	Fe II	5.55	-2.64	2.2	6	1
6446.4	Fe II	6.22	-2.11	2.2	3.7	1
6456.38	Fe II	3.9	-2.07	2.2	61.5	1
5342.71	Co I	4.02	0.54	2.2	32.7	2
5352.05	Co I	3.58	0.06	2.2	26.5	2
6455	Co I	3.63	-0.24	2.2	16.2	3
5082.35	Ni I	3.66	-0.59	2.2	69.1	2
5088.54	Ni I	3.85	-1.04	2.2	33.6	2
5088.96	Ni I	3.68	-1.24	2.2	31.3	2
5094.42	Ni I	3.83	-1.07	2.2	32.6	2
5115.4	Ni I	3.83	-0.28	2.2	79.2	2
5847.01	Ni I	1.68	-3.41	2.2	23.2	1
6086.28	Ni I	4.26	-0.51	2.2	37.9	1
6111.08	Ni I	4.09	-0.81	2.2	35.8	2
6130.14	Ni I	4.27	-0.94	2.2	22.4	2
6175.37	Ni I	4.09	-0.53	2.2	50.5	1
6176.8	Ni I	4.09	-0.53	2.2	67.3	2
6177.25	Ni I	1.82	-3.51	2.2	15.2	2
6204.61	Ni I	4.09	-1.11	2.2	22.8	2
6327.6	Ni I	1.68	-3.23	2.2	40	1
6378.26	Ni I	4.15	-1	2.2	33.1	1
6414.59	Ni I	4.15	-1.18	2.2	16.2	1
6482.81	Ni I	1.93	-2.97	2.2	40.7	1
6532.88	Ni I	1.93	-3.47	2.2	17.9	1
6598.61	Ni I	4.23	-1.02	2.2	21	1
6635.14	Ni I	4.42	-0.82	2.2	19.2	1
6643.64	Ni I	1.68	-2.01	2.2	101.4	1

Continued on next page

Table A.1 – *Continued from previous page*

Wavelength	Ion	χ_l	$\log(gf)$	Damping Constant	Solar EQW	Reference
6767.78	Ni I	1.83	-1.89	2.2	70.1	1
6772.32	Ni I	3.66	-0.98	2.2	50.9	1
6842.04	Ni I	3.66	-1.48	2.2	25.8	1
5105.55	Cu I	1.52	-1.52	2.2	90.8	2
5218.21	Cu I	3.82	0.47	2.2	55.6	2
5220.09	Cu I	3.82	-0.45	2.2	16.1	2
4810.54	Zn I	4.08	-0.17	2.2	90.8	2
6362.35	Zn I	5.79	0.14	2.2	55.6	2
4854.87	Y II	0.99	-0.01	2.2	16.1	4
4900.12	Y II	1.03	-0.09	2.2	57.4	2
5087.43	Y II	1.08	-0.17	2.2	48.6	2
5200.42	Y II	0.99	-0.49	2.2	39	2
5473.39	Y II	1.74	-0.83	2.2	9.4	3
6506.35	Zr I	0.63	-0.64	2.2	2.5	3
5112.28	Zr II	1.66	-0.59	2.2	9.7	2
5570.39	Mo I	1.33	0.43	2.2	9.6	3
5853.69	Ba II	0.6	-1	2.2	66.7	1
6141.73	Ba II	0.7	-0.07	2.2	132.8	1
6496.91	Ba II	0.6	-0.41	2.2	112.2	1
6320.42	La I	0.17	-1.39	2.2	5.2	3
6390.49	La I	0.32	-1.47	2.2	3.2	3
4773.96	Ce II	0.92	0.25	2.2	10.5	2
5092.8	Nd II	0.38	-0.65	2.2	7.6	2
5319.82	Nd II	0.55	-0.28	2.2	11.7	2
6645.13	Eu II	1.38	0.2	2.2	5.6	2
5311.63	Hf	1.78	0.13	2.2	4.4	3

Table A.2: All stars parameters

Star HD	Temperature (K)	±	MtVel kms^{-1}	±	log(g)	[Fe/H]	±
361	5978	50	1.39	0.19	4.7	-0.08	0.07
1002	5894	52	1.04	0.12	4.57	0.21	0.07
1237	5639	78	1.22	0.18	4.73	0.19	0.09
1893	5652	66	0.97	0.13	4.56	0.31	0.09
1926	6015	51	1.38	0.3	4.59	-0.24	0.08
2098	6070	56	1.25	0.1	4.63	0.25	0.07
2222	5808	47	1.22	0.1	4.24	0.25	0.08
3359	5613	58	1	0.11	4.47	0.27	0.08
4333	5572	58	0.93	0.11	4.45	0.31	0.08
4392	5808	61	1.1	0.13	4.63	0.17	0.08
6236	6101	57	1.56	0.16	4.69	0.14	0.08
6790	6151	66	1.21	0.2	4.56	0.13	0.09
6880	5417	42	0.97	0.11	4.57	-0.07	0.06
6910	6107	55	1.47	0.1	4.26	0.41	0.09
7134	5985	48	1.97	0.35	4.54	-0.28	0.07
7449	6117	60	1.64	0.33	4.71	-0.06	0.09
7661	5586	49	1.21	0.11	4.66	0.1	0.07
8076	6014	55	1.56	0.19	4.71	0.07	0.08
8129	5693	43	0.97	0.11	4.61	0.05	0.07
8406	5788	49	1.11	0.13	4.6	-0.05	0.07
9175	5856	45	1.23	0.1	4.32	0.14	0.08
9782	6099	56	1.36	0.16	4.6	0.14	0.08
9847	5866	51	1.05	0.09	4.45	0.4	0.08
9905	5395	69	0.73	0.14	4.52	0.23	0.09
10008	5415	46	1.16	0.09	4.6	0	0.07
10226	6129	66	1.32	0.16	4.71	0.22	0.08
10370	5731	44	1.41	0.15	4.65	-0.04	0.07
10519	5706	41	1.84	0.35	4.27	-0.58	0.08
10576	6042	53	1.5	0.15	4.32	0.06	0.09
10611	5449	56	1.21	0.13	4.7	0.08	0.08
10678	5671	51	1.01	0.1	4.48	0.13	0.07
11264	5874	56	1.09	0.12	4.55	0.15	0.07
11754	5906	60	1.25	0.09	4.23	0.31	0.08
12585	5845	54	1.01	0.11	4.45	0.18	0.08
12951	6086	53	1.92	0.24	4.3	-0.13	0.08
13060	5329	58	0.86	0.11	4.48	0.16	0.08
13350	5712	69	1.09	0.12	4.45	0.47	0.1
13386	5332	76	0.84	0.17	4.62	0.33	0.1
14758	5828	55	1.16	0.2	4.57	-0.13	0.07
15507	5778	58	1.27	0.13	4.56	0.16	0.06

Continued on next page

Table A.2 – *Continued from previous page*

Star	Temperature	±	MtVel	±	log(g)	[Fe/H]	±
15590	5990	50	1.39	0.1	4.15	0.28	0.08
15767	5097	77	1.06	0.2	4.71	-0.11	0.11
16950	6164	57	1.58	0.15	4.41	0.28	0.09
17134	5914	51	1.18	0.16	4.45	0.02	0.07
17289	5970	46	1.23	0.18	4.44	-0.1	0.08
18168	5236	61	1.27	0.13	4.4	0	0.11
18708	5960	50	1.19	0.14	4.53	0.23	0.07
18754	5736	53	1.25	0.1	4.22	0.29	0.09
18819	6107	56	1.78	0.15	4.09	0.17	0.08
19603	6191	61	1.31	0.18	4.56	0.33	0.08
19916	6312	105	1.78	0.25	4.58	0.36	0.12
20155	6138	56	1.39	0.15	4.44	0.28	0.09
20407	5799	67	1.57	0.39	4.38	-0.45	0.1
20584	6281	71	1.83	0.2	4.35	0.24	0.1
20657	6032	43	1.33	0.11	4.45	0.24	0.07
20675	6029	92	1.43	0.21	4.51	0.27	0.13
21036	5782	60	1.1	0.12	4.72	0.23	0.08
21089	5692	53	1.23	0.1	4.16	0.32	0.1
22177	5745	40	0.96	0.09	4.39	0.3	0.07
22582	5612	64	0.93	0.14	4.56	0.05	0.09
23576	6059	65	1.14	0.16	4.52	0.19	0.08
24331	5052	51	0.91	0.11	4.39	-0.24	0.09
25912	5984	67	1.07	0.16	4.61	0.22	0.09
26040	6105	82	1.05	0.4	4.45	-0.01	0.11
26071	5702	48	1.11	0.1	4.32	0.31	0.09
26864	5844	60	1.14	0.14	4.29	0.13	0.1
27328	5585	87	1.1	0.17	4.48	0.18	0.12
27446	5832	56	1.16	0.12	4.58	0.05	0.07
27905	5898	62	1.22	0.2	4.61	-0.08	0.08
27939	5874	60	1.21	0.11	4.33	0.28	0.09
28185	5731	58	1.1	0.1	4.51	0.26	0.08
28701	5792	75	1	0.26	4.57	-0.21	0.1
28821	5727	47	1.25	0.14	4.49	-0.08	0.07
29231	5541	73	0.96	0.14	4.51	0.23	0.1
29263	5855	64	1.24	0.17	4.49	0.12	0.1
29813	5976	53	1.18	0.19	4.66	0.03	0.07
30278	5493	50	1.05	0.12	4.59	-0.1	0.07
30306	5603	60	1.13	0.11	4.44	0.25	0.09
30501	5218	63	0.92	0.14	4.6	0.03	0.09
30669	5473	55	0.94	0.12	4.52	0.19	0.08
31392	5451	49	1.03	0.1	4.58	0.11	0.07
32564	5682	73	0.97	0.15	4.7	0.1	0.09
32724	5846	40	1.59	0.15	4.37	-0.16	0.07
32804	5998	46	1.08	0.13	4.7	0.16	0.06
33093	5988	50	1.82	0.16	4.25	0	0.08

Continued on next page

Table A.2 – *Continued from previous page*

Star	Temperature	±	MtVel	±	log(g)	[Fe/H]	±
33214	5214	86	0.96	0.16	4.49	0.22	0.11
33822	5817	49	1.13	0.08	4.32	0.34	0.08
33873	5857	69	1.29	0.14	4.68	0.21	0.09
34195	6147	65	1.87	0.24	4.44	0.1	0.1
34230	5564	69	1.07	0.12	4.5	0.27	0.08
34377	5822	70	1.41	0.18	4.62	0.15	0.07
34599	5981	66	1.32	0.18	4.75	0.22	0.07
35376	5865	70	1.35	0.18	4.49	0.11	0.08
35676	5737	47	1.17	0.11	4.63	0.2	0.07
36152	5864	57	1.02	0.13	4.56	0.15	0.08
36329	6066	87	1.29	0.29	4.81	0.17	0.11
37351	6022	44	1.4	0.16	4.65	0.13	0.05
37706	5578	43	1.25	0.14	4.67	-0.21	0.07
37761	5702	44	1.37	0.09	4.07	0.19	0.08
37986	5583	73	0.93	0.12	4.48	0.35	0.09
38467	5903	48	1.23	0.1	4.45	0.33	0.08
38554	5748	66	1.16	0.12	4.59	0.29	0.09
38667	6269	72	1.55	0.19	4.63	0.25	0.09
38677	6224	56	1.44	0.16	4.54	0.23	0.08
39126	5426	64	1.23	0.13	4.64	0.09	0.09
39503	5701	68	1.07	0.13	4.61	0.24	0.09
39804	5750	54	1.05	0.13	4.62	0.1	0.07
39855	5558	60	1.46	0.28	4.68	-0.44	0.08
40105	5192	56	1.09	0.09	3.96	0.1	0.1
40403	5970	54	1.12	0.1	4.47	0.44	0.08
41155	6314	63	1.56	0.21	4.44	0.29	0.1
42044	6266	78	1.95	0.34	4.32	0.04	0.12
42287	6189	78	1.22	0.26	4.72	0.17	0.08
42538	6141	63	1.48	0.15	4.36	0.26	0.09
42719	6032	60	1.38	0.1	4.36	0.37	0.09
42778	6015	71	1.27	0.14	4.52	0.25	0.09
43470	6250	98	1.45	0.33	4.45	0.12	0.14
44569	5826	47	1.37	0.16	4.53	-0.15	0.06
44573	5114	59	0.97	0.13	4.55	0.02	0.08
45133	5756	63	1.01	0.11	4.49	0.4	0.09
45987	5978	81	1.2	0.15	4.59	0.33	0.11
46175	6191	75	1.47	0.28	4.75	0.22	0.08
46435	6037	94	0.72	0.29	4.67	0.23	0.12
46894	5507	55	1.16	0.1	4.11	0.16	0.1
47017	6006	54	1.59	0.15	4.21	0.15	0.1
47186	5759	56	1.1	0.11	4.51	0.29	0.08
48056	6191	62	1.5	0.21	4.4	0.13	0.1
48265	5848	60	1.28	0.1	4.14	0.42	0.09
49035	5687	61	1	0.11	4.46	0.34	0.09
49866	5931	47	1.49	0.1	4.16	0.15	0.08

Continued on next page

Table A.2 – *Continued from previous page*

Star	Temperature	±	MtVel	±	log(g)	[Fe/H]	±
50117	6015	31	1.28	0.12	4.44	0.12	0.07
50255	5784	76	1.08	0.23	4.65	-0.02	0.11
50652	5812	57	1.15	0.12	4.46	0.36	0.09
51608	5484	55	0.95	0.12	4.55	0.04	0.08
52217	5636	78	1.02	0.15	4.55	0.28	0.11
52756	5222	85	0.9	0.18	4.55	0.19	0.12
56413	5855	74	0.97	0.15	4.66	0.38	0.09
56662	5972	57	1.64	0.26	4.66	-0.11	0.08
56972	5722	55	1.05	0.1	4.47	0.31	0.08
58111	5280	83	1.22	0.18	4.67	0.04	0.12
58556	6218	73	1.89	0.32	4.78	0.05	0.09
58696	6000	59	1.65	0.19	4.36	0.02	0.09
59711	5840	52	1.41	0.18	4.66	-0.07	0.07
59824	6017	55	1.16	0.11	4.53	0.29	0.07
61051	5550	55	0.98	0.15	4.72	0.06	0.07
61475	5437	73	1.22	0.14	4.59	0.28	0.1
62549	5999	55	1.42	0.19	4.49	0.04	0.08
62644	5533	35	1.17	0.08	4.06	0.09	0.07
64114	5695	60	1.09	0.15	4.65	0.05	0.06
64144	5689	54	1.18	0.15	4.59	0.01	0.08
65427	5827	56	1.34	0.15	4.44	0.08	0.07
66039	6224	62	1.27	0.15	4.67	0.24	0.08
66058	5938	56	1.24	0.12	4.54	0.17	0.08
66791	5811	40	1.3	0.09	4.33	0.13	0.07
70081	5872	53	1.35	0.11	4.34	0.19	0.09
72579	5578	65	0.92	0.12	4.58	0.31	0.09
72687	5936	76	1.64	0.27	4.71	0.02	0.11
72892	5855	89	1.3	0.18	4.6	0.23	0.12
73267	5398	66	0.85	0.13	4.48	0.13	0.09
73744	5854	53	1.53	0.29	4.55	-0.3	0.07
74698	5888	42	1.32	0.12	4.45	0.15	0.07
74733	5910	56	1.27	0.2	4.54	-0.1	0.08
74935	6114	59	1.37	0.17	4.55	0.14	0.08
75288	5807	61	1.02	0.11	4.52	0.18	0.08
75351	6028	59	1.71	0.16	4.29	0.18	0.09
77338	5498	92	1.22	0.17	4.62	0.32	0.13
77417	5627	65	0.95	0.13	4.57	0.33	0.09
77683	5344	55	1.05	0.08	4.04	0.27	0.09
78130	5907	57	1.17	0.13	4.6	0.21	0.08
78286	5907	66	1.15	0.13	4.55	0.29	0.09
79985	5837	63	1.21	0.14	4.22	0.08	0.1
81110	5850	61	1.02	0.11	4.64	0.34	0.08
81700	5973	51	1.11	0.13	4.68	0.2	0.07
82282	5371	81	1.31	0.2	4.73	-0.04	0.12
82400	5796	74	1.29	0.18	4.67	0.12	0.1

Continued on next page

Table A.2 – *Continued from previous page*

Star	Temperature	±	MtVel	±	log(g)	[Fe/H]	±
82516	5215	73	0.93	0.16	4.5	0.09	0.1
82977	5490	68	1.28	0.15	4.67	0.02	0.1
83365	6026	67	1.49	0.18	4.62	0.15	0.09
83517	5751	51	1.28	0.16	4.4	-0.01	0.06
84652	6123	59	1.37	0.18	4.5	0.06	0.08
85380	6132	58	1.67	0.19	4.33	0.12	0.09
85390	5281	62	1.08	0.15	4.42	0.01	0.08
86006	5866	49	1.21	0.1	4.32	0.37	0.08
86226	5950	52	1.65	0.22	4.71	-0.01	0.05
86249	5070	66	0.84	0.17	4.58	0.11	0.11
86397	5714	58	0.94	0.14	4.6	0.24	0.09
86652	6026	78	1.64	0.2	4.71	0.12	0.09
87931	5609	55	0.96	0.12	4.6	0.12	0.07
87998	5922	55	1.74	0.28	4.57	-0.14	0.07
88864	5919	63	1.39	0.19	4.2	0.07	0.08
89178	5538	57	1.31	0.11	4.13	0.07	0.11
89418	6032	69	1.88	0.36	4.6	-0.15	0.1
89988	5900	46	1.42	0.11	4.17	0.2	0.08
90028	5992	58	1.3	0.12	4.45	0.32	0.09
90702	5851	84	1.46	0.18	4.66	0.23	0.11
91320	6157	56	1.57	0.17	4.34	0.12	0.08
91901	5155	57	1.05	0.12	4.57	0.02	0.08
92069	5746	43	1.13	0.08	4.38	0.23	0.08
92719	5830	50	1.54	0.21	4.6	-0.11	0.06
93083	5089	63	0.85	0.14	4.5	0.19	0.1
94151	5681	46	1.18	0.12	4.53	0.11	0.05
94387	5605	66	0.97	0.11	4.51	0.33	0.09
94482	6141	71	1.67	0.28	4.55	0.02	0.09
94527	5622	54	1.24	0.16	4.67	-0.11	0.07
94690	5923	67	1.17	0.14	4.62	0.33	0.09
94838	5993	52	1.17	0.14	4.7	0.12	0.07
95136	5893	59	1.22	0.14	4.54	0.23	0.08
95338	5277	66	0.94	0.14	4.57	0.17	0.09
95521	5809	52	1.6	0.26	4.68	-0.14	0.06
95533	5479	59	0.84	0.12	4.59	0.26	0.08
95542	6090	66	1.47	0.24	4.68	0.02	0.08
96020	5729	69	1.02	0.13	4.5	0.43	0.1
96276	6128	52	1.64	0.23	4.66	-0.01	0.07
98163	5804	47	1.19	0.1	4.28	0.17	0.08
98459	6014	43	1.38	0.13	4.44	0.22	0.08
98764	6022	58	1.29	0.16	4.72	0.14	0.08
99116	5604	54	0.92	0.15	4.63	-0.01	0.08
101093	6064	56	1.28	0.2	4.53	-0.08	0.08
101171	5449	51	1.14	0.17	4.59	-0.02	0.07
101181	5733	47	1.06	0.1	4.5	0.23	0.07

Continued on next page

Table A.2 – *Continued from previous page*

Star	Temperature	±	MtVel	±	log(g)	[Fe/H]	±
101896	5475	75	0.89	0.17	4.53	0.29	0.11
102574	6181	66	1.72	0.16	4.22	0.23	0.1
102579	5344	59	0.85	0.1	4.51	0.09	0.08
102843	5544	70	0.95	0.13	4.51	0.27	0.1
103559	5707	58	1.26	0.15	4.56	0.05	0.08
103673	5767	55	1.11	0.16	4.7	0.1	0.08
104645	5446	42	1.04	0.08	4.05	0.12	0.08
104760	6026	62	1.41	0.15	4.6	0.17	0.08
104982	5731	49	1.58	0.25	4.57	-0.18	0.06
105690	5797	79	1.46	0.22	4.76	0.05	0.1
105904	5853	57	1.39	0.09	4.59	0.33	0.08
106275	5167	80	0.81	0.2	4.57	0.03	0.11
106869	6156	53	1.59	0.16	4.51	0.13	0.08
106937	5654	54	1.11	0.09	4.24	0.39	0.09
107008	5495	60	0.99	0.1	4.46	0.29	0.08
107181	5766	50	1.19	0.08	4.25	0.39	0.08
108953	5655	90	0.89	0.18	4.58	0.43	0.12
109591	5788	53	1.21	0.13	4.58	-0.04	0.07
109908	6040	61	1.39	0.15	4.64	0.1	0.08
109930	5297	63	0.99	0.12	4.52	0.09	0.08
109988	5348	76	0.95	0.16	4.61	0.27	0.11
110605	5718	58	1.01	0.11	4.5	0.36	0.08
110619	5723	57	1.73	0.36	4.74	-0.36	0.08
111431	5999	51	1.53	0.14	4.32	0.12	0.08
112121	5728	62	1.07	0.13	4.54	0.28	0.09
112540	5642	56	1.02	0.15	4.66	-0.07	0.08
113027	6070	56	1.95	0.33	4.62	-0.03	0.06
113255	5930	51	1.19	0.12	4.47	0.19	0.08
113513	5824	65	1.13	0.15	4.71	0.18	0.07
114294	5495	47	1.25	0.09	4.13	0.16	0.09
114432	5695	66	1.34	0.17	4.57	0.17	0.07
114884	6051	57	1.27	0.13	4.57	0.27	0.07
115080	5661	40	1.38	0.14	4.41	-0.17	0.06
115674	5670	44	1.44	0.18	4.57	-0.18	0.06
116920	5146	70	0.93	0.19	4.65	-0.1	0.1
117653	6051	59	1.71	0.21	4.52	0.17	0.06
117860	5924	54	1.28	0.16	4.46	0.1	0.06
119070	5464	56	0.93	0.15	4.61	-0.04	0.09
119119	6197	50	1.52	0.21	4.44	0.17	0.08
119507	5786	46	1.14	0.1	4.39	0.15	0.08
119782	5239	63	0.93	0.14	4.55	0.04	0.09
120100	5560	66	0.95	0.1	4.43	0.29	0.08
120329	5794	89	1.32	0.17	4.44	0.4	0.15
121504	6006	60	1.33	0.14	4.49	0.13	0.07
122078	5849	50	1.24	0.09	4.23	0.31	0.08

Continued on next page

Table A.2 – *Continued from previous page*

Star	Temperature	±	MtVel	±	log(g)	[Fe/H]	±
124553	6162	58	1.84	0.18	4.45	0.19	0.08
125968	5952	64	1.3	0.15	4.51	0.17	0.09
126653	6121	82	1.5	0.27	4.44	0.07	0.12
127321	6133	63	1.26	0.18	4.26	0.13	0.09
128214	5836	85	1.31	0.15	4.43	0.36	0.13
128760	6160	72	1.53	0.23	4.51	0.16	0.1
128987	5617	48	1.23	0.09	4.63	0.05	0.07
129679	6090	97	1.45	0.3	4.52	0.07	0.12
129764	6041	57	1.36	0.15	4.51	0.18	0.07
129946	5719	55	1.08	0.18	4.7	-0.08	0.08
131900	5614	59	1.12	0.11	4.55	0.2	0.08
132648	5486	44	1.54	0.24	4.65	-0.33	0.06
133014	5754	57	1.07	0.11	4.4	0.38	0.1
135005	5778	45	1.28	0.09	4.21	0.17	0.07
135309	6014	55	1.17	0.13	4.59	0.23	0.07
135562	6127	70	1.35	0.16	4.37	0.24	0.11
135625	6036	55	1.33	0.14	4.43	0.17	0.09
135725	5719	49	1.04	0.12	4.55	0.03	0.07
136130	5711	44	1.26	0.1	4.09	0.05	0.07
136548	5792	57	1.04	0.16	4.52	-0.01	0.08
136894	5474	40	1.15	0.1	4.43	-0.07	0.05
137214	6177	68	1.35	0.18	4.51	0.17	0.09
140643	5210	83	0.99	0.19	4.55	0.2	0.12
141105	5450	43	1.07	0.09	3.91	-0.13	0.08
141366	5889	74	1.51	0.15	4.03	0.22	0.12
141514	6262	61	1.88	0.24	4.67	0.13	0.08
141598	5678	44	1.03	0.12	4.52	-0.04	0.07
141599	5701	65	1.05	0.12	4.63	0.3	0.09
141885	6085	76	1.66	0.16	4.23	0.37	0.12
142137	6071	71	1.66	0.17	4.22	0.3	0.12
143120	5770	62	1.23	0.11	4.26	0.38	0.11
143137	6289	84	1.86	0.23	4.18	0.21	0.12
143295	5075	65	0.94	0.14	4.53	0.07	0.1
143673	5566	52	0.87	0.11	4.37	0.23	0.09
144087	5730	72	1.14	0.17	4.69	0.18	0.1
144088	5424	88	1.06	0.19	4.71	0.17	0.12
144167	5977	67	1.19	0.12	4.19	0.43	0.11
144550	5855	63	1.33	0.11	4.21	0.3	0.1
144848	5870	49	1.24	0.1	4.29	0.27	0.08
144899	5953	62	1.41	0.11	4.09	0.35	0.09
145518	5979	58	1.41	0.17	4.61	-0.03	0.08
145666	5998	59	1.36	0.21	4.67	-0.02	0.08
146817	5778	46	1.47	0.16	4.42	-0.06	0.08
146835	5937	71	1.9	0.38	4.55	-0.21	0.1
147018	5601	60	1.05	0.12	4.59	0.22	0.09

Continued on next page

Table A.2 – *Continued from previous page*

Star	Temperature	±	MtVel	±	log(g)	[Fe/H]	±
147619	6157	66	1.67	0.15	4.13	0.25	0.1
148156	6196	60	1.46	0.14	4.3	0.24	0.09
148628	6136	85	1.48	0.31	4.42	-0.05	0.13
149189	5966	62	1.27	0.12	4.29	0.34	0.1
150761	6210	117	1.71	0.28	4.41	0.28	0.16
151450	6155	78	1.78	0.34	4.65	-0.02	0.1
152388	5389	57	1	0.13	4.61	0.1	0.09
153631	5901	41	1.46	0.16	4.35	-0.07	0.07
154682	5918	50	1.46	0.16	4.38	-0.07	0.08
154697	5692	55	1.05	0.12	4.55	0.17	0.08
156152	5814	44	1.23	0.08	4.22	0.09	0.07
156643	5828	49	1.55	0.21	4.55	-0.22	0.07
157798	5919	84	0.95	0.17	4.21	0.29	0.14
157830	5623	43	1.12	0.13	4.65	-0.17	0.06
158469	6201	71	1.46	0.26	4.45	0.07	0.1
158630	5974	46	1.51	0.21	4.61	-0.14	0.07
159902	5779	46	1.27	0.18	4.54	-0.19	0.07
160411	5956	60	1.43	0.12	4.13	0.22	0.1
160859	5934	52	1.36	0.17	4.68	-0.04	0.07
161098	5660	44	1.19	0.14	4.58	-0.2	0.06
162907	5528	64	0.87	0.13	4.43	0.21	0.09
165011	6279	54	1.86	0.19	4.41	0.16	0.08
165204	5715	65	1.04	0.11	4.44	0.35	0.09
165271	5877	41	1.46	0.08	4.19	0.12	0.07
165385	6176	72	1.6	0.23	4.34	0.07	0.11
165449	5995	50	1.52	0.17	4.5	-0.05	0.07
165920	5413	76	0.94	0.13	4.45	0.37	0.1
169303	6163	58	1.98	0.25	4.44	0.03	0.08
169506	6026	86	1.77	0.16	4.02	0.34	0.12
171990	6040	48	1.67	0.13	4.17	0.04	0.07
172063	5520	63	0.93	0.11	4.4	0.13	0.1
172582	5636	69	0.79	0.27	4.6	-0.23	0.1
174494	5862	53	1.32	0.1	4.16	0.22	0.09
174541	5754	54	1.47	0.23	4.44	-0.23	0.1
175073	5287	59	0.73	0.16	4.64	0.01	0.08
175169	5829	78	1.02	0.15	4.53	0.34	0.1
176110	5848	82	1.46	0.17	4.31	0.21	0.14
176151	5807	61	1.3	0.12	4.26	0.22	0.1
176986	5105	84	0.86	0.21	4.58	0.13	0.12
177122	6073	58	1.35	0.26	4.68	-0.06	0.08
177409	5976	48	1.29	0.14	4.69	0	0.07
178076	5555	54	1.19	0.1	4.59	0.02	0.07
179640	5702	61	0.97	0.11	4.51	0.44	0.08
180204	6233	60	1.5	0.17	4.51	0.31	0.08
180257	6046	53	1.39	0.11	4.22	0.29	0.08

Continued on next page

Table A.2 – *Continued from previous page*

Star	Temperature	±	MtVel	±	log(g)	[Fe/H]	±
181010	5394	66	0.83	0.12	4.67	0.16	0.08
182228	6010	36	1.13	0.1	4.44	0.27	0.08
182498	6030	64	1.46	0.22	4.54	0.07	0.08
184317	5984	52	1.31	0.13	4.54	0.11	0.08
185283	5005	87	0.88	0.22	4.62	0.09	0.13
185615	5646	50	1.2	0.11	4.44	0.13	0.07
186160	6000	52	1.5	0.31	4.64	-0.25	0.08
186265	5647	57	1.02	0.09	4.38	0.45	0.1
186651	6222	66	1.4	0.24	4.64	0.1	0.09
186803	5787	55	1.14	0.14	4.68	0.03	0.07
187154	6025	84	1.47	0.19	4.47	0.17	0.1
189310	5252	69	0.92	0.16	4.56	0.09	0.1
190125	5760	80	1.32	0.16	4.53	0.19	0.11
190613	5836	44	1.32	0.11	4.37	0.04	0.08
191760	5978	54	1.3	0.11	4.35	0.34	0.09
193567	5754	55	1.02	0.11	4.52	0.29	0.08
193728	5575	49	1.16	0.09	4.04	0.14	0.09
193995	5852	55	1.22	0.1	4.3	0.35	0.09
195145	5739	58	0.93	0.12	4.57	0.29	0.08
195284	5696	48	0.98	0.11	4.6	0.17	0.07
196397	5482	90	0.92	0.17	4.53	0.37	0.13
197069	6085	87	1.01	0.17	4.51	0.32	0.1
197210	5641	42	1.1	0.13	4.59	0.02	0.07
197499	6164	74	1.73	0.26	4.54	0.12	0.1
197818	5904	67	1.51	0.26	4.63	-0.13	0.09
197823	5584	82	1.05	0.17	4.72	0.25	0.11
198477	5663	88	0.88	0.19	4.6	0.29	0.12
199065	6114	55	1.28	0.15	4.71	0.21	0.07
200733	6464	90	1.94	0.34	4.47	0.24	0.11
200869	5552	79	1.11	0.15	4.55	0.37	0.11
201757	5712	59	1.18	0.1	4.3	0.23	0.09
202282	5835	63	1.21	0.14	4.49	0.11	0.09
202457	5780	51	1.06	0.09	4.37	0.14	0.08
203432	5742	60	0.92	0.12	4.59	0.41	0.08
205045	6132	72	1.31	0.18	4.51	0.25	0.1
205067	5814	44	1.19	0.13	4.44	-0.04	0.07
205158	6151	57	1.83	0.17	4.3	0.25	0.1
206025	6213	50	1.69	0.2	4.44	0.16	0.08
206255	5773	54	1.22	0.1	4.11	0.19	0.09
206683	6070	63	1.16	0.12	4.57	0.39	0.08
207970	5604	54	1.04	0.12	4.43	0.1	0.08
208704	5867	40	1.25	0.11	4.44	-0.05	0.07
209566	5632	70	0.94	0.15	4.63	0.24	0.1
209659	6085	51	1.66	0.13	4.29	0.21	0.08
210193	5920	56	1.19	0.15	4.64	0.17	0.07

Continued on next page

Table A.2 – *Continued from previous page*

Star	Temperature	±	MtVel	±	log(g)	[Fe/H]	±
211366	5970	81	1.21	0.18	4.73	0.3	0.08
213429	6056	64	1.3	0.21	4.45	0.02	0.1
213717	5486	59	0.95	0.12	4.56	0.13	0.08
213941	5688	50	1.71	0.24	4.64	-0.39	0.07
214691	5658	49	0.91	0.09	4.41	0.2	0.08
215456	5872	46	1.41	0.16	4.32	-0.03	0.07
216054	5472	56	0.95	0.15	4.59	-0.12	0.08
218760	5029	86	0.9	0.2	4.57	0.02	0.12
219011	5871	62	1.18	0.11	4.46	0.4	0.1
219533	5946	51	1.32	0.1	4.36	0.34	0.08
219556	5602	57	0.96	0.1	4.52	0.22	0.08
220426	6355	60	1.22	0.14	4.58	0.38	0.08
220476	5755	52	1.28	0.14	4.66	0.02	0.08
220689	6004	45	1.51	0.17	4.56	0.01	0.07
220718	5949	54	1.37	0.11	4.13	0.26	0.09
220829	5268	86	0.86	0.18	4.58	0.15	0.11
220945	5149	82	1.07	0.2	4.69	0.13	0.1
220981	5659	65	1.2	0.14	4.36	0.23	0.09
221257	5869	49	1.32	0.16	4.44	-0.09	0.09
221275	5512	58	1	0.11	4.55	0.2	0.08
221954	5768	78	1.03	0.15	4.33	0.43	0.12
222422	5593	56	1.01	0.15	4.73	-0.03	0.08
222669	5966	50	1.16	0.11	4.57	0.11	0.07
224010	6015	55	1.36	0.13	4.45	0.26	0.09
224022	6153	52	1.46	0.17	4.47	0.15	0.08
224143	6049	82	1.46	0.3	4.79	0.08	0.1
224433	5656	66	1.21	0.15	4.58	0.17	0.08
224538	6209	70	1.5	0.14	4.41	0.34	0.09
224789	5249	52	1.12	0.11	4.52	0.05	0.07
225155	5716	48	1.08	0.1	4.35	0.25	0.08
225299	5820	64	1.24	0.13	4.52	0.22	0.08

Table A.3: All stars abundances for Fe, C, O, Na, Mg, Al, Si, and S.

Star	[Fe/H]	±	[C/H]	±	[O/H]	±	[Na/H]	±	[Mg/H]	±	[Al/H]	±	[Si/H]	±	[S/H]	±
361	-0.08	0.07	-	-	-	-	-0.3	0.04	-	-	-0.27	0.01	-0.19	0.04	-0.18	0.13
1002	0.21	0.07	0.08	0.04	0.19	*	0.11	0.11	0.15	*	0.06	0.01	0.06	0.05	0.04	0.04
1237	0.19	0.09	-	-	0.4	*	0.03	0.18	0.15	0.14	0.13	0.02	0.03	0.07	-0.15	0.06
1893	0.31	0.09	-0.03	0.01	0.48	*	0.33	0.11	0.28	0.05	0.29	0.03	0.13	0.06	-0.07	0.18
1926	-0.24	0.08	-0.28	0.12	-0.04	*	-0.4	0.01	-	-	-0.35	0.05	-0.25	0.04	-0.19	0.13
2098	0.25	0.07	0.18	0.04	0.28	*	-0.01	0.03	0.11	0.03	-0.01	0.01	0.08	0.05	0.2	0.12
2222	0.25	0.08	0.14	0.01	0.17	*	0.09	0.19	0.16	0.04	0.21	0.01	0.15	0.06	0.2	0.11
3359	0.27	0.08	-	-	0.47	*	0.41	*	0.28	*	-	-	0.14	0.05	-	-
4333	0.31	0.08	-0.01	0.18	0.45	0.13	0.44	0.08	0.31	0.06	0.35	0.04	0.13	0.07	0.07	0.08
4392	0.17	0.08	0.06	0.02	0.41	0.14	0.19	0.04	0.13	0.04	0.1	0.04	0.04	0.04	0.05	0.07
6236	0.14	0.08	0.03	0.11	0.18	0.11	-0.14	0.06	-0.03	*	-0.1	0.01	-0.02	0.04	0.11	*
6790	0.13	0.09	-	-	0.03	*	-0.16	0.08	-	-	-0.08	0.39	-0.1	0.05	0.01	0.16
6880	-0.07	0.06	-	-	-0.07	*	0.04	0.02	0.14	0.06	0.09	0.03	-0.16	0.04	-0.28	0.09
6910	0.41	0.09	0.56	0.05	0.53	*	0.21	0.06	0.18	0.03	0.19	*	0.27	0.07	0.46	0.13
7134	-0.28	0.07	-0.31	0.1	-	-	-0.47	0.02	-	-	-0.41	*	-0.3	0.03	-0.32	0.1
7449	-0.06	0.09	-0.18	0.15	-	-	-0.35	0.03	-0.14	0.05	-0.35	0.01	-0.21	0.04	-0.16	0.18
7661	0.1	0.07	-	-	0.12	*	0.09	0.12	0.16	0.05	0.11	0.01	-0.08	0.06	-0.2	0.13
8076	0.07	0.08	0.04	0.04	0.12	*	-0.13	0.02	-0.01	0.03	-0.1	0.01	-0.07	0.1	0.04	0.17
8129	0.05	0.07	-	-	-	-	-0.06	0.02	0.06	0.03	0.02	0.02	-0.08	0.04	-0.21	0.08
8406	-0.05	0.07	-	-	-	-	-0.18	0.03	-0.04	0.1	-0.13	0.02	-0.15	0.04	-0.26	0.04
9175	0.14	0.08	0.1	0.1	-	-	0.02	0.05	0.14	0.02	0.13	0.04	0.06	0.06	0.03	0.05
9782	0.14	0.08	0.08	0.17	0.17	*	-0.09	0.03	-0.03	0.04	-0.13	0.01	-0.02	0.05	0.12	0.18
9847	0.4	0.08	0.39	0.13	0.54	*	0.37	0.08	0.28	0.06	0.32	0.01	0.26	0.07	0.41	0.01
9905	0.23	0.09	-	-	0.41	0.08	0.46	0.05	0.25	0.09	0.4	0.01	0.08	0.06	-0.03	*
10008	0	0.07	-	-	0.32	*	0.05	0.03	0.15	0.11	0.07	*	-0.14	0.07	-0.38	0.04
10226	0.22	0.08	0.06	0.15	-	-	-0.06	0.01	0.04	0.01	-0.02	0.01	0.05	0.06	0.13	0.16
10370	-0.04	0.07	-0.24	0.01	-	-	-0.02	0.03	0.04	*	0	0.01	-0.1	0.04	-0.16	0.1
10519	-0.58	0.08	-0.4	0.16	-	-	-0.48	0.03	-	-	-0.24	0.01	-0.3	0.03	-0.4	0.02
10576	0.06	0.09	0.04	0.09	0.37	*	-0.17	0.06	-0.05	0.08	-0.12	0.01	-0.06	0.06	0.11	0.15
10611	0.08	0.08	-	-	0.11	*	0.14	0.14	0.16	0.1	0.14	0.05	-0.14	0.06	-0.45	0.19
10678	0.13	0.07	-0.15	0.08	0.17	*	0.12	0.01	0.15	0.03	0.12	*	0.01	0.04	-0.19	0.01
11264	0.15	0.07	-0.02	0.04	-	-	0.05	0.04	0.06	0.06	0.07	*	0.03	0.05	0.02	0.04
11754	0.31	0.08	0.36	0.04	0.37	0.09	0.14	0.23	0.19	0.02	0.21	0.11	0.22	0.07	0.37	0.12
12585	0.18	0.08	-0.12	0.21	0.15	*	0.08	0.07	0.13	0.02	0.1	0.03	0.05	0.05	0.01	*
12951	-0.13	0.08	0.04	0.1	-	-	-0.31	0.07	-	-	-0.31	0.04	-0.18	0.05	-0.02	0.15
13060	0.16	0.08	-	-	0.42	*	0.25	0.04	0.32	0.06	0.39	0.01	-0.02	0.05	-0.1	*

Continued on next page

Table A.3 – *Continued from previous page*

Star	[Fe/H]	±	[C/H]	±	[O/H]	±	[Na/H]	±	[Mg/H]	±	[Al/H]	±	[Si/H]	±	[S/H]	±
13350	0.47	0.1	0.32	0.1	0.66	0.11	0.49	0.15	0.4	0.06	0.47	0.01	0.34	0.08	0.33	0.08
13386	0.33	0.1	-	-	0.56	*	0.54	0.11	0.41	0.07	0.49	0.01	0.11	0.06	-0.12	*
14758	-0.13	0.07	-0.28	0.06	-	-	-0.28	0.03	-0.05	0.03	-0.18	*	-0.21	0.04	-0.25	0.02
15507	0.16	0.06	0.1	0.23	0.34	0.2	0.11	0.05	0.13	0.01	0.11	0.03	0.04	0.05	-0.03	0.04
15590	0.28	0.08	0.33	0.05	0.57	*	0.2	0.04	0.1	0.05	0.04	0.06	0.17	0.05	0.44	0.05
15767	-0.11	0.11	-0.27	*	0.45	*	0.24	0.05	0.14	0.22	0.26	0.04	-0.28	0.07	-	-
16950	0.28	0.09	0.5	0.14	0.43	*	0.14	0.08	0.04	0.06	0.07	0.05	0.17	0.09	0.36	0.1
17134	0.02	0.07	-0.07	0.11	-	-	-0.19	0.05	-0.04	0.02	-0.1	0.01	-0.12	0.03	-0.14	0.01
17289	-0.1	0.08	0.03	0.05	-	-	-0.31	0.02	-0.15	0.03	-0.22	0.04	-0.21	0.07	-0.16	0.15
18168	0	0.11	-0.27	*	0.02	*	0.38	0.04	0.25	0.21	0.31	0.09	-0.14	0.05	-0.11	*
18708	0.23	0.07	0.17	0.12	0.33	*	0.12	0.04	0.01	0.05	0.1	0.03	0.1	0.06	0.17	0.05
18754	0.29	0.09	0.25	0.08	0.33	0.09	0.35	0.15	0.24	0.03	0.25	0.04	0.24	0.08	0.32	0.06
18819	0.17	0.08	0.5	0.06	-	-	0	0.07	-0.01	0.08	-0.05	0.04	0.1	0.06	0.38	0.15
19603	0.33	0.08	0.49	0.07	0.38	*	0.13	0.01	0.07	*	0.03	0.04	0.13	0.06	0.37	0.12
19916	0.36	0.12	0.41	0.18	0.57	*	0.1	0.2	0.03	0.04	0.08	0.34	0.18	0.1	0.49	*
20155	0.28	0.09	0.51	0.07	0.36	*	0.11	0.08	0.01	0.03	0.04	0.05	0.12	0.06	0.39	0.16
20407	-0.45	0.1	-0.43	0.2	-	-	-0.43	0.01	-	-	-0.5	0.03	-0.37	0.09	-0.28	*
20584	0.24	0.1	0.31	0.22	0.36	*	-0.05	0.19	-0.03	*	0.03	*	0.07	0.09	0.35	0.25
20657	0.24	0.07	0.31	0.12	0.28	*	0.12	0.01	0.12	0.06	0.06	0.02	0.12	0.05	0.31	0.07
20675	0.27	0.13	0.47	0.07	0.2	0.23	0.18	0.13	0.08	0.11	0.09	0.06	0.12	0.06	0.37	0.06
21036	0.23	0.08	-	-	0.17	*	0.06	0.09	0.13	0.06	0.11	0.01	0.02	0.05	-0.09	*
21089	0.32	0.1	0.23	0.09	0.64	0.16	0.45	0.16	0.27	0.12	0.31	0.05	0.26	0.08	0.4	0.08
22177	0.3	0.07	0.17	0.1	0.53	*	0.22	0.08	0.26	*	0.29	0.04	0.17	0.05	0.19	0.08
22582	0.05	0.09	-0.31	0.19	0.07	0.03	0.1	0.04	0.21	0.04	0.22	0.04	-0.02	0.04	-0.21	0.17
23576	0.19	0.08	0.1	0.07	0.32	*	-0.14	0.11	-0.02	0.03	-0.1	0.02	-0.06	0.06	0.04	0.11
24331	-0.24	0.09	-0.33	*	-	-	0.19	0.03	0.2	0.13	0.23	0.03	-0.34	0.07	-	-
25912	0.22	0.09	-0.04	0.16	-0.08	*	-0.09	0.04	0.02	0.02	0	0.01	0	0.1	-0.02	0.14
26040	-0.01	0.11	0.01	0.22	-	-	-0.15	0.15	-0.14	*	-0.37	0.01	-0.22	0.06	0.12	*
26071	0.31	0.09	0.23	0.04	0.7	0.13	0.39	0.12	0.37	0.04	0.37	0.02	0.24	0.07	0.37	0.16
26864	0.13	0.1	-0.01	0.01	0.41	0.1	-0.08	0.1	0.08	0.11	-0.34	0.28	-0.01	0.09	-0.01	0.01
27328	0.18	0.12	-	-	-	-	0.26	0.08	0.3	0.07	0.22	0.09	0.04	0.1	-	-
27446	0.05	0.07	-0.21	0.14	-	-	-0.16	0.03	0.01	0.01	-0.08	0.06	-0.07	0.05	-0.12	0.01
27905	-0.08	0.08	-	-	-	-	-0.23	0.03	-0.09	0.02	-0.18	0.01	-0.19	0.06	-0.27	0.18
27939	0.28	0.09	0.24	0.05	0.33	*	0.28	0.13	0.22	0.04	0.23	0.11	0.2	0.08	0.34	0.18
28185	0.26	0.08	0.07	0.05	0.55	0.04	0.39	0.13	0.22	0.01	0.25	0.01	0.16	0.07	0.08	*
28701	-0.21	0.1	-0.26	0.1	-	-	-0.22	0.1	0.03	0.07	-0.1	0.02	-0.15	0.08	-0.21	0.03
28821	-0.08	0.07	-0.33	0.23	-	-	-0.19	0.03	0.04	0.02	-0.01	0.01	-0.11	0.03	-0.28	0.03

Continued on next page

Table A.3 – *Continued from previous page*

Star	[Fe/H]	±	[C/H]	±	[O/H]	±	[Na/H]	±	[Mg/H]	±	[Al/H]	±	[Si/H]	±	[S/H]	±
29231	0.23	0.1	-	-	0.22	0.04	0.27	0.04	0.26	0.06	0.23	0.04	0.09	0.08	-0.21	*
29263	0.12	0.1	0.1	0.11	-	-	0.01	0.04	0.08	0.07	0.02	0.05	0.01	0.04	0.08	0.01
29813	0.03	0.07	-0.21	0.16	-	-	-0.21	0.01	-0.05	0.01	-0.09	0.13	-0.12	0.04	-0.17	0.11
30278	-0.1	0.07	-	-	0.27	*	-0.03	0.08	0.1	0.14	0.09	*	-0.16	0.06	-0.54	*
30306	0.25	0.09	-	-	0.36	0.19	0.27	0.07	0.26	0.01	0.28	0.04	0.15	0.05	-	-
30501	0.03	0.09	-	-	0.13	*	0.26	0.01	0.22	0.11	0.28	0.01	-0.13	0.07	-	-
30669	0.19	0.08	-	-	0.56	0.03	0.27	0.06	0.28	0.07	0.33	0.02	0.06	0.06	-0.21	0.05
31392	0.11	0.07	-	-	-	-	0.24	0.04	0.23	0.06	0.22	*	0	0.05	-0.23	0.16
32564	0.1	0.09	-	-	0.25	*	0.06	0.04	0.13	0.06	0.12	0.01	-0.05	0.04	-0.2	*
32724	-0.16	0.07	-0.21	0.17	-	-	-0.23	0.04	-0.08	0.02	-0.14	0.04	-0.15	0.05	-0.25	0.23
32804	0.16	0.06	-0.08	0.14	0.04	*	-0.14	0.01	-0.01	0.05	-0.11	0.01	-0.04	0.05	-0.06	0.11
33093	0	0.08	0.06	0.09	0.33	*	-0.13	0.12	-0.13	*	-0.16	0.02	-0.08	0.05	0.07	0.08
33214	0.22	0.11	-	-	-	-	0.56	0.13	0.38	0.16	0.49	0.01	0.05	0.07	-	-
33822	0.34	0.08	0.26	0.04	0.46	*	0.33	0.12	0.33	0.01	0.3	*	0.23	0.06	0.37	0.06
33873	0.21	0.09	-0.02	*	0.19	*	0.13	0.07	0.15	0.04	0.13	0.03	0.06	0.06	0	0.01
34195	0.1	0.1	0.37	0.13	0.29	*	-0.1	0.05	0.01	0.18	-0.15	*	0.03	0.06	0.32	0.14
34230	0.27	0.08	-0.02	0.09	0.47	*	0.35	0.1	0.29	*	0.34	0.01	0.15	0.04	0	0.06
34377	0.15	0.07	-0.12	*	0.15	*	0.05	0.08	0.06	0.07	0.03	0.01	0.02	0.05	0.04	0.01
34599	0.22	0.07	-0.05	0.06	0.25	*	0.05	0.06	0.04	*	0	0.01	0.01	0.06	-0.01	0.11
35376	0.11	0.08	0.03	0.15	0.15	*	-0.01	0.04	0.08	*	0.18	0.22	0.01	0.05	-0.02	0.04
35676	0.2	0.07	-	-	0.09	*	0.16	0.13	0.2	0.1	0.13	0.03	0.03	0.06	-0.05	0.01
36152	0.15	0.08	0.03	0.19	-0.01	*	0	0.01	0.04	0.01	0.01	0.01	-0.01	0.05	-0.04	0.01
36329	0.17	0.11	-	-	-	-	-0.17	0.12	-0.14	0.23	-0.28	0.11	-0.09	0.08	-0.2	0.07
37351	0.13	0.05	0.02	0.12	0.35	*	-0.04	0.11	0.02	*	-0.11	0.08	-0.03	0.04	0.04	0.13
37706	-0.21	0.07	-	-	-	-	-0.14	0.09	-0.06	0.13	-0.12	0.01	-0.25	0.06	-0.6	*
37761	0.19	0.08	0.12	0.21	0.41	*	0.16	0.07	0.22	*	0.31	0.16	0.12	0.05	0.16	0.06
37986	0.35	0.09	-	-	0.56	0.23	0.49	0.1	0.32	*	0.41	0.04	0.22	0.08	0.22	0.23
38467	0.33	0.08	0.22	0.01	0.39	*	0.29	0.05	0.25	0.04	0.25	0.01	0.23	0.05	0.37	0.05
38554	0.29	0.09	0.14	0.04	0.53	0.1	0.38	0.15	0.27	0.01	0.29	0.06	0.16	0.06	0.19	0.06
38667	0.25	0.09	0.33	0.15	0.29	*	-0.01	*	0.16	0.08	-0.07	0.04	0.09	0.06	0.3	0.23
38677	0.23	0.08	0.36	0.04	0.35	*	-0.04	0.06	-0.04	0.02	-0.11	0.04	0.05	0.05	0.26	0.14
39126	0.09	0.09	-	-	0.29	*	0.16	0.06	0.21	0.13	0.17	0.01	-0.1	0.06	-0.31	0.21
39503	0.24	0.09	-0.11	0.21	0.5	0.03	0.31	0.14	0.2	0.09	0.26	0.04	0.11	0.06	0.02	*
39804	0.1	0.07	-0.24	0.02	-	-	-0.04	0.04	0.06	*	0.03	0.03	-0.04	0.05	-0.17	0.01
39855	-0.44	0.08	-	-	-	-	-0.33	0.04	-0.15	0.13	-0.29	0.01	-0.44	0.05	-	-
40105	0.1	0.1	-	-	0.59	0.21	0.43	0.13	0.37	0.01	0.45	0.01	0.06	0.06	-0.31	*
40403	0.44	0.08	0.39	0.16	0.52	0.01	0.36	0.14	0.24	0.03	0.28	0.01	0.26	0.06	0.42	0.06

Continued on next page

Table A.3 – *Continued from previous page*

Star	[Fe/H]	±	[C/H]	±	[O/H]	±	[Na/H]	±	[Mg/H]	±	[Al/H]	±	[Si/H]	±	[S/H]	±
41155	0.29	0.1	0.47	0.14	0.56	*	0.03	0.11	-0.01	0.03	-0.1	0.03	0.08	0.08	0.39	0.28
42044	0.04	0.12	0.3	0.04	0.4	*	-0.2	0.09	-	-	-0.36	0.04	-0.12	0.06	0.3	0.25
42287	0.17	0.08	0.06	0.05	0.22	*	-0.22	0.01	-0.1	*	-0.26	*	-0.08	0.07	0.22	*
42538	0.26	0.09	0.36	0.07	0.27	*	0	0.08	-0.03	0.13	0.06	0.01	0.09	0.08	0.25	0.24
42719	0.37	0.09	0.56	0.06	0.48	*	0.21	0.08	0.22	0.1	0.29	0.02	0.26	0.07	0.45	0.11
42778	0.25	0.09	0.08	0.03	0.35	*	0	0.11	-0.01	0.08	-0.08	0.01	0.05	0.06	0.13	0.2
43470	0.12	0.14	0.16	0.12	0.35	*	-0.15	0.13	-	-	-0.25	0.05	-0.09	0.07	0.1	0.17
44569	-0.15	0.06	-0.21	0.08	-	-	-0.28	*	-0.08	0.08	-0.15	0.04	-0.17	0.05	-0.18	0.03
44573	0.02	0.08	-	-	-	-	0.43	0.14	0.21	0.18	0.36	0.04	-0.15	0.06	-	-
45133	0.4	0.09	0.22	0.08	0.43	0.02	0.39	0.04	0.26	0.03	0.32	0.01	0.26	0.06	0.26	0.01
45987	0.33	0.11	0.19	0.14	0.61	0.1	0.14	0.04	0.22	0.03	0.18	0.06	0.15	0.04	0.3	0.01
46175	0.22	0.08	0.17	0.12	0.31	*	-0.06	0.05	-0.13	*	-0.09	0.07	0.01	0.05	0.15	0.22
46435	0.23	0.12	0.25	0.21	0.35	*	-0.01	0.08	-	-	-0.06	0.12	-0.01	0.07	0.19	0.04
46894	0.16	0.1	-0.04	0.16	0.38	0.01	0.29	0.02	0.18	0.03	0.29	0.02	0.13	0.06	0	0.1
47017	0.15	0.1	0.53	0.1	0.55	*	0.09	0.05	0.09	0.02	-0.02	*	0.07	0.07	0.46	0.12
47186	0.29	0.08	-0.03	0.24	0.56	0.11	0.41	0.08	0.23	0.09	0.29	0.04	0.17	0.06	0.12	0.01
48056	0.13	0.1	0.19	0.13	0.34	*	-0.11	0.06	-0.05	0.01	-0.11	0.05	-0.03	0.07	0.13	0.11
48265	0.42	0.09	0.37	0.06	0.68	0.11	0.52	0.16	0.26	0.02	0.38	0.01	0.34	0.08	0.47	0.02
49035	0.34	0.09	-0.03	0.24	-	-	0.41	0.13	0.29	0.08	0.34	0.01	0.2	0.05	0.16	0.13
49866	0.15	0.08	0.26	0.07	0.43	*	0.07	0.13	0.02	0.11	0.04	0.01	0.07	0.05	0.34	0.12
50117	0.12	0.07	0.14	0.12	0.32	0.09	-0.05	0.04	-0.02	*	-0.07	0.05	-0.01	0.05	0.11	0.13
50255	-0.02	0.11	-	-	-	-	-0.12	0.17	-0.06	0.06	-0.18	0.09	-0.14	0.06	-0.34	0.09
50652	0.36	0.09	0.12	0.19	0.43	*	0.25	0.06	0.24	0.05	0.3	0.01	0.18	0.05	0.26	0.04
51608	0.04	0.08	-	-	-	-	0.09	0.08	0.22	0.01	0.2	0.02	-0.06	0.06	-0.21	0.16
52217	0.28	0.11	-0.01	0.08	-	-	0.37	0.05	0.31	0.01	0.31	0.01	0.14	0.04	0.14	0.18
52756	0.19	0.12	-	-	-	-	0.61	0.17	0.35	0.13	0.53	0.04	0.02	0.07	-	-
56413	0.38	0.09	-	-	0.29	*	0.23	0.08	0.23	0.01	0.25	0.01	0.18	0.12	0.06	0.03
56662	-0.11	0.08	-	-	0.34	*	-0.21	0.1	-	-	-0.24	0.01	-0.2	0.05	-0.13	0.13
56972	0.31	0.08	-0.06	0.21	0.45	0.08	0.28	0.11	0.28	0.01	0.29	0.03	0.18	0.06	0.22	0.04
58111	0.04	0.12	-	-	0.19	*	0.39	*	0.27	0.2	0.34	0.01	-0.12	0.07	-	-
58556	0.05	0.09	-0.01	0.19	0.24	*	-0.22	0.13	-	-	-0.31	0.01	-0.09	0.06	-0.08	0.3
58696	0.02	0.09	0.1	0.08	0.2	*	-0.12	0.08	-0.06	0.03	-0.13	0.01	-0.07	0.04	0.13	0.01
59711	-0.07	0.07	-0.34	0.2	0.24	*	-0.12	0.07	-0.08	0.07	-0.13	0.01	-0.15	0.05	-0.29	0.11
59824	0.29	0.07	0.31	0.19	0.32	0.17	0.12	0.04	0.16	0.04	0.12	0.01	0.11	0.05	0.17	0.04
61051	0.06	0.07	-	-	0.23	*	0.15	0.07	0.24	0.03	0.3	0.01	-0.03	0.03	-0.15	0.15
61475	0.28	0.1	-	-	-	-	0.33	0.08	0.35	0.14	0.43	0.03	0.13	0.05	-0.17	*
62549	0.04	0.08	-0.03	0.14	0.12	*	-0.16	0.02	-0.03	0.04	-0.1	0.03	-0.05	0.04	0.06	0.01

Continued on next page

Table A.3 – *Continued from previous page*

Star	[Fe/H]	±	[C/H]	±	[O/H]	±	[Na/H]	±	[Mg/H]	±	[Al/H]	±	[Si/H]	±	[S/H]	±
62644	0.09	0.07	-0.19	0.15	-	-	0.14	0.02	0.11	0.07	0.15	0.04	0.06	0.04	0.01	0.04
64114	0.05	0.06	-	-	0.12	*	-0.05	0.01	0.08	*	-	-	-0.07	0.06	-0.17	0.01
64144	0.01	0.08	-	-	0.03	*	0	0.09	0.05	0.07	-0.01	0.01	-0.09	0.04	-0.17	0.18
65427	0.08	0.07	0.2	0.12	0.24	*	0.09	0.05	0.07	*	0.09	0.01	0.01	0.07	0.13	0.11
66039	0.24	0.08	0.11	0.09	0.11	*	-0.14	0.03	-0.05	0.08	-0.12	0.06	0.01	0.07	0.13	0.25
66058	0.17	0.08	0.18	0.05	0.12	*	0.07	0.07	0.05	0.05	0.03	0.03	0.04	0.04	0.14	0.13
66791	0.13	0.07	0.16	0.04	0.13	*	0.05	0.06	0.14	0.01	0.05	0.02	0.07	0.05	0.11	*
70081	0.19	0.09	0.27	0.07	0.42	0.18	0.1	0.04	0.15	0.06	0.12	0.03	0.11	0.04	0.24	*
72579	0.31	0.09	-	-	0.44	0.01	0.37	0.08	0.32	0.06	0.37	0.01	0.15	0.05	0.04	0.08
72687	0.02	0.11	-0.3	0.01	-	-	-0.24	0.12	-0.07	0.08	-0.06	0.21	-0.13	0.05	-0.17	*
72892	0.23	0.12	0.09	0.01	0.3	0.02	0.1	0.17	0.17	0.04	0.18	0.03	0.09	0.05	0.1	0.01
73267	0.13	0.09	-	-	-	-	0.26	0.08	0.33	0.07	0.33	0.07	0.01	0.06	0.05	*
73744	-0.3	0.07	-0.41	0.17	-	-	-0.46	0.04	-	-	-0.36	0.06	-0.3	0.04	-0.29	0.04
74698	0.15	0.07	0.12	0.06	0.12	*	-0.01	0.05	0.11	0.04	0.06	0.01	0.04	0.05	0.15	0.08
74733	-0.1	0.08	-	-	-	-	-0.27	0.01	-0.14	0.04	-0.26	0.02	-0.21	0.05	-0.1	0.03
74935	0.14	0.08	0.17	0.11	0.19	*	-0.05	0.08	-0.07	0.04	-0.15	0.03	-0.01	0.05	0.17	0.11
75288	0.18	0.08	0.08	0.07	0.19	*	0.12	0.05	0.09	0.05	0.13	0.01	0.06	0.04	-0.01	0.02
75351	0.18	0.09	0.34	0.07	0.42	*	0.16	0.16	0.09	0.02	0.07	0.02	0.14	0.07	0.3	0.13
77338	0.32	0.13	-0.07	0.06	-	-	0.66	*	0.37	0.1	0.45	0.01	0.2	0.06	0.02	0.14
77417	0.33	0.09	-0.02	0.08	-	-	0.36	0.07	0.31	0.01	0.37	0.01	0.18	0.05	0.17	0.16
77683	0.27	0.09	-	-	0.41	*	0.36	0.15	0.35	0.01	0.38	0.03	0.17	0.07	-	-
78130	0.21	0.08	0.04	0.01	0.01	*	0.13	0.06	0.1	0.01	0.04	0.01	0.06	0.04	0.07	0.08
78286	0.29	0.09	0.2	0.03	0.52	*	0.2	0.11	0.19	0.03	0.17	0.04	0.16	0.05	0.21	0.05
79985	0.08	0.1	0.13	0.19	0.4	*	-0.05	0.04	-0.01	0.04	-0.01	0.06	-0.02	0.05	0.1	0.06
81110	0.34	0.08	0.16	*	0.41	0.15	0.31	0.12	0.2	0.01	0.22	0.03	0.17	0.07	0.16	0.12
81700	0.2	0.07	-0.13	0.1	0.03	*	-0.01	0.05	0.03	0.03	-0.03	0.01	0	0.04	-0.04	0.11
82282	-0.04	0.12	-	-	-	-	0.16	0.04	0.16	0.16	0.08	0.05	-0.16	0.07	-0.35	*
82400	0.12	0.1	-0.12	0.01	0.16	*	0.03	*	0.05	0.08	0	0.1	-0.05	0.06	-0.05	0.09
82516	0.09	0.1	-0.29	*	0.39	*	0.5	0.06	0.31	0.15	0.43	0.01	-0.1	0.06	-	-
82977	0.02	0.1	-	-	-	-	0.05	0.12	0.16	0.08	0.11	0.04	-0.12	0.05	-	-
83365	0.15	0.09	0.1	0.11	0.25	*	-0.01	*	0.05	0.02	-0.01	*	0.04	0.05	0.14	0.1
83517	-0.01	0.06	0.01	*	-	-	0.09	0.16	0.04	*	-0.03	0.09	-0.04	0.03	-0.05	*
84652	0.06	0.08	0.1	0.14	0.5	*	-0.1	*	-	-	-0.29	0.04	-0.08	0.08	0.18	0.01
85380	0.12	0.09	0.3	0.13	0.29	*	-0.12	0.04	0.02	0.14	-0.1	0.08	0.02	0.07	0.3	0.11
85390	0.01	0.08	-	-	-	-	-	-	-	-	0.29	*	-0.12	0.05	-0.46	*
86006	0.37	0.08	0.39	0.06	0.5	0.18	0.36	0.11	0.25	0.02	0.28	*	0.25	0.06	0.38	0.02
86226	-0.01	0.05	-0.05	*	-	-	-0.17	0.03	-	-	-0.16	*	-0.08	0.04	0.04	*

Continued on next page

Table A.3 – *Continued from previous page*

Star	[Fe/H]	±	[C/H]	±	[O/H]	±	[Na/H]	±	[Mg/H]	±	[Al/H]	±	[Si/H]	±	[S/H]	±
86249	0.11	0.11	-	-	-	-	0.51	0.09	0.28	0.17	0.46	*	-0.12	0.09	-	-
86397	0.24	0.09	0.03	0.11	0.33	*	0.13	0.15	0.23	0.03	0.24	0.01	0.11	0.05	0.08	0.12
86652	0.12	0.09	0.14	0.2	0.06	*	0	0.04	0	0.01	-0.02	0.03	0	0.08	0.11	0.05
87931	0.12	0.07	-	-	0.35	*	0.15	0.07	0.18	0.03	0.16	0.03	-0.02	0.05	-0.17	0.11
87998	-0.14	0.07	-0.14	*	-	-	-0.31	0.05	-0.08	*	-0.18	0.03	-0.19	0.04	-0.16	*
88864	0.07	0.08	0.31	*	-	-	0.18	*	0.03	*	0.08	0.28	0.02	0.05	0.24	*
89178	0.07	0.11	-0.18	0.02	-	-	0.04	0.09	0.15	0.03	0.16	0.02	0.02	0.06	-0.1	0.18
89418	-0.15	0.1	-	-	-	-	-0.32	0.07	-	-	-0.37	0.04	-0.2	0.06	-0.16	0.2
89988	0.2	0.08	0.2	0.15	0.31	0.05	0.16	0.07	0.14	0.09	0.11	*	0.14	0.05	0.32	0.05
90028	0.32	0.09	0.46	0.06	0.59	*	0.52	*	0.22	0.05	0.19	0.02	0.21	0.07	0.39	0.09
90702	0.23	0.11	0.03	0.06	0.12	*	0.24	*	0.2	0.01	0.15	0.04	0.12	0.04	0.11	0.15
91320	0.12	0.08	0.29	0.21	0.5	*	0.06	0.06	-0.05	0.01	-0.09	0.01	0	0.06	0.25	0.14
91901	0.02	0.08	-0.31	*	0.58	*	0.26	0.1	0.27	0.18	0.3	0.02	-0.17	0.07	-	-
92069	0.23	0.08	0.13	0.08	0.31	0.01	0.15	0.09	0.22	0.01	0.27	0.01	0.14	0.05	0.13	0.04
92719	-0.11	0.06	-	-	-	-	-0.23	0.04	-0.06	*	-0.16	0.01	-0.15	0.04	-0.23	*
93083	0.19	0.1	-	-	0.46	0.22	0.6	0.05	0.39	0.1	0.59	0.03	0	0.06	-	-
94151	0.11	0.05	-0.2	*	-	-	0.12	0.06	-	-	0.09	0.01	0.03	0.05	-0.13	*
94387	0.33	0.09	-	-	0.5	0.05	0.5	0.13	0.37	0.04	0.4	0.01	0.19	0.07	-	-
94482	0.02	0.09	0.11	0.14	0.31	*	-0.11	*	-	-	-0.23	0.04	-0.1	0.07	0.02	0.31
94527	-0.11	0.07	-0.45	0.13	-	-	-0.12	0.05	0.03	0.08	-0.14	0.06	-0.18	0.04	-0.34	0.18
94690	0.33	0.09	0.27	0.06	0.29	0.01	0.29	0.06	0.2	*	0.22	*	0.2	0.06	0.29	0.06
94838	0.12	0.07	-0.07	0.05	-	-	-0.18	0.04	-0.02	0.01	-0.14	0.01	-0.05	0.05	-0.09	0.12
95136	0.23	0.08	-0.05	0.21	0.14	0.02	0.1	0.1	0.13	0.05	0.14	0.01	0.09	0.06	0.16	0.01
95338	0.17	0.09	-	-	-	-	0.45	0.05	0.35	0.08	0.44	0.02	0.02	0.04	-0.34	0.05
95521	-0.14	0.06	-0.38	*	-	-	-0.19	*	-	-	-0.18	0.03	-0.17	0.04	-0.24	*
95533	0.26	0.08	-	-	0.24	0.18	0.29	0.1	0.28	*	0.38	0.01	0.1	0.06	-	-
95542	0.02	0.08	-0.17	0.13	-	-	-0.31	0.02	-	-	-0.32	0.02	-0.15	0.05	-0.15	0.09
96020	0.43	0.1	0.07	0.14	0.33	*	0.36	0.05	0.36	0.01	0.38	0.02	0.24	0.07	0.35	*
96276	-0.01	0.07	0.05	0.05	0.18	*	-0.14	0.05	-	-	-0.23	0.02	-0.14	0.05	-0.01	0.16
98163	0.17	0.08	0.14	0.02	0.24	*	0.05	0.05	0.16	0.03	0.11	0.03	0.09	0.04	0.17	0.02
98459	0.22	0.08	0.27	0.11	0.29	*	0.12	0.02	0.1	0.03	0.1	0.02	0.11	0.05	0.3	0.08
98764	0.14	0.08	-0.08	0.06	0.13	*	-0.13	0.04	0.01	0.01	-0.07	0.01	-0.02	0.05	-0.02	0.08
99116	-0.01	0.08	-0.38	0.17	-	-	0.02	0.01	0.09	0.06	0.01	0.01	-0.11	0.04	-0.31	*
101093	-0.08	0.08	-0.16	0.01	-	-	-0.35	0.06	-	-	-0.35	0.01	-0.22	0.04	-0.11	0.02
101171	-0.02	0.07	-	-	-	-	0.1	0.01	0.13	0.04	0.12	0.03	-0.1	0.05	-0.3	0.13
101181	0.23	0.07	-	-	0.4	0.01	0.29	0.01	0.17	0.05	0.17	*	0.12	0.06	0.08	0.04
101896	0.29	0.11	-	-	0.39	*	0.42	0.14	0.42	0.1	0.41	0.08	0.09	0.06	-	-

Continued on next page

Table A.3 – *Continued from previous page*

Star	[Fe/H]	±	[C/H]	±	[O/H]	±	[Na/H]	±	[Mg/H]	±	[Al/H]	±	[Si/H]	±	[S/H]	±
102574	0.23	0.1	0.31	0.12	0.44	*	-0.02	0.11	0.02	0.01	-0.1	0.11	0.1	0.08	0.36	0.11
102579	0.09	0.08	-0.22	*	-	-	0.38	0.03	0.32	0.16	0.31	0.01	-0.05	0.07	-0.14	*
102843	0.27	0.1	-	-	-	-	0.32	0.08	0.48	0.16	0.37	0.01	0.1	0.05	-0.12	*
103559	0.05	0.08	-0.32	0.01	-	-	-0.12	0.05	0.04	*	0	0.01	-0.06	0.04	-0.19	0.13
103673	0.1	0.08	-	-	-	-	-0.13	0.19	0.08	0.04	-0.04	0.02	-0.09	0.05	-0.27	0.04
104645	0.12	0.08	-	-	0.67	*	0.27	0.04	0.21	0.06	0.22	0.01	0.04	0.04	-0.05	0.25
104760	0.17	0.08	0.15	0.07	0.11	*	-0.01	0.04	-0.01	0.05	-0.03	0.03	0.05	0.04	0.17	0.01
104982	-0.18	0.06	-0.4	*	-	-	-0.16	*	-	-	-0.13	0.01	-0.19	0.04	-0.28	*
105690	0.05	0.1	-	-	-	-	-0.12	0.08	-0.07	0.21	-0.09	0.32	-0.11	0.07	-0.28	*
105904	0.33	0.08	0.13	0.05	0.65	0.13	0.32	0.11	0.31	0.04	0.26	0.01	0.17	0.06	0.28	0.06
106275	0.03	0.11	-0.36	*	0.25	*	0.34	0.07	0.3	0.16	0.39	0.03	-0.17	0.06	-	-
106869	0.13	0.08	0.18	0.14	0.4	*	-0.05	0.06	-	-	-0.11	0.01	-0.01	0.07	0.15	0.26
106937	0.39	0.09	0.16	0.08	0.56	0.06	0.38	0.06	0.35	0.01	0.43	0.01	0.27	0.07	0.26	0.11
107008	0.29	0.08	-	-	0.44	0.14	0.53	0.05	0.35	0.01	0.35	0.07	0.15	0.08	0.02	*
107181	0.39	0.08	0.28	0.02	0.59	0.08	0.38	0.06	0.31	0.01	0.35	0.02	0.29	0.07	0.33	0.02
108953	0.43	0.12	-	-	-	-	0.59	0.1	0.42	0.03	0.45	0.02	0.32	0.18	-	-
109591	-0.04	0.07	-0.09	0.14	-0.04	*	-0.02	0.05	0.07	0.13	0.07	0.02	-0.04	0.06	-0.14	0.09
109908	0.1	0.08	0	0.19	0.01	*	-0.13	0.06	-0.09	0.01	-0.22	0.06	-0.05	0.08	-0.02	0.18
109930	0.09	0.08	-	-	0.16	*	0.32	0.06	0.28	0.08	0.37	0.04	-0.03	0.06	-0.32	*
109988	0.27	0.11	-	-	-	-	0.66	0.09	0.42	0.06	0.54	0.04	0.1	0.07	-	-
110605	0.36	0.08	0.07	0.11	0.41	0.12	0.49	0.04	0.26	0.03	0.29	0.01	0.22	0.06	0.12	0.07
110619	-0.36	0.08	-	-	-	-	-0.29	0.02	-0.18	0.14	-0.3	0.04	-0.35	0.05	-0.42	*
111431	0.12	0.08	0.25	0.04	0.3	*	0	0.06	0.05	0.01	-0.05	0.04	0.02	0.06	0.2	0.07
112121	0.28	0.09	-0.08	0.17	0.45	0.18	0.26	0.05	0.21	*	0.25	0.06	0.14	0.06	0.13	0.02
112540	-0.07	0.08	-	-	-	-	-0.03	0.04	0.05	0.05	-0.07	0.01	-0.17	0.05	-0.23	0.07
113027	-0.03	0.06	0.11	*	-	-	-0.22	*	-	-	-0.3	0.03	-0.11	0.05	0.16	*
113255	0.19	0.08	0.06	0.17	0.27	*	-0.02	0.07	0.03	0.04	0.04	0.08	0.02	0.08	0.11	0.16
113513	0.18	0.07	-	-	-	-	-0.01	0.08	-0.04	*	0.02	0.02	-0.04	0.05	-0.12	0.08
114294	0.16	0.09	-	-	0.22	0.14	0.19	0.11	0.2	0.08	0.27	0.01	0.09	0.06	0.03	0.11
114432	0.17	0.07	-0.16	*	-	-	0.2	*	-	-	0.12	0.01	0.05	0.04	-0.07	*
114884	0.27	0.07	0.16	0.1	-	-	0.12	0.11	0.06	*	0.07	0.01	0.1	0.04	0.2	0.11
115080	-0.17	0.06	-0.14	*	-	-	-0.05	0.07	0.08	*	0.14	0.11	-0.09	0.03	-	-
115674	-0.18	0.06	-0.42	*	-	-	-0.19	*	-	-	-0.16	0.02	-0.2	0.04	-0.33	*
116920	-0.1	0.1	-0.37	*	-	-	0.26	0.06	0.21	0.21	0.23	0.06	-0.31	0.08	-	-
117653	0.17	0.06	0.28	0.06	0.34	*	0.04	0.11	0.06	*	-0.01	0.02	0.05	0.06	0.36	*
117860	0.1	0.06	-0.04	*	-	-	-0.1	0.04	-0.01	*	-0.15	0.01	-0.03	0.05	0.12	*
119070	-0.04	0.09	-0.43	0.07	-	-	0.13	0.03	0.13	0.06	0.12	0.04	-0.13	0.05	-0.29	0.12

Continued on next page

Table A.3 – *Continued from previous page*

Star	[Fe/H]	±	[C/H]	±	[O/H]	±	[Na/H]	±	[Mg/H]	±	[Al/H]	±	[Si/H]	±	[S/H]	±
119119	0.17	0.08	0.34	0.09	0.26	*	-0.21	0.04	-	-	-0.17	0.05	-0.03	0.07	0.25	0.26
119507	0.15	0.08	0.11	0.12	0.18	0.04	0.11	0.06	0.18	0.02	0.18	*	0.07	0.06	0.15	0.04
119782	0.04	0.09	-0.31	*	-	-	0.27	0.01	0.22	0.13	0.28	0.01	-0.11	0.05	-0.39	*
120100	0.29	0.08	-	-	0.43	0.02	0.3	0.08	0.32	0.04	0.37	0.01	0.17	0.06	0.1	0.18
120329	0.4	0.15	0.34	0.15	0.55	0.19	0.46	*	0.32	0.04	0.4	0.04	0.26	0.07	0.18	*
121504	0.13	0.07	0.14	0.11	0.26	*	-0.06	0.03	0	0.02	-0.08	*	0.01	0.05	0.13	0.11
122078	0.31	0.08	0.31	0.03	0.38	*	0.28	0.09	0.21	0.02	0.2	0.05	0.21	0.06	0.37	0.05
124553	0.19	0.08	0.33	0.07	0.54	*	0.2	0.1	0.03	0.01	0	0.02	0.06	0.1	0.28	0.21
125968	0.17	0.09	0.19	0.05	0.32	0.08	0.06	0.06	0.04	0.06	0.07	0.01	0.05	0.07	0.19	0.11
126653	0.07	0.12	0.17	0.09	0.46	*	-0.14	0.09	-	-	-0.43	0.03	-0.11	0.07	0.08	0.31
127321	0.13	0.09	0.23	0.02	0.14	*	-0.16	0.06	-0.1	0.01	-0.18	0.09	-0.07	0.06	0.13	0.16
128214	0.36	0.13	0.31	0.06	0.67	0.15	0.43	*	0.27	0.02	0.25	0.02	0.24	0.09	0.37	0.01
128760	0.16	0.1	0.13	0.19	0.15	*	-0.02	*	-	-	-0.21	0.11	-0.01	0.08	0.27	0.18
128987	0.05	0.07	-	-	0.14	*	0.05	0.09	0.09	0.12	0.02	0.04	-0.08	0.06	-0.33	0.05
129679	0.07	0.12	0	0.15	-	-	-0.16	*	-0.22	0.16	-0.39	*	-0.13	0.09	-0.17	0.16
129764	0.18	0.07	0.07	0.13	0.22	*	-0.06	0.02	-0.01	0.08	-0.06	*	0.02	0.05	0.08	0.16
129946	-0.08	0.08	-0.48	0.08	-	-	-0.39	0.11	-0.07	0.06	-0.17	0.01	-0.2	0.06	-0.33	0.04
131900	0.2	0.08	-0.07	0.25	0.43	0.01	0.44	0.01	0.26	0.08	0.3	*	0.1	0.04	-0.02	0.19
132648	-0.33	0.06	-	-	-	-	-0.09	0.13	-0.2	*	-0.17	0.01	-0.32	0.05	-	-
133014	0.38	0.1	0.22	0.09	0.51	0.1	0.3	0.09	0.41	0.09	0.37	0.03	0.25	0.05	0.36	0.01
135005	0.17	0.07	-0.02	0.06	0.32	*	0.12	0.05	0.11	0.03	0.14	0.02	0.1	0.05	0.12	0.04
135309	0.23	0.07	-	-	0.32	0.05	-0.1	0.06	0.01	*	0	0.13	0.04	0.05	-0.08	0.04
135562	0.24	0.11	0.32	0.09	0.44	*	0.09	0.05	0.02	0.04	-0.02	0.01	0.09	0.06	0.28	0.18
135625	0.17	0.09	0.23	0.08	0.28	*	0.02	0.03	0.09	0.08	0	0.04	0.05	0.06	0.14	0.06
135725	0.03	0.07	-	-	-	-	-0.01	0.09	0.04	0.08	-0.01	0.01	-0.09	0.06	-0.21	0.01
136130	0.05	0.07	-0.12	0.07	0.23	0.17	0	0.05	0.07	0.01	0.1	0.01	0.01	0.05	-0.03	0.16
136548	-0.01	0.08	-0.09	0.02	-	-	-0.27	0.06	0.05	0.02	-0.1	0.02	-0.07	0.05	-0.09	0.01
136894	-0.07	0.05	-0.47	*	-0.22	*	0.05	0.09	-	-	0.09	*	-0.12	0.04	-0.29	*
137214	0.17	0.09	0.26	0.06	0.32	*	-0.11	0.04	-	-	-0.16	0.03	0.01	0.08	0.17	0.18
140643	0.2	0.12	-	-	0.4	0.18	0.62	0.06	0.4	0.1	0.59	0.05	0.05	0.06	-0.29	0.04
141105	-0.13	0.08	-0.34	0.02	0.29	*	0.01	0.02	-0.02	0.01	0.03	0.01	-0.14	0.09	-0.24	0.18
141366	0.22	0.12	0.22	0.1	0.46	*	0.16	*	0.14	0.09	0.27	0.35	0.16	0.08	0.33	0.18
141514	0.13	0.08	0.22	0.16	0.55	*	-0.1	0.12	-	-	-0.16	0.04	-0.04	0.06	0.15	0.23
141598	-0.04	0.07	-0.15	0.11	0.11	*	-0.01	0.08	0.1	0.02	0.06	0.03	-0.06	0.05	-0.16	0.01
141599	0.3	0.09	-	-	0.17	*	0.28	0.04	0.23	0.05	0.26	0.01	0.16	0.05	0.13	0.05
141885	0.37	0.12	0.62	0.11	0.61	*	0.17	0.2	0.23	0.07	0.26	0.32	0.27	0.11	0.47	0.15
142137	0.3	0.12	0.47	0.17	-	-	0.21	0.12	0.12	0.01	0.09	0.09	0.22	0.1	0.48	0.1

Continued on next page

Table A.3 – *Continued from previous page*

Star	[Fe/H]	±	[C/H]	±	[O/H]	±	[Na/H]	±	[Mg/H]	±	[Al/H]	±	[Si/H]	±	[S/H]	±
143120	0.38	0.11	0.3	0.01	-	-	-	-	0.34	0.05	0.39	0.01	0.28	0.06	0.38	0.04
143137	0.21	0.12	0.43	0.2	0.6	0.1	-0.14	0.21	-	-	-0.07	0.08	0.05	0.07	0.35	0.25
143295	0.07	0.1	-	-	0.31	0.06	0.36	0.1	0.25	0.22	0.35	0.01	-0.16	0.08	-	-
143673	0.23	0.09	-	-	0.3	0.18	0.21	0.09	0.25	0.09	0.29	0.06	0.08	0.06	0.16	0.08
144087	0.18	0.1	-	-	0.49	*	0.12	0.08	0.17	0.11	0.12	0.01	-0.01	0.05	-0.04	0.16
144088	0.17	0.12	-	-	0.61	*	0.28	0.11	0.26	0.17	0.27	*	-0.04	0.06	-0.41	*
144167	0.43	0.11	0.51	0.09	0.59	0.13	0.34	0.19	0.29	0.08	0.28	0.04	0.31	0.09	0.34	*
144550	0.3	0.1	0.26	0.04	0.5	0.06	0.34	0.08	0.26	0.01	0.24	0.01	0.24	0.06	0.38	0.16
144848	0.27	0.08	0.19	0.06	0.53	0.02	0.2	0.05	0.18	0.01	0.15	0.05	0.14	0.07	0.33	0.01
144899	0.35	0.09	0.4	0.01	-	-	0.37	0.08	0.21	0.1	0.19	0.07	0.25	0.08	0.5	0.14
145518	-0.03	0.08	-0.15	0.07	-	-	-0.2	0.01	-0.13	0.03	-0.24	0.06	-0.16	0.06	-0.12	0.14
145666	-0.02	0.08	-0.13	0.07	-	-	-0.18	0.06	-0.14	0.06	-0.25	0.06	-0.14	0.06	-0.19	0.23
146817	-0.06	0.08	-	-	0.44	*	0.02	0.06	0.13	0.05	0.09	0.01	-0.04	0.05	-0.01	0.07
146835	-0.21	0.1	-0.22	0.08	-	-	-0.26	0.04	-	-	-0.48	*	-0.26	0.09	-0.05	*
147018	0.22	0.09	-	-	0.61	*	-	-	0.23	0.1	0.27	0.04	0.05	0.06	0.04	0.15
147619	0.25	0.1	0.43	0.18	-	-	0.15	0.06	0.1	0.04	0.03	0.05	0.12	0.07	0.48	0.23
148156	0.24	0.09	0.37	0.12	0.34	*	0.07	0.08	0.03	0.04	-0.09	0.1	0.1	0.06	0.23	0.08
148628	-0.05	0.13	0.16	0.15	0.5	*	-0.37	0.02	-	-	-0.33	0.12	-0.21	0.03	-	-
149189	0.34	0.1	0.46	0.11	0.56	*	0.29	0.01	0.17	0.04	0.13	0.02	0.22	0.06	0.44	0.11
150761	0.28	0.16	0.5	0.17	-	-	0.16	0.24	0.06	0.03	0.1	0.11	0.17	0.1	0.2	*
151450	-0.02	0.1	-0.09	0.14	0.19	*	-0.13	0.04	-	-	-0.27	0.01	-0.13	0.05	-0.04	0.23
152388	0.1	0.09	-	-	-0.25	*	0.2	0.05	0.19	0.12	0.2	0.02	-0.07	0.04	-0.32	*
153631	-0.07	0.07	-0.07	0.07	0.03	*	-0.12	0.01	-0.11	0.01	-0.16	0.01	-0.14	0.03	-0.08	0.06
154682	-0.07	0.08	0.04	0.14	-	-	-0.31	0.04	-	-	-0.25	0.01	-0.15	0.04	-0.08	0.09
154697	0.17	0.08	-	-	0.02	*	0.14	0.06	0.15	0.06	0.13	0.02	0.04	0.05	-0.04	0.04
156152	0.09	0.07	0.01	0.18	0.33	*	-0.06	0.07	0.01	0.05	0.07	0.03	-0.02	0.05	0.08	0.09
156643	-0.22	0.07	-0.31	0.08	0.05	*	-0.22	0.08	-0.19	0.06	-0.26	0.01	-0.24	0.05	-0.42	0.14
157798	0.29	0.14	0.24	0.17	0.46	*	-	-	0.17	0.11	0.1	0.06	0.14	0.1	0.32	0.09
157830	-0.17	0.06	-0.54	0.09	-	-	-0.19	0.04	-0.06	0.1	-0.16	0.05	-0.23	0.05	-0.45	0.06
158469	0.07	0.1	0.19	0.16	0.54	*	-0.2	*	-	-	-0.17	0.07	-0.1	0.04	0.14	0.23
158630	-0.14	0.07	-	-	-	-	-0.36	0.01	-	-	-0.28	0.01	-0.21	0.05	-0.2	0.13
159902	-0.19	0.07	-0.4	0.12	-	-	-0.28	0.02	-0.13	0.05	-0.22	0.05	-0.24	0.06	-0.36	0.14
160411	0.22	0.1	0.32	0.07	0.38	0.21	0.1	0.08	0.06	0.03	0.04	0.01	0.1	0.06	0.36	0.14
160859	-0.04	0.07	-0.34	0.11	-	-	-0.25	0.01	-0.03	0.02	-0.15	0.05	-0.14	0.04	-0.17	0.06
161098	-0.2	0.06	-	-	-	-	-0.22	0.01	-0.05	0.01	-0.17	0.04	-0.25	0.04	-0.35	0.06
162907	0.21	0.09	-0.05	0.12	0.17	*	0.27	0.08	0.36	0.05	0.25	0.06	0.14	0.07	-0.11	*
165011	0.16	0.08	0.39	0.14	0.43	*	-0.12	0.04	-	-	-0.17	0.06	0	0.07	0.32	0.25

Continued on next page

Table A.3 – *Continued from previous page*

Star	[Fe/H]	±	[C/H]	±	[O/H]	±	[Na/H]	±	[Mg/H]	±	[Al/H]	±	[Si/H]	±	[S/H]	±
165204	0.35	0.09	0.07	0.16	0.37	0.06	0.27	0.05	0.3	0.01	0.36	0.02	0.2	0.06	0.23	0.06
165271	0.12	0.07	0.13	0.12	0.28	*	0.06	0.07	0.04	0.02	0.06	0.02	0.07	0.06	0.16	0.04
165385	0.07	0.11	0.27	0.14	0.44	*	-0.03	0.01	-	-	-0.28	0.01	-0.06	0.07	0.21	0.21
165449	-0.05	0.07	-0.05	0.11	0.02	*	-0.2	0.01	-0.07	0.06	-0.18	0.01	-0.12	0.05	-0.08	0.13
165920	0.37	0.1	-	-	0.63	0.01	0.56	0.13	0.41	0.12	0.52	0.02	0.19	0.07	-0.05	*
169303	0.03	0.08	0.27	0.07	0.29	*	-0.2	0.04	-	-	-0.14	0.22	-0.04	0.07	0.14	0.19
169506	0.34	0.12	0.59	0.1	0.74	*	0.31	0.15	0.23	0.08	0.16	0.04	0.3	0.11	0.54	0.2
171990	0.04	0.07	0.3	0.03	0.26	*	-0.08	0.03	-0.04	0.06	-0.1	0.01	-0.02	0.04	0.21	0.15
172063	0.13	0.1	-	-	0.36	*	0.3	0.05	0.22	0.04	0.28	*	0.05	0.06	-0.07	0.11
172582	-0.23	0.1	-0.26	*	-	-	-0.22	0.11	-0.13	0.08	-0.18	0.05	-0.32	0.04	-	-
174494	0.22	0.09	-	-	0.34	0.17	0.27	0.22	0.18	0.13	0.15	0.03	0.15	0.08	0.28	0.1
174541	-0.23	0.1	-0.08	0.16	-	-	-0.15	0.13	0.04	0.04	-0.2	0.18	-0.13	0.05	0.1	0.19
175073	0.01	0.08	-	-	-	-	0.26	0.08	0.16	0.13	0.16	0.01	-0.17	0.06	-0.55	*
175169	0.34	0.1	0.18	0.06	0.2	0.2	0.23	0.03	0.25	0.01	0.26	0.04	0.18	0.05	0.23	0.02
176110	0.21	0.14	0.23	0.08	0.55	*	0.24	0.2	0.11	0.11	0.11	*	0.12	0.09	0.31	*
176151	0.22	0.1	0.2	0.25	0.43	*	0.22	0.09	0.18	0.11	0.1	0.03	0.12	0.06	0.32	0.08
176986	0.13	0.12	-	-	-	-	0.57	0.06	0.34	0.16	0.47	0.03	-0.11	0.07	-	-
177122	-0.06	0.08	0	0.13	0.12	*	-0.24	0.05	-	-	-0.31	0.07	-0.18	0.05	-0.02	0.03
177409	0	0.07	-0.23	0.18	-	-	-0.22	0.02	-0.05	0.07	-0.17	0.01	-0.11	0.05	-0.12	0.18
178076	0.02	0.07	-	-	-0.11	*	-0.04	0.06	0.12	0.08	0.03	0.01	-0.13	0.06	-0.41	0.01
179640	0.44	0.08	0.13	0.15	0.47	0.11	0.43	0.09	0.38	0.01	0.41	0.02	0.24	0.06	0.23	0.06
180204	0.31	0.08	0.33	0.24	0.39	*	0.09	0.08	0.02	0.04	0.01	0.05	0.11	0.07	0.39	0.16
180257	0.29	0.08	0.39	0.1	0.4	*	0.14	0.11	0.08	0.02	0.08	0.01	0.15	0.07	0.41	0.06
181010	0.16	0.08	-	-	-	-	0.31	0.08	0.25	0.07	0.31	*	-0.05	0.05	-0.27	0.19
182228	0.27	0.08	0.32	0.02	0.43	0.12	0.11	0.08	0.17	0.07	0.1	0.01	0.12	0.06	0.26	*
182498	0.07	0.08	0.04	0.09	-	-	-0.27	0.01	-	-	-0.1	0.01	-0.07	0.07	0.02	0.11
184317	0.11	0.08	0.07	0.1	-	-	-0.02	0.06	0.05	0.04	-0.02	0.01	0.01	0.05	0.07	0.03
185283	0.09	0.13	-0.12	*	-	-	0.52	0.13	-	-	0.54	0.02	-0.19	0.1	-	-
185615	0.13	0.07	-0.06	*	0.2	*	0.16	0.06	0.3	*	0.29	0.02	0.09	0.04	0.05	0.12
186160	-0.25	0.08	-0.39	0.11	-	-	-0.44	0.06	-	-	-0.43	0.03	-0.32	0.05	-0.24	0.13
186265	0.45	0.1	0.08	0.22	0.64	*	0.43	0.07	0.41	0.05	0.45	0.05	0.3	0.07	0.33	0.23
186651	0.1	0.09	0.11	0.1	0.09	*	-0.16	0.08	-	-	-0.23	0.04	-0.08	0.05	0.07	0.18
186803	0.03	0.07	-0.37	0.05	-	-	-0.13	0.02	0.22	0.25	-0.05	0.01	-0.09	0.05	-0.27	0.01
187154	0.17	0.1	-	-	-	-	-0.01	0.15	0.03	0.05	0.05	0.22	0.04	0.04	0.04	0.18
189310	0.09	0.1	-	-	0.43	*	0.33	0.04	0.37	0.09	0.34	0.02	-0.1	0.08	-	-
190125	0.19	0.11	-	-	0.23	0.11	0.08	0.03	0.2	0.01	0.17	0.02	0.09	0.07	0.09	0.01
190613	0.04	0.08	-0.11	0.2	0.04	0.04	-0.15	0.04	0.06	0.01	-	-	-0.04	0.05	-0.02	0.12

Continued on next page

Table A.3 – *Continued from previous page*

Star	[Fe/H]	±	[C/H]	±	[O/H]	±	[Na/H]	±	[Mg/H]	±	[Al/H]	±	[Si/H]	±	[S/H]	±
191760	0.34	0.09	0.35	0.1	-	-	0.27	0.1	0.14	*	0.16	0.05	0.23	0.06	0.42	0.05
193567	0.29	0.08	-0.04	0.17	0.42	*	0.22	0.08	0.26	0.01	0.22	0.05	0.15	0.06	0.01	0.06
193728	0.14	0.09	0.07	0.12	0.19	*	0.15	0.1	0.24	0.01	0.26	0.04	0.13	0.05	-	-
193995	0.35	0.09	0.39	0.06	0.5	*	0.31	0.08	0.24	0.04	0.21	0.01	0.2	0.07	0.36	0.06
195145	0.29	0.08	0.08	0.04	0.51	0.08	0.27	0.08	0.23	0.01	0.23	0.01	0.15	0.06	0.01	0.03
195284	0.17	0.07	-	-	0.2	*	0.06	0.04	0.17	0.11	0.1	0.01	0.01	0.06	-0.07	0.06
196397	0.37	0.13	-	-	0.57	0.1	0.59	0.12	0.41	0.08	0.52	0.09	0.21	0.07	-0.13	*
197069	0.32	0.1	0.42	0.13	0.13	*	0.15	*	0.02	0.04	-0.02	0.04	0.13	0.06	0.45	0.16
197210	0.02	0.07	-	-	0.22	0.01	-0.01	0.04	0.09	0.04	0.01	0.01	-0.08	0.06	-0.22	0.14
197499	0.12	0.1	0.21	0.1	0.34	*	-0.18	*	-0.03	*	-0.31	0.23	-0.04	0.06	0.15	0.13
197818	-0.13	0.09	-0.36	0.17	-0.08	*	-0.18	0.11	-0.1	0.01	-0.22	0.01	-0.19	0.04	-0.27	0.04
197823	0.25	0.11	-	-	0.53	*	0.31	0.12	0.27	0.03	0.24	0.02	0.07	0.07	-0.17	*
198477	0.29	0.12	-	-	0.47	*	0.28	0.13	0.34	0.07	0.3	0.08	0.11	0.09	0.1	*
199065	0.21	0.07	0	0.18	0.04	*	-0.1	0.06	0	0.02	-0.06	0.01	-0.02	0.06	0.01	0.11
200733	0.24	0.11	0.43	0.13	0.63	*	-0.16	0.17	-0.12	0.04	-0.25	0.04	0.02	0.09	0.36	0.25
200869	0.37	0.11	-0.01	0.03	0.47	0.19	0.57	*	0.44	0.01	0.5	0.06	0.22	0.06	0.17	*
201757	0.23	0.09	0.16	0.05	0.42	0.14	0.35	0.16	0.23	0.15	0.16	0.04	0.15	0.07	0.22	*
202282	0.11	0.09	-0.03	0.04	0.32	*	0.03	0.05	0.06	0.01	-0.03	0.01	0	0.05	-0.06	0.26
202457	0.14	0.08	0.11	0.02	0.38	0.22	0.03	0.07	0.17	0.01	0.18	0.02	0.08	0.04	0.12	0.06
203432	0.41	0.08	0.12	0.04	0.46	0.18	0.41	0.11	0.29	0.01	0.36	0.01	0.21	0.07	0.2	0.11
205045	0.25	0.1	0.43	0.06	0.48	0.05	0.17	0.04	0.02	0.05	-0.08	0.09	0.08	0.08	0.24	0.22
205067	-0.04	0.07	-0.13	0.02	-	-	-0.25	0.01	0.02	0.06	-0.03	0.01	-0.08	0.04	-0.07	*
205158	0.25	0.1	0.44	0.1	0.49	*	0.06	0.11	0.03	0.02	0.05	0.07	0.13	0.07	0.37	0.16
206025	0.16	0.08	0.35	0.07	0.31	*	-0.11	0.12	-	-	-0.12	0.01	0.04	0.07	0.25	0.23
206255	0.19	0.09	0.18	0.01	0.09	0.08	0.18	0.06	0.18	0.07	0.16	*	0.11	0.05	0.2	0.01
206683	0.39	0.08	0.3	0.12	0.38	0.13	0.31	0.11	0.2	0.01	0.22	0.04	0.21	0.05	0.31	0.15
207970	0.1	0.08	-0.02	0.06	-	-	0.16	0.1	0.26	0.02	0.26	0.02	0.06	0.04	-0.02	0.02
208704	-0.05	0.07	-0.19	0.1	-	-	-0.35	0.05	-0.03	0.04	-0.15	0.01	-0.14	0.05	-0.1	0.11
209566	0.24	0.1	-	-	0.48	*	0.28	0.08	0.29	0.02	0.29	0.02	0.09	0.06	0.02	*
209659	0.21	0.08	0.35	0.22	0.41	0.01	0.11	0.13	0.04	0.04	0.01	0.01	0.1	0.06	0.36	0.14
210193	0.17	0.07	0.06	0.03	0.31	0.14	0.11	0.03	0.08	0.04	0.05	*	0.03	0.05	0.06	0.04
211366	0.3	0.08	0.12	0.09	0.35	*	0.25	0.02	0.02	*	0	0.08	0.11	0.04	0.26	0.01
213429	0.02	0.1	0.1	0.12	0.19	*	-0.22	0.13	-0.17	0.05	-0.14	*	-0.17	0.05	-0.1	0.25
213717	0.13	0.08	-	-	0.02	*	0.28	0.11	0.26	0.04	0.24	0.04	-0.02	0.05	0.13	*
213941	-0.39	0.07	-0.59	0.11	-	-	-0.29	*	-0.03	0.04	-0.09	0.04	-0.23	0.04	-0.44	0.03
214691	0.2	0.08	-0.01	0.11	0.37	*	0.1	0.19	0.27	0.02	0.32	0.03	0.12	0.07	0.08	0.05
215456	-0.03	0.07	0.05	0.09	-	-	-0.21	0.01	-0.06	0.06	-0.12	0.01	-0.11	0.04	-0.05	0.1

Continued on next page

Table A.3 – *Continued from previous page*

Star	[Fe/H]	±	[C/H]	±	[O/H]	±	[Na/H]	±	[Mg/H]	±	[Al/H]	±	[Si/H]	±	[S/H]	±
216054	-0.12	0.08	-	-	-	-	-0.09	0.07	0.1	0.04	0.04	0.01	-0.2	0.04	-0.32	*
218760	0.02	0.12	-0.35	*	-0.05	*	0.43	0.05	0.3	0.16	0.48	0.04	-0.2	0.08	-	-
219011	0.4	0.1	0.16	0.12	0.76	0.24	0.28	0.1	0.24	0.02	0.34	0.02	0.2	0.09	0.31	0.05
219533	0.34	0.08	0.22	*	0.33	*	0.22	0.14	0.22	0.01	0.24	0.03	0.22	0.07	0.3	0.06
219556	0.22	0.08	-	-	0.45	0.16	0.27	0.05	0.22	0.11	0.23	0.02	0.08	0.06	0.11	0.3
220426	0.38	0.08	0.43	0.09	0.52	*	0.14	0.07	-	-	-0.11	*	0.16	0.09	0.38	0.23
220476	0.02	0.08	-	-	0.03	*	-0.12	0.04	0.03	0.05	-0.06	0.02	-0.11	0.06	-0.26	0.05
220689	0.01	0.07	-0.01	0.09	0.19	*	0	0.01	-0.03	0.01	-0.13	0.02	-0.08	0.05	-0.02	0.11
220718	0.26	0.09	0.36	0.07	0.64	*	0.18	0.1	0.12	0.1	0.09	0.02	0.16	0.07	0.4	0.05
220829	0.15	0.11	-	-	0.46	*	0.38	0.03	0.22	*	0.39	0.01	-0.04	0.07	-0.25	0.24
220945	0.13	0.1	-	-	-	-	0.47	0.16	0.14	*	0.42	0.15	-0.06	0.1	-	-
220981	0.23	0.09	0.33	0.23	0.68	*	0.28	0.1	0.27	0.04	0.22	0.11	0.18	0.07	0.2	0.09
221257	-0.09	0.09	-0.13	0.1	-	-	-0.19	0.06	-0.12	0.03	-0.2	*	-0.16	0.04	-0.16	0.07
221275	0.2	0.08	-	-	-	-	0.24	0.16	0.32	0.08	0.29	0.02	0.07	0.06	-	-
221954	0.43	0.12	0.2	0.16	0.58	0.24	0.36	0.13	0.29	*	0.35	0.05	0.26	0.06	0.36	0.01
222422	-0.03	0.08	-	-	-0.02	*	-0.02	0.09	0.07	0.01	0.05	0.03	-0.15	0.04	-0.4	0.06
222669	0.11	0.07	0.05	0.05	0.04	*	-0.07	0.09	-0.04	0.07	-0.07	0.07	-0.05	0.06	-0.03	0.08
224010	0.26	0.09	0.37	0.07	0.26	*	0.19	0.11	0.16	0.03	0.07	0.05	0.17	0.06	0.22	0.16
224022	0.15	0.08	0.23	0.16	0.28	*	-0.08	0.04	-	-	-0.12	0.01	0.01	0.06	0.19	0.23
224143	0.08	0.1	-	-	-	-	-0.15	0.16	-0.08	0.02	-0.21	0.11	-0.11	0.06	-0.19	0.2
224433	0.17	0.08	-	-	0.33	*	0.2	0.08	0.2	0.06	0.15	0.08	0.05	0.05	-0.16	0.06
224538	0.34	0.09	0.5	0.13	0.54	*	0.17	0.11	0.05	0.04	0.01	0.03	0.21	0.08	0.54	0.19
224789	0.05	0.07	-	-	0.3	0.09	0.34	0.09	0.28	0.11	0.29	0.01	-0.08	0.06	-0.48	*
225155	0.25	0.08	0.11	0.15	0.51	*	0.17	0.1	0.26	0.01	0.3	0.02	0.17	0.05	0.21	0.03
225299	0.22	0.08	-	-	0.24	*	0.16	0.06	0.17	0.02	0.13	0.04	0.07	0.05	0.13	0.14

Table A.4: All stars abundances for Ca, Sc, Ti, V, Cr, Mn and Co.

Star	[Ca/H]	±	[Sc/H]	±	[Ti/H]	±	[V/H]	±	[Cr/H]	±	[Mn/H]	±	[Co/H]	±
361	-0.15	0.12	-0.16	0.04	-0.23	0.05	-0.3	0.03	-0.23	0.1	-0.43	0.21	-0.29	0.06
1002	0.11	0.14	0.1	0.03	0.14	0.11	0.17	0.04	0.08	0.12	0.2	0.05	0.1	0.03
1237	0.29	0.12	-0.03	0.08	0.39	0.1	0.46	0.09	0.33	0.06	0.45	0.08	0.14	0.08
1893	0.35	0.17	0.04	0.07	0.44	0.11	0.57	0.11	0.29	0.18	0.66	0.18	0.33	0.04
1926	-0.31	0.14	-0.19	*	-0.36	0.06	-0.44	0.03	-0.43	0.16	-0.91	0.25	-0.4	0.08
2098	0.01	0.12	0.11	0.07	-0.03	0.08	-0.03	0.03	0.03	0.09	-0.02	0.16	0.03	0.04
2222	0.14	0.13	0.27	0.05	0.21	0.1	0.25	0.05	0.19	0.1	0.41	0.14	0.23	0.07
3359	0.25	0.14	0.08	0.08	0.43	0.11	0.57	0.11	0.26	0.19	0.8	0.17	0.32	0.08
4333	0.32	0.14	0.14	0.06	0.52	0.13	0.63	0.14	0.32	0.18	0.72	0.22	0.37	0.04
4392	0.08	0.12	0.07	0.03	0.13	0.09	0.19	0.06	0.06	0.07	0.29	0.09	0.11	0.05
6236	-0.04	0.11	0.03	0.03	-0.11	0.07	-0.18	0.08	-0.08	0.12	-0.17	0.23	-0.15	0.09
6790	-0.13	0.18	0.05	0.03	-0.23	0.09	-0.35	0.08	-0.14	0.17	-0.46	0.26	-0.23	0.03
6880	0.18	0.14	-0.14	0.09	0.34	0.1	0.43	0.08	0.03	0.25	0.42	0.2	0.06	0.02
6910	0.16	0.14	0.5	0.02	0.14	0.1	0.16	0.08	0.23	0.17	0.37	0.15	0.25	0.06
7134	-0.31	0.12	-0.14	*	-0.38	0.06	-	-	-0.37	0.13	-0.7	0.2	-0.42	0.08
7449	-0.22	0.11	-0.13	0.02	-0.31	0.04	-	-	-0.31	0.16	-0.59	0.23	-0.33	0.07
7661	0.28	0.16	-0.13	0.12	0.35	0.12	0.42	0.07	0.18	0.22	0.43	0.08	0.08	0.06
8076	-0.06	0.11	-0.06	0.12	-0.11	0.04	-0.14	0.04	-0.04	0.08	-0.15	0.15	-0.09	0.05
8129	0.09	0.11	-0.11	0.06	0.15	0.08	0.19	0.05	0.02	0.11	0.21	0.09	0.01	0.08
8406	-0.05	0.1	-0.14	0.05	-0.03	0.14	-0.08	0.01	-0.12	0.08	-0.12	0.08	-0.12	0.01
9175	0.08	0.11	0.19	0.02	0.06	0.11	0.08	0.03	0.04	0.08	0.11	0.06	0.11	0.02
9782	-0.1	0.13	0.06	0.06	-0.16	0.05	-0.19	0.05	-0.06	0.17	-0.23	0.2	-0.13	0.09
9847	0.23	0.15	0.34	0.05	0.3	0.14	0.38	0.09	0.28	0.08	0.59	0.17	0.41	0.08
9905	0.38	0.22	0.06	0.09	0.66	0.14	0.83	0.18	0.3	0.27	0.73	0.22	0.42	0.14
10008	0.35	0.18	-0.17	0.08	0.46	0.09	0.53	0.11	0.2	0.25	0.54	0.2	0.06	0.03
10226	0	0.1	0.07	0.03	-0.05	0.04	-0.05	0.09	-0.02	0.11	-0.12	0.19	-0.07	0.06
10370	0.02	0.11	-0.08	0.03	0.06	0.07	0.08	0.07	-0.08	0.1	0.14	0.08	-0.01	0.03
10519	-0.25	0.11	-0.11	0.01	-0.17	0.04	-0.31	0.02	-0.53	0.14	-0.95	0.18	-0.39	0.1
10576	-0.1	0.12	0.16	0.05	-0.1	0.05	-0.18	0.06	-0.07	0.17	-0.39	0.19	-0.09	0.08
10611	0.38	0.19	-0.15	0.13	0.53	0.12	0.62	0.1	-	-	0.52	0.11	0.13	0.05
10678	0.17	0.11	0.04	0.09	0.2	0.1	0.27	0.05	0.12	0.1	0.37	0.11	0.12	0.01
11264	0.05	0.11	0.11	0.05	0.07	0.11	0.11	0.02	-0.01	0.1	0.14	0.05	0.08	0.04
11754	0.16	0.15	0.35	0.04	0.19	0.08	0.21	0.04	0.21	0.11	0.43	0.15	0.32	0.06
12585	0.07	0.1	0.06	0.03	0.07	0.14	0.12	0.04	0.03	0.08	0.21	0.06	0.08	0.05
12951	-0.27	0.16	0.06	0.02	-0.34	0.06	-0.44	0.06	-0.28	0.21	-0.64	0.24	-0.34	0.11
13060	0.45	0.23	-0.05	0.08	0.7	0.13	0.88	0.17	-	-	0.72	0.26	0.31	0.06

Continued on next page

Table A.4 – *Continued from previous page*

Star	[Ca/H]	±]	[Sc/H]	±	[Ti/H]	±	[V/H]	±	[Cr/H]	±	[Mn/H]	±	[Co/H]	±
13350	0.38	0.15	0.39	0.08	0.54	0.14	0.7	0.16	0.44	0.13	0.83	0.23	0.6	0.06
13386	0.57	0.28	0.12	0.11	0.92	0.18	1.2	0.22	-	-	0.88	0.24	0.53	0.05
14758	-0.12	0.12	-0.09	0.04	-0.12	0.06	-0.13	0.09	-0.25	0.08	-0.42	0.17	-0.23	0.06
15507	0.14	0.11	0.06	0.06	0.15	0.11	0.21	0.04	0.15	0.04	0.3	0.08	0.08	0.02
15590	0.05	0.12	0.4	0.02	0.06	0.08	0.11	0.05	0.15	0.11	0.25	0.07	0.12	0.04
15767	-	-	-0.23	0.12	0.85	0.16	1.06	0.17	-	-	0.67	0.25	0.06	0.1
16950	0	0.17	0.36	0.04	0.02	0.24	-0.04	0.09	0.12	0.25	0.03	0.2	0.07	0.09
17134	-0.09	0.11	0	0.02	-0.08	0.07	-0.11	0.12	-0.12	0.08	-0.22	0.13	-0.16	0.09
17289	-0.18	0.15	-0.06	0.05	-0.24	0.08	-0.17	0.11	-0.21	0.17	-0.54	0.27	-0.3	0.06
18168	0.46	0.2	-0.05	0.08	0.74	0.13	1.01	0.15	-	-	0.76	0.29	0.32	0.09
18708	0.03	0.11	0.19	*	-0.01	0.12	0.04	0.05	0.1	0.02	0.18	0.06	0.17	0.03
18754	0.24	0.16	0.41	0.02	0.37	0.14	0.42	0.08	0.32	0.1	0.67	0.22	0.37	0.01
18819	-0.07	0.16	0.38	0.02	-0.08	0.08	-0.11	0.08	0.02	0.23	-0.12	0.23	-0.01	0.09
19603	0	0.13	0.27	0.03	-0.06	0.07	-0.02	0.06	0.07	0.05	0.15	0.09	0.07	0.08
19916	0	0.2	0.36	0.05	0.01	0.18	-0.03	0.05	0.14	0.22	0.03	0.25	0.1	0.18
20155	-0.03	0.14	0.31	0.01	-0.06	0.07	-0.01	0.1	0.05	0.15	0.04	0.19	0.07	0.07
20407	-0.47	0.13	-0.25	0.08	-0.41	0.19	-0.48	0.11	-0.52	0.18	-0.87	0.21	-0.49	0.06
20584	-0.07	0.21	0.33	0.03	-0.14	0.19	-0.19	0.09	0.05	0.19	-0.16	0.26	-0.02	0.03
20657	0.03	0.13	0.26	0.02	0.02	0.1	0.01	0.06	0.09	0.13	0.13	0.12	0.12	0.03
20675	0.07	0.12	0.3	0.04	0.07	0.13	0.04	0.03	0.08	0.11	0.13	0.11	0.14	0.06
21036	0.21	0.14	0	0.03	0.27	0.12	0.32	0.07	0.18	0.14	0.38	0.1	0.14	0.06
21089	0.28	0.14	0.39	0.05	0.41	0.13	0.49	0.08	0.3	0.1	0.71	0.24	0.45	0.03
22177	0.24	0.14	0.24	0.03	0.35	0.12	0.39	0.08	0.25	0.05	0.49	0.15	0.26	0.17
22582	0.17	0.14	0.03	0.03	0.34	0.1	0.38	0.07	0	0.18	0.24	0.13	0.12	0.02
23576	-0.05	0.15	0.01	0.03	-0.09	0.09	-0.13	0.07	-0.05	0.14	-0.26	0.22	-0.13	0.03
24331	-	-	-0.26	0.07	0.76	0.16	-	-	-	-	0.61	0.27	0.09	0.13
25912	0.04	0.13	0.1	0.07	0.04	0.08	0.04	0.05	0.04	0.11	0	0.06	-0.03	0.06
26040	-0.22	0.14	-0.09	*	-	-	-0.22	0.12	-	-	-	-	-0.28	0.15
26071	0.32	0.17	0.35	0.06	0.46	0.13	0.53	0.09	0.33	0.09	0.63	0.16	0.47	0.03
26864	0.12	0.19	-0.03	0.07	0.08	0.14	-0.02	0.09	0.05	0.11	-0.02	0.15	0.05	0.04
27328	0.3	0.17	-0.01	0.06	0.48	0.05	0.62	0.15	0.21	0.23	0.57	0.23	0.3	0.09
27446	0.02	0.13	-0.09	0.03	-0.01	0.09	0.02	0.04	-0.07	0.1	-0.06	0.07	-0.08	0.1
27905	-0.15	0.1	-0.12	0.04	-0.17	0.04	-0.18	0.05	-0.24	0.12	-0.34	0.19	-0.21	0.09
27939	0.24	0.12	0.25	0.05	0.26	0.11	0.28	0.07	0.18	0.1	0.45	0.13	0.27	0.08
28185	0.21	0.14	0.18	0.07	0.3	0.12	0.43	0.11	0.21	0.15	0.59	0.13	0.26	0.1
28701	-0.1	0.1	-0.09	0.05	-0.03	0.1	-0.16	0.07	-0.31	0.07	-0.71	0.22	-0.19	0.05
28821	-0.01	0.09	-0.05	0.03	0.04	0.09	0.03	0.03	-0.12	0.06	-0.15	0.11	-0.11	0.07

Continued on next page

Table A.4 – *Continued from previous page*

Star	[Ca/H]	±]	[Sc/H]	±	[Ti/H]	±	[V/H]	±	[Cr/H]	±	[Mn/H]	±	[Co/H]	±
29231	0.37	0.16	0	0.08	0.48	0.12	0.6	0.14	0.27	0.19	0.68	0.23	0.29	0.07
29263	0	0.11	0.09	0.02	0.06	0.08	0.07	0.04	0	0.05	0.05	0.08	0.03	0.07
29813	-0.11	0.12	-0.07	0.03	-0.14	0.07	-0.19	0.03	-0.17	0.09	-0.28	0.17	-0.17	0.05
30278	0.14	0.13	-0.11	0.06	0.29	0.1	0.31	0.09	-0.02	0.17	0.25	0.13	-0.05	0.03
30306	0.3	0.15	0.13	0.09	0.42	0.13	0.53	0.12	0.28	0.14	0.61	0.21	0.3	0.06
30501	0.5	0.22	-0.17	0.11	0.74	0.14	0.96	0.17	-	-	0.7	0.25	0.12	0.1
30669	0.37	0.22	0.08	0.06	0.56	0.11	0.71	0.18	0.24	0.23	0.65	0.24	0.35	0.04
31392	0.33	0.18	-0.07	0.14	0.48	0.12	0.62	0.14	0.18	0.23	0.64	0.2	0.23	0.04
32564	0.16	0.14	-0.05	0.05	0.28	0.09	0.31	0.05	0.05	0.12	0.34	0.13	0.11	0.01
32724	-0.1	0.14	0.06	0.05	-0.1	0.04	-0.16	0.11	-0.18	0.1	-0.47	0.19	-0.27	0.09
32804	0.03	0.12	-0.04	0.03	-0.06	0.1	-0.04	0.05	0.04	0.12	-0.08	0.15	-0.1	0.02
33093	-0.1	0.16	0.19	0.01	-0.1	0.05	-0.16	0.13	-0.04	0.18	-0.24	0.17	-0.21	0.16
33214	0.6	0.25	-0.02	0.14	0.89	0.17	1.19	0.25	-	-	0.91	0.25	0.44	0.03
33822	0.25	0.16	0.3	0.04	0.28	0.11	0.34	0.05	0.26	0.1	0.58	0.15	0.37	0.04
33873	0.18	0.12	-0.01	0.09	0.2	0.12	0.25	0.04	0.14	0.09	0.34	0.07	0.16	0.05
34195	-0.09	0.21	0.23	0.05	-0.18	0.12	-0.24	0.08	-0.08	0.28	-0.29	0.24	-0.09	0.04
34230	0.38	0.19	-	-	0.49	0.14	0.63	0.13	0.43	0.03	0.64	0.21	0.4	0.07
34377	0.19	0.15	0.06	0.04	0.15	0.05	0.13	0.03	0.19	0.03	0.28	0.09	0.15	0.01
34599	0.07	0.13	0.01	0.05	0.04	0.05	0.11	0.07	0.12	0.02	0.15	0.06	0.04	*
35376	0.01	0.12	0.15	0.04	0.05	0.14	0.05	0.06	0.04	0.03	0.09	0.08	0.06	0.02
35676	0.28	0.14	0.04	0.08	0.27	0.09	0.34	0.06	0.19	0.12	0.43	0.11	0.19	0.03
36152	0.05	0.12	0.01	0.04	0.07	0.11	0.07	0.05	0.01	0.08	0.11	0.03	0.01	0.03
36329	0.01	0.15	-0.12	0.04	-	-	0.03	0.2	-0.04	0.16	-0.1	0.18	-0.09	0.12
37351	0	0.12	0	0.01	-0.12	0.05	-0.15	0.02	0.02	0.03	0	0.04	-0.08	0.04
37706	0	0.11	-0.21	0.09	0.1	0.08	0.08	0.04	-0.15	0.13	-0.01	0.11	-0.2	0.04
37761	0.19	0.14	0.4	0.05	0.29	0.12	0.36	0.04	0.24	0.03	0.46	0.18	0.28	0.03
37986	0.42	0.19	0.21	0.1	0.56	0.13	0.74	0.2	0.36	0.18	0.79	0.23	0.51	0.07
38467	0.19	0.11	0.35	0.02	0.22	0.11	0.28	0.06	0.21	0.12	0.4	0.09	0.34	0.04
38554	0.23	0.17	0.2	0.07	0.34	0.1	0.42	0.07	0.25	0.09	0.6	0.15	0.34	0.05
38667	-0.09	0.12	0.17	0.01	-0.1	0.12	-0.18	0.07	-0.04	0.17	-0.23	0.21	-0.04	0.05
38677	-0.08	0.12	0.15	0.03	-0.18	0.05	-0.18	0.05	0.01	0.21	-0.2	0.24	-0.12	0.16
39126	0.41	0.21	-0.11	0.1	0.55	0.13	0.65	0.12	-	-	0.63	0.21	0.14	0.07
39503	0.24	0.18	0.16	0.09	0.36	0.11	0.42	0.12	0.21	0.13	0.63	0.22	0.3	0.01
39804	0.1	0.13	-0.01	0.12	0.13	0.05	0.16	0.07	0.02	0.13	0.22	0.06	0.04	0.05
39855	-0.13	0.11	-0.37	0.04	-0.07	0.1	-0.1	0.03	-0.33	0.14	-0.33	0.15	-0.31	0.08
40105	0.53	0.29	0.28	0.07	0.88	0.15	1.08	0.18	0.41	0.26	-	-	0.56	0.08
40403	0.2	0.14	0.33	0.03	0.22	0.13	0.29	0.06	0.25	0.08	0.46	0.12	0.37	0.01

Continued on next page

Table A.4 – *Continued from previous page*

Star	[Ca/H]	±]	[Sc/H]	±	[Ti/H]	±	[V/H]	±	[Cr/H]	±	[Mn/H]	±	[Co/H]	±
41155	-0.05	0.22	0.37	0.04	-0.15	0.13	-0.25	0.1	0.06	0.23	-0.25	0.27	-0.12	0.11
42044	-0.18	0.21	0.21	0.09	-0.25	0.19	-0.38	0.06	-0.06	0.27	-0.57	0.25	-0.29	0.08
42287	-0.09	0.19	-0.04	0.02	-0.13	0.16	-0.2	0.14	-0.08	0.07	-0.17	0.06	-0.18	0.1
42538	-0.02	0.21	0.32	0.04	-0.03	0.08	-0.06	0.13	0.03	0.19	-0.13	0.23	0.01	0.1
42719	0.16	0.19	0.48	0.03	0.17	0.12	0.19	0.06	0.18	0.1	0.29	0.09	0.29	0.09
42778	0.1	0.19	0.07	0.06	0.03	0.08	-0.01	0.1	0.07	0.1	0.01	0.18	0.01	0.09
43470	-0.22	0.18	0.12	0.06	-0.34	0.13	-0.26	0.25	-	-	-	-	-0.31	0.18
44569	-0.15	0.15	-0.08	0.01	-0.16	0.1	-0.17	0.04	-0.29	0.09	-0.47	0.15	-0.22	0.09
44573	-	-	-0.21	0.14	0.85	0.17	1.09	0.18	-	-	0.76	0.28	0.22	0.06
45133	0.31	0.16	0.3	0.06	0.38	0.13	0.51	0.12	0.31	0.09	0.66	0.2	0.41	0.06
45987	0.13	0.14	0.24	0.02	0.19	0.15	0.22	0.02	0.13	0.11	0.31	0.08	0.26	0.07
46175	-0.08	0.13	0.06	0.03	-0.14	0.05	-0.16	0.07	-0.01	0.04	0	0.04	-0.1	0.06
46435	-0.04	0.26	0.03	0.1	-0.05	0.12	0.02	0.16	-0.04	0.15	-0.16	0.05	0	0.11
46894	0.27	0.15	0.35	0.04	0.43	0.13	0.56	0.15	0.25	0.1	-	-	0.31	0.04
47017	-0.01	0.15	0.3	0.05	-0.01	0.09	-0.06	0.15	0.07	0.2	0.07	0.17	0.05	0.03
47186	0.21	0.13	0.21	0.07	0.32	0.1	0.42	0.12	0.22	0.14	0.63	0.15	0.32	0.03
48056	-0.15	0.16	0.16	0.03	-0.19	0.07	-	-	-0.02	0.22	-0.38	0.28	-0.14	0.12
48265	0.31	0.15	0.51	0.03	0.4	0.14	0.5	0.12	0.34	0.09	0.76	0.22	0.48	0.09
49035	0.32	0.17	0.29	0.12	0.42	0.11	0.54	0.12	0.3	0.13	0.65	0.17	0.44	0.01
49866	0.03	0.15	0.33	*	0.02	0.11	0.05	0.08	0.06	0.14	0.11	0.08	0.08	0.05
50117	-0.08	0.11	0.15	0.04	-0.12	0.06	-0.17	0.03	-0.04	0.15	-0.2	0.18	-0.04	0.03
50255	0	0.15	-0.17	0.06	0.02	0.11	-0.03	0.16	-0.14	0.11	-0.06	0.05	-0.2	0.07
50652	0.24	0.12	0.29	0.02	0.33	0.06	0.37	0.07	0.28	0.08	0.5	0.14	0.23	0.11
51608	0.25	0.17	-0.03	0.05	0.45	0.08	0.51	0.13	0.06	0.29	0.47	0.19	0.27	0.23
52217	0.32	0.14	0.12	0.09	0.43	0.11	0.57	0.12	-	-	0.66	0.22	0.39	0.1
52756	0.63	0.27	0.02	0.11	0.96	0.17	1.22	0.21	-	-	0.88	0.24	0.45	0.01
56413	0.22	0.12	0.17	0.05	0.3	0.11	0.4	0.1	0.22	0.12	0.58	0.21	0.36	0.06
56662	-0.19	0.1	-0.1	0.07	-0.23	0.07	-0.28	0.12	-0.19	0.11	-0.44	0.21	-0.33	0.05
56972	0.28	0.15	0.22	0.06	0.35	0.1	0.42	0.07	0.27	0.09	0.61	0.19	0.34	0.04
58111	0.45	0.25	-0.12	0.12	0.74	0.12	0.96	0.17	-	-	0.78	0.26	0.25	0.04
58556	-0.15	0.15	-0.03	0.06	-0.24	0.1	-0.37	0.1	-0.14	0.15	-0.44	0.26	-0.35	0.12
58696	-0.11	0.14	0.18	0.05	-0.15	0.07	-0.17	0.08	-0.05	0.19	-0.26	0.17	-0.12	0.07
59711	-0.08	0.12	-0.08	0.07	-0.1	0.12	-0.09	0.07	-0.12	0.04	-0.16	0.12	-0.18	0.07
59824	0.08	0.13	0.24	0.06	0.05	0.15	0.06	0.03	0.05	0.09	0.2	0.13	0.15	0.04
61051	0.24	0.16	0	0.02	0.49	0.1	0.57	0.15	0.08	0.25	0.3	0.09	0.22	0.02
61475	0.55	0.25	0.05	0.16	0.71	0.13	0.93	0.19	0.4	0.25	0.91	0.26	0.43	0.05
62549	-0.12	0.1	0.07	0.02	-0.15	0.09	-0.13	0.1	-0.11	0.11	-0.32	0.14	-0.07	0.08

Continued on next page

Table A.4 – *Continued from previous page*

Star	[Ca/H]	±]	[Sc/H]	±	[Ti/H]	±	[V/H]	±	[Cr/H]	±	[Mn/H]	±	[Co/H]	±
62644	0.21	0.16	0.25	0.05	0.34	0.1	0.44	0.1	0.14	0.1	0.57	0.27	0.23	0.05
64114	0.1	0.13	-0.1	0.08	0.08	0.16	0.17	0.02	0.09	0.01	0.15	0.11	-0.07	*
64144	0.09	0.1	-0.12	0.06	0.13	0.08	0.15	0.05	0.02	0.1	0.19	0.06	-0.02	0.03
65427	0.06	0.13	0.13	0.01	0.08	0.08	0.17	0.08	0.06	0.03	0.17	0.07	-0.01	0.12
66039	-0.06	0.11	0.08	0.04	-0.11	0.13	-0.22	0.04	-0.06	0.17	-0.31	0.27	-0.09	0.07
66058	0.01	0.12	0.13	0.04	0	0.09	0.04	0.05	0.04	0.12	0.11	0.08	0.02	0.05
66791	0.15	0.15	0.23	0.03	0.15	0.09	0.13	0.06	0.06	0.09	0.16	0.06	0.1	0.06
70081	0.1	0.12	0.21	0.04	0.11	0.1	0.14	0.03	0.1	0.09	0.25	0.07	0.17	0.06
72579	0.35	0.18	0.17	0.09	0.6	0.24	0.73	0.14	0.3	0.2	0.72	0.25	0.43	0.07
72687	0.01	0.14	-0.13	0.08	-0.02	0.13	-0.08	0.03	0.03	0.09	-0.14	0.13	-0.22	0.11
72892	0.12	0.11	0.17	0.05	0.2	0.14	0.25	0.07	0.15	0.06	0.35	0.09	0.19	0.05
73267	0.35	0.17	0.03	0.06	0.61	0.13	0.73	0.13	0.23	0.23	0.62	0.24	0.41	0.24
73744	-0.3	0.11	-0.22	0.02	-0.32	0.05	-0.35	0.06	-0.42	0.14	-0.72	0.19	-0.34	0.06
74698	0.06	0.13	0.14	0.02	0.06	0.1	0.06	0.04	0.03	0.08	0.1	0.03	0.06	0.02
74733	-0.18	0.13	-0.15	0.02	-0.2	0.03	-0.26	0.05	-0.23	0.09	-0.46	0.21	-0.26	0.01
74935	-0.1	0.16	0.08	0.02	-0.16	0.08	-0.19	0.06	-0.08	0.16	-0.29	0.26	-0.1	0.06
75288	0.07	0.11	0.08	0.03	0.11	0.1	0.2	0.08	0.07	0.07	0.27	0.07	0.16	0.04
75351	0.01	0.15	0.34	*	0.04	0.08	0.02	0.03	0.09	0.16	0.1	0.15	0.14	0.07
77338	0.5	0.19	0.19	0.09	0.72	0.13	0.92	0.16	0.42	0.24	0.89	0.27	0.55	0.09
77417	0.36	0.15	0.16	0.08	0.48	0.14	0.63	0.11	0.29	0.17	0.71	0.23	0.4	0.04
77683	0.47	0.25	0.35	0.07	0.7	0.17	0.9	0.16	0.46	0.19	-	-	0.53	0.1
78130	0.11	0.13	0.04	0.04	0.08	0.1	0.15	0.04	0.05	0.11	0.23	0.05	0.1	0.05
78286	0.13	0.09	0.26	0.07	0.15	0.14	0.22	0.04	0.14	0.08	0.36	0.1	0.19	0.06
79985	0	0.13	0.2	0.02	0.04	0.08	0.03	0.1	0	0.14	0.05	0.07	0.02	0.03
81110	0.23	0.14	0.16	0.08	0.24	0.12	0.36	0.09	0.22	0.12	0.51	0.12	0.26	0.03
81700	0.08	0.14	0.02	0.06	0	0.08	0.03	0.05	0.01	0.08	0.03	0.1	-0.06	0.06
82282	0.39	0.22	-0.26	0.16	0.52	0.1	0.62	0.12	-	-	0.54	0.2	0.09	0.11
82400	0.15	0.17	-0.05	0.08	0.15	0.09	0.17	0.03	0.06	0.15	0.18	0.04	0.01	0.06
82516	-	-	-0.08	0.09	0.9	0.18	1.13	0.21	-	-	0.82	0.26	0.37	0.07
82977	0.26	0.14	-0.17	0.07	0.38	0.09	0.47	0.07	0.17	0.27	0.47	0.19	0.07	0.06
83365	-0.01	0.13	0.08	0.03	-0.05	0.12	-0.1	0.02	-0.02	0.1	-0.05	0.14	0	0.02
83517	0.09	0.16	0.03	*	0.1	0.09	0.14	0.06	-	-	-	-	-0.06	*
84652	-0.23	0.15	0.03	0.04	-0.24	0.1	-0.34	0.22	-0.14	0.15	-0.49	0.27	-0.2	0.05
85380	-0.11	0.14	0.25	0.04	-0.19	0.1	-0.23	0.1	-0.05	0.28	-0.32	0.22	-0.1	0.13
85390	-	-	-0.03	*	0.58	0.22	-	-	-	-	-	-	-	-
86006	0.24	0.11	0.41	0.02	0.28	0.13	0.38	0.1	0.25	0.09	0.62	0.19	0.44	0.08
86226	-0.05	0.12	-0.05	0.04	-0.12	0.04	-0.21	0.05	-	-	-	-	-0.29	*

Continued on next page

Table A.4 – *Continued from previous page*

Star	[Ca/H]	±]	[Sc/H]	±	[Ti/H]	±	[V/H]	±	[Cr/H]	±	[Mn/H]	±	[Co/H]	±
86249	-	-	-0.07	0.11	1.04	0.18	-	-	-	-	0.84	0.25	0.32	0.06
86397	0.22	0.16	0.13	0.03	0.3	0.09	0.37	0.06	0.18	0.12	0.48	0.16	0.28	0.09
86652	-0.02	0.1	-0.01	0.13	-0.07	0.14	0	0.07	-0.01	0.08	0.02	0.12	-0.01	0.07
87931	0.23	0.15	-0.03	0.06	0.3	0.09	0.41	0.09	0.15	0.15	0.46	0.17	0.07	0.07
87998	-0.12	0.11	-0.02	0.01	-0.17	0.03	-0.26	0.03	-	-	-	-	-0.43	*
88864	0.1	0.08	0.17	*	0.04	0.16	0.14	0.16	-	-	-	-	-0.18	*
89178	0.2	0.13	0.25	0.04	0.36	0.08	0.44	0.09	0.12	0.15	-	-	0.19	0.02
89418	-0.26	0.11	-0.12	0.05	-0.34	0.04	-0.38	0.06	-0.28	0.13	-0.61	0.23	-0.4	0.06
89988	0.08	0.12	0.32	0.02	0.06	0.12	0.1	0.02	0.14	0.12	0.25	0.1	0.13	0.05
90028	0.13	0.16	0.36	0.07	0.14	0.12	0.16	0.06	0.2	0.09	0.37	0.09	0.23	0.01
90702	0.2	0.11	0.1	0.07	0.21	0.13	0.28	0.05	0.19	0.06	0.43	0.09	0.16	0.03
91320	-0.14	0.14	0.18	0.01	-0.15	0.1	-0.23	0.05	-0.1	0.2	-0.3	0.25	-0.05	0.06
91901	-	-	-0.15	0.1	0.82	0.14	1.01	0.16	-	-	0.77	0.25	0.19	0.07
92069	0.22	0.13	0.29	0.03	0.34	0.1	0.35	0.07	0.2	0.08	0.41	0.13	0.28	0.07
92719	-0.1	0.11	-0.13	0.03	-0.13	0.03	-0.22	0.06	-	-	-	-	-0.23	*
93083	0.66	0.29	0.02	0.13	1.04	0.19	-	-	-	-	0.9	0.26	0.46	0.05
94151	0.13	0.13	0	0.06	0.17	0.12	0.22	*	-	-	-	-	0.06	*
94387	0.39	0.16	0.17	0.1	0.53	0.14	0.71	0.12	0.34	0.19	0.77	0.23	0.49	0.11
94482	-0.18	0.16	0.06	0.03	-0.23	0.07	-0.28	0.04	-0.18	0.18	-0.47	0.21	-0.22	0.07
94527	0.06	0.12	-0.21	0.08	0.11	0.12	0.14	0.04	-0.08	0.14	0.06	0.08	-0.12	0.07
94690	0.16	0.14	0.21	0.03	0.19	0.16	0.28	0.09	0.17	0.09	0.44	0.13	0.28	0.08
94838	-0.01	0.12	-0.05	0.03	-0.04	0.06	-0.08	0.03	-0.08	0.09	-0.19	0.16	-0.14	0.11
95136	0.13	0.15	0.2	0.05	0.13	0.13	0.17	0.07	0.1	0.09	0.25	0.06	-	-
95338	-	-	-0.03	0.14	0.83	0.15	1.08	0.21	-	-	0.83	0.27	0.44	0.08
95521	-0.05	0.06	-0.15	0.01	-0.1	0.03	-0.21	*	-	-	-	-	-0.32	*
95533	0.41	0.23	0.12	0.07	0.66	0.13	0.82	0.16	0.33	0.23	0.7	0.23	0.41	0.04
95542	-0.13	0.13	-0.09	0.05	-0.22	0.06	-0.32	0.05	-0.18	0.14	-0.48	0.22	-0.11	0.1
96020	0.32	0.15	0.24	0.08	0.44	0.15	0.55	0.09	0.37	0.13	0.75	0.26	0.46	0.06
96276	-0.21	0.12	-0.02	0.03	-0.31	0.05	-0.42	0.04	-0.2	0.15	-0.51	0.24	-0.18	0.17
98163	0.11	0.13	0.24	0.03	0.14	0.09	0.15	0.05	0.1	0.08	0.27	0.08	0.16	0.02
98459	0.02	0.12	0.26	0.02	-0.01	0.11	0.02	0.03	0.07	0.1	0.11	0.13	0.12	0.06
98764	0.02	0.12	0.03	0.12	-0.02	0.05	-0.06	0.04	-0.01	0.1	-0.12	0.16	-0.11	0.02
99116	0.1	0.12	-0.13	0.05	0.16	0.1	-	-	0.03	0.14	0.24	0.1	0.04	0.06
101093	-0.28	0.13	-0.18	0.01	-0.37	0.04	-0.35	0.08	-0.33	0.16	-0.74	0.24	-0.38	0.03
101171	0.24	0.18	-0.06	0.09	0.37	0.1	0.46	0.09	0.11	0.24	0.39	0.12	0.08	0.01
101181	0.16	0.11	0.14	0.05	0.29	0.18	0.36	0.09	0.15	0.11	0.44	0.12	0.21	0.01
101896	0.43	0.2	0.08	0.16	0.69	0.16	0.89	0.18	0.32	0.26	0.76	0.25	0.44	0.06

Continued on next page

Table A.4 – *Continued from previous page*

Star	[Ca/H]	±]	[Sc/H]	±	[Ti/H]	±	[V/H]	±	[Cr/H]	±	[Mn/H]	±	[Co/H]	±
102574	-0.04	0.14	0.29	0.03	-0.11	0.14	-0.07	0.19	-0.03	0.25	-0.13	0.2	-0.01	0.11
102579	0.39	0.18	-0.07	0.08	0.61	0.12	0.81	0.17	0.23	0.29	0.68	0.24	0.3	0.06
102843	0.38	0.16	0.13	0.08	0.57	0.12	0.7	0.11	0.31	0.2	0.67	0.2	0.39	0.03
103559	0.17	0.13	-0.07	0.05	0.17	0.07	0.18	0.04	0.13	0.03	0.12	0.01	-0.06	0.1
103673	0.11	0.13	-0.15	0.1	0.16	0.07	0.19	0.06	0.01	0.15	0.13	0.03	0.11	0.25
104645	0.28	0.21	0.25	0.06	0.51	0.13	0.61	0.12	0.2	0.16	0.68	0.28	0.33	0.01
104760	-0.03	0.12	0.06	0.02	-0.08	0.14	-0.04	0.07	-0.03	0.1	-0.04	0.12	0.01	0.05
104982	-0.06	0.05	-0.12	0.03	-0.16	0.23	-0.13	*	-	-	-	-	-0.25	*
105690	0.13	0.17	-0.22	0.13	0.15	0.23	0.17	0.1	0.1	0.12	0.1	0.08	-0.13	0.12
105904	0.21	0.12	0.24	0.07	0.29	0.15	0.39	0.09	0.32	0.1	0.72	0.12	0.32	0.04
106275	0.52	0.27	-0.14	0.11	0.86	0.15	1.07	0.19	-	-	0.69	0.26	0.28	0.01
106869	-0.12	0.13	0.16	0.06	-0.17	0.08	-0.29	0.07	-0.06	0.16	-0.29	0.23	-0.14	0.05
106937	0.4	0.16	0.39	0.06	0.55	0.15	0.69	0.2	0.37	0.14	0.77	0.26	0.53	0.15
107008	0.45	0.19	0.08	0.11	0.58	0.13	0.77	0.12	0.38	0.23	0.81	0.23	0.46	0.04
107181	0.32	0.15	0.4	0.04	0.39	0.11	0.51	0.1	0.36	0.08	0.73	0.24	0.43	0.07
108953	0.39	0.16	0.23	0.15	0.6	0.14	0.74	0.17	0.44	0.16	0.77	0.19	0.6	0.11
109591	-0.01	0.1	0.1	0.03	0.07	0.09	0.07	0.06	-0.11	0.06	-0.16	0.11	0.01	0.09
109908	-0.01	0.22	-0.05	0.04	-0.06	0.11	-0.07	0.23	-0.07	0.08	-0.27	0.25	-0.26	0.18
109930	0.47	0.26	-0.01	0.06	0.71	0.14	0.92	0.2	-	-	0.73	0.27	0.31	0.05
109988	0.58	0.25	0.1	0.12	0.89	0.2	1.2	0.21	0.6	0.04	0.81	0.16	0.53	0.07
110605	0.29	0.16	0.22	0.06	0.35	0.13	0.51	0.15	0.27	0.09	0.64	0.19	0.38	0.03
110619	-0.2	0.08	-0.32	0.05	-0.16	0.09	-0.23	0.05	-0.35	0.12	-0.42	0.14	-0.23	0.02
111431	-0.03	0.15	0.24	0.06	-0.04	0.08	-0.08	0.08	0.03	0.16	-0.06	0.13	0	0.04
112121	0.24	0.17	0.16	0.03	0.32	0.11	0.45	0.12	0.21	0.09	0.51	0.2	0.25	0.09
112540	0.06	0.11	-0.17	0.06	0.14	0.07	0.16	0.05	-0.08	0.12	0.08	0.08	-0.07	0.04
113027	-0.14	0.15	-0.07	0.01	-0.28	0.04	-0.46	*	-	-	-	-	-0.35	*
113255	0.01	0.11	0.16	0.01	0.03	0.09	0.03	0.04	0.02	0.09	0.06	0.08	0.12	0.1
113513	0.14	0.12	-0.09	0.07	0.13	0.11	0.18	0.04	0.18	0.05	0.22	0.04	-0.02	0.05
114294	0.32	0.18	0.23	0.04	0.5	0.1	0.6	0.12	0.33	0.12	-	-	0.32	0.03
114432	0.32	0.06	-0.02	0.1	0.22	0.13	0.31	*	-	-	-	-	0.11	*
114884	0.07	0.18	0.2	0.02	0.02	0.12	0.03	0.09	0.06	0.1	0.17	0.05	0.15	0.12
115080	0.02	0.13	0.06	*	0.14	0.08	0.14	0.04	-	-	-	-	-0.12	*
115674	-0.01	0.05	-0.16	0.06	-0.03	0.09	-0.09	0.02	-	-	-	-	-0.19	*
116920	-	-	-0.27	0.09	0.8	0.14	1.01	0.2	-	-	0.64	0.24	0.05	0.09
117653	0.01	0.14	0.2	0.02	-0.05	0.03	0.07	0.21	0.08	0.09	0.1	0.06	-0.07	*
117860	0.01	0.14	-0.06	0.04	-0.06	0.03	-0.06	*	-	-	-	-	-0.14	*
119070	0.2	0.16	-0.1	0.07	0.38	0.1	0.48	0.1	0.07	0.24	0.4	0.19	0.03	0.08

Continued on next page

Table A.4 – *Continued from previous page*

Star	[Ca/H]	±]	[Sc/H]	±	[Ti/H]	±	[V/H]	±	[Cr/H]	±	[Mn/H]	±	[Co/H]	±
119119	-0.12	0.14	0.24	0.04	-0.24	0.07	-0.28	0.05	-0.06	0.21	-0.31	0.19	-0.17	0.07
119507	0.15	0.13	0.3	0.09	0.25	0.1	0.27	0.07	0.09	0.07	0.24	0.1	0.19	0.06
119782	0.44	0.22	-0.13	0.13	0.69	0.15	0.9	0.19	-	-	0.68	0.26	0.2	0.05
120100	0.38	0.18	0.2	0.07	0.55	0.12	0.67	0.13	0.31	0.16	0.65	0.23	0.44	0.05
120329	0.39	0.23	0.37	0.05	0.39	0.12	0.52	0.09	0.34	0.14	0.74	0.23	0.54	0.15
121504	-0.04	0.11	0.05	0.02	-0.13	0.11	-0.13	0.02	-0.05	0.17	-0.17	0.17	-0.1	0.05
122078	0.18	0.15	0.34	0.02	0.24	0.12	0.31	0.06	0.21	0.09	0.5	0.12	0.3	0.04
124553	0.02	0.13	0.23	0.13	-0.04	0.11	-0.15	0.05	0.09	0.2	-0.06	0.18	0.01	0.04
125968	0.02	0.12	0.13	*	0.02	0.13	0.04	0.04	0.05	0.12	0.13	0.1	0.08	0.07
126653	-0.12	0.19	0.14	0.03	-0.28	0.22	-0.28	0.11	-0.16	0.22	-0.49	0.28	-0.12	0.25
127321	-0.17	0.16	0.2	0.03	-0.2	0.1	-0.19	0.2	-0.16	0.22	-0.44	0.27	-0.12	0.06
128214	0.23	0.13	0.33	0.02	0.3	0.13	0.36	0.07	0.27	0.12	0.62	0.16	0.36	0.06
128760	-0.16	0.23	0.08	0.05	-0.17	0.12	-0.26	0.1	-0.05	0.24	-0.29	0.25	-0.11	0.27
128987	0.26	0.21	-0.08	0.11	0.28	0.1	0.29	0.05	0.11	0.17	0.35	0.09	-0.01	0.05
129679	-0.11	0.17	-0.13	0.04	-0.12	0.28	-0.24	0.16	-0.01	0.17	-	-	-0.3	0.14
129764	0.02	0.11	0.08	0.04	-0.06	0.08	-0.09	0.06	0	0.13	-0.14	0.19	-0.1	0.08
129946	0	0.12	-0.2	0.04	0.02	0.04	-0.01	0.06	-0.11	0.06	-0.16	0.12	-0.18	0.05
131900	0.31	0.18	0.08	0.05	0.42	0.11	0.54	0.09	0.24	0.17	0.66	0.2	0.33	0.03
132648	-0.02	0.11	-0.29	0.05	0.03	0.1	0.06	0.03	-	-	-	-	-0.22	*
133014	0.3	0.14	0.36	0.06	0.42	0.12	0.49	0.1	0.35	0.09	0.65	0.21	0.44	0.07
135005	0.15	0.17	0.33	0.01	0.2	0.13	0.21	0.04	0.11	0.08	0.35	0.11	0.21	0.04
135309	0.08	0.14	0.14	0.11	0.03	0.04	0.06	0.05	0.03	0.09	0	0.08	-0.03	0.07
135562	-0.06	0.14	0.27	0.05	-0.08	0.11	-0.09	0.1	0.03	0.19	-0.11	0.17	0.09	0.08
135625	0	0.14	0.19	0.02	-0.06	0.07	-0.08	0.02	0.01	0.13	-0.07	0.2	0.04	0.09
135725	0.09	0.16	-0.06	0.07	0.14	0.1	0.14	0.05	-0.02	0.14	0.2	0.06	0.04	0.04
136130	0.13	0.16	0.23	0.02	0.19	0.1	0.2	0.04	0.04	0.08	0.19	0.09	0.1	0.06
136548	-0.03	0.1	-0.02	0.03	-0.01	0.07	-0.05	0.04	-0.09	0.05	-0.18	0.11	-0.06	0.06
136894	0.17	0.14	-0.12	0.08	0.27	0.09	0.29	0.01	-	-	-	-	-0.02	*
137214	-0.11	0.12	0.14	0.08	-0.2	0.21	-0.29	0.04	-0.09	0.19	-0.33	0.27	-0.11	0.11
140643	0.65	0.26	0.07	0.1	0.97	0.18	1.29	0.23	-	-	0.91	0.26	0.49	0.02
141105	0.08	0.18	0.14	0.02	0.26	0.1	0.29	0.07	-0.01	0.07	0.28	0.26	0.03	0.02
141366	0.17	0.11	0.42	0.07	0.14	0.13	0.15	0.11	0.15	0.18	0.24	0.06	0.13	0.08
141514	-0.05	0.15	0.1	0.08	-0.19	0.13	-0.34	0.09	-0.06	0.19	-0.38	0.27	-0.19	0.06
141598	0.05	0.14	0.01	0.06	0.17	0.14	0.17	0.07	-0.09	0.11	0.03	0.06	-	-
141599	0.27	0.14	0.09	0.06	0.36	0.12	0.49	0.1	0.24	0.15	0.59	0.19	0.35	0.09
141885	0.1	0.21	0.47	0.08	0.09	0.14	0.12	0.06	0.22	0.23	0.25	0.19	0.21	0.11
142137	0.06	0.19	0.41	0.05	0.04	0.13	0.02	0.05	0.18	0.17	0.23	0.13	0.13	0.16

Continued on next page

Table A.4 – *Continued from previous page*

Star	[Ca/H]	±]	[Sc/H]	±	[Ti/H]	±	[V/H]	±	[Cr/H]	±	[Mn/H]	±	[Co/H]	±
143120	0.27	0.1	0.47	0.06	0.4	0.11	0.5	0.14	0.34	0.09	0.74	0.24	0.5	0.06
143137	-0.13	0.2	0.29	0.04	-	-	-0.34	0.11	0	0.28	-	-	-0.06	0.09
143295	-	-	-0.16	0.12	0.98	0.16	1.16	0.2	-	-	0.81	0.25	0.28	0.07
143673	0.27	0.19	0.1	0.03	0.46	0.12	-	-	0.31	0.17	0.57	0.23	0.33	0.09
144087	0.23	0.11	-0.03	0.07	0.29	0.1	0.35	0.05	0.14	0.15	0.4	0.09	0.19	0.02
144088	0.44	0.19	-0.07	0.12	0.65	0.14	0.83	0.12	-	-	0.71	0.22	0.36	0.1
144167	0.2	0.15	0.44	*	0.25	0.1	0.28	0.11	0.29	0.14	0.42	0.12	0.3	0.08
144550	0.16	0.17	0.34	0.03	0.23	0.14	0.31	0.09	0.2	0.13	0.55	0.18	0.35	0.11
144848	0.09	0.16	0.27	0.03	0.15	0.09	0.17	0.06	0.14	0.1	0.35	0.08	0.14	0.07
144899	0.12	0.12	0.41	0.08	0.11	0.14	0.22	0.02	0.23	0.12	0.47	0.14	0.39	0.08
145518	-0.14	0.12	-0.17	0.04	-0.17	0.08	-	-	-0.2	0.1	-0.4	0.19	-0.29	0.11
145666	-0.12	0.13	-0.09	0.06	-0.21	0.06	-0.2	0.14	-0.16	0.09	-0.32	0.25	-0.32	0.11
146817	0.02	0.11	0.11	0.06	0.08	0.08	0.05	0.05	-0.05	0.08	-0.13	0.11	0	0.03
146835	-0.24	0.14	-0.25	0.03	-0.3	0.08	-0.31	0.1	-0.27	0.11	-0.57	0.21	-0.33	0.06
147018	0.27	0.14	0.05	0.07	0.46	0.09	0.55	0.12	0.23	0.15	0.61	0.2	0.25	0.04
147619	-0.05	0.15	0.38	0.08	-0.13	0.1	-0.08	0.15	0.11	0.23	-0.05	0.21	0.07	0.08
148156	-0.04	0.2	0.21	0.08	-	-	-0.21	0.07	0.03	0.22	-0.17	0.23	-0.01	0.06
148628	-0.28	0.16	-0.06	0.03	-0.39	0.07	-	-	-0.23	0.24	-	-	-0.35	0.12
149189	0.11	0.15	0.35	0.04	0.12	0.13	0.15	0.06	0.19	0.13	0.41	0.19	0.22	0.02
150761	-0.04	0.29	0.28	0.04	-	-	0	0.12	0.13	0.21	-	-	0.14	0.16
151450	-0.22	0.13	-0.03	0.02	-0.31	0.05	-0.33	0.11	-0.21	0.2	-0.54	0.28	-0.27	0.09
152388	0.37	0.15	-0.12	0.09	0.54	0.11	0.67	0.14	-	-	0.62	0.25	0.16	0.02
153631	-0.13	0.12	0.04	0.03	-0.17	0.05	-0.23	0.02	-0.16	0.14	-0.38	0.18	-0.21	0.06
154682	-0.15	0.11	0	0.02	-0.19	0.05	-0.26	0.05	-0.16	0.16	-0.39	0.17	-0.25	0.03
154697	0.2	0.13	0.03	0.05	0.24	0.11	0.33	0.07	0.15	0.12	0.44	0.13	0.18	0.05
156152	0.11	0.15	0.09	0.07	0.05	0.09	-0.01	0.03	0.04	0.09	0.01	0.1	0	0.03
156643	-0.19	0.1	-0.14	0.06	-0.19	0.08	-0.23	0.04	-0.25	0.05	-0.4	0.17	-0.3	0.08
157798	0.07	0.25	0.48	0.29	0.18	0.11	0.29	0.26	0.13	0.19	0.27	0.16	-	-
157830	-0.02	0.11	-0.22	0.03	0.02	0.1	0.02	0.04	-0.19	0.16	-0.08	0.06	-0.18	0.06
158469	-0.21	0.17	0.06	0.02	-0.3	0.09	-0.39	0.09	-0.17	0.24	-	-	-0.24	0.12
158630	-0.2	0.11	-0.14	0.02	-0.26	0.05	-0.29	0.06	-0.27	0.1	-0.54	0.21	-0.29	0.03
159902	-0.11	0.13	-0.17	0.01	-0.16	0.05	-0.17	0.07	-0.28	0.09	-0.4	0.16	-0.24	0.04
160411	0.04	0.14	0.35	0.02	0.03	0.14	0.05	0.07	0.1	0.13	0.11	0.07	0.08	0.07
160859	-0.09	0.09	-0.06	0.04	-0.1	0.04	-0.14	0.09	-0.15	0.06	-0.39	0.18	-0.16	0.04
161098	-0.09	0.1	-0.2	0.06	-0.01	0.07	-0.05	0.05	-0.18	0.08	-0.14	0.09	-0.17	0.06
162907	0.34	0.16	0.1	0.05	0.59	0.25	0.67	0.13	0.24	0.21	0.61	0.21	0.34	0.02
165011	-0.15	0.14	0.23	0.03	-0.24	0.12	-0.29	0.15	-0.07	0.25	-0.36	0.23	-0.15	0.1

Continued on next page

Table A.4 – *Continued from previous page*

Star	[Ca/H]	±]	[Sc/H]	±	[Ti/H]	±	[V/H]	±	[Cr/H]	±	[Mn/H]	±	[Co/H]	±
165204	0.34	0.18	0.27	0.05	0.44	0.14	0.5	0.12	0.32	0.1	0.65	0.18	0.41	0.01
165271	0.03	0.12	0.27	0.01	0.05	0.05	0.06	0.07	0.06	0.1	0.12	0.06	0.06	0.04
165385	-0.21	0.14	0.16	0.04	-0.31	0.09	-0.33	0.07	-0.11	0.25	-	-	-0.18	0.06
165449	-0.17	0.11	0.01	0.01	-0.19	0.07	-0.24	0.08	-0.18	0.14	-0.41	0.19	-0.22	0.06
165920	0.57	0.27	0.18	0.13	0.78	0.17	1.02	0.23	0.45	0.26	0.91	0.27	0.6	0.1
169303	-0.21	0.18	0.16	0.03	-0.25	0.09	-0.29	0.18	-0.1	0.23	-0.4	0.27	-0.24	0.11
169506	0.14	0.19	0.49	0.03	0.14	0.15	0.14	0.17	0.2	0.26	0.29	0.2	0.3	0.23
171990	-0.11	0.11	0.22	0.02	-0.17	0.04	-0.19	0.09	-0.11	0.19	-0.23	0.16	-0.12	0.05
172063	0.3	0.24	0.05	0.07	0.39	0.14	0.5	0.1	0.2	0.14	0.56	0.19	0.3	0.04
172582	-0.11	0.12	-0.28	0.04	0	0.04	-0.09	0.05	-0.25	0.13	-0.3	0.13	-0.2	0.06
174494	0.1	0.14	0.35	0.04	0.12	0.13	0.16	0.03	0.11	0.13	0.38	0.14	0.2	0.09
174541	-0.1	0.11	0.06	0.05	0.01	0.09	-0.04	0.09	-0.23	0.08	-0.55	0.17	-0.13	0.08
175073	0.36	0.16	-0.21	0.09	0.6	0.14	0.77	0.16	-	-	0.54	0.22	0.15	0.06
175169	0.17	0.12	0.21	0.07	0.25	0.14	0.32	0.04	0.24	0.08	0.5	0.12	0.19	0.15
176110	0.02	0.16	0.29	0.01	0.09	0.12	-	-	0.13	0.13	0.28	0.15	0.18	0.06
176151	0.12	0.16	0.32	0.03	0.19	0.07	0.24	0.06	0.13	0.12	0.43	0.13	0.28	0.08
176986	-	-	-0.06	0.11	0.99	0.14	-	-	-	-	0.85	0.24	0.34	0.1
177122	-0.24	0.11	-0.1	0.04	-0.32	0.07	-0.4	0.05	-0.2	0.22	-0.59	0.27	-0.33	0.08
177409	-0.08	0.12	-0.05	0.03	-0.15	0.06	-0.22	0.06	-0.13	0.09	-0.33	0.18	-0.16	0.06
178076	0.23	0.12	-0.17	0.09	0.31	0.08	0.37	0.07	0.1	0.19	0.38	0.13	0.01	0.04
179640	0.38	0.17	0.33	0.09	0.54	0.14	0.64	0.14	0.38	0.15	0.76	0.26	0.49	0.06
180204	-0.03	0.16	0.23	0.01	-0.12	0.06	-0.1	0.1	0.08	0.18	-0.06	0.25	0.04	0.07
180257	0.1	0.18	0.39	0.05	0.1	0.11	0.03	0.08	0.14	0.14	0.18	0.14	0.19	0.18
181010	0.42	0.21	-0.04	0.09	0.67	0.13	0.84	0.16	-	-	0.59	0.17	0.26	0.05
182228	0.05	0.15	0.25	0.02	0.05	0.05	0.05	0.01	0.06	0.15	0.14	0.14	0.13	0.07
182498	-0.06	0.16	0.03	0.01	-0.16	0.07	-0.2	0.03	-0.06	0.1	-0.25	0.03	-0.2	*
184317	-0.04	0.11	0.08	0.01	-0.08	0.07	-0.11	0.02	-0.04	0.12	-0.07	0.14	-0.08	0.07
185283	-	-	-0.04	0.19	1.16	0.18	-	-	-	-	0.83	0.26	0.28	0.17
185615	0.2	0.13	0.15	0.04	0.34	0.11	0.41	0.08	0.17	0.13	0.39	0.14	0.24	0.04
186160	-0.32	0.14	-0.24	0.05	-0.39	0.05	-0.48	0.05	-0.42	0.13	-0.79	0.26	-0.4	0.06
186265	0.47	0.23	0.32	0.06	0.59	0.15	0.72	0.14	0.45	0.14	0.85	0.24	0.58	0.12
186651	-0.15	0.16	0	0.03	-0.28	0.07	-0.29	0.1	-0.17	0.2	-0.49	0.27	-0.26	0.09
186803	0.09	0.07	-0.13	0.06	0.07	0.08	0.08	0.04	-0.05	0.13	0.05	0.05	-0.1	0.04
187154	0.06	0.2	-	-	0.01	0.11	-0.01	0.09	0.05	0.16	-0.11	0.2	0	0.03
189310	0.5	0.23	-0.1	0.11	0.76	0.15	0.89	0.11	-	-	0.73	0.27	0.31	0.09
190125	0.22	0.16	0.11	0.08	0.27	0.12	0.37	0.12	0.14	0.13	0.44	0.09	0.12	0.04
190613	-0.01	0.11	0.11	0.06	0.02	0.06	-0.03	0.06	-0.03	0.08	-0.07	0.09	-0.07	0.04

Continued on next page

Table A.4 – *Continued from previous page*

Star	[Ca/H]	±]	[Sc/H]	±	[Ti/H]	±	[V/H]	±	[Cr/H]	±	[Mn/H]	±	[Co/H]	±
191760	0.12	0.13	0.36	0.04	0.18	0.09	0.2	0.09	0.22	0.2	0.35	0.07	0.28	0.1
193567	0.25	0.11	0.14	0.04	0.33	0.09	0.43	0.07	-	-	0.56	0.18	0.36	0.06
193728	0.25	0.16	0.28	0.03	0.33	0.12	0.39	0.06	0.19	0.11	0.5	0.17	0.27	0.07
193995	0.22	0.15	0.32	0.02	0.26	0.14	0.36	0.07	0.26	0.07	0.54	0.17	0.32	0.07
195145	0.25	0.14	0.1	0.06	0.36	0.12	0.43	0.12	0.22	0.16	0.56	0.14	0.3	0.04
195284	0.22	0.15	0.04	0.17	0.26	0.1	0.32	0.08	0.14	0.14	0.42	0.11	0.16	0.04
196397	0.49	0.2	0.19	0.12	0.74	0.16	0.95	0.18	0.42	0.26	0.87	0.26	0.46	0.04
197069	0.01	0.09	0.19	0.02	-0.08	0.09	-0.04	0.04	0.07	0.18	-0.04	0.21	-0.01	0.06
197210	0.1	0.09	-0.12	0.05	0.17	0.11	0.19	0.04	0.02	0.12	0.25	0.11	0.01	0.05
197499	-0.11	0.14	0.1	0.14	-0.1	0.26	-0.19	0.08	-0.1	0.17	-0.3	0.16	-0.11	0.02
197818	-0.12	0.11	-0.1	0.02	-0.18	0.07	-0.24	0.02	-0.23	0.1	-0.46	0.18	-0.16	0.07
197823	0.36	0.18	0.04	0.08	0.52	0.11	0.67	0.16	0.26	0.19	0.68	0.21	0.35	0.05
198477	0.28	0.2	0.22	0.08	0.46	0.14	0.62	0.11	0.26	0.21	0.59	0.13	0.39	0.19
199065	-0.03	0.14	-0.01	0.01	-0.05	0.08	-0.05	0.08	-0.03	0.09	-0.14	0.2	-0.07	0.13
200733	-0.2	0.2	0.24	0.02	-0.32	0.18	-0.21	0.15	-	-	-	-	-0.16	0.1
200869	0.49	0.2	0.23	0.06	0.69	0.17	0.87	0.15	0.43	0.21	0.87	0.26	0.55	0.07
201757	0.25	0.13	0.29	0.08	0.3	0.12	0.45	0.1	0.2	0.14	0.5	0.13	0.29	0.07
202282	0.05	0.16	0.02	0.05	0.08	0.08	0.06	0.02	0.04	0.11	0.13	0.09	-0.05	0.1
202457	0.1	0.13	0.21	0.01	0.2	0.06	0.21	0.07	0.08	0.07	0.2	0.07	0.21	0.08
203432	0.32	0.16	0.2	0.07	0.46	0.15	0.57	0.11	0.34	0.12	0.68	0.17	0.44	0.07
205045	-0.02	0.15	0.24	0.02	-0.04	0.14	-0.1	0.05	-0.01	0.13	-0.14	0.22	0.07	0.15
205067	-0.05	0.11	0.03	0.02	0	0.1	-0.05	0.05	-0.13	0.08	-0.23	0.12	-0.07	0.01
205158	0.03	0.16	0.3	0.03	-0.03	0.1	-0.13	0.12	0.11	0.23	-0.01	0.2	0.03	0.1
206025	-0.1	0.16	0.25	0.03	-0.21	0.12	-0.31	0.17	-0.01	0.27	-0.35	0.27	-0.16	0.11
206255	0.13	0.16	0.3	0.03	0.2	0.09	0.23	0.04	0.14	0.08	0.42	0.15	0.25	0.12
206683	0.13	0.13	0.28	0.01	0.11	0.09	0.19	0.09	0.15	0.14	0.35	0.14	0.27	0.06
207970	0.2	0.16	0.09	0.02	0.36	0.11	0.41	0.1	0.14	0.11	0.41	0.16	0.27	0.02
208704	-0.13	0.11	-0.02	0.03	-0.15	0.05	-0.15	0.05	-0.16	0.1	-0.24	0.14	-0.19	0.01
209566	0.31	0.16	0.1	0.07	0.45	0.11	0.58	0.16	0.22	0.17	0.59	0.19	0.32	0.01
209659	0.01	0.17	0.35	0.04	-0.04	0.09	-0.07	0.05	0.06	0.16	-0.03	0.15	0.04	0.1
210193	0.04	0.1	0.07	0.02	0.04	0.11	0.1	0.07	0.02	0.11	0.17	0.07	0.07	0.04
211366	0.13	0.07	0.11	0.04	0.1	0.18	0.13	0.08	0.16	0.05	0.27	0.07	0.08	*
213429	-0.12	0.15	-0.04	0.04	-0.11	0.15	-0.15	0.11	-0.12	0.18	-	-	-0.24	0.09
213717	0.36	0.2	-0.02	0.09	0.52	0.11	0.66	0.11	0.2	0.2	0.61	0.23	0.48	0.25
213941	-0.06	0.16	-0.17	0.04	-0.01	0.09	-0.08	0.04	-0.31	0.08	-0.52	0.12	-0.2	0.07
214691	0.21	0.14	0.14	0.02	0.36	0.1	0.43	0.09	0.14	0.13	0.43	0.16	0.29	0.11
215456	-0.1	0.12	0.11	0.01	-0.12	0.07	-0.13	0.08	-0.13	0.12	-0.22	0.12	-0.15	0.06

Continued on next page

Table A.4 – *Continued from previous page*

Star	[Ca/H]	±]	[Sc/H]	±	[Ti/H]	±	[V/H]	±	[Cr/H]	±	[Mn/H]	±	[Co/H]	±
216054	0.13	0.15	-0.2	0.07	0.26	0.08	0.3	0.06	-0.02	0.18	0.21	0.16	-0.03	0.01
218760	-	-	-0.1	0.09	1.05	0.16	-	-	-	-	0.81	0.26	0.29	0.07
219011	0.26	0.14	0.32	0.04	0.32	0.11	0.41	0.08	0.28	0.09	0.54	0.14	0.37	0.09
219533	0.15	0.13	0.36	0.03	0.19	0.15	0.27	0.07	0.19	0.1	0.37	0.07	0.27	0.05
219556	0.28	0.13	0.06	0.05	0.43	0.09	0.5	0.08	0.19	0.17	0.59	0.22	0.26	0.06
220426	-0.03	0.18	0.23	0.01	-0.11	0.1	-0.14	0.11	0.05	0.22	-0.07	0.27	0.02	0.09
220476	0.13	0.16	-0.14	0.05	0.11	0.07	0.07	0.05	0.02	0.09	0.07	0.08	0.03	0.09
220689	-0.15	0.11	0.01	0.01	-0.15	0.07	-0.19	0.06	-0.12	0.11	-0.26	0.18	-0.13	0.04
220718	0.13	0.21	0.38	0.02	0.11	0.07	0.15	0.08	0.11	0.13	0.27	0.08	0.15	0.13
220829	0.48	0.24	0.01	0.04	0.83	0.2	1.01	0.21	-	-	0.64	0.16	0.34	0.13
220945	-	-	0.02	0.09	0.93	0.22	1.2	0.21	0.6	0.01	0.65	0.09	0.34	*
220981	0.28	0.17	0.27	0.06	0.38	0.14	0.47	0.12	0.31	0.04	0.42	0.11	0.31	*
221257	-0.15	0.1	-0.06	0.01	-0.18	0.04	-0.18	0.04	-0.21	0.07	-0.39	0.18	-0.22	0.03
221275	0.35	0.18	0.04	0.09	0.53	0.11	0.69	0.17	0.22	0.27	0.68	0.21	0.37	0.04
221954	0.32	0.16	0.4	0.03	0.44	0.18	0.58	0.15	0.38	0.11	0.63	0.21	0.39	0.13
222422	0.18	0.13	-0.13	0.07	0.24	0.07	0.31	0.06	0	0.16	0.17	0.05	-0.03	0.04
222669	-0.05	0.12	-0.03	0.02	-0.08	0.04	-0.09	0.08	-0.06	0.1	-0.1	0.12	-0.1	0.07
224010	0.03	0.12	0.27	0.03	0.1	0.13	0.05	0.07	0.08	0.1	0.24	0.15	0.14	0.06
224022	-0.1	0.16	0.18	0.03	-0.17	0.11	-0.27	0.06	-0.07	0.19	-0.28	0.25	-0.1	0.14
224143	-0.05	0.18	-0.15	0.08	-0.09	0.08	-0.08	0.18	-0.04	0.03	-0.2	0.19	-0.08	0.07
224433	0.23	0.13	-0.01	0.06	0.29	0.13	0.37	0.08	-	-	0.41	0.1	0.1	*
224538	-0.02	0.16	0.31	0.03	-0.07	0.1	-0.08	0.07	0.08	0.17	0.07	0.28	0.09	0.08
224789	0.5	0.23	-0.07	0.11	0.68	0.13	0.87	0.16	-	-	0.79	0.27	0.25	0.06
225155	0.2	0.14	0.29	0.04	0.33	0.12	0.4	0.1	0.21	0.08	0.47	0.14	0.32	0.07
225299	0.18	0.15	0.1	0.07	0.2	0.15	0.23	0.09	0.13	0.09	0.39	0.1	0.15	0.05

Table A.5: All stars abundances for Ni, Cu, Zn, Y, Zr, Mo and Ba.

Star	[Ni/H]	±	[Cu/H]	±	[Zn/H]	±	[Y/H]	±	[Zr/H]	±	[Mo/H]	±	[Ba/H]	±
361	-0.25	0.09	-0.32	0.06	-0.94	*	-0.06	0.01	-0.2	*	0	-	-0.08	0.1
1002	0.08	0.14	0.23	0.19	-0.75	*	0.09	0.03	-	-	-0.36	*	-0.09	0.13
1237	0.18	0.12	0.35	*	-0.94	*	0.31	*	-0.14	*	-	-	0.12	0.09
1893	0.31	0.13	0.31	0.19	-0.77	*	0.09	0.07	0.28	0.17	-0.11	*	-0.06	0.06
1926	-0.4	0.13	-0.44	0.1	-0.9	*	-	-	-	-	-	-	-0.37	0.06
2098	0.03	0.12	0.03	0.04	-0.64	*	0.03	0.09	-0.1	*	-	-	-0.12	0.17
2222	0.23	0.12	0.24	0.06	-0.63	*	0.2	0.17	0.84	*	-0.12	*	0.02	0.14
3359	0.3	0.15	0.37	0.21	-0.8	*	0.12	0.26	0.13	*	-0.07	*	-0.17	0.11
4333	0.32	0.14	0.34	0.18	-0.78	*	-	-	0.02	*	0.03	*	-0.12	0.07
4392	0.13	0.12	0.19	0.11	-0.74	*	0.07	0.12	-0.07	*	-	-	-0.16	0.09
6236	-0.07	0.1	-0.09	0.03	-0.75	*	0.02	0.15	0.19	0.13	-0.3	*	-0.03	0.13
6790	-0.16	0.16	-0.3	0.12	-0.84	*	-0.06	0.11	0.06	0.04	-	-	-0.08	0.18
6880	0.04	0.17	-0.08	0.06	-	-	0.05	0.16	0.5	*	-0.35	*	-0.13	0.05
6910	0.24	0.13	0.32	0.04	-0.44	*	0.31	0.2	0.5	*	-	-	0.17	0.18
7134	-0.38	0.09	-0.4	0.09	-0.93	*	-0.25	0.01	-0.33	*	-	-	-0.34	0.14
7449	-0.3	0.1	-0.28	0.19	-0.9	*	-0.14	0.14	-0.1	*	-	-	-0.12	0.11
7661	0.1	0.12	0.08	0.24	-0.99	*	0.09	0.14	0.83	*	-	-	0.1	0.06
8076	-0.1	0.1	-0.19	0.04	-0.85	*	0.01	0.09	0.29	*	-	-	-0.01	0.11
8129	0	0.09	-0.02	0.16	-0.92	*	-0.08	0.09	-0.05	*	-	-	-0.11	0.07
8406	-0.13	0.09	-0.17	0.08	-0.91	*	-0.13	0.14	-0.08	*	-	-	-0.13	0.09
9175	0.08	0.12	0.1	0.1	-0.69	*	0.09	0.02	0.1	*	-	-	-0.1	0.13
9782	-0.08	0.1	-0.11	0.02	-0.69	*	-0.01	0.17	0.14	0.05	-	-	-0.09	0.14
9847	0.35	0.13	0.47	0.04	-0.52	*	0.28	0.13	-	-	-0.35	*	-0.04	0.1
9905	0.34	0.16	0.42	0.23	-0.87	*	0.04	0.2	0.18	*	-0.14	*	-0.11	0.02
10008	0.09	0.16	0.07	0.23	-	-	0.11	0.16	0.14	*	-	-	0.16	0.11
10226	-0.01	0.11	-0.23	0.26	-0.73	*	-0.02	0.21	0.14	*	-	-	-0.01	0.1
10370	-0.02	0.09	0.01	0.05	-0.82	*	-0.07	0.08	-0.12	*	-	-	-0.2	0.13
10519	-0.42	0.11	-0.46	0.05	-	-	-	-	-0.19	*	-	-	-0.49	0.14
10576	-0.08	0.12	-0.18	0.01	-0.76	*	0.06	0.11	0.07	*	-	-	-0.07	0.17
10611	0.11	0.15	-	-	-	-	0.14	0.14	0.08	*	-	-	0.16	0.11
10678	0.12	0.13	0.1	0.13	-0.9	*	0.12	0.14	-0.27	*	-	-	-0.08	0.07
11264	0.07	0.11	0.11	0.14	-0.74	*	-0.1	0.22	0.02	*	-	-	-0.15	0.1
11754	0.28	0.13	0.3	0.08	-0.53	*	0.28	0.09	0.35	0.21	-0.14	*	0.04	0.15
12585	0.08	0.1	0.06	0.05	-0.74	*	-	-	-	-	-0.26	*	-0.13	0.03
12951	-0.28	0.12	-0.35	0.13	-0.81	*	-0.12	0.24	-0.02	*	-	-	-0.1	0.15
13060	0.28	0.16	0.3	0.23	-	-	-	-	0.13	*	-	-	-0.08	0.07

Continued on next page

Table A.5 – *Continued from previous page*

Star	[Ni/H]	±	[Cu/H]	±	[Zn/H]	±	[Y/H]	±	[Zr/H]	±	[Mo/H]	±	[Ba/H]	±
13350	0.47	0.15	0.54	0.15	-0.54	*	-	-	-	-	-0.07	*	0.03	0.11
13386	0.43	0.2	0.47	0.22	-0.8	*	-	-	-	-	-	-	-	-
14758	-0.23	0.09	-0.18	0.05	-0.94	*	-0.23	0.03	-	-	-	-	-0.28	0.09
15507	0.12	0.1	0.18	0.1	-0.75	*	-	-	-	-	-	-	-0.08	0.1
15590	0.22	0.17	0.21	0.04	-0.51	*	0.24	0.21	0.36	0.15	0.02	*	0.13	0.15
15767	0.05	0.19	-	-	-	-	-	-	0.8	*	-	-	-0.01	0.1
16950	0.09	0.14	0.25	0.02	-0.49	*	0.14	0.22	0.28	0.22	-	-	0.05	0.12
17134	-0.11	0.12	-0.12	0.12	-0.84	*	-0.17	0.03	-0.15	*	-	-	-0.21	0.11
17289	-0.28	0.12	-0.33	0.07	-0.94	*	0.08	0.21	-0.19	*	-	-	-0.13	0.08
18168	0.22	0.25	-	-	-	-	-0.09	*	-0.17	*	-	-	-0.08	0.1
18708	0.13	0.11	0.09	0.05	-0.62	*	0.26	0.14	-	-	-	-	-0.06	0.17
18754	0.35	0.13	0.46	0.19	-0.55	*	0.42	0.11	0.14	0.15	0.01	*	0.08	0.14
18819	0.01	0.13	0.02	0.09	-0.54	*	0.2	0.22	0.33	0.07	-	-	0.23	0.15
19603	0.12	0.13	0.14	0.04	-0.6	*	0.23	*	0.41	*	-	-	-0.04	0.13
19916	0.09	0.16	0.2	*	-0.62	*	0.26	0.02	0.53	*	-	-	-0.01	0.17
20155	0.1	0.12	0.16	0.05	-0.5	*	0.13	0.17	0.13	*	-0.28	*	0.04	0.16
20407	-0.47	0.16	-0.5	0.08	-	-	-0.46	0.04	-	-	-	-	-0.48	0.09
20584	-0.04	0.13	0	0.04	-0.71	*	0.31	0.04	0.45	*	-	-	0.19	0.13
20657	0.14	0.13	0.19	0.1	-0.54	*	0.24	0.16	0.25	0.09	-	-	0.01	0.19
20675	0.14	0.12	0.21	0.11	-0.48	*	0.36	0.17	0.37	0.06	-0.48	*	-0.05	0.12
21036	0.11	0.11	0.11	0.14	-0.93	*	0.12	0.03	0.07	*	-	-	0.1	0.09
21089	0.4	0.19	0.43	0.11	-0.56	*	0.22	0.14	-	-	-0.01	*	0	0.09
22177	0.26	0.12	0.34	0.03	-0.67	*	0.23	0.02	0.35	*	-0.31	*	-0.02	0.11
22582	0.08	0.12	0.19	0.11	-0.82	*	-0.03	0.11	0.05	*	-	-	-0.23	0.06
23576	-0.1	0.1	-0.16	0.04	-0.82	*	0.11	0.27	-0.22	*	-	-	-0.17	0.15
24331	0.04	0.2	-	-	-	-	-0.53	*	-	-	-	-	-0.14	0.01
25912	0.01	0.17	-0.02	0.12	-0.88	*	0.14	0.04	0.36	*	-	-	-0.05	0.14
26040	-0.29	0.12	-0.27	0.25	-	-	0.02	0.11	-	-	-0.58	*	-0.12	0.08
26071	0.36	0.16	0.44	0.07	-0.55	*	0.21	0.05	0.26	0.12	-0.12	*	-0.05	0.11
26864	-0.01	0.17	-0.12	0.16	-0.99	*	0.13	0.21	0.07	*	-	-	0.12	0.13
27328	0.22	0.16	0.22	0.22	-0.96	*	-	-	0.23	0.23	-	-	-0.11	0.02
27446	-0.06	0.12	-0.09	0.13	-0.95	*	0.13	0.16	-	-	-	-	-0.01	0.08
27905	-0.22	0.1	-0.21	0.05	-0.88	*	-0.17	0.04	-	-	-	-	-0.23	0.03
27939	0.25	0.14	0.26	0.09	-0.58	*	0.13	0.04	0.08	*	-0.3	*	-0.13	0.13
28185	0.28	0.11	0.29	0.09	-0.63	*	-	-	-0.16	*	-0.31	*	-0.15	0.06
28701	-0.23	0.12	-0.14	0.06	-0.9	*	-0.02	0.13	-0.06	*	-	-	-0.1	0.12
28821	-0.07	0.12	-0.03	0.07	-0.95	*	-0.18	0.05	-0.16	*	-	-	-0.26	0.08

Continued on next page

Table A.5 – *Continued from previous page*

Star	[Ni/H]	±	[Cu/H]	±	[Zn/H]	±	[Y/H]	±	[Zr/H]	±	[Mo/H]	±	[Ba/H]	±
29231	0.26	0.16	0.27	0.15	-0.88	*	0.11	0.04	0.43	*	-0.14	*	-0.08	0.09
29263	0.1	0.2	0.08	0.18	-0.68	*	0.09	0.22	-	-	-	-	-0.15	0.07
29813	-0.13	0.12	-0.17	0.07	-0.89	*	-0.1	0.14	-0.02	*	-	-	-0.12	0.12
30278	-0.02	0.11	0.02	0.16	-1	*	-0.16	0.16	-0.26	*	-	-	-0.25	0.08
30306	0.27	0.15	0.35	0.16	-0.74	*	0.08	0.11	0.11	0.13	-	-	-0.1	0.13
30501	0.18	0.19	-	-	-	-	-	-	0.55	*	-	-	0	0.03
30669	0.27	0.14	0.3	0.21	-0.87	*	0.07	0.13	0.09	*	-	-	-0.14	0.05
31392	0.19	0.23	0.22	0.23	-0.99	*	0.05	0.16	0.21	*	-0.16	*	-0.04	0.07
32564	0.08	0.11	0.21	0.2	-0.85	*	-0.07	0.08	-0.31	*	-	-	-0.18	0.03
32724	-0.2	0.1	-0.18	0.04	-0.79	*	-0.12	0.01	-0.26	*	-	-	-0.17	0.14
32804	-0.06	0.09	-0.14	*	-0.84	*	0.2	0.12	0.15	*	-	-	0.12	0.15
33093	-0.09	0.1	-0.12	0.06	-0.7	*	0.06	0.29	0.09	*	-	-	0.1	0.14
33214	0.45	0.28	0.46	0.26	-0.79	*	-	-	-	-	-	-	-0.04	0.08
33822	0.31	0.13	0.4	0.09	-0.58	*	0.23	0.04	0.27	0.06	-0.33	*	-0.02	0.17
33873	0.13	0.11	0.26	0.23	-0.75	*	0.09	0.07	0.12	*	-0.46	*	-0.08	0.04
34195	-0.06	0.19	-0.13	0.04	-0.63	*	0.11	0.13	0.32	0.01	-	-	0.06	0.15
34230	0.34	0.11	-	-	-0.73	*	-	-	0.11	0.11	-0.18	*	-0.12	0.05
34377	0.1	0.11	0.15	*	-0.81	*	-	-	0.09	*	-	-	0.04	0.13
34599	0.08	0.12	0.15	*	-0.74	*	-	-	-	-	-	-	0.03	0.03
35376	0.06	0.09	0.24	*	-0.71	*	0.45	*	0.24	*	-	-	-0.13	0.13
35676	0.16	0.11	0.1	0.16	-0.84	*	0.14	0.03	-0.19	*	-	-	0.07	0.06
36152	0.04	0.1	0.03	0.1	-0.8	*	0.07	0.04	-	-	-0.49	*	-0.13	0.09
36329	-0.15	0.15	-0.17	0.13	-0.96	*	0.04	*	-0.18	*	-	-	0.11	0.09
37351	-0.03	0.1	-0.13	*	-0.76	*	-	-	-	-	-	-	-0.03	0.08
37706	-0.15	0.1	-0.15	0.1	-	-	-0.11	0.09	-0.44	*	-	-	-0.17	0.06
37761	0.27	0.14	0.39	0.18	-0.65	*	0.48	0.03	0.37	*	-	-	0.19	0.19
37986	0.41	0.16	0.49	0.18	-0.64	*	0.23	*	-0.08	*	-0.09	*	-0.09	0.07
38467	-	-	0.38	0.17	-0.53	*	0.18	0.22	0.37	*	-	-	-0.01	0.13
38554	0.31	0.15	0.31	0.06	-0.55	*	0.06	0.01	0.23	0.15	-0.36	*	-0.12	0.12
38667	-0.01	0.18	-0.06	0.02	-0.58	*	0.12	0.09	-	-	-	-	-0.01	0.14
38677	-0.05	0.12	-0.08	0.06	-0.63	*	0.08	0.18	0.14	0.18	-	-	-0.1	0.15
39126	0.15	0.18	-	-	-	-	-	-	0.02	*	-	-	0.11	0.11
39503	0.26	0.13	0.32	0.16	-0.67	*	0.19	0.16	-0.12	*	-0.17	*	-0.12	0.07
39804	0.05	0.09	0	0.19	-0.91	*	0.03	0.03	-0.05	*	-	-	-0.08	0.06
39855	-0.31	0.1	-0.28	0.11	-	-	-0.41	0.03	-0.25	*	-	-	-0.33	0.07
40105	0.4	0.24	0.55	0.23	-0.93	*	0.27	0.3	0.42	*	0.13	*	0.01	0.12
40403	0.32	0.11	0.41	0.08	-0.5	*	0.16	0.06	0.37	0.22	0.06	*	0.05	0.12

Continued on next page

Table A.5 – *Continued from previous page*

Star	[Ni/H]	±	[Cu/H]	±	[Zn/H]	±	[Y/H]	±	[Zr/H]	±	[Mo/H]	±	[Ba/H]	±
41155	-0.03	0.16	-0.02	0.18	-0.57	*	0.24	0.19	0.35	0.18	-	-	0.2	0.13
42044	-0.27	0.12	-0.21	0.27	-	-	0.06	0.23	-	-	-	-	0.09	0.21
42287	-0.16	0.13	-0.32	*	-0.85	*	-	-	-	-	-	-	0.07	0.11
42538	0.04	0.15	0.02	0.01	-0.61	*	0.35	0.18	0.32	*	-	-	0.1	0.11
42719	0.24	0.14	0.33	0.09	-0.46	*	0.28	0.09	0.33	0.04	-	-	0.18	0.15
42778	0.03	0.13	-0.01	0.01	-0.77	*	0.07	0.16	0.16	*	-	-	0.09	0.12
43470	-0.2	0.13	-0.28	0.21	-0.71	*	0.09	0.25	0.43	0.26	-	-	-0.03	0.19
44569	-0.21	0.12	-0.16	0.08	-0.93	*	-0.16	0.08	-	-	-	-	-0.28	0.06
44573	0.2	0.22	-	-	-	-	-	-	0.7	*	-	-	0.01	0.08
45133	0.37	0.12	0.38	0.12	-0.55	*	0.17	0.28	0.13	0.19	-0.21	*	-0.04	0.08
45987	0.24	0.19	0.29	0.15	-0.54	*	-	-	-	-	-0.51	*	-0.05	0.12
46175	-0.01	0.13	-0.1	*	-0.67	*	-	-	-	-	-	-	-0.05	0.11
46435	0.02	0.17	-	-	-0.79	*	-	-	0.11	*	-0.4	*	-0.26	0.15
46894	0.31	0.15	0.36	0.1	-0.77	*	0.26	0.16	0.26	0.12	-	-	0.06	0.17
47017	0.06	0.12	0.14	0.12	-0.56	*	0.17	0.14	0.37	*	-	-	0.01	0.18
47186	0.31	0.15	0.33	0.17	-0.62	*	0.15	0.06	0.05	*	-0.2	*	-0.13	0.05
48056	-0.09	0.14	-0.16	0.06	-0.71	*	0.17	0.06	0.14	*	-	-	-0.02	0.22
48265	0.45	0.15	0.58	0.12	-0.42	*	0.63	0.27	0.34	0.15	-	-	0.12	0.12
49035	0.34	0.17	0.43	0.06	-0.65	*	0.18	0.08	-	-	-0.27	*	-0.01	0.04
49866	0.11	0.11	0.1	0.2	-	-	0.31	0.14	0.23	0.11	-	-	0.11	0.17
50117	-0.04	0.09	0.01	0.04	-0.67	*	-	-	0.15	0.07	-	-	-0.08	0.14
50255	-0.16	0.14	-0.29	0.1	-1	*	-0.05	0.25	0.1	*	-	-	-0.02	0.02
50652	0.28	0.12	0.43	0.16	-0.55	*	0.28	0.01	0.31	0.13	-0.25	*	-0.03	0.13
51608	0.16	0.16	0.14	0.2	-	-	0.02	0.29	0.72	*	-	-	-0.19	0.07
52217	0.33	0.16	0.25	0.04	-0.73	*	0.18	0.17	0.41	*	-0.36	*	-0.18	0.08
52756	0.4	0.22	0.44	0.29	-0.89	*	-	-	0.48	*	-	-	-0.07	0.06
56413	0.29	0.12	0.27	0.06	-0.73	*	0.23	0.04	-	-	-	-	-0.08	0.09
56662	-0.23	0.09	-0.31	0.08	-0.85	*	-0.1	0.05	-0.24	*	-	-	-0.21	0.12
56972	0.29	0.12	0.13	0.26	-0.67	*	0.23	0.21	0.18	0.09	-0.15	*	-0.08	0.16
58111	0.22	0.22	-	-	-	-	-	-	-	-	-	-	-0.15	0.1
58556	-0.21	0.1	-0.36	0.18	-0.76	*	0.06	0.05	-0.08	*	-	-	-0.01	0.1
58696	-0.09	0.09	-0.08	0.07	-0.68	*	0.09	0.07	0.22	0.23	-	-	-0.05	0.2
59711	-0.12	0.1	-0.14	0.05	-0.85	*	-0.13	0.04	-0.32	*	-	-	-0.21	0.09
59824	0.15	0.1	0.22	0.07	-0.61	*	0.07	0.19	0.15	*	-0.29	*	-0.08	0.11
61051	0.12	0.1	0.24	0.19	-0.83	*	-0.16	*	0.27	*	-	-	-0.18	0.03
61475	0.4	0.18	-	-	-	-	0.16	0.16	0.51	*	-	-	-0.1	0.1
62549	-0.1	0.09	-0.06	0.03	-0.78	*	-0.08	0.04	-0.03	*	-	-	-0.18	0.13

Continued on next page

Table A.5 – *Continued from previous page*

Star	[Ni/H]	±	[Cu/H]	±	[Zn/H]	±	[Y/H]	±	[Zr/H]	±	[Mo/H]	±	[Ba/H]	±
62644	0.21	0.13	0.28	0.21	-0.8	*	0.5	0.21	0.13	*	-	-	0.09	0.15
64114	0.05	0.11	-	-	-0.93	*	-	-	-0.04	*	-	-	-0.13	0.04
64144	0	0.08	0.02	0.08	-0.89	*	-0.07	0.04	-0.15	*	-0.46	*	-0.09	0.06
65427	0.08	0.11	0.24	*	-0.7	*	-	-	0.26	*	-	-	-0.14	0.15
66039	-0.08	0.1	-0.23	0.17	-0.79	*	0.13	0.09	0.25	0.04	-	-	0.08	0.1
66058	0.07	0.12	0.11	0.11	-0.67	*	0.11	0.02	0.44	*	-	-	-0.1	0.11
66791	0.12	0.12	0.14	0.17	-0.71	*	0.08	0.09	-	-	-	-	-0.03	0.11
70081	0.16	0.16	0.22	0.13	-0.64	*	0.25	0.12	0.17	0.04	-	-	-0.08	0.18
72579	0.33	0.14	0.54	0.18	-0.73	*	0.11	0.07	0.12	0.15	-0.13	*	-0.1	0.08
72687	-0.13	0.15	-0.13	*	-	-	-	-	-	-	-	-	0.14	0.06
72892	0.17	0.1	0.25	0.1	-0.69	*	0.17	0.29	-	-	-0.33	*	-0.12	0.14
73267	0.23	0.15	0.3	0.23	-0.88	*	-	-	0.24	0.1	-0.22	*	-0.17	0.1
73744	-0.36	0.09	-0.37	0.08	-	-	-0.33	0.01	-	-	-	-	-0.4	0.06
74698	0.06	0.12	0.14	0.14	-0.72	*	0.05	0.03	-	-	-0.63	*	-0.06	0.11
74733	-0.23	0.12	-0.25	0.1	-0.93	*	-0.11	0.06	-0.08	*	-	-	-0.15	0.08
74935	-0.06	0.12	-0.07	0.08	-0.68	*	0.27	0.14	0.34	*	-	-	0.03	0.11
75288	0.14	0.1	0.12	0.06	-0.69	*	0	0.06	0.25	*	-	-	-0.14	0.08
75351	0.12	0.12	0.11	0.04	-0.53	*	0.16	0.23	0.34	0.21	-	-	-0.01	0.14
77338	0.43	0.16	-	-	-0.68	*	0.34	0.26	0.09	*	-0.02	*	-0.05	0.08
77417	-	-	0.36	0.05	-0.72	*	0.23	0.27	0.04	*	-0.25	*	-0.14	0.07
77683	0.43	0.2	0.4	0.17	-0.81	*	0.35	0.1	-	-	-0.02	*	0.07	0.14
78130	0.13	0.11	0.14	0.13	-0.75	*	0.11	0.1	-	-	0.66	*	-0.09	0.06
78286	0.21	0.13	0.17	0.27	-0.62	*	0.2	0.02	-0.05	*	-	-	-0.13	0.15
79985	0.02	0.11	0.09	0.08	-0.74	*	0.1	0.15	0.02	*	-	-	0	0.15
81110	0.27	0.12	0.29	0.13	-0.66	*	0.13	0.01	-0.07	*	-	-	-0.08	0.04
81700	0.04	0.14	-0.05	0.05	-0.82	*	0	0.15	0.12	*	-	-	0.02	0.11
82282	0.06	0.16	-	-	-	-	0.08	0.26	0.36	*	-	-	0.15	0.08
82400	0.03	0.12	0.04	0.11	-0.89	*	0.11	0.11	-0.22	*	-	-	0.09	0.07
82516	0.29	0.24	0.44	0.28	-	-	-	-	0.9	0.23	-	-	-0.11	0.06
82977	0.08	0.16	0.12	0.23	-0.98	*	0.13	0.21	0.14	*	-0.14	*	0.06	0.07
83365	0.02	0.1	-0.01	0.05	-0.67	*	0.13	0.13	0.16	*	-	-	-0.06	0.09
83517	0	0.1	-	-	-0.74	*	-	-	-	-	-	-	-0.23	0.01
84652	-0.17	0.09	-0.3	0.1	-0.8	*	0.02	0.11	0.17	0.06	-	-	-0.13	0.17
85380	-0.06	0.14	0	0.13	-0.66	*	0.1	0.18	0.37	0.13	-	-	0.03	0.13
85390	0.2	0.16	-	-	-	-	-0.18	*	-	-	-	-	-0.23	0.13
86006	0.36	0.13	0.41	0.1	-0.5	*	0.38	0.21	0.43	0.27	-0.26	*	0.05	0.12
86226	-0.15	0.24	-	-	-0.77	*	0.77	*	-	-	-	-	-0.17	0.06

Continued on next page

Table A.5 – *Continued from previous page*

Star	[Ni/H]	±	[Cu/H]	±	[Zn/H]	±	[Y/H]	±	[Zr/H]	±	[Mo/H]	±	[Ba/H]	±
86249	0.26	0.19	-	-	-	-	-0.31	*	-	-	-	-	-0.07	0.05
86397	0.24	0.12	0.24	0.15	-0.78	*	0.2	0.27	-	-	-0.18	*	-0.11	0.09
86652	0.02	0.08	0.03	0.05	-0.64	*	0.04	0.02	0.03	*	-	-	-0.13	0.11
87931	0.14	0.12	0.16	0.21	-0.9	*	-0.07	0.14	-0.22	*	-0.22	*	-0.14	0.06
87998	-0.22	0.1	-	-	-0.9	*	-	-	-	-	0.42	*	-0.29	0.08
88864	-0.02	0.15	0.64	*	-0.76	*	-	-	-	-	-	-	-0.09	0.05
89178	0.2	0.17	0.24	0.24	-0.82	*	0.29	0.06	0.14	*	-0.12	*	0.08	0.16
89418	-0.32	0.1	-0.42	0.12	-0.85	*	-0.14	0.07	-0.23	*	-	-	-0.17	0.14
89988	0.21	0.14	0.18	0.09	-0.52	*	0.36	0.11	0.37	0.13	-	-	0.02	0.19
90028	0.24	0.13	0.27	0.03	-0.49	*	0.29	0.19	0.33	0.11	-0.41	*	-0.07	0.19
90702	0.16	0.11	0.22	0.1	-0.68	*	0.1	0.06	0.36	*	-	-	0	0.06
91320	-0.09	0.14	-0.13	0.04	-0.65	*	0.06	0.1	0.49	*	-	-	-0.03	0.2
91901	0.2	0.23	-	-	-	-	-0.17	*	0.72	*	-	-	0.07	0.12
92069	0.25	0.15	0.31	0.22	-0.68	*	0.04	0.27	-0.04	*	-	-	-0.02	0.15
92719	-0.17	0.07	-	-	-0.88	*	-	-	-	-	-	-	-0.2	0.01
93083	-	-	-	-	-	-	-	-	0.66	*	-	-	-0.13	0.07
94151	0.15	0.1	-	-	-0.8	*	0.85	*	-	-	-	-	-0.22	0.03
94387	0.39	0.14	0.42	0.06	-0.71	*	0.29	0.17	-0.17	*	-0.17	*	-0.13	0.03
94482	-0.2	0.1	-0.26	0.01	-0.69	*	-0.05	0.17	0.02	*	-	-	-0.07	0.13
94527	-0.1	0.11	-0.11	0.14	-0.99	*	-0.05	0.11	-0.17	*	-	-	-0.1	0.1
94690	0.27	0.11	0.31	0.02	-0.62	*	0.13	0.02	0.21	0.21	-0.46	*	-0.16	0.06
94838	-0.1	0.1	-0.21	0.08	-0.92	*	-0.01	0.13	-	-	-	-	0.06	0.08
95136	0.17	0.11	0.23	0.11	-0.65	*	0.2	0.1	-0.17	*	-0.38	*	-0.09	0.12
95338	0.33	0.21	-	-	-0.91	*	-	-	0.63	*	-	-	-0.17	0.09
95521	-0.15	0.1	-	-	-0.93	*	-	-	-	-	-	-	-0.23	0.04
95533	0.31	0.17	-	-	-0.88	*	-	-	0.05	*	-	-	-0.09	0.1
95542	-0.23	0.11	-0.32	0.15	-0.91	*	-	-	0.08	*	-	-	-0.05	0.13
96020	0.38	0.14	0.48	0.16	-0.68	*	-	-	0.36	0.19	-0.17	*	-0.08	0.12
96276	-0.24	0.11	-0.3	0.08	-0.77	*	-0.13	0.15	0.21	*	-	-	-0.16	0.13
98163	0.14	0.11	0.18	0.03	-0.66	*	0.23	0.12	0.2	*	-	-	-0.03	0.12
98459	0.13	0.11	0.18	0.05	-0.53	*	0.21	0.01	0.28	0.06	-	-	-0.03	0.18
98764	-0.08	0.11	-0.13	0.06	-0.81	*	0	0.12	0.13	*	-0.43	*	0.09	0.13
99116	0.05	0.13	0	0.18	-0.96	*	-0.01	0.14	-0.2	*	-0.52	*	-0.16	0.08
101093	-0.34	0.11	-0.47	0.09	-0.99	*	-0.07	0.06	-0.08	*	-	-	-0.07	0.09
101171	0.11	0.11	0.16	0.27	-0.99	*	-	-	0.25	*	-	-	-0.13	0.06
101181	0.2	0.13	0.32	0.22	-0.72	*	-	-	-0.1	*	-0.55	*	-0.14	0.14
101896	0.33	0.19	0.36	0.24	-0.93	*	-	-	0.07	*	-0.03	*	-0.12	0.06

Continued on next page

Table A.5 – *Continued from previous page*

Star	[Ni/H]	±	[Cu/H]	±	[Zn/H]	±	[Y/H]	±	[Zr/H]	±	[Mo/H]	±	[Ba/H]	±
102574	0.01	0.14	0.11	0.03	-0.67	*	0.25	0.15	0.45	0.04	-	-	0.09	0.14
102579	0.24	0.2	0.3	0.27	-	-	-	-	0.39	*	-0.08	*	-0.2	0.06
102843	0.31	0.17	0.2	0.21	-0.86	*	0.02	0.08	0.1	*	-0.22	*	-0.1	0.11
103559	0	0.11	0.07	*	-	-	-0.08	*	-	-	-	-	0.11	0.07
103673	-0.01	0.12	-0.06	0.21	-0.94	*	0.17	0.13	0.23	*	-	-	0.06	0.15
104645	0.3	0.21	0.3	0.1	-0.82	*	0.31	0.25	0.23	*	-0.11	*	0.1	0.12
104760	0.01	0.1	0.11	0.22	-0.69	*	0	0.18	0.37	0.13	-	-	-0.16	0.09
104982	-0.13	0.09	-	-	-0.9	*	-	-	-	-	-	-	-0.3	0.01
105690	-0.08	0.19	-0.01	0.16	-	-	0.1	0.14	-0.18	*	-0.34	*	0.1	0.12
105904	0.26	0.1	0.37	0.1	-0.55	*	0.18	0.06	0.06	*	-0.14	*	-0.12	0.17
106275	0.17	0.19	-	-	-	-	-0.43	*	0.47	0.27	-	-	-0.16	0.08
106869	-0.07	0.13	-0.14	0.06	-0.61	*	0.11	0.09	-0.05	*	-	-	-0.05	0.11
106937	0.41	0.14	0.44	0.15	-0.6	*	0.3	0.3	0.22	0.06	-	-	0.06	0.12
107008	0.38	0.14	0.38	0.26	-0.72	*	0.15	0.22	0.22	*	-0.15	*	-0.06	0.06
107181	0.41	0.13	0.43	0.09	-0.56	*	0.33	0.04	0.26	0.18	-0.13	*	0.1	0.15
108953	0.48	0.19	0.48	0.17	-0.54	*	0.07	0.16	0.67	*	-0.14	*	-	-
109591	-0.03	0.13	0.03	0.1	-0.72	*	-0.09	0.04	-0.13	*	-0.39	*	-0.19	0.09
109908	-0.12	0.12	-0.24	0.11	-0.82	*	-0.01	0.14	0.1	*	-	-	0.04	0.06
109930	0.25	0.18	-	-	-	-	0.01	0.25	-	-	-	-	-0.17	0.02
109988	0.45	0.17	0.54	0.23	-	-	-	-	-	-	-	-	-0.17	0.06
110605	0.36	0.13	0.42	0.09	-0.62	*	0.17	0.1	0.24	0.28	-0.29	*	-0.1	0.04
110619	-0.32	0.09	-0.22	0.09	-0.98	*	-0.31	0.01	-0.38	*	-	-	-0.3	0.06
111431	0.02	0.12	0.07	0.08	-0.65	*	0.1	0.12	0.22	0.01	-	-	-0.03	0.17
112121	0.25	0.15	0.24	0.11	-0.68	*	0.14	0.11	-	-	-0.3	*	-0.12	0.13
112540	-0.07	0.11	-0.08	0.27	-	-	-0.06	0.16	-0.05	*	-	-	-0.13	0.08
113027	-0.2	0.11	-	-	-0.75	*	-	-	-	-	-	-	-0.1	0.02
113255	0.07	0.09	0.12	0.1	-0.7	*	0.04	0.06	-	-	-	-	-0.07	0.1
113513	0.11	0.16	0.47	*	-0.92	*	-	-	-	-	-	-	0.11	0.12
114294	0.28	0.16	0.32	0.1	-	-	-	-	-	-	-	-	-	-
114432	0.2	0.1	-	-	-0.85	*	-	-	-	-	-	-	0.02	0.04
114884	0.1	0.1	0.12	0.15	-0.58	*	0.14	0.1	0.19	*	-	-	-0.06	0.07
115080	-0.07	0.1	-	-	-0.78	*	-	-	-	-	-	-	-0.35	0.01
115674	-0.15	0.09	-	-	-0.96	*	-	-	-	-	-	-	-0.19	0.01
116920	0.05	0.2	-	-	-	-	-	-	-	-	-	-	-0.12	0.08
117653	0.06	0.14	-	-	-0.56	*	0.34	*	-	-	-	-	-0.07	0.12
117860	-0.05	0.08	-	-	-0.81	*	-	-	-	-	-	-	0.01	0.06
119070	0.05	0.12	0.07	0.18	-	-	0.05	0.28	-0.06	*	-0.25	*	-0.17	0.08

Continued on next page

Table A.5 – *Continued from previous page*

Star	[Ni/H]	±	[Cu/H]	±	[Zn/H]	±	[Y/H]	±	[Zr/H]	±	[Mo/H]	±	[Ba/H]	±
119119	-0.12	0.13	-0.18	0.04	-0.68	*	0.22	0.17	0.36	0.21	-	-	0.16	0.17
119507	0.15	0.13	0.06	0.21	-0.68	*	0.18	0.03	0.1	*	-0.17	*	-0.03	0.12
119782	0.2	0.22	0.27	0.26	-	-	-0.22	*	0.14	*	-	-	-0.1	0.08
120100	0.33	0.14	0.41	0.25	-0.72	*	0	0.04	-	-	-0.15	*	-0.05	0.1
120329	0.38	0.18	0.31	0.14	-0.52	*	0.36	0.02	0.36	*	0.12	*	0	0.16
121504	-0.06	0.11	-0.11	0.05	-0.75	*	0.11	0.09	-	-	-	-	-0.06	0.08
122078	0.29	0.11	0.36	0.12	-0.56	*	0.35	0.18	0.23	*	-0.23	*	-0.02	0.1
124553	0.01	0.11	0.11	0.08	-0.55	*	0.2	0.09	0.28	0.07	-	-	0.11	0.14
125968	0.08	0.1	0.1	0.11	-0.7	*	-0.11	0.27	-	-	-	-	-0.08	0.14
126653	-0.18	0.15	-0.19	0.16	-0.83	*	-	-	0.05	0.15	-0.37	*	0	0.12
127321	-0.14	0.11	-0.26	0.19	-0.74	*	0.11	0.26	0.11	*	-	-	0.01	0.22
128214	0.28	0.26	0.36	0.1	-0.55	*	0.22	0.2	0.98	0.07	-0.52	*	-0.03	0.12
128760	-0.07	0.18	-0.22	0.06	-0.67	*	-	-	-0.01	*	-0.08	*	0.01	0.16
128987	0.04	0.1	0.01	0.16	-0.95	*	-	-	0.04	*	-	-	0.12	0.1
129679	-0.28	0.11	-0.35	0.12	-	-	0.17	0.16	-	-	-	-	0.12	0.16
129764	-0.03	0.11	-0.11	0.06	-0.79	*	-0.01	0.15	0.29	*	-	-	0.04	0.12
129946	-0.16	0.09	-0.21	0.06	-	-	-0.08	0.13	-0.05	*	-	-	0.04	0.08
131900	0.29	0.13	0.32	0.2	-0.76	*	0.06	0.06	-	-	-0.09	*	-0.2	0.05
132648	-0.18	0.1	-	-	-	-	-	-	-	-	-	-	-0.33	0.06
133014	0.35	0.13	0.44	0.06	-0.58	*	0.25	0.08	-0.13	*	-0.19	*	0.09	0.16
135005	0.19	0.11	0.26	0.21	-0.66	*	0.14	0.09	0.31	*	-0.21	*	0.04	0.11
135309	0.05	0.12	0	0.11	-0.89	*	0.11	0.07	0.17	*	-	-	0.05	0.13
135562	0.04	0.13	0.02	0.05	-0.59	*	0.26	0.2	0.21	*	-0.67	*	-0.08	0.31
135625	0.04	0.17	0	0.08	-0.65	*	0.09	0.09	0.03	*	-	-	-0.07	0.14
135725	0	0.09	0.01	0.16	-0.87	*	-0.15	0.24	-0.01	*	-0.38	*	-0.01	0.16
136130	0.09	0.11	0.13	0.16	-0.79	*	0.21	0.12	0.4	*	-	-	-0.02	0.12
136548	-0.08	0.1	-0.07	0.11	-0.87	*	-	-	0.34	*	-0.39	*	-0.16	0.05
136894	0.02	0.09	-	-	-	-	-	-	-	-	-	-	-0.27	0.06
137214	-0.1	0.12	-0.1	0.09	-0.7	*	0.04	0.08	0.36	*	-	-	-0.09	0.14
140643	0.37	0.19	0.53	0.28	-0.93	*	-0.18	*	0.61	*	-	-	-0.11	0.06
141105	0.03	0.13	0.12	0.16	-0.97	*	0.16	0.02	0.17	*	-	-	0	0.11
141366	0.17	0.16	-	-	-0.57	*	0.41	0.17	0.4	0.01	-0.56	*	0.19	0.15
141514	-0.16	0.13	-0.14	0.16	-0.64	*	0.01	0.2	0.14	*	-	-	-0.01	0.15
141598	-0.04	0.1	0.07	0.19	-0.81	*	-0.1	0.03	0.01	*	-	-	-0.23	0.04
141599	0.3	0.13	0.33	0.11	-0.74	*	0.15	0.09	-0.1	*	-	-	-0.07	0.04
141885	0.21	0.21	-	-	-0.53	*	0.49	0.04	0.45	0.24	-	-	0.16	0.16
142137	0.17	0.15	0.3	0.01	-0.52	*	0.19	0.27	0.4	0.14	-	-	-0.08	0.29

Continued on next page

Table A.5 – *Continued from previous page*

Star	[Ni/H]	±	[Cu/H]	±	[Zn/H]	±	[Y/H]	±	[Zr/H]	±	[Mo/H]	±	[Ba/H]	±
143120	0.43	0.15	0.53	0.19	-0.44	*	0.37	0.15	0.53	0.15	-0.47	*	0	0.12
143137	-0.12	0.16	-0.13	0.15	-0.7	*	0.27	0.17	0.53	0.03	-	-	0.18	0.17
143295	0.21	0.26	-	-	-	-	-	-	-	-	-	-	0.08	0.08
143673	0.26	0.16	0.29	0.14	-0.9	*	0.06	0.11	0.12	*	-0.29	*	-0.17	0.12
144087	0.13	0.11	0.13	0.17	-0.83	*	0.12	0.03	0.07	*	-	-	0.06	0.08
144088	0.22	0.14	0.26	0.28	-0.89	*	0.17	0.21	0.3	*	0.08	*	0.02	0.01
144167	0.33	0.13	0.31	0.02	-0.43	*	-	-	-	-	-	-	-	-
144550	0.29	0.27	0.33	0.16	-0.55	*	0.24	0.11	0.28	*	-0.19	*	-0.06	0.12
144848	0.23	0.13	0.36	0.25	-0.58	*	0.17	0.07	0.53	0.18	-0.34	*	-0.01	0.15
144899	0.29	0.13	0.4	0.16	-0.48	*	0.25	0.16	0.54	0.02	-0.34	*	0.06	0.18
145518	-0.21	0.11	-0.27	0.07	-0.87	*	-0.04	0.01	0.04	*	-	-	-0.09	0.11
145666	-0.2	0.1	-0.28	0.1	-0.86	*	-0.06	*	-0.14	*	-	-	-0.1	0.13
146817	-0.02	0.1	0.11	0.09	-0.66	*	-0.06	0.01	0.01	*	-0.58	*	-0.22	0.13
146835	-0.31	0.12	-0.41	0.22	-	-	-0.19	0.23	-0.17	*	-	-	-0.11	0.09
147018	0.28	0.17	0.3	0.11	-0.87	*	0.09	0.13	-	-	-	-	-0.11	0.09
147619	0.08	0.16	0.12	0.06	-0.48	*	0.25	0.23	0.47	0.18	-	-	0.09	0.24
148156	0.03	0.18	-0.09	0.05	-0.56	*	0.18	0.01	0.29	*	-	-	-0.13	0.17
148628	-0.32	0.17	-0.35	0.23	-0.8	*	-0.08	0.12	-0.03	0.12	-	-	-0.09	0.1
149189	0.24	0.14	0.28	0.12	-0.42	*	0.49	0.22	0.27	*	-	-	-0.01	0.2
150761	0.04	0.17	0.11	0.04	-0.5	*	0.05	0.23	0.59	*	-	-	-0.11	0.16
151450	-0.24	0.1	-0.28	0.12	-0.8	*	-0.02	0.07	-0.03	*	-	-	-0.17	0.16
152388	0.18	0.14	0.13	0.21	-	-	0.13	0.25	0.18	*	-	-	0.06	0.09
153631	-0.18	0.08	-0.22	0.05	-0.83	*	-0.1	0.06	-0.13	*	-	-	-0.2	0.12
154682	-0.21	0.1	-0.23	0.08	-0.86	*	-0.05	0.04	-0.03	*	-	-	-0.16	0.12
154697	0.16	0.12	0.17	0.18	-0.84	*	0.22	0.23	-0.02	*	-	-	-0.06	0.1
156152	0	0.11	-0.03	0.09	-0.83	*	0.1	0.09	-	-	-0.36	*	-0.02	0.16
156643	-0.23	0.1	-0.25	0.01	-0.87	*	-0.22	0.01	-0.35	*	-	-	-0.28	0.12
157798	0.17	0.14	0.19	0.1	-0.62	*	0.51	0.21	0.31	0.22	-0.38	*	-0.21	0.08
157830	-0.15	0.1	-0.16	0.12	-	-	-0.04	0.25	-0.15	*	-	-	-0.15	0.09
158469	-0.18	0.16	-0.27	0.14	-0.67	*	-0.05	0.13	0.25	*	-	-	-0.07	0.05
158630	-0.29	0.1	-0.34	0.1	-0.92	*	-0.14	0.1	-0.13	*	-	-	-0.17	0.12
159902	-0.23	0.08	-0.24	0.08	-0.93	*	-0.23	0.07	-0.24	*	-	-	-0.28	0.1
160411	0.15	0.15	0.16	0.14	-0.58	*	-	-	0.63	0.28	-	-	0.21	0.23
160859	-0.15	0.11	-0.24	0.05	-0.93	*	-0.07	0.06	0.34	*	-	-	-0.12	0.09
161098	-0.17	0.09	-0.16	0.08	-	-	-0.2	0.07	-0.27	*	-	-	-0.27	0.06
162907	0.28	0.17	0.33	0.2	-0.78	*	-	-	-0.09	*	-0.07	*	-0.14	0.13
165011	-0.13	0.14	-0.18	0.1	-0.58	*	0.07	0.23	0.25	0.08	-	-	0.12	0.15

Continued on next page

Table A.5 – *Continued from previous page*

Star	[Ni/H]	±	[Cu/H]	±	[Zn/H]	±	[Y/H]	±	[Zr/H]	±	[Mo/H]	±	[Ba/H]	±
165204	0.31	0.11	0.33	0.1	-0.66	*	0.22	0.08	0.17	0.1	-0.15	*	-0.01	0.09
165271	0.08	0.11	0.11	0.13	-0.65	*	0.11	0.11	0.27	0.12	-	-	0.06	0.17
165385	-0.16	0.12	-0.23	0.07	-0.65	*	0.09	0.13	-	-	-	-	-0.04	0.18
165449	-0.17	0.11	-0.2	0.07	-0.77	*	-0.08	0.01	-0.05	*	-	-	-0.21	0.13
165920	0.45	0.17	0.52	0.17	-0.79	*	0.33	0.28	0.24	0.23	-	-	-0.09	0.08
169303	-0.18	0.12	-0.19	0.15	-0.72	*	0.2	0.04	0.14	*	-	-	0.02	0.13
169506	0.26	0.21	0.41	0.07	-0.39	*	0.32	0.24	-	-	-	-	0.2	0.17
171990	-0.08	0.1	-0.05	0.04	-0.64	*	0.14	0.09	0.24	0.06	-	-	0.02	0.17
172063	0.23	0.11	0.27	0.17	-0.86	*	-	-	-	-	-0.23	*	-0.12	0.1
172582	-0.23	0.11	-0.18	0.14	-	-	-	-	-0.1	*	-	-	-0.32	0.01
174494	0.18	0.1	0.26	0.14	-0.51	*	0.27	0.19	0.34	0.21	-0.12	*	0.17	0.23
174541	-0.17	0.1	-0.12	0.14	-0.87	*	-0.15	0.1	0.1	*	-	-	-0.35	0.09
175073	0.13	0.18	0.19	0.28	-	-	-	-	0.43	*	-	-	-0.1	0.08
175169	0.3	0.19	0.25	0.18	-0.63	*	0.2	0.03	0.15	0.14	-0.36	*	-0.11	0.17
176110	0.16	0.13	0.23	0.12	-0.65	*	-	-	-	-	-0.33	*	-0.19	0.16
176151	0.23	0.12	0.32	0.2	-0.66	*	0.33	0.21	0.45	*	-	-	0.1	0.16
176986	0.27	0.21	-	-	-	-	-	-	0.65	*	-	-	-0.1	0.07
177122	-0.28	0.11	-0.35	0.04	-0.86	*	-	-	0.03	*	-	-	-0.13	0.09
177409	-0.16	0.12	-0.21	0.06	-0.84	*	-0.04	0.05	-0.25	*	-	-	-0.09	0.1
178076	0.03	0.11	-0.01	0.2	-	-	0.14	0.17	0.07	*	-	-	0.14	0.1
179640	0.39	0.16	0.43	0.06	-0.74	*	0.31	0.18	0.04	*	-0.07	*	-0.06	0.12
180204	0.04	0.15	0.09	0.06	-0.59	*	0.15	0.06	0.25	0.25	-	-	-0.04	0.12
180257	0.16	0.11	0.05	0.17	-0.55	*	0.18	0.26	0.47	0.04	-	-	0.13	0.17
181010	0.21	0.15	-	-	-0.89	*	-0.16	*	-	-	-	-	-0.11	0.06
182228	0.13	0.12	0.18	0.05	-	-	0.26	0.02	0.36	0.03	-	-	-0.07	0.12
182498	-0.13	0.11	-0.36	*	-0.84	*	-	-	0.28	*	-	-	0.01	0.13
184317	-0.03	0.1	-0.02	0.14	-0.67	*	0.03	0.01	0.03	*	-	-	-0.08	0.11
185283	-	-	-	-	-	-	-0.35	0.25	-	-	-	-	-0.07	0.07
185615	0.21	0.12	0.39	0.13	-0.69	*	-0.18	*	-0.18	*	-0.31	*	-0.17	0.1
186160	-0.42	0.1	-0.55	0.12	-	-	-0.24	0.03	-0.34	*	-	-	-0.2	0.09
186265	0.45	0.14	0.47	0.14	-0.64	*	0.36	0.08	0.31	0.03	-0.21	*	-0.04	0.12
186651	-0.2	0.12	-0.31	0.04	-0.79	*	0.06	0.07	0.14	0.27	-	-	-0.13	0.15
186803	-0.06	0.09	-0.09	0.06	-0.93	*	0.01	0.01	-0.07	*	-	-	-0.01	0.05
187154	0	0.13	-0.04	0.05	-0.67	*	0.14	0.1	-	-	-0.54	*	0.17	0.09
189310	0.21	0.12	-	-	-	-	-0.22	*	0.41	*	-	-	-0.09	0.04
190125	0.17	0.17	0.21	0.07	-0.79	*	0.12	0.07	0.19	0.17	-0.8	*	-0.04	0.09
190613	-0.05	0.11	-0.07	0.05	-0.83	*	-0.03	0.01	0.02	*	-	-	-0.16	0.09

Continued on next page

Table A.5 – *Continued from previous page*

Star	[Ni/H]	±	[Cu/H]	±	[Zn/H]	±	[Y/H]	±	[Zr/H]	±	[Mo/H]	±	[Ba/H]	±
191760	0.25	0.11	0.3	0.03	-0.5	*	0.22	0.19	0.6	0.06	-	-	0.06	0.2
193567	0.26	0.13	0.32	0.06	-0.77	*	0.18	0.09	-	-	-	-	-0.1	0.14
193728	0.21	0.12	0.34	0.07	-0.67	*	0.11	0.18	0.01	*	-0.49	*	0.05	0.18
193995	0.29	0.14	0.36	0.07	-0.52	*	0.44	0.19	0.5	*	-0.36	*	0.05	0.13
195145	0.26	0.12	0.22	0.09	-0.8	*	-	-	0.21	0.16	-	-	-0.09	0.13
195284	0.12	0.12	0.05	0.16	-0.87	*	0.08	0.01	0.02	*	-	-	-0.02	0.04
196397	0.44	0.18	0.61	0.19	-0.68	*	0.18	0.12	0.36	0.01	-0.11	*	-0.04	0.02
197069	0.05	0.14	0.07	0.03	-0.68	*	0.1	0.18	0.1	*	-	-	-0.1	0.08
197210	0.04	0.09	0.03	0.12	-0.92	*	-0.14	0.15	-0.17	*	-	-	-0.1	0.05
197499	-0.14	0.13	-0.17	0.02	-0.74	*	-0.08	0.2	0.33	*	-	-	0.03	0.18
197818	-0.22	0.08	-0.25	0.07	-0.9	*	-0.1	0.03	0.04	0.18	-	-	-0.25	*
197823	0.27	0.14	0.26	0.22	-0.85	*	0.26	0.23	0.18	*	-	-	-0.05	0.06
198477	0.28	0.18	0.33	0.23	-0.86	*	0.23	0.21	-0.23	*	-	-	-0.19	0.26
199065	-0.06	0.12	-0.12	0.03	-0.82	*	-0.15	0.25	0.11	*	-	-	0.04	0.08
200733	-0.16	0.13	-0.2	0.11	-0.67	*	0.06	0.22	-	-	-0.66	*	0.18	0.18
200869	0.45	0.16	0.51	0.25	-0.67	*	-	-	0.37	0.29	-0.17	*	-0.1	0.11
201757	0.25	0.21	0.32	0.2	-0.63	*	-	-	0.28	0.08	-	-	0	0.15
202282	0.05	0.11	0.02	0.16	-0.69	*	0.01	0.04	0.1	*	-0.26	*	-0.12	0.1
202457	0.13	0.11	0.27	0.1	-0.67	*	-	-	0.15	0.05	-0.55	*	-0.09	0.12
203432	0.37	0.14	0.37	0.08	-0.67	*	-	-	0.04	*	-0.1	*	-0.07	0.03
205045	0.04	0.13	0.02	0.06	-0.62	*	0.15	0.18	0.44	*	-	-	-0.07	0.11
205067	-0.1	0.1	-0.06	0.1	-0.78	*	-0.11	0.09	-	-	-	-	-0.18	0.1
205158	0.06	0.14	0.08	*	-0.52	*	-	-	0.39	0.08	-	-	0.1	0.13
206025	-0.09	0.14	-0.12	0.11	-0.62	*	0.19	0.15	0.26	*	-	-	0.18	0.15
206255	0.21	0.14	0.22	0.15	-0.62	*	0.26	0.18	0.36	0.01	-	-	0.06	0.21
206683	0.26	0.15	0.19	0.13	-0.52	*	-	-	0.38	0.16	-	-	-0.12	0.13
207970	0.16	0.13	0.19	0.12	-0.79	*	0.04	0.13	-0.15	*	-0.42	*	-0.12	0.05
208704	-0.13	0.11	-0.12	0.05	-0.85	*	-0.11	0.09	-0.03	*	-	-	-0.25	0.08
209566	0.27	0.14	0.35	0.13	-0.75	*	-0.07	0.21	-	-	-	-	-0.14	0.1
209659	0.09	0.17	0.14	0.04	-0.49	*	0.21	0.18	0.25	*	-0.68	*	0.11	0.13
210193	0.08	0.1	0.06	0.02	-0.73	*	0.03	*	0.02	*	-	-	-0.17	0.13
211366	0.18	0.12	-	-	-0.65	*	-	-	-	-	-	-	-0.16	0.02
213429	-0.22	0.13	-0.32	0.11	-0.87	*	0.04	0.18	0.03	*	-	-	-0.08	0.15
213717	0.2	0.13	0.38	0.25	-	-	0.15	0.27	-	-	-0.39	*	-0.09	0.06
213941	-0.25	0.1	-0.27	0.14	-0.91	*	-0.35	0.04	-0.33	*	-	-	-0.5	0.08
214691	0.22	0.13	0.2	0.1	-0.7	*	0	0.11	-	-	-0.32	*	-0.11	0.08
215456	-0.1	0.11	-0.09	0.09	-0.8	*	0.02	*	-	-	-	-	-0.09	0.12

Continued on next page

Table A.5 – *Continued from previous page*

Star	[Ni/H]	±	[Cu/H]	±	[Zn/H]	±	[Y/H]	±	[Zr/H]	±	[Mo/H]	±	[Ba/H]	±
216054	-0.05	0.13	0.01	0.18	-	-	-0.21	0.14	-0.02	*	-	-	-0.24	0.05
218760	0.25	0.29	-	-	-	-	-	-	0.92	*	-	-	-0.13	0.06
219011	0.31	0.19	0.36	0.07	-0.49	*	0.21	0.15	0.06	0.17	-0.33	*	0.01	0.09
219533	0.29	0.16	0.27	0.11	-0.63	*	0.23	0.02	-	-	-	-	0.04	0.17
219556	0.26	0.12	0.28	0.14	-0.77	*	0.01	0.14	-	-	-	-	-0.11	0.11
220426	0.04	0.13	0.05	0.09	-0.61	*	0.17	0.02	0.27	0.23	-	-	-0.12	0.18
220476	-0.06	0.1	-0.08	0.1	-0.94	*	0.09	0.21	0.05	*	-	-	0.16	0.09
220689	-0.1	0.11	-0.11	0.03	-0.77	*	-0.05	0.02	-0.1	*	-	-	-0.22	0.15
220718	0.19	0.2	0.23	0.13	-0.54	*	0.33	0.13	0.33	*	-0.56	*	0.12	0.19
220829	0.28	0.16	0.34	0.26	-	-	-0.19	*	0.49	0.04	-	-	-0.15	0.06
220945	0.33	0.16	-	-	-	-	-	-	0.28	*	-	-	-0.04	0.06
220981	0.31	0.14	-	-	-0.62	*	-	-	-	-	-	-	-0.1	0.06
221257	-0.19	0.09	-0.19	0.05	-0.84	*	-0.13	0.05	-0.2	*	-	-	-0.25	0.12
221275	0.29	0.15	0.38	0.18	-0.78	*	0.21	0.26	0.07	*	-0.34	*	-0.12	0.11
221954	0.39	0.14	0.39	0.11	-0.57	*	0.33	0.11	-	-	-0.23	*	0.05	0.16
222422	-0.01	0.11	-0.06	0.19	-	-	0.11	0.22	0.02	*	-	-	-0.03	0.06
222669	-0.06	0.11	-0.13	0.12	-0.82	*	0.07	0.03	-0.03	*	-	-	-0.07	0.1
224010	0.17	0.11	0.23	0.16	-0.54	*	0.08	0.27	0.43	0.1	-0.54	*	-0.15	0.23
224022	-0.07	0.13	-0.11	0.01	-0.66	*	0.01	0.19	0.16	*	-	-	-0.11	0.12
224143	-0.17	0.12	-0.25	0.01	-0.9	*	0.09	0.06	-	-	-	-	0.12	0.08
224433	0.21	0.08	-	-	-0.86	*	0.99	*	-0.01	*	-	-	-0.22	0.05
224538	0.11	0.14	0.13	0.04	-0.46	*	0.22	0.21	0.01	*	-	-	0.01	0.19
224789	0.24	0.21	0.29	0.27	-0.97	*	-	-	0.43	*	0.09	*	0.03	0.09
225155	0.25	0.13	0.32	0.06	-0.62	*	0.24	0.15	0.09	0.19	-0.32	*	-0.02	0.07
225299	0.16	0.13	0.15	0.15	-0.8	*	0.16	0.11	-0.1	*	-0.56	*	-0.11	0.12

Table A.6: All stars abundances for La, Ce, Nd, Eu, Hf, Mg/Si ratio and C/O ratio

Star	[La/H]	±	[Ce/H]	±	[Nd/H]	±	[Eu/H]	±	[Hf/H]	±	Mg/Si	C/O
361	-0.02	*	-	-	0.04	0.04	-	-	-	-	1.24	-
1002	0.06	*	-	-	-0.03	0.11	0.36	*	0.37	*	1.36	0.46
1237	-0.01	*	-	-	-	-	-0.1	*	0.36	*	1.06	0.19
1893	0.19	*	-	-	0.26	0.14	-	-	-	-	1.26	0.25
1926	-0.16	*	-	-	-0.19	0.01	-0.01	*	-	-	1.52	0.3
2098	0.08	0.1	0.29	*	0.09	0.06	-	-	0.38	*	1.26	0.38
2222	0.31	0.1	-	-	0.2	0.06	0.32	*	0.66	*	1.16	0.46
3359	0.25	*	-	-	0.19	0.11	-	-	0.45	*	1.39	0.19
4333	0.27	0.01	-	-	0.22	0.09	-	-	0.5	*	1.24	0.32
4392	0.15	*	-	-	0.04	0.03	-	-	-0.12	*	1.2	0.3
6236	-0.02	0.12	-	-	0.03	0.16	0.43	*	-	-	1.15	0.35
6790	0.29	0.18	-	-	0.06	0.12	-	-	-	-	1.17	0.3
6880	0.23	0.01	-	-	0.09	0.17	-	-	0.5	*	1.43	0.35
6910	0.13	0.08	-	-	0.21	0.23	-	-	0.69	*	1.02	0.34
7134	-	-	-	-	-0.15	0.04	-	-	-	-	1.4	-
7449	-0.17	*	-	-	-0.06	*	-0.02	*	-	-	1.34	-
7661	-0.1	*	1.15	*	0.22	0.16	-	-	0.63	*	1.33	0.26
8076	0.07	0.08	-	-	0.07	0.04	0.18	*	0.4	*	1.26	0.46
8129	0.03	*	-	-	0.09	0.01	0.25	*	0.43	*	1.28	-
8406	-0.05	*	-	-	-0.04	0.08	0.02	*	-	-	1.32	-
9175	0.05	0.23	-	-	0.1	0.11	-	-	0.49	*	1.35	0.24
9782	-0.11	*	-	-	-0.02	0.01	0.27	*	0.34	*	1.19	0.37
9847	0.27	*	-	-	0.2	*	0.34	*	0.56	*	1.13	0.39
9905	0.44	0.2	-	-	0.16	0.04	-	-	0.29	*	1.01	0.32
10008	0.2	0.06	-	-	0.29	0.1	-	-	0.32	*	1.28	0.16
10226	0.02	*	-	-	0.07	*	0.35	*	0.35	*	1.18	-
10370	-	-	-	-	0.08	0.19	0.41	*	-	-	1.29	-
10519	-	-	0.2	*	-0.2	0.13	-0.03	*	-	-	1.55	-
10576	0.32	0.05	-	-	0.13	0.07	0.21	*	0.3	*	1.27	0.19
10611	0.03	0.18	-	-	0.31	0.1	-	-	0.65	*	1.28	0.38
10678	0.03	0.11	-	-	-0.05	0.11	-	-	0.83	*	1.3	0.35
11264	0.07	0.12	-	-	0	0.03	0.36	*	0.57	*	1.17	0.27
11754	0.32	0.03	-	-	0.14	0.06	0.83	*	0.18	*	1.09	0.45
12585	0.13	*	-	-	0.13	*	0.41	*	0.19	*	1.3	0.32
12951	-0.12	*	-	-	0	0.05	-	-	-	-	1.32	-

Continued on next page

Table A.6 – *Continued from previous page*

Star	[La/H]	±	[Ce/H]	±	[Nd/H]	±	[Eu/H]	±	[Hf/H]	±	Mg/Si	C/O
13060	0.26	*	-	-	0.35	0.11	-0.31	*	0.35	*	1.37	0.18
13350	0.45	*	-	-	0.27	0.03	-	-	0.72	*	1.08	0.31
13386	-	-	-	-	-	-	-	-	-	-	1.14	0.32
14758	-	-	-	-	0.03	0.14	0.18	*	-	-	1.55	-
15507	0.06	*	-	-	0.16	*	0.46	*	0.37	*	1.19	0.37
15590	0.24	0.05	-	-	0.14	0.01	-	-	0.45	*	1.06	0.21
15767	0.58	*	-	-	-	-	-	-	0.65	*	1.05	0.6
16950	-0.05	*	-	-	0.1	*	0.42	*	0.36	*	0.94	0.42
17134	-0.15	*	-	-	-0.01	*	0.25	*	0.3	*	1.4	-
17289	-	-	-	-	-0.07	0.01	-	-	-	-	1.41	-
18168	0.48	0.06	-	-	0.13	*	-	-	-0.06	*	1.39	0.89
18708	0.01	*	-	-	0.1	*	0.22	*	0.44	*	0.9	0.35
18754	0.42	0.02	-	-	-	-	-	-	0.69	*	1.03	0.48
18819	0.22	*	-	-	0.23	*	0.43	*	-	-	1.05	0.47
19603	-0.06	*	-	-	0.04	*	-	-	0.37	*	0.97	0.49
19916	0.17	*	-	-	-	-	-	-	-	-	0.89	0.23
20155	0.15	*	-	-	0.11	0.01	0.49	*	0.49	*	1	0.53
20407	-0.06	*	-	-	-0.03	*	-	-	-	-	1.27	-
20584	-	-	-	-	0.11	*	0.36	*	-	-	1.04	0.27
20657	0.17	*	-	-	0.12	*	0.28	*	0.78	*	1.19	0.46
20675	0.26	*	-	-	0.12	*	0.39	*	0.63	*	1.05	0.83
21036	0.09	*	0.58	*	0.27	*	-	-	0.43	*	1.2	0.31
21089	0.45	0.13	-	-	0.45	*	-	-	1.03	*	1.06	0.22
22177	0.27	0.02	-	-	0.3	*	-	-	0.45	*	1.25	0.28
22582	0.12	*	-	-	0.07	*	0.4	*	0.22	*	1.46	0.4
23576	0.2	*	-	-	0.06	*	-	-	-	-	1.35	0.27
24331	-	-	-	-	-0.04	*	-	-	-	-	1.57	-
25912	0.23	*	-	-	0.25	0.08	0.32	*	0.56	*	1.21	0.59
26040	0.3	*	-	-	-0.06	*	-	-	-	-	1.3	-
26071	0.41	0.08	-	-	0.29	0.11	0.47	*	0.77	*	1.33	0.21
26864	0.44	0.02	-	-	0	0.06	-	-	0.69	*	1.41	0.2
27328	-	-	-	-	-	-	-	-	0.69	*	1.55	-
27446	0.03	0.02	-	-	0.08	0.08	0.09	*	-	-	1.27	-
27905	-	-	-	-	-0.06	*	0.05	*	-	-	1.38	-
27939	-	-	-	-	0.23	*	0.36	*	-	-	1.2	0.42
28185	0.3	*	-	-	0.12	*	0.46	*	0.75	*	1.09	0.22
28701	-	-	-	-	0.26	0.27	0.31	*	-	-	1.6	-

Continued on next page

Table A.6 – *Continued from previous page*

Star	[La/H]	±	[Ce/H]	±	[Nd/H]	±	[Eu/H]	±	[Hf/H]	±	Mg/Si	C/O
28821	-0.02	0.08	-	-	0.06	*	0.28	*	0.3	*	1.44	-
29231	0.36	*	-	-	0.13	0.13	-	-	0.43	*	1.19	0.3
29263	0.27	0.1	-	-	-	-	-	-	0.69	*	1.28	-
29813	-0.09	*	-	-	0.02	*	-	-	0.41	*	1.3	-
30278	-0.08	*	-	-	0.17	0.05	0.24	*	0.47	*	1.41	0.17
30306	0.47	0.06	-	-	0.3	0.2	0.09	*	0.44	*	1.1	0.18
30501	0.25	0.09	-	-	0.37	0.21	-	-	0.2	*	1.15	0.63
30669	0.22	0.11	-	-	0.09	0.1	-	-	0.1	*	1.24	0.12
31392	0.18	0.01	-	-	0.18	0.12	-	-	0.44	*	1.22	-
32564	-	-	-	-	0.04	0.02	-	-	0.64	*	1.29	0.29
32724	-	-	-	-	0.12	*	-	-	-	-	1.3	-
32804	-0.01	0.06	0.08	*	0.19	*	0.24	*	-	-	1.16	0.43
33093	0.02	0.14	-	-	0.21	0.1	0.32	*	-	-	1.06	0.22
33214	0.13	0.28	0.44	*	0.24	0.21	0.56	*	0.45	*	1.13	0.32
33822	0.25	0.1	-	-	0.2	0.01	0.43	*	0.75	*	1.35	0.33
33873	0.11	*	-	-	0.1	*	0.43	*	0.54	*	1.21	0.4
34195	-	-	-	-	0.02	0.04	0.21	*	-	-	1.18	0.45
34230	0.27	0.01	-	-	0.23	*	0.42	*	-	-	1.02	0.31
34377	0.14	0.14	-	-	0.11	*	0.46	*	0.44	*	1.07	0.31
34599	0.04	*	0.29	*	0.09	*	-	-	0.29	*	1.1	0.3
35376	0.05	*	-	-	-	-	-	-	0.42	*	1.09	0.43
35676	0.14	0.13	-	-	0.19	0.03	0.43	*	0.38	*	1.36	0.39
36152	-0.07	*	-0.16	*	0.14	0.11	0.34	*	0.21	*	1.22	0.68
36329	0.21	*	-0.33	*	0.06	0.25	0.24	*	0.37	*	0.97	-
37351	-0.21	*	-	-	0.01	*	-	-	0.47	*	1.09	0.25
37706	-0.03	*	-	-	0.12	0.02	0.11	*	0.42	*	1.24	-
37761	0.4	0.01	-	-	0.51	*	0.65	*	-	-	1.18	0.25
37986	0.37	*	-	-	0.23	*	0.67	*	0.73	*	1.04	0.22
38467	0.29	0.14	1.07	*	0.19	0.06	-	-	0.39	*	1.16	0.33
38554	0.18	0.07	-	-	0.1	*	-	-	0.67	*	1.19	0.28
38667	-	-	-	-	-	-	0.29	*	0.83	*	1.47	0.4
38677	-0.09	*	-	-	0.01	*	-	-	0.52	*	1.02	0.37
39126	0.15	0.07	-	-	0.25	*	-	-	-	-	1.28	0.22
39503	0.23	*	-	-	0.08	0.11	-	-	0.37	*	1.09	0.21
39804	0.02	0.16	-	-	0.18	*	0.3	*	-	-	1.17	0.26
39855	-	-	0.1	*	-0.17	0.1	-	-	-	-	1.59	-
40105	0.49	0.08	-	-	0.47	0.01	0.43	*	0.58	*	1.35	0.1

Continued on next page

Table A.6 – *Continued from previous page*

Star	[La/H]	±	[Ce/H]	±	[Nd/H]	±	[Eu/H]	±	[Hf/H]	±	Mg/Si	C/O
40403	0.3	*	-	-	-	-	-	-	-	-	1.08	0.35
41155	-	-	-	-	0.22	0.06	0.35	*	0.48	*	1.09	0.25
42044	0.15	0.01	-	-	0.06	0.04	0.05	*	0.37	*	0.96	0.24
42287	-	-	-	-	0.04	*	-	-	0.19	*	0.95	0.31
42538	0.06	*	-	-	0.2	*	0.5	*	-	-	0.98	0.44
42719	0.29	0.09	-	-	0.31	0.11	0.66	*	0.11	*	1.09	0.49
42778	-	-	-	-	0.06	*	0.32	*	0.47	*	1	0.25
43470	-	-	-	-	0.03	0.11	-	-	-	-	1.21	0.22
44569	-0.1	*	-	-	-0.08	0.02	-	-	-	-	1.32	-
44573	0.16	0.24	-	-	0.4	0.25	-	-	-	-	1.03	-
45133	0.28	*	1.43	*	0.29	*	0.34	*	0.31	*	0.98	0.4
45987	0.21	0.17	-	-	0.18	0.08	-	-	0.58	*	1.31	0.2
46175	-	-	-	-	0.01	*	0.18	*	0.49	*	0.74	0.33
46435	0.39	*	-	-	-	-	-	-	-	-	0.7	0.42
46894	0.35	0.06	-	-	0.45	0.1	0.35	*	0.78	*	1.03	0.3
47017	0.22	*	-	-	0.15	0.04	0.28	*	-	-	1.28	0.37
47186	0.18	*	-	-	0.1	*	-	-	0.66	*	1.13	0.17
48056	-	-	-	-	0.04	0.02	0.3	*	0.3	*	1.25	0.25
48265	0.28	0.13	-	-	0.38	*	0.52	*	0.87	*	0.94	0.2
49035	0.21	*	-	-	0.19	*	-	-	-	-	1.15	0.24
49866	0.28	0.08	-	-	0.21	0.07	0.45	*	0.49	*	1.09	0.28
50117	-0.02	0.03	-	-	0.06	0.01	0.3	*	-	-	1.2	0.29
50255	-0.08	*	-	-	-	-	0.14	*	0.28	*	1.22	-
50652	0.39	0.2	-	-	0.28	*	0.66	*	0.77	*	1.17	0.3
51608	0.11	*	-	-	0.19	0.07	0.27	*	-	-	1.46	0.3
52217	0.44	0.07	-	-	-0.01	*	-0.18	*	-	-	1.27	0.4
52756	0.32	*	-	-	0.44	0.25	-	-	0.05	*	1.09	0.15
56413	0.33	0.16	-	-	0.09	*	-	-	0.76	*	1.1	0.52
56662	-	-	-	-	-0.01	0.06	0.08	*	0.43	*	1.23	0.18
56972	0.35	0.11	-	-	0.29	*	0.35	*	-	-	1.22	0.21
58111	0.24	0.17	-	-	0.26	0.29	-	-	-0.16	*	1.31	0.51
58556	-	-	0.21	*	0.08	*	0.23	*	-	-	1.04	0.25
58696	-0.1	*	-	-	0.13	0.01	0.29	*	0.52	*	1.24	0.34
59711	-0.15	*	-0.19	*	-0.03	0.11	0.21	*	0.38	*	1.2	0.19
59824	0.12	*	-	-	0.12	*	0.52	*	-	-	1.31	0.45
61051	0.16	*	-	-	0.24	*	0.5	*	-	-	1.38	0.28
61475	0.34	0.04	-	-	0.06	0.03	0.14	*	0.7	*	1.09	0.25

Continued on next page

Table A.6 – *Continued from previous page*

Star	[La/H]	±	[Ce/H]	±	[Nd/H]	±	[Eu/H]	±	[Hf/H]	±	Mg/Si	C/O
62549	-	-	-	-	-0.01	0.08	-	-	0.46	*	1.26	0.33
62644	0.28	0.04	-	-	0.47	0.11	0.47	*	0.16	*	1.08	-
64114	0.04	0.07	-	-	-	-	0.22	*	-	-	1.32	0.32
64144	-0.04	*	-	-	0.01	0.11	0.35	*	0.39	*	1.28	0.29
65427	0.02	*	-	-	0.12	*	0.28	*	-	-	1.15	0.55
66039	0.03	*	-	-	0.05	0.08	0.24	*	-	-	1.1	0.4
66058	0.07	0.1	-	-	0.05	0.03	-	-	-	-	1.16	0.57
66791	0.15	0.07	-	-	0.28	0.04	0.39	*	0.12	*	1.27	0.56
70081	0.15	0.05	-	-	0.21	0.12	0.42	*	0.46	*	1.21	0.37
72579	0.23	0.02	-	-	0.21	*	0.15	*	0.28	*	1.16	0.29
72687	-	-	-	-	0	0.04	-	-	-	-	1.17	-
72892	0.18	0.06	-	-	0.15	*	-	-	0.47	*	1.24	0.38
73267	0.3	*	-	-	0.19	0.21	-	-	-0.17	*	1.45	0.13
73744	-	-	-	-	-0.18	0.09	-	-	-	-	1.44	-
74698	0.09	*	-	-	0.23	0.11	-	-	0.15	*	1.31	0.55
74733	-0.03	*	-	-	-0.05	0.07	0.08	*	-	-	1.33	-
74935	-0.02	*	-	-	0.16	0.18	-	-	0.46	*	1.08	0.41
75288	0.22	0.2	-	-	0.06	0.12	0.44	*	0.65	*	1.13	0.49
75351	0.01	*	-	-	0.14	0.08	0.45	*	0.41	*	1.06	0.33
77338	0.38	0.18	-	-	0.17	*	-	-	0.61	*	1.01	0.19
77417	0.37	0.09	-	-	0.04	0.06	-	-	0.68	*	1.13	0.41
77683	0.42	*	-	-	0.43	0.16	0.18	*	0.41	*	1.13	0.28
78130	0.09	*	-	-	0.06	0.04	-	-	-	-	1.19	0.6
78286	0.13	*	-	-	0.2	0.01	0.43	*	0.36	*	1.17	0.27
79985	0.14	*	-	-	0.21	0.01	-	-	0.47	*	1.19	0.26
81110	0.1	*	1	*	0.09	0.12	-	-	0.3	*	1.06	0.36
81700	-0.07	*	-	-	0.06	0.04	-	-	-	-	1.19	0.4
82282	0.2	0.26	-	-	0.4	0.21	-	-	-	-	1.25	-
82400	0.17	*	-	-	0.2	0.04	-	-	0.24	*	1.19	0.38
82516	0.36	0.11	-	-	-	-	-	-	-	-	1.39	0.4
82977	0.22	0.04	-	-	0.28	0.07	-	-	0.42	*	1.35	-
83365	0.14	0.06	-	-	0.01	0.06	-	-	-	-	1.16	0.36
83517	-0.02	*	-	-	-	-	-	-	-	-	1.27	-
84652	-	-	-	-	0.02	0.11	-	-	-	-	1.29	0.16
85380	-	-	-	-	0	0.06	-	-	-	-	1.26	0.37
85390	-	-	-	-	-	-	-	-	-	-	0	1
86006	0.29	0.04	-	-	0.28	*	0.48	*	0.44	*	1.08	0.4

Continued on next page

Table A.6 – *Continued from previous page*

Star	[La/H]	±	[Ce/H]	±	[Nd/H]	±	[Eu/H]	±	[Hf/H]	±	Mg/Si	C/O
86226	-	-	0.1	*	-	-	-	-	-	-	0	-
86249	0.38	0.14	-	-	-	-	-	-	-	-	1	0.89
86397	0.24	0.21	-	-	-0.09	0.11	0.65	*	0.25	*	1.24	0.38
86652	0.02	*	-	-	0.14	0.05	0.33	*	0.45	*	1.08	0.65
87931	0.21	*	-	-	-	-	-	-	-	-	1.31	0.23
87998	-	-	-	-	-	-	-	-	-	-	1.4	-
88864	-	-	-	-	-	-	0.36	*	-	-	1.14	-
89178	0.36	0.07	-	-	0.44	0.02	-	-	-	-	1.25	0.17
89418	-	-	-	-	-0.06	0.01	-	-	-	-	1	-
89988	0.21	*	-	-	0.24	*	-	-	0.53	*	1.17	0.34
90028	0.11	*	-	-	0.18	0.11	-	-	0.75	*	1.22	0.33
90702	0.17	0.08	-	-	-	-	-	-	-	-	1.15	0.53
91320	-	-	-	-	-0.16	*	0.22	*	-	-	1.17	0.22
91901	0.27	0.12	-	-	-	-	0.37	*	-	-	1.28	0.32
92069	0.32	0.01	-	-	0.35	0.02	0.59	*	0.26	*	1.26	0.39
92719	-	-	-	-	-	-	-	-	-	-	1.26	-
93083	0.42	0.16	-	-	0.37	0.28	-	-	-	-	1.08	0.46
94151	0.05	0.08	0.97	*	-	-	-	-	-	-	0	-
94387	0.54	*	-	-	0.03	*	0.36	*	0.38	*	1.24	0.24
94482	-	-	-	-	0.09	0.13	-	-	-	-	1.2	0.27
94527	0.06	*	-	-	0.09	0.02	0.38	*	0.14	*	1.37	-
94690	0.17	*	-	-	0.16	0.18	-	-	0.49	*	1.05	0.52
94838	0.09	0.13	-	-	0.15	0.13	0.19	*	-	-	1.17	-
95136	0.38	0.21	-	-	0.15	0.16	0.43	*	0.4	*	1.21	0.38
95338	0.38	0.06	-	-	-	-	-	-	-0.01	*	1.18	0.2
95521	-	-	-	-	-	-	-	-	-	-	0	-
95533	0.2	*	-	-	-	-	-	-	-	-	0.99	0.22
95542	-	-	-	-	0.08	0.04	0.28	*	-	-	1.32	-
96020	0.36	0.08	-	-	0.14	0.04	-	-	0.41	*	1.23	0.38
96276	-	-	-	-	-0.06	0.02	0.25	*	-	-	1.19	0.35
98163	0.2	0.02	-0.62	*	0.22	0.06	-	-	0.21	*	1.31	0.42
98459	0.16	0.04	-	-	0.16	*	0.41	*	0.54	*	1.16	0.42
98764	0.08	0.13	-	-	0.12	0.03	-	-	-	-	1.19	0.34
99116	-0.03	*	-	-	0.12	0.25	-	-	0.13	*	1.37	-
101093	-	-	-	-	-0.01	0.07	-	-	-	-	1.19	-
101171	0.2	0.03	-	-	0.22	*	0.42	*	0.39	*	1.19	0.25
101181	0.06	*	-	-	0.28	0.09	-	-	0.6	*	1.13	0.45

Continued on next page

Table A.6 – *Continued from previous page*

Star	[La/H]	±	[Ce/H]	±	[Nd/H]	±	[Eu/H]	±	[Hf/H]	±	Mg/Si	C/O
101896	0.27	*	-	-	0.19	*	0.25	*	0.78	*	1.56	0.22
102574	0.12	*	-	-	0.05	0.13	-	-	-	-	1.07	0.23
102579	0.33	0.26	-	-	0.15	0.25	0.02	*	0.4	*	1.5	0.64
102843	0.31	0.01	-	-	0.21	0.01	0.3	*	0.54	*	1.9	0.22
103559	0.2	0.13	-0.16	*	-	-	-	-	-	-	1.09	-
103673	0.12	*	-	-	0.12	0.04	0.04	*	0.49	*	1.38	-
104645	0.31	0.08	-	-	0.41	0.16	-	-	0.35	*	1.28	0.08
104760	0.13	*	-	-	0.13	0.23	-	-	-	-	1.01	0.55
104982	-0.19	*	-	-	-	-	0.21	*	-	-	0	-
105690	-	-	-	-	0.2	*	-	-	0.84	*	1	-
105904	0.39	*	-	-	0.15	0.02	0.39	*	0.8	*	1.36	0.19
106275	0.28	0.08	-	-	0.25	0.12	-	-	-	-	1.46	0.6
106869	-0.09	*	-	-	0.04	*	0.24	*	0.24	*	0.97	0.23
106937	0.41	0.1	-	-	0.35	0.13	-	-	0.25	*	1.15	0.27
107008	0.26	*	-	-	0.09	0.13	0.61	*	0.65	*	1.2	0.25
107181	0.32	0.11	-	-	0.35	0.05	0.25	*	0.41	*	1.09	0.25
108953	0.52	0.14	-	-	-	-	-	-	-	-	1.08	0.18
109591	0.1	*	0.51	*	0.15	0.11	0.32	*	0.06	*	1.31	0.65
109908	0.53	*	-	-	0.13	*	-	-	0.51	*	1.06	0.5
109930	0.24	0.01	0.34	*	0.23	0.24	-	-	-0.07	*	1.24	0.33
109988	0.48	0.1	-	-	0.3	0.21	0.19	*	-	-	1.19	0.13
110605	0.35	*	-	-	0.25	0.01	-	-	0.66	*	1.04	0.33
110619	-	-	-	-	-0.33	0.04	-	-	-	-	1.33	-
111431	0.12	0.16	-	-	0.17	0.07	0.43	*	-	-	1.31	0.37
112121	-	-	-	-	0.27	0.02	-0.03	*	0.06	*	1.1	0.21
112540	0	0.19	-	-	0.15	0.01	-	-	-	-	1.45	-
113027	-	-	-	-	-	-	0.14	*	-	-	1.21	-
113255	0.06	0.11	-	-	0.18	0.01	0.14	*	0.25	*	1.16	0.32
113513	0.03	0.04	0.94	*	0.13	*	-	-	-	-	0.84	-
114294	-	-	-	-	-	-	-	-	-	-	1.13	0.28
114432	-0.08	*	-	-	-	-	0.43	*	-	-	0	-
114884	0.1	*	-	-	0.03	*	-	-	0.49	*	1.04	-
115080	-	-	-	-	-	-	-	-	-	-	1.48	-
115674	-	-	-	-	-	-	0.1	*	-	-	1.48	-
116920	0.16	*	-	-	0.28	0.25	-	-	-	-	1.51	-
117653	0.2	*	-	-	-	-	-	-	-	-	1.15	0.39
117860	0.03	*	-	-	-	-	-	-	-	-	1.15	-

Continued on next page

Table A.6 – *Continued from previous page*

Star	[La/H]	±	[Ce/H]	±	[Nd/H]	±	[Eu/H]	±	[Hf/H]	±	Mg/Si	C/O
119070	0.08	*	-	-	0.16	0.1	-	-	0.25	*	1.31	-
119119	0.01	*	-	-	0.24	0.06	0.31	*	0.41	*	1.01	0.42
119507	0.43	0.13	-	-	0.31	0.14	-	-	0.36	*	1.35	0.52
119782	0.26	*	-	-	0.33	0.18	-	-	-	-	1.16	-
120100	0.24	0.05	-	-	0.36	0.15	-	-	0.36	*	1.16	0.21
120329	0.47	0.08	-	-	0.51	*	-	-	-	-	1.16	0.35
121504	-0.17	*	-	-	0.01	*	0.32	*	-	-	1.16	0.35
122078	0.25	0.05	-	-	0.31	0.06	-	-	0.8	*	1.13	0.43
124553	0.28	0.27	-	-	0.18	*	0.62	*	0.56	*	1.14	0.22
125968	0.03	*	-	-	-	-	0.31	*	0.49	*	1.13	0.38
126653	-	-	-	-	0.17	0.1	-	-	-	-	1.13	0.2
127321	0.05	*	-	-	-	-	0.28	*	0.67	*	1.37	0.43
128214	0.22	*	-	-	0.27	0.11	-	-	0.69	*	1.11	0.24
128760	-	-	-	-	0.1	0.18	-	-	0.36	*	0.97	0.37
128987	-	-	-	-	0.16	0.12	-	-	0.62	*	1.21	0.22
129679	-	-	-0.05	*	-	-	-	-	-	-	1.01	-
129764	-	-	-	-	0.18	*	0.19	*	-	-	1.12	0.31
129946	0.05	*	-	-	0.09	*	0.12	*	0.37	*	1.25	-
131900	0.29	*	-	-	0.08	*	0.04	*	0.57	*	1.21	0.29
132648	-	-	-0.59	*	-	-	-	-	-	-	1.07	1
133014	0.32	0.07	-	-	0.31	*	0.68	*	0.73	*	1.47	0.19
135005	0.34	*	-	-	0.29	0.06	-	-	0.24	*	1.14	0.25
135309	-	-	-	-	0.19	*	-0.2	*	0.28	*	0.93	0.2
135562	-	-	-	-	0	0.19	-	-	0.54	*	1.11	0.28
135625	0.03	*	-	-	0.19	*	0.34	*	0.55	*	1.36	0.38
135725	0.34	*	-	-	0.05	*	-0.02	*	0.31	*	1.3	-
136130	0.24	0.08	-	-	-	-	-	-	-	-	1.29	0.25
136548	-0.05	*	-	-	0.07	0.04	0.32	*	0.14	*	1.39	0.46
136894	-	-	-	-	-	-	0.24	*	-	-	0	0.54
137214	-0.05	0.07	-	-	-0.04	*	0.3	*	-	-	1.25	0.33
140643	0.58	0.01	-	-	0.36	0.16	-	-	-	-	1.13	0.51
141105	0.07	*	-	-	0.39	0.13	-0.01	*	0.25	*	1.28	0.17
141366	0.38	0.28	-	-	0.41	*	0.63	*	0.72	*	1.14	0.22
141514	-	-	-	-	0.02	0.07	0.52	*	-	-	1.14	0.18
141598	-	-	-	-	0.15	0.16	-	-	-	-	1.44	0.44
141599	0.14	*	-	-	-	-	-	-	-	-	1.01	0.39
141885	0.41	*	0.05	*	0.2	0.22	0.39	*	0.58	*	1.13	0.35

Continued on next page

Table A.6 – *Continued from previous page*

Star	[La/H]	±	[Ce/H]	±	[Nd/H]	±	[Eu/H]	±	[Hf/H]	±	Mg/Si	C/O
142137	-	-	-	-	0.19	*	-	-	0.47	*	0.99	0.43
143120	0.51	0.07	-	-	0.27	0.1	-	-	0.6	*	1.2	0.47
143137	-	-	-	-	0.13	0.01	-	-	0.55	*	1.18	0.18
143295	0.47	0.12	-	-	0.41	0.14	-	-	0.61	*	1.1	0.49
143673	0.3	0.1	-	-	0.23	0.02	-	-	0.24	*	1.28	0.17
144087	-	-	-	-	0.04	0.01	-	-	0.22	*	1.37	0.2
144088	-	-	-	-	0.25	0.17	-	-	0.16	*	1.24	0.19
144167	-	-	-	-	-	-	-	-	-	-	1.19	0.27
144550	0.37	0.07	-	-	-	-	-	-	-	-	1.18	0.26
144848	0.32	0.03	-	-	0.25	*	-	-	0.42	*	1.24	0.23
144899	0.2	0.05	-	-	-	-	-	-	-	-	1.12	0.84
145518	-0.06	*	-	-	-	-	0.06	*	-	-	1.21	-
145666	-0.01	*	-	-	0.07	*	-	-	0.5	*	1.13	0.42
146817	-0.01	*	-	-	0.19	0.06	0.25	*	0.51	*	1.58	0.27
146835	-	-	-	-	-0.24	*	-	-	-	-	1.1	-
147018	0.18	0.18	-	-	0.3	0.19	-	-	0.2	*	1.22	0.11
147619	-	-	0.1	*	0.19	0.1	0.39	*	-	-	1.26	0.35
148156	0.21	*	-	-	-0.1	0.06	-	-	0.74	*	1.15	0.35
148628	-0.07	*	-	-	-0.04	0.06	0.01	*	0.51	*	1.44	0.18
149189	0.52	0.25	-	-	0.25	0.04	-	-	0.36	*	1.07	0.32
150761	-0.05	*	-	-	-0.09	*	-	-	0.72	*	1	0.46
151450	-	-	-	-	0	0.05	-	-	-	-	1.03	0.24
152388	0.16	0.11	-	-	0.3	0.13	-	-	0.17	*	1.16	0.6
153631	-	-	-	-	0.02	0.01	-	-	-	-	1.27	0.41
154682	-0.12	*	-	-	0.05	*	-	-	0.51	*	1.34	-
154697	-	-	-	-	0.06	0.11	-	-	0.29	*	1.19	0.42
156152	0.47	*	-	-	0.09	0.12	-	-	-	-	1.24	0.25
156643	-	-	-	-	-0.14	0.1	0.06	*	-	-	1.16	0.28
157798	0.1	0.18	-	-	0.04	*	-	-	0.51	*	1.36	0.27
157830	-	-	-0.19	*	0.05	0.01	-	-	-	-	1.25	-
158469	-0.03	*	-	-	-0.16	0.09	-	-	-	-	1.3	0.16
158630	-0.17	*	-0.59	*	-0.08	0.06	-	-	-	-	1.37	-
159902	-	-	-	-	-0.03	0.07	0.06	*	-	-	1.37	-
160411	0.5	0.23	-	-	0.29	0.01	-	-	-	-	1.14	0.33
160859	0.01	0.05	0.04	*	0.05	0.01	0.09	*	0.4	*	1.37	-
161098	-0.19	*	-	-	-0.05	0.01	-	-	-	-	1.46	-
162907	0.2	*	0.38	*	0.14	0.07	-	-	0.95	*	1.35	0.6

Continued on next page

Table A.6 – *Continued from previous page*

Star	[La/H]	±	[Ce/H]	±	[Nd/H]	±	[Eu/H]	±	[Hf/H]	±	Mg/Si	C/O
165011	-0.11	*	-	-	0.1	0.03	0.27	*	0.4	*	1.12	0.28
165204	0.35	0.07	-	-	0.2	0.17	0.15	*	0.29	*	1.17	0.36
165271	0.08	0.15	-	-	0.16	0.1	0.4	*	0.24	*	1.12	0.33
165385	-	-	-	-	0.05	*	0.39	*	-	-	1.01	0.24
165449	-	-	-	-	0.01	0.03	0.12	*	-	-	1.32	0.41
165920	0.49	0.21	-	-	0.29	0.02	-	-	0.92	*	1.15	0.22
169303	0.13	*	-	-	0.05	0.06	-	-	-	-	1.08	0.35
169506	0.29	*	0.08	*	0.12	*	0.5	*	0.75	*	1.06	0.21
171990	0.07	*	-	-	0.13	*	0.23	*	-	-	1.21	0.4
172063	0.78	*	-	-	0.11	0.16	-	-	0.63	*	1.22	0.26
172582	-	-	-	-	-	-	-	-	-	-	1.41	-
174494	0.32	*	-	-	0.16	0.13	-	-	0.71	*	1.26	0.33
174541	0.41	*	-	-	0.06	0.08	-	-	-	-	1.6	-
175073	-	-	-	-	0.25	0.23	-	-	0.48	*	1.21	-
175169	0.43	0.15	-	-	0.28	0.16	-	-	0.35	*	1.22	0.55
176110	0.26	*	-	-	0.35	0.27	-	-	-	-	1.07	0.24
176151	0.39	0.25	-	-	0.24	0.02	-	-	0.85	*	1.25	0.32
176986	0.41	0.23	-	-	-	-	0.13	*	0.35	*	1.21	-
177122	-0.18	*	-	-	0.06	0.2	-	-	0.22	*	1.14	0.4
177409	-	-	-	-	0.06	0.04	0.23	*	0.29	*	1.26	-
178076	0.08	0.14	-	-	0.21	0.06	-	-	0.56	*	1.4	0.34
179640	0.38	0.04	-	-	0.33	0.01	-	-	0.94	*	1.26	0.34
180204	-	-	-	-	0.03	*	0.33	*	0.57	*	1.03	0.3
180257	-	-	-	-	0.23	0.04	-	-	0.51	*	1.06	0.36
181010	-	-	-	-	0.23	0.12	-	-	0.75	*	1.2	0.31
182228	0.05	*	1.31	*	0.14	*	0.45	*	0.64	*	1.35	0.34
182498	0.14	0.13	-	-	0.17	*	0.24	*	0.48	*	1.2	-
184317	0.01	*	-	-	0.14	*	-	-	0.22	*	1.25	0.28
185283	-	-	-	-	-	-	-	-	-	-	1.09	-
185615	0.19	*	-	-	-	-	-	-	-	-	1.36	0.41
186160	-	-	-	-	-0.17	0.07	-	-	-	-	1.54	-
186265	0.45	0.12	-	-	0.41	0.04	-	-	0.5	*	1.15	0.21
186651	-	-	-	-	-0.05	0.02	-	-	-	-	1.11	0.42
186803	0.15	*	-	-	0.18	0.06	-	-	-	-	2	-
187154	0.44	0.15	-	-	0.04	0.03	-	-	0.53	*	1.17	-
189310	0.19	*	-	-	0.36	0.26	-	-	0.71	*	1.63	2.45
190125	-	-	-	-	0.16	0.08	-	-	0.41	*	1.3	0.28

Continued on next page

Table A.6 – *Continued from previous page*

Star	[La/H]	±	[Ce/H]	±	[Nd/H]	±	[Eu/H]	±	[Hf/H]	±	Mg/Si	C/O
190613	0.11	0.04	-	-	0.03	*	-	-	-	-	1.4	0.4
191760	0.06	*	-	-	0.24	0.05	0.57	*	0.69	*	0.97	0.35
193567	0.24	0.02	-	-	0.24	0.08	0.36	*	0.43	*	1.28	0.24
193728	0.5	0.15	-	-	0.38	0.02	-	-	0.38	*	1.29	0.51
193995	0.48	*	-	-	0.36	0.06	0.6	*	0.95	*	1.21	0.38
195145	0.38	0.06	-	-	-0.04	*	0.33	*	0.46	*	1.12	0.25
195284	0.1	*	-	-	0.2	0.06	-	-	0.55	*	1.33	0.26
196397	-	-	-	-	0.27	0.04	-	-	0.43	*	1.13	0.2
197069	-	-	-	-	0.07	0.16	-	-	0.5	*	1	0.83
197210	0.06	0.06	-	-	0.09	*	-	-	-	-	1.32	0.2
197499	-	-	-	-	0.08	0.02	0.11	*	0.15	*	1.24	0.29
197818	-0.03	*	-	-	-0.06	0.03	0.25	*	-	-	1.31	0.33
197823	0.26	0.02	-	-	0.19	0.13	-	-	0.65	*	1.16	0.18
198477	0.13	*	-	-	0.18	*	-	-	0.41	*	1.5	0.19
199065	-0.08	*	-	-	-0.05	0.19	0.26	*	0.43	*	1.23	0.45
200733	0.19	0.11	-	-	0.07	0.03	0.39	*	0.41	*	1	0.16
200869	0.53	0.02	-	-	0.16	0.16	-	-	0.79	*	1.26	0.33
201757	0.25	0.05	-	-	-	-	-	-	0.82	*	1.22	0.33
202282	0.04	*	-	-	0.01	*	-	-	0.5	*	1.24	0.25
202457	0.19	0.02	-	-	0.23	0.01	0.43	*	0.35	*	1.35	0.3
203432	0.1	*	-	-	0.09	0.11	0.6	*	0.62	*	1.1	0.32
205045	0.16	*	-	-	0.13	0.13	0.28	*	0.14	*	1.11	0.35
205067	0.13	0.13	-	-	0.1	0.03	0.2	*	-	-	1.38	0.36
205158	-0.16	*	-	-	0.14	0.04	-	-	-	-	0.98	0.3
206025	0.25	0.04	-	-	0.19	0.06	-	-	-	-	1.63	0.37
206255	0.45	*	-	-	0.35	*	-	-	0.72	*	1.35	0.58
206683	0.25	*	-	-	0.12	*	-	-	0.61	*	1.12	0.39
207970	0.54	*	-	-	0.17	0.2	-	-	0.48	*	1.45	0.44
208704	-0.18	*	-	-	-0.03	0.04	0.14	*	0.41	*	1.45	0.57
209566	0.27	*	-	-	-0.04	0.15	-0.12	*	0.9	*	1.32	0.16
209659	0.19	*	-	-	0.17	0.02	0.39	*	0.44	*	1.06	0.32
210193	-	-	-	-	0.01	*	0.41	*	0.3	*	1.17	0.35
211366	0.06	*	1.39	*	-	-	-	-	-	-	0.83	0.33
213429	-0.27	*	-	-	-0.14	0.16	0.24	*	-	-	1.26	0.35
213717	0.26	*	-	-	0.07	0.05	0.54	*	0.91	*	1.42	0.33
213941	-	-	-	-	-0.22	*	-	-	-	-	1.42	-
214691	0.56	*	-	-	0.2	*	-	-	0.39	*	1.35	0.32

Continued on next page

Table A.6 – *Continued from previous page*

Star	[La/H]	±	[Ce/H]	±	[Nd/H]	±	[Eu/H]	±	[Hf/H]	±	Mg/Si	C/O
215456	-0.05	*	-	-	0.16	*	0.31	*	0.37	*	1.29	-
216054	0.01	0.01	-	-	0.04	*	0.21	*	0.18	*	1.49	-
218760	0.33	0.18	-	-	-	-	-	-	-	-	1.25	1.66
219011	0.36	0.06	-	-	0.34	*	0.63	*	0.92	*	1.17	0.13
219533	0.22	0.04	-	-	0.2	0.07	0.62	*	0.49	*	1.16	0.33
219556	0.15	*	-	-	0.2	0.08	0.58	*	0.53	*	1.19	0.15
220426	0.04	*	-	-	-0.1	0.09	0.3	*	-	-	1.68	0.27
220476	0.05	0.01	-	-	0.13	*	-	-	0.37	*	1.28	0.39
220689	-	-	-	-	-0.1	0.08	0.33	*	-	-	1.31	0.62
220718	0.3	0.17	-	-	0.29	*	-	-	0.61	*	1.13	0.21
220829	0.08	*	-	-	-	-	0.46	*	0.71	*	0.98	0.3
220945	0.21	*	-0.01	*	-	-	0.24	*	0.82	*	0.66	1
220981	-	-	-	-	-	-	-	-	-	-	1.13	0.33
221257	-	-	-	-	-0.02	0.06	0.21	*	-	-	1.25	-
221275	0.37	*	-	-	0.01	0.21	0.19	*	0.6	*	1.35	0.09
221954	0.29	0.08	-	-	0.35	*	0.31	*	0.96	*	0.92	0.25
222422	0.21	0.14	-	-	0.22	0.05	0.35	*	-	-	1.33	0.3
222669	0.04	*	-	-	0.02	0.01	0.15	*	0.5	*	1.19	0.54
224010	0.08	*	-	-	0.1	0.15	0.4	*	0.29	*	1.16	0.58
224022	0.13	*	-	-	-0.03	0.03	0.26	*	0.48	*	1.17	0.34
224143	0.04	*	-	-	0.1	*	0.16	*	-	-	1.2	-
224433	0.14	0.13	-0.06	*	-	-	0.36	*	-	-	1.26	0
224538	0.16	*	-	-	-	-	-	-	-	-	0.91	0.28
224789	0.28	0.11	-	-	0.24	0.11	-0.03	*	-0.06	*	1.26	0.29
225155	0.22	0.01	-	-	0.19	0.1	0.52	*	0.35	*	1.24	0.27
225299	0.2	*	-0.28	*	0.07	0.05	-	-	0.53	*	1.27	0.28

Table A.7: Absolute abundances normalized to 10^6 Si atoms

Star	Fe	C	O	Na	Mg	Si	Al	Ca
1002	1.19E+06	7.40E+06	1.59E+07	4.70E+04	1.36E+06	1.00E+06	9.50E+04	6.44E+04
1893	1.27E+06	6.51E+06	2.62E+07	5.35E+04	1.26E+06	1.00E+06	1.03E+05	6.45E+04
2098	1.15E+06	6.73E+06	1.76E+07	3.76E+04	1.26E+06	1.00E+06	8.41E+04	5.34E+04
2222	1.11E+06	6.04E+06	1.31E+07	3.81E+04	1.16E+06	1.00E+06	1.05E+05	5.19E+04
4333	1.25E+06	7.77E+06	2.39E+07	7.92E+04	1.24E+06	1.00E+06	1.08E+05	5.61E+04
4392	1.16E+06	8.46E+06	2.83E+07	7.20E+04	1.20E+06	1.00E+06	9.83E+04	5.24E+04
6236	1.19E+06	6.38E+06	1.82E+07	4.84E+04	1.15E+06	1.00E+06	9.02E+04	5.85E+04
6910	1.06E+06	6.80E+06	1.98E+07	4.65E+04	1.02E+06	1.00E+06	8.76E+04	5.03E+04
8076	1.18E+06	8.59E+06	1.88E+07	3.92E+04	1.26E+06	1.00E+06	9.41E+04	5.67E+04
9782	1.14E+06	6.46E+06	1.74E+07	4.17E+04	1.19E+06	1.00E+06	8.41E+04	5.51E+04
9847	1.10E+06	8.39E+06	2.16E+07	5.00E+04	1.13E+06	1.00E+06	9.86E+04	5.09E+04
10576	1.09E+06	6.07E+06	3.16E+07	3.80E+04	1.27E+06	1.00E+06	9.44E+04	5.92E+04
10678	1.17E+06	6.36E+06	1.81E+07	4.88E+04	1.30E+06	1.00E+06	1.02E+05	6.32E+04
11754	1.04E+06	7.48E+06	1.65E+07	4.88E+04	1.09E+06	1.00E+06	9.20E+04	5.11E+04
12585	1.13E+06	4.72E+06	1.49E+07	4.35E+04	1.30E+06	1.00E+06	1.02E+05	5.83E+04
13350	1.14E+06	7.63E+06	2.44E+07	6.20E+04	1.08E+06	1.00E+06	1.03E+05	4.75E+04
15507	1.09E+06	9.23E+06	2.48E+07	5.89E+04	1.19E+06	1.00E+06	1.00E+05	5.69E+04
15590	1.07E+06	6.20E+06	2.94E+07	4.94E+04	1.06E+06	1.00E+06	7.56E+04	4.71E+04
16950	9.87E+05	8.15E+06	1.96E+07	4.69E+04	9.36E+05	1.00E+06	8.63E+04	4.60E+04
18168	1.26E+06	1.64E+07	1.84E+07	6.74E+04	1.39E+06	1.00E+06	1.28E+05	7.07E+04
18708	1.05E+06	6.64E+06	1.90E+07	4.45E+04	8.99E+05	1.00E+06	9.52E+04	4.93E+04
18754	9.87E+05	7.37E+06	1.55E+07	6.23E+04	1.03E+06	1.00E+06	8.50E+04	4.69E+04
19603	1.19E+06	9.58E+06	1.94E+07	5.35E+04	9.73E+05	1.00E+06	9.18E+04	5.76E+04
19916	1.07E+06	5.51E+06	2.41E+07	4.28E+04	8.94E+05	1.00E+06	9.05E+04	4.60E+04
20155	1.11E+06	9.88E+06	1.87E+07	4.86E+04	1.00E+06	1.00E+06	9.15E+04	4.99E+04
20584	1.07E+06	5.33E+06	2.01E+07	4.06E+04	1.04E+06	1.00E+06	1.13E+05	5.14E+04
20657	1.06E+06	7.58E+06	1.65E+07	4.64E+04	1.19E+06	1.00E+06	9.15E+04	5.06E+04
20675	1.14E+06	1.14E+07	1.37E+07	7.10E+04	1.05E+06	1.00E+06	9.36E+04	5.44E+04
21089	1.03E+06	6.53E+06	2.99E+07	7.50E+04	1.06E+06	1.00E+06	9.12E+04	4.80E+04
22177	1.12E+06	7.64E+06	2.71E+07	3.96E+04	1.25E+06	1.00E+06	1.08E+05	5.70E+04
22582	1.02E+06	6.09E+06	1.53E+07	5.61E+04	1.46E+06	1.00E+06	1.27E+05	5.87E+04
23576	1.35E+06	7.09E+06	2.59E+07	3.92E+04	1.35E+06	1.00E+06	9.20E+04	7.00E+04
25912	1.33E+06	5.51E+06	9.36E+06	3.56E+04	1.21E+06	1.00E+06	9.80E+04	6.69E+04
26071	1.04E+06	7.41E+06	3.55E+07	6.61E+04	1.33E+06	1.00E+06	1.06E+05	5.44E+04
26864	1.22E+06	6.61E+06	3.24E+07	4.84E+04	1.41E+06	1.00E+06	4.42E+04	7.78E+04
27939	1.03E+06	6.70E+06	1.59E+07	4.93E+04	1.20E+06	1.00E+06	9.83E+04	6.09E+04

Continued on next page

Table A.7 – *Continued from previous page*

Star	Fe	C	O	Na	Mg	Si	Al	Ca
28185	1.08E+06	6.51E+06	3.01E+07	8.01E+04	1.09E+06	1.00E+06	9.86E+04	4.99E+04
32804	1.21E+06	5.84E+06	1.35E+07	3.43E+04	1.16E+06	1.00E+06	8.13E+04	6.87E+04
33093	1.11E+06	7.27E+06	3.32E+07	4.28E+04	1.06E+06	1.00E+06	8.94E+04	5.37E+04
33822	1.09E+06	6.70E+06	2.05E+07	5.39E+04	1.35E+06	1.00E+06	1.04E+05	5.55E+04
33873	1.22E+06	6.49E+06	1.63E+07	5.04E+04	1.21E+06	1.00E+06	1.04E+05	6.27E+04
34195	9.49E+05	9.32E+06	2.07E+07	3.81E+04	1.18E+06	1.00E+06	7.43E+04	4.83E+04
34230	1.10E+06	7.70E+06	2.51E+07	4.52E+04	1.02E+06	1.00E+06	1.04E+05	5.78E+04
34377	1.16E+06	5.19E+06	1.68E+07	5.96E+04	1.07E+06	1.00E+06	9.02E+04	6.79E+04
34599	1.39E+06	6.61E+06	2.19E+07	5.07E+04	1.10E+06	1.00E+06	1.04E+05	6.65E+04
35376	1.02E+06	7.15E+06	1.65E+07	3.91E+04	1.09E+06	1.00E+06	1.36E+05	5.11E+04
36152	1.22E+06	8.10E+06	1.19E+07	4.17E+04	1.22E+06	1.00E+06	9.66E+04	6.27E+04
37351	1.12E+06	6.78E+06	2.74E+07	4.35E+04	1.09E+06	1.00E+06	8.28E+04	6.08E+04
37761	1.09E+06	6.71E+06	2.64E+07	4.69E+04	1.18E+06	1.00E+06	1.35E+05	5.51E+04
38467	1.06E+06	5.58E+06	1.70E+07	5.39E+04	1.16E+06	1.00E+06	9.80E+04	5.07E+04
38554	1.16E+06	7.67E+06	2.79E+07	7.59E+04	1.19E+06	1.00E+06	1.06E+05	4.93E+04
38667	1.06E+06	6.47E+06	1.61E+07	4.14E+04	1.47E+06	1.00E+06	7.72E+04	4.81E+04
38677	1.07E+06	7.41E+06	2.00E+07	4.12E+04	1.02E+06	1.00E+06	7.67E+04	5.26E+04
39503	1.15E+06	6.04E+06	2.93E+07	7.04E+04	1.09E+06	1.00E+06	1.07E+05	5.53E+04
40403	1.17E+06	6.81E+06	1.96E+07	7.04E+04	1.08E+06	1.00E+06	9.50E+04	5.16E+04
41155	1.13E+06	7.18E+06	2.90E+07	4.76E+04	1.09E+06	1.00E+06	-	5.77E+04
42287	1.23E+06	6.26E+06	2.00E+07	3.51E+04	9.55E+05	1.00E+06	6.92E+04	7.01E+04
42538	1.13E+06	7.19E+06	1.62E+07	4.03E+04	9.77E+05	1.00E+06	1.00E+05	5.37E+04
42719	1.03E+06	9.22E+06	1.87E+07	3.99E+04	1.09E+06	1.00E+06	1.06E+05	4.90E+04
42778	1.24E+06	5.51E+06	2.19E+07	3.95E+04	1.00E+06	1.00E+06	7.27E+04	6.73E+04
45133	1.13E+06	6.81E+06	1.72E+07	6.38E+04	9.77E+05	1.00E+06	9.02E+04	5.15E+04
45987	1.24E+06	6.38E+06	3.25E+07	5.64E+04	1.31E+06	1.00E+06	1.01E+05	5.53E+04
46175	1.20E+06	6.89E+06	2.08E+07	4.20E+04	7.39E+05	1.00E+06	8.48E+04	5.49E+04
46894	1.05E+06	7.34E+06	2.44E+07	5.92E+04	1.03E+06	1.00E+06	-	5.11E+04
47017	1.05E+06	1.35E+07	3.69E+07	4.98E+04	1.28E+06	1.00E+06	8.66E+04	5.16E+04
47186	1.12E+06	5.07E+06	2.93E+07	8.63E+04	1.13E+06	1.00E+06	1.07E+05	5.13E+04
48056	1.07E+06	6.03E+06	2.44E+07	4.29E+04	1.25E+06	1.00E+06	9.17E+04	5.57E+04
48265	1.04E+06	5.43E+06	2.66E+07	8.41E+04	9.44E+05	1.00E+06	1.00E+05	5.12E+04
49866	1.06E+06	7.89E+06	2.84E+07	4.51E+04	1.09E+06	1.00E+06	9.31E+04	5.24E+04
50117	1.10E+06	7.34E+06	2.53E+07	5.80E+04	1.20E+06	1.00E+06	8.99E+04	5.52E+04
50652	1.24E+06	6.08E+06	2.03E+07	4.24E+04	1.17E+06	1.00E+06	1.09E+05	5.52E+04
56972	1.15E+06	4.76E+06	2.23E+07	5.92E+04	1.22E+06	1.00E+06	1.02E+05	5.59E+04
58696	1.09E+06	7.96E+06	2.33E+07	4.39E+04	1.24E+06	1.00E+06	9.28E+04	5.44E+04

Continued on next page

Table A.7 – *Continued from previous page*

Star	Fe	C	O	Na	Mg	Si	Al	Ca
59711	1.13E+06	6.06E+06	3.25E+07	4.54E+04	1.20E+06	1.00E+06	1.01E+05	5.71E+04
59824	1.14E+06	8.06E+06	1.79E+07	6.14E+04	1.31E+06	1.00E+06	9.95E+04	5.81E+04
62549	1.05E+06	5.94E+06	1.79E+07	3.79E+04	1.26E+06	1.00E+06	-	5.28E+04
65427	1.07E+06	1.25E+07	2.29E+07	5.19E+04	1.15E+06	1.00E+06	1.17E+05	6.07E+04
66039	1.22E+06	5.22E+06	1.29E+07	3.60E+04	1.10E+06	1.00E+06	8.06E+04	6.25E+04
66058	1.13E+06	8.06E+06	1.42E+07	5.08E+04	1.16E+06	1.00E+06	9.36E+04	5.30E+04
66791	1.04E+06	8.20E+06	1.46E+07	4.20E+04	1.27E+06	1.00E+06	8.89E+04	6.03E+04
70081	1.05E+06	9.16E+06	2.48E+07	5.48E+04	1.21E+06	1.00E+06	-	5.27E+04
72892	1.21E+06	7.20E+06	1.92E+07	5.40E+04	1.24E+06	1.00E+06	1.09E+05	5.27E+04
74698	1.13E+06	8.00E+06	1.47E+07	3.81E+04	1.31E+06	1.00E+06	9.80E+04	5.60E+04
74935	1.10E+06	7.18E+06	1.75E+07	4.54E+04	1.08E+06	1.00E+06	7.81E+04	5.58E+04
75288	1.14E+06	8.12E+06	1.65E+07	4.48E+04	1.13E+06	1.00E+06	1.05E+05	5.31E+04
75351	9.52E+05	7.58E+06	2.32E+07	5.14E+04	1.06E+06	1.00E+06	9.25E+04	4.41E+04
78130	1.21E+06	6.38E+06	1.06E+07	5.43E+04	1.19E+06	1.00E+06	9.12E+04	6.17E+04
78286	1.13E+06	7.20E+06	2.65E+07	4.56E+04	1.17E+06	1.00E+06	9.52E+04	5.20E+04
79985	1.12E+06	8.59E+06	3.30E+07	4.40E+04	1.19E+06	1.00E+06	9.63E+04	6.01E+04
81110	1.18E+06	6.92E+06	1.93E+07	7.00E+04	1.06E+06	1.00E+06	9.33E+04	5.64E+04
81700	1.30E+06	5.03E+06	1.24E+07	4.22E+04	1.19E+06	1.00E+06	9.12E+04	7.00E+04
82400	1.32E+06	7.52E+06	2.00E+07	5.14E+04	1.19E+06	1.00E+06	9.58E+04	7.10E+04
83365	1.11E+06	6.94E+06	1.93E+07	4.32E+04	1.16E+06	1.00E+06	8.81E+04	5.26E+04
85380	1.01E+06	7.56E+06	2.07E+07	3.67E+04	1.26E+06	1.00E+06	8.51E+04	4.93E+04
86006	1.10E+06	8.35E+06	2.07E+07	6.92E+04	1.08E+06	1.00E+06	9.55E+04	5.20E+04
86397	1.15E+06	7.54E+06	1.98E+07	3.96E+04	1.24E+06	1.00E+06	1.04E+05	5.72E+04
86652	1.14E+06	8.98E+06	1.38E+07	4.52E+04	1.08E+06	1.00E+06	9.89E+04	5.23E+04
89988	1.00E+06	6.30E+06	1.85E+07	6.27E+04	1.17E+06	1.00E+06	9.17E+04	4.96E+04
90028	1.07E+06	9.24E+06	2.77E+07	9.61E+04	1.22E+06	1.00E+06	9.72E+04	4.99E+04
90702	1.09E+06	6.24E+06	1.17E+07	5.62E+04	1.15E+06	1.00E+06	9.12E+04	5.29E+04
91320	1.01E+06	7.51E+06	3.49E+07	5.85E+04	1.17E+06	1.00E+06	9.17E+04	5.20E+04
92069	1.08E+06	7.39E+06	1.88E+07	5.23E+04	1.26E+06	1.00E+06	1.13E+05	5.66E+04
94690	1.09E+06	7.20E+06	1.39E+07	6.72E+04	1.05E+06	1.00E+06	9.39E+04	4.86E+04
95136	1.17E+06	4.98E+06	1.31E+07	5.74E+04	1.21E+06	1.00E+06	1.07E+05	5.94E+04
96020	1.28E+06	5.31E+06	1.40E+07	4.32E+04	1.23E+06	1.00E+06	1.04E+05	5.32E+04
98163	1.08E+06	7.46E+06	1.79E+07	4.05E+04	1.31E+06	1.00E+06	9.50E+04	5.67E+04
98459	1.06E+06	7.44E+06	1.76E+07	4.68E+04	1.16E+06	1.00E+06	1.00E+05	4.98E+04
98764	1.18E+06	5.63E+06	1.64E+07	3.54E+04	1.19E+06	1.00E+06	9.09E+04	6.41E+04
102574	1.03E+06	5.37E+06	2.38E+07	3.90E+04	1.07E+06	1.00E+06	7.18E+04	4.99E+04
104760	1.10E+06	7.36E+06	1.35E+07	4.12E+04	1.01E+06	1.00E+06	8.61E+04	4.97E+04

Continued on next page

Table A.7 – *Continued from previous page*

Star	Fe	C	O	Na	Mg	Si	Al	Ca
105904	1.21E+06	6.80E+06	3.61E+07	7.20E+04	1.36E+06	1.00E+06	1.07E+05	4.99E+04
106275	1.23E+06	1.71E+07	2.84E+07	5.23E+04	1.46E+06	1.00E+06	1.35E+05	7.16E+04
106937	1.13E+06	6.51E+06	2.37E+07	5.62E+04	1.15E+06	1.00E+06	1.06E+05	5.64E+04
107181	1.10E+06	6.13E+06	2.41E+07	6.20E+04	1.09E+06	1.00E+06	9.50E+04	5.24E+04
109591	9.35E+05	8.56E+06	1.33E+07	4.24E+04	1.31E+06	1.00E+06	1.18E+05	5.18E+04
109908	1.18E+06	6.77E+06	1.36E+07	3.97E+04	1.06E+06	1.00E+06	7.14E+04	6.38E+04
110605	1.14E+06	5.88E+06	1.78E+07	8.44E+04	1.04E+06	1.00E+06	9.04E+04	5.11E+04
111431	1.09E+06	8.63E+06	2.32E+07	4.48E+04	1.31E+06	1.00E+06	9.15E+04	5.35E+04
112121	1.18E+06	5.28E+06	2.46E+07	6.04E+04	1.10E+06	1.00E+06	1.01E+05	5.55E+04
113255	1.20E+06	6.53E+06	2.07E+07	3.94E+04	1.16E+06	1.00E+06	1.02E+05	5.60E+04
117653	1.12E+06	9.55E+06	2.45E+07	5.01E+04	1.15E+06	1.00E+06	1.00E+05	5.71E+04
119507	1.05E+06	8.44E+06	1.63E+07	5.77E+04	1.35E+06	1.00E+06	1.14E+05	6.08E+04
120329	1.23E+06	8.20E+06	2.31E+07	8.11E+04	1.16E+06	1.00E+06	1.17E+05	6.12E+04
121504	1.10E+06	7.42E+06	2.11E+07	-	1.16E+06	1.00E+06	8.59E+04	5.59E+04
122078	1.10E+06	7.74E+06	1.81E+07	4.77E+04	1.13E+06	1.00E+06	8.89E+04	5.22E+04
124553	1.08E+06	7.52E+06	3.36E+07	6.94E+04	1.14E+06	1.00E+06	9.69E+04	5.78E+04
125968	1.12E+06	8.44E+06	2.22E+07	6.11E+04	1.13E+06	1.00E+06	1.04E+05	5.55E+04
127321	1.24E+06	7.86E+06	1.83E+07	4.44E+04	1.37E+06	1.00E+06	8.95E+04	6.57E+04
128214	1.14E+06	7.48E+06	3.15E+07	8.20E+04	1.11E+06	1.00E+06	8.89E+04	4.69E+04
129764	1.18E+06	5.67E+06	1.82E+07	4.03E+04	1.12E+06	1.00E+06	8.71E+04	6.44E+04
131900	1.10E+06	7.75E+06	2.65E+07	-	1.21E+06	1.00E+06	1.13E+05	5.85E+04
133014	1.15E+06	6.40E+06	2.14E+07	5.51E+04	1.47E+06	1.00E+06	1.05E+05	5.28E+04
135005	1.10E+06	5.42E+06	2.18E+07	4.19E+04	1.14E+06	1.00E+06	1.01E+05	5.74E+04
135562	1.07E+06	6.68E+06	2.37E+07	4.84E+04	1.11E+06	1.00E+06	8.22E+04	5.04E+04
135625	1.09E+06	7.54E+06	1.97E+07	4.45E+04	1.36E+06	1.00E+06	9.52E+04	5.92E+04
136130	1.05E+06	5.58E+06	2.27E+07	5.20E+04	1.29E+06	1.00E+06	1.11E+05	6.67E+04
141105	1.08E+06	6.90E+06	4.02E+07	6.44E+04	1.28E+06	1.00E+06	1.13E+05	6.72E+04
141366	1.04E+06	5.59E+06	2.50E+07	4.65E+04	1.14E+06	1.00E+06	1.28E+05	5.10E+04
141598	9.99E+05	8.92E+06	2.01E+07	4.20E+04	1.44E+06	1.00E+06	-	5.86E+04
141885	1.03E+06	8.84E+06	2.49E+07	3.81E+04	1.13E+06	1.00E+06	1.03E+05	4.23E+04
144167	1.09E+06	-	2.19E+07	6.48E+04	1.19E+06	1.00E+06	9.04E+04	5.14E+04
144550	1.01E+06	5.85E+06	2.25E+07	7.29E+04	1.18E+06	1.00E+06	9.50E+04	4.55E+04
144848	1.15E+06	6.83E+06	2.97E+07	6.49E+04	1.24E+06	1.00E+06	9.50E+04	4.90E+04
148156	1.01E+06	6.24E+06	1.80E+07	4.79E+04	1.15E+06	1.00E+06	7.16E+04	5.32E+04
149189	1.10E+06	8.06E+06	2.55E+07	5.84E+04	1.07E+06	1.00E+06	7.97E+04	4.83E+04
153631	1.07E+06	7.93E+06	1.92E+07	4.81E+04	1.27E+06	1.00E+06	9.83E+04	5.89E+04
156152	1.17E+06	7.20E+06	2.87E+07	3.82E+04	1.24E+06	1.00E+06	1.15E+05	7.28E+04

Continued on next page

Table A.7 – *Continued from previous page*

Star	Fe	C	O	Na	Mg	Si	Al	Ca
156643	1.01E+06	7.56E+06	2.66E+07	4.57E+04	1.16E+06	1.00E+06	9.44E+04	5.57E+04
160411	1.14E+06	7.73E+06	2.34E+07	6.31E+04	1.14E+06	1.00E+06	9.02E+04	5.43E+04
162907	1.01E+06	7.73E+06	1.29E+07	3.81E+04	1.35E+06	1.00E+06	8.34E+04	5.60E+04
165204	1.19E+06	6.10E+06	1.70E+07	5.31E+04	1.17E+06	1.00E+06	1.08E+05	6.11E+04
165271	1.03E+06	6.91E+06	2.10E+07	4.34E+04	1.12E+06	1.00E+06	9.72E+04	5.09E+04
165449	1.02E+06	6.94E+06	1.70E+07	3.99E+04	1.32E+06	1.00E+06	9.25E+04	5.32E+04
169506	9.60E+05	7.09E+06	3.34E+07	4.94E+04	1.06E+06	1.00E+06	7.83E+04	4.20E+04
171990	9.64E+05	9.02E+06	2.28E+07	4.25E+04	1.21E+06	1.00E+06	9.09E+04	5.11E+04
175169	1.19E+06	6.55E+06	1.19E+07	5.77E+04	1.22E+06	1.00E+06	1.01E+05	4.98E+04
176110	1.10E+06	7.99E+06	3.37E+07	6.06E+04	1.07E+06	1.00E+06	9.07E+04	4.06E+04
176151	1.13E+06	8.12E+06	2.55E+07	4.97E+04	1.25E+06	1.00E+06	8.54E+04	5.14E+04
179640	1.29E+06	6.51E+06	1.93E+07	6.76E+04	1.26E+06	1.00E+06	1.06E+05	5.83E+04
180204	1.12E+06	5.67E+06	1.89E+07	4.81E+04	1.03E+06	1.00E+06	8.75E+04	5.07E+04
180257	1.09E+06	7.24E+06	2.00E+07	4.68E+04	1.06E+06	1.00E+06	8.91E+04	5.84E+04
182228	1.12E+06	7.73E+06	2.29E+07	5.96E+04	1.35E+06	1.00E+06	9.44E+04	5.50E+04
185615	9.82E+05	6.92E+06	1.68E+07	4.42E+04	1.36E+06	1.00E+06	1.26E+05	5.14E+04
186265	1.16E+06	5.34E+06	2.52E+07	4.13E+04	1.15E+06	1.00E+06	1.00E+05	5.91E+04
193567	1.17E+06	5.31E+06	2.23E+07	4.25E+04	1.28E+06	1.00E+06	9.74E+04	5.89E+04
193728	9.82E+05	7.82E+06	1.55E+07	3.55E+04	1.29E+06	1.00E+06	1.05E+05	5.55E+04
193995	1.20E+06	8.96E+06	2.39E+07	7.12E+04	1.21E+06	1.00E+06	9.17E+04	5.58E+04
195145	1.15E+06	6.82E+06	2.68E+07	6.15E+04	1.12E+06	1.00E+06	9.31E+04	5.76E+04
197069	1.17E+06	8.68E+06	1.04E+07	4.94E+04	9.97E+05	1.00E+06	7.22E+04	5.56E+04
197499	1.13E+06	7.68E+06	2.62E+07	3.62E+04	1.24E+06	1.00E+06	6.01E+04	5.64E+04
197818	1.06E+06	5.47E+06	1.66E+07	4.53E+04	1.31E+06	1.00E+06	9.47E+04	6.23E+04
199065	1.31E+06	5.67E+06	1.26E+07	3.98E+04	1.23E+06	1.00E+06	9.55E+04	6.33E+04
200733	1.07E+06	5.91E+06	3.64E+07	3.73E+04	1.00E+06	1.00E+06	6.63E+04	4.96E+04
200869	1.18E+06	6.82E+06	2.04E+07	8.01E+04	1.26E+06	1.00E+06	1.16E+05	5.69E+04
201757	1.09E+06	7.94E+06	2.37E+07	7.76E+04	1.22E+06	1.00E+06	8.41E+04	5.79E+04
202282	1.14E+06	6.46E+06	2.57E+07	4.79E+04	1.24E+06	1.00E+06	8.51E+04	5.83E+04
202457	1.02E+06	7.61E+06	2.55E+07	4.75E+04	1.35E+06	1.00E+06	1.13E+05	5.47E+04
203432	1.27E+06	6.31E+06	2.00E+07	7.16E+04	1.10E+06	1.00E+06	1.04E+05	5.66E+04
205045	1.11E+06	9.38E+06	2.65E+07	8.10E+04	1.11E+06	1.00E+06	7.39E+04	5.55E+04
205158	1.06E+06	7.81E+06	2.59E+07	4.24E+04	9.83E+05	1.00E+06	9.28E+04	5.04E+04
206255	1.10E+06	7.16E+06	1.23E+07	6.53E+04	1.35E+06	1.00E+06	1.01E+05	5.61E+04
206683	1.12E+06	5.88E+06	1.52E+07	7.43E+04	1.12E+06	1.00E+06	9.90E+04	5.28E+04
209659	1.06E+06	7.56E+06	2.34E+07	6.66E+04	1.06E+06	1.00E+06	8.59E+04	5.07E+04
210193	1.17E+06	7.76E+06	2.24E+07	6.76E+04	1.17E+06	1.00E+06	9.77E+04	5.51E+04

Continued on next page

Table A.7 – *Continued from previous page*

Star	Fe	C	O	Na	Mg	Si	Al	Ca
211366	1.33E+06	7.12E+06	2.13E+07	6.20E+04	8.27E+05	1.00E+06	7.99E+04	5.22E+04
213429	1.23E+06	9.08E+06	2.58E+07	4.33E+04	1.26E+06	1.00E+06	1.18E+05	7.67E+04
214691	1.06E+06	7.06E+06	2.18E+07	3.15E+04	1.35E+06	1.00E+06	1.21E+05	5.41E+04
219011	1.29E+06	5.50E+06	4.22E+07	6.46E+04	1.17E+06	1.00E+06	1.22E+05	6.06E+04
219533	1.11E+06	5.11E+06	1.53E+07	4.83E+04	1.16E+06	1.00E+06	1.02E+05	4.95E+04
220689	1.07E+06	7.18E+06	1.15E+07	5.72E+04	1.31E+06	1.00E+06	9.39E+04	5.09E+04
220718	1.08E+06	7.45E+06	3.62E+07	4.77E+04	1.13E+06	1.00E+06	8.49E+04	5.80E+04
220981	9.50E+05	1.29E+07	3.90E+07	4.13E+04	1.13E+06	1.00E+06	8.35E+04	5.13E+04
1237	1.23E+06	-	2.84E+07	4.01E+04	1.06E+06	1.00E+06	8.98E+04	6.10E+04
6880	1.15E+06	-	1.64E+07	4.12E+04	1.43E+06	1.00E+06	1.10E+05	5.96E+04
7661	1.33E+06	-	1.96E+07	4.20E+04	1.33E+06	1.00E+06	1.05E+05	7.24E+04
9905	1.14E+06	-	2.43E+07	7.27E+04	1.01E+06	1.00E+06	1.09E+05	5.28E+04
10008	1.24E+06	-	3.69E+07	4.05E+04	1.28E+06	1.00E+06	9.39E+04	7.50E+04
10611	1.41E+06	-	2.15E+07	4.80E+04	1.28E+06	1.00E+06	1.08E+05	7.83E+04
13060	1.23E+06	-	3.17E+07	3.77E+04	1.37E+06	1.00E+06	1.28E+05	6.64E+04
13386	1.22E+06	-	2.83E+07	6.35E+04	1.14E+06	1.00E+06	1.03E+05	5.56E+04
21036	1.38E+06	-	1.70E+07	4.27E+04	1.20E+06	1.00E+06	9.89E+04	6.78E+04
29231	1.19E+06	-	1.60E+07	5.74E+04	1.19E+06	1.00E+06	9.09E+04	6.52E+04
30278	1.12E+06	-	3.70E+07	3.92E+04	1.41E+06	1.00E+06	1.21E+05	6.29E+04
30306	1.08E+06	-	2.00E+07	5.39E+04	1.10E+06	1.00E+06	9.47E+04	5.18E+04
30501	1.18E+06	-	2.07E+07	4.43E+04	1.15E+06	1.00E+06	1.05E+05	6.89E+04
30669	1.18E+06	-	3.82E+07	5.59E+04	1.24E+06	1.00E+06	1.14E+05	6.11E+04
32564	1.16E+06	-	2.41E+07	4.59E+04	1.29E+06	1.00E+06	1.09E+05	6.36E+04
35676	1.30E+06	-	1.43E+07	4.68E+04	1.36E+06	1.00E+06	-	7.54E+04
37986	1.12E+06	-	2.45E+07	7.08E+04	1.04E+06	1.00E+06	1.00E+05	5.65E+04
39126	1.31E+06	-	2.89E+07	4.04E+04	1.28E+06	1.00E+06	9.92E+04	7.21E+04
40105	1.03E+06	-	4.40E+07	6.22E+04	1.35E+06	1.00E+06	1.16E+05	6.14E+04
56413	1.25E+06	-	1.40E+07	4.49E+04	1.10E+06	1.00E+06	9.49E+04	5.42E+04
58111	1.24E+06	-	2.39E+07	6.59E+04	1.31E+06	1.00E+06	1.27E+05	6.20E+04
61051	1.05E+06	-	2.23E+07	4.15E+04	1.38E+06	1.00E+06	1.41E+05	5.72E+04
64144	1.17E+06	-	1.74E+07	4.33E+04	1.28E+06	1.00E+06	1.00E+05	6.26E+04
72579	1.17E+06	-	2.21E+07	6.01E+04	1.16E+06	1.00E+06	1.04E+05	5.29E+04
77683	1.12E+06	-	2.16E+07	3.50E+04	1.13E+06	1.00E+06	8.89E+04	5.38E+04
87931	1.18E+06	-	2.84E+07	4.44E+04	1.31E+06	1.00E+06	1.05E+05	6.40E+04
93083	1.08E+06	-	2.74E+07	6.27E+04	1.08E+06	1.00E+06	1.18E+05	5.22E+04
94387	1.15E+06	-	2.37E+07	8.04E+04	1.24E+06	1.00E+06	1.08E+05	5.80E+04
95533	1.18E+06	-	1.59E+07	5.08E+04	9.92E+05	1.00E+06	1.09E+05	5.91E+04

Continued on next page

Table A.7 – *Continued from previous page*

Star	Fe	C	O	Na	Mg	Si	Al	Ca
101181	1.13E+06	-	2.36E+07	7.20E+04	1.13E+06	1.00E+06	9.28E+04	5.05E+04
101896	1.32E+06	-	2.28E+07	5.22E+04	1.56E+06	1.00E+06	1.20E+05	6.44E+04
104645	1.14E+06	-	5.66E+07	6.57E+04	1.28E+06	1.00E+06	1.01E+05	6.09E+04
107008	1.16E+06	-	2.28E+07	8.37E+04	1.20E+06	1.00E+06	9.50E+04	6.08E+04
109930	1.13E+06	-	1.86E+07	4.40E+04	1.24E+06	1.00E+06	1.20E+05	6.39E+04
114294	1.13E+06	-	1.81E+07	5.11E+04	1.13E+06	1.00E+06	1.04E+05	5.77E+04
120100	1.10E+06	-	2.16E+07	5.19E+04	1.16E+06	1.00E+06	1.04E+05	5.67E+04
128987	1.24E+06	-	2.15E+07	4.65E+04	1.21E+06	1.00E+06	9.39E+04	7.57E+04
135309	1.25E+06	-	2.20E+07	4.49E+04	9.28E+05	1.00E+06	9.17E+04	6.86E+04
140643	1.07E+06	-	2.33E+07	7.54E+04	1.13E+06	1.00E+06	1.30E+05	6.01E+04
141599	1.17E+06	-	1.19E+07	4.62E+04	1.01E+06	1.00E+06	9.33E+04	5.11E+04
143673	1.21E+06	-	1.96E+07	5.34E+04	-	1.00E+06	1.10E+05	5.98E+04
144087	1.38E+06	-	3.87E+07	5.04E+04	1.37E+06	1.00E+06	1.05E+05	7.13E+04
144088	1.35E+06	-	5.11E+07	5.06E+04	1.24E+06	1.00E+06	1.07E+05	7.01E+04
146817	9.29E+05	-	4.17E+07	6.46E+04	-	1.00E+06	1.29E+05	5.59E+04
152388	1.25E+06	-	7.74E+06	4.02E+04	1.16E+06	1.00E+06	9.86E+04	6.28E+04
154697	1.18E+06	-	1.17E+07	4.32E+04	1.19E+06	1.00E+06	9.66E+04	6.07E+04
165920	1.19E+06	-	2.99E+07	6.86E+04	1.15E+06	1.00E+06	1.09E+05	6.12E+04
172063	1.08E+06	-	2.56E+07	4.98E+04	1.22E+06	1.00E+06	1.13E+05	6.24E+04
174494	1.05E+06	-	1.95E+07	7.76E+04	1.26E+06	1.00E+06	9.66E+04	5.15E+04
178076	1.32E+06	-	1.38E+07	3.60E+04	1.40E+06	1.00E+06	1.01E+05	7.36E+04
189310	1.25E+06	-	3.81E+07	5.14E+04	1.63E+06	1.00E+06	1.16E+05	7.10E+04
190125	1.17E+06	-	1.79E+07	5.04E+04	1.30E+06	1.00E+06	1.07E+05	6.21E+04
195284	1.26E+06	-	1.92E+07	4.24E+04	1.33E+06	1.00E+06	9.72E+04	6.99E+04
196397	1.17E+06	-	2.50E+07	7.56E+04	1.13E+06	1.00E+06	1.12E+05	5.48E+04
197210	1.15E+06	-	2.57E+07	5.19E+04	1.32E+06	1.00E+06	9.44E+04	5.90E+04
197823	1.25E+06	-	3.28E+07	4.58E+04	1.16E+06	1.00E+06	9.36E+04	5.96E+04
198477	1.28E+06	-	2.63E+07	5.07E+04	1.50E+06	1.00E+06	1.11E+05	5.96E+04
209566	1.20E+06	-	2.88E+07	4.62E+04	1.32E+06	1.00E+06	1.11E+05	6.12E+04
213717	1.24E+06	-	1.36E+07	5.23E+04	1.42E+06	1.00E+06	1.14E+05	7.25E+04
219556	1.19E+06	-	2.83E+07	6.33E+04	1.19E+06	1.00E+06	1.00E+05	5.94E+04
220476	1.24E+06	-	1.81E+07	4.11E+04	1.28E+06	1.00E+06	9.74E+04	7.45E+04
220829	1.22E+06	-	3.49E+07	6.21E+04	9.85E+05	1.00E+06	1.17E+05	6.12E+04
7449	1.14E+06	6.05E+06	-	4.69E+04	1.34E+06	1.00E+06	7.88E+04	6.03E+04
9175	1.06E+06	6.78E+06	-	5.32E+04	1.35E+06	1.00E+06	1.11E+05	5.85E+04
10226	1.16E+06	5.44E+06	-	5.04E+04	1.18E+06	1.00E+06	9.17E+04	5.94E+04
10370	1.11E+06	7.70E+06	-	6.11E+04	1.29E+06	1.00E+06	1.11E+05	5.48E+04

Continued on next page

Table A.7 – *Continued from previous page*

Star	Fe	C	O	Na	Mg	Si	Al	Ca
11264	1.13E+06	6.44E+06	-	5.92E+04	1.17E+06	1.00E+06	1.03E+05	5.79E+04
14758	1.11E+06	7.46E+06	-	4.86E+04	1.55E+06	1.00E+06	1.04E+05	6.63E+04
17134	1.21E+06	7.41E+06	-	5.25E+04	1.40E+06	1.00E+06	1.05E+05	6.49E+04
17289	1.09E+06	1.03E+07	-	5.11E+04	1.41E+06	1.00E+06	1.02E+05	6.85E+04
18819	9.68E+05	9.08E+06	-	5.51E+04	1.05E+06	1.00E+06	8.06E+04	4.56E+04
26040	1.26E+06	7.41E+06	-	8.32E+04	1.30E+06	1.00E+06	7.76E+04	8.35E+04
27446	1.17E+06	5.74E+06	-	4.51E+04	1.27E+06	1.00E+06	9.20E+04	6.41E+04
28701	8.09E+05	7.34E+06	-	4.83E+04	1.60E+06	1.00E+06	1.08E+05	6.09E+04
28821	1.02E+06	5.83E+06	-	4.45E+04	1.44E+06	1.00E+06	1.14E+05	5.92E+04
29263	1.12E+06	8.79E+06	-	5.59E+04	1.28E+06	1.00E+06	9.61E+04	5.31E+04
29813	1.15E+06	5.50E+06	-	4.90E+04	1.30E+06	1.00E+06	1.06E+05	6.01E+04
32724	9.27E+05	6.75E+06	-	4.98E+04	1.30E+06	1.00E+06	1.02E+05	5.73E+04
39804	1.20E+06	5.60E+06	-	4.82E+04	1.17E+06	1.00E+06	-	6.07E+04
44569	9.85E+05	7.81E+06	-	4.48E+04	1.32E+06	1.00E+06	1.03E+05	5.31E+04
49035	1.15E+06	5.16E+06	-	7.10E+04	1.15E+06	1.00E+06	1.03E+05	5.56E+04
52217	1.20E+06	7.46E+06	-	6.96E+04	1.27E+06	1.00E+06	1.05E+05	5.86E+04
62644	1.05E+06	5.67E+06	-	5.29E+04	1.08E+06	1.00E+06	9.41E+04	5.67E+04
72687	1.29E+06	5.00E+06	-	4.56E+04	1.17E+06	1.00E+06	1.16E+05	6.86E+04
77338	1.11E+06	7.36E+06	-	9.41E+04	1.01E+06	1.00E+06	1.01E+05	5.19E+04
77417	1.18E+06	6.79E+06	-	6.08E+04	1.13E+06	1.00E+06	1.04E+05	5.58E+04
83517	1.12E+06	9.39E+06	-	8.08E+04	1.27E+06	1.00E+06	1.04E+05	7.27E+04
87998	1.09E+06	7.36E+06	-	4.86E+04	1.40E+06	1.00E+06	1.10E+05	6.24E+04
88864	1.07E+06	9.46E+06	-	9.68E+04	1.14E+06	1.00E+06	1.25E+05	6.55E+04
89178	1.14E+06	6.35E+06	-	4.54E+04	1.25E+06	1.00E+06	1.05E+05	5.61E+04
94527	1.15E+06	7.27E+06	-	5.14E+04	1.37E+06	1.00E+06	8.73E+04	6.36E+04
94838	1.22E+06	6.42E+06	-	4.49E+04	1.17E+06	1.00E+06	8.08E+04	6.45E+04
99116	1.19E+06	7.46E+06	-	5.91E+04	1.37E+06	1.00E+06	1.01E+05	6.27E+04
102579	1.15E+06	1.25E+07	-	7.70E+04	1.50E+06	1.00E+06	1.18E+05	6.43E+04
103559	1.17E+06	5.41E+06	-	4.30E+04	1.09E+06	1.00E+06	9.51E+04	7.18E+04
114884	1.12E+06	5.75E+06	-	6.21E+04	1.04E+06	1.00E+06	9.18E+04	5.68E+04
115080	8.91E+05	9.33E+06	-	6.03E+04	1.48E+06	1.00E+06	1.62E+05	5.82E+04
117860	1.24E+06	5.52E+06	-	5.58E+04	1.15E+06	1.00E+06	8.17E+04	6.93E+04
119070	1.17E+06	9.31E+06	-	6.66E+04	1.31E+06	1.00E+06	-	6.46E+04
119782	1.17E+06	1.42E+07	-	5.61E+04	1.16E+06	1.00E+06	1.04E+05	6.19E+04
129679	1.26E+06	6.43E+06	-	6.14E+04	1.01E+06	1.00E+06	6.14E+04	7.03E+04
129946	1.22E+06	5.93E+06	-	3.19E+04	1.25E+06	1.00E+06	8.98E+04	6.78E+04
136548	1.05E+06	8.17E+06	-	3.50E+04	1.39E+06	1.00E+06	8.79E+04	5.75E+04

Continued on next page

Table A.7 – *Continued from previous page*

Star	Fe	C	O	Na	Mg	Si	Al	Ca
142137	1.00E+06	7.15E+06	-	6.40E+04	9.91E+05	1.00E+06	7.87E+04	4.34E+04
144899	1.08E+06	5.67E+06	-	8.10E+04	1.12E+06	1.00E+06	8.68E+04	4.46E+04
145518	1.17E+06	6.92E+06	-	-	1.21E+06	1.00E+06	8.68E+04	6.08E+04
145666	1.16E+06	7.04E+06	-	4.34E+04	1.13E+06	1.00E+06	8.18E+04	6.26E+04
147619	1.06E+06	6.49E+06	-	7.48E+04	1.26E+06	1.00E+06	8.99E+04	4.69E+04
150761	9.93E+05	7.41E+06	-	6.68E+04	1.00E+06	1.00E+06	9.44E+04	4.30E+04
157830	1.10E+06	6.86E+06	-	4.86E+04	1.25E+06	1.00E+06	9.36E+04	6.00E+04
159902	1.09E+06	6.57E+06	-	5.16E+04	1.37E+06	1.00E+06	9.94E+04	6.72E+04
160859	1.11E+06	5.02E+06	-	4.65E+04	1.37E+06	1.00E+06	9.72E+04	6.10E+04
172582	1.19E+06	1.55E+07	-	5.96E+04	1.41E+06	1.00E+06	1.14E+05	7.15E+04
174541	8.07E+05	1.08E+07	-	5.43E+04	1.60E+06	1.00E+06	8.32E+04	5.29E+04
177409	1.10E+06	5.41E+06	-	4.75E+04	1.26E+06	1.00E+06	8.84E+04	6.08E+04
184317	1.05E+06	6.75E+06	-	5.66E+04	1.25E+06	1.00E+06	9.28E+04	5.24E+04
186803	1.18E+06	4.95E+06	-	4.57E+04	2.00E+06	1.00E+06	9.44E+04	6.61E+04
191760	1.07E+06	6.17E+06	-	6.61E+04	9.66E+05	1.00E+06	8.32E+04	4.67E+04
205067	1.01E+06	6.82E+06	-	3.92E+04	1.38E+06	1.00E+06	1.06E+05	5.77E+04
207970	1.00E+06	9.40E+06	-	5.51E+04	1.45E+06	1.00E+06	1.19E+05	5.52E+04
208704	1.08E+06	6.58E+06	-	3.72E+04	1.45E+06	1.00E+06	9.66E+04	5.67E+04
213941	7.35E+05	5.92E+06	-	4.45E+04	1.42E+06	1.00E+06	1.24E+05	5.72E+04
215456	1.05E+06	9.73E+06	-	4.75E+04	1.29E+06	1.00E+06	9.58E+04	5.69E+04
221257	1.07E+06	7.84E+06	-	5.70E+04	1.25E+06	1.00E+06	9.15E+04	5.73E+04
8129	1.20E+06	-	-	5.03E+04	1.28E+06	1.00E+06	1.03E+05	6.40E+04
8406	1.16E+06	-	-	5.14E+04	1.32E+06	1.00E+06	9.58E+04	6.33E+04
27328	1.25E+06	-	-	6.84E+04	1.55E+06	1.00E+06	1.07E+05	6.73E+04
27905	1.14E+06	-	-	5.37E+04	1.38E+06	1.00E+06	1.01E+05	6.13E+04
31392	1.15E+06	-	-	5.75E+04	1.22E+06	1.00E+06	9.89E+04	5.84E+04
33214	1.15E+06	-	-	6.74E+04	1.13E+06	1.00E+06	1.07E+05	5.66E+04
36329	1.41E+06	-	-	4.91E+04	9.68E+05	1.00E+06	6.47E+04	7.55E+04
37706	1.09E+06	-	-	5.50E+04	1.24E+06	1.00E+06	1.04E+05	5.98E+04
39855	1.10E+06	-	-	5.77E+04	1.59E+06	1.00E+06	1.14E+05	6.74E+04
50255	1.24E+06	-	-	5.59E+04	1.22E+06	1.00E+06	8.37E+04	6.90E+04
51608	1.15E+06	-	-	5.19E+04	1.46E+06	1.00E+06	1.17E+05	6.29E+04
52756	1.14E+06	-	-	8.08E+04	1.09E+06	1.00E+06	1.24E+05	6.55E+04
61475	1.19E+06	-	-	4.70E+04	1.09E+06	1.00E+06	1.08E+05	6.22E+04
73267	1.14E+06	-	-	5.58E+04	1.45E+06	1.00E+06	1.15E+05	5.84E+04
74733	1.15E+06	-	-	-	1.33E+06	1.00E+06	8.99E+04	6.28E+04
82282	1.23E+06	-	-	6.11E+04	1.25E+06	1.00E+06	9.36E+04	7.32E+04

Continued on next page

Table A.7 – *Continued from previous page*

Star	Fe	C	O	Na	Mg	Si	Al	Ca
82977	1.30E+06	-	-	5.17E+04	1.35E+06	1.00E+06	1.09E+05	6.57E+04
92719	1.07E+06	-	-	4.97E+04	1.26E+06	1.00E+06	9.81E+04	5.56E+04
101171	1.12E+06	-	-	5.52E+04	1.19E+06	1.00E+06	1.03E+05	5.99E+04
102843	1.25E+06	-	-	6.22E+04	1.90E+06	1.00E+06	1.20E+05	6.42E+04
103673	1.35E+06	-	-	4.42E+04	1.38E+06	1.00E+06	9.33E+04	7.07E+04
105690	1.35E+06	-	-	4.97E+04	1.00E+06	1.00E+06	9.15E+04	7.46E+04
108953	1.06E+06	-	-	7.48E+04	1.08E+06	1.00E+06	8.99E+04	4.57E+04
109988	1.08E+06	-	-	8.94E+04	1.19E+06	1.00E+06	1.21E+05	5.95E+04
110619	1.03E+06	-	-	5.85E+04	1.33E+06	1.00E+06	1.04E+05	5.63E+04
112540	1.18E+06	-	-	6.26E+04	1.45E+06	1.00E+06	9.80E+04	6.56E+04
113513	1.34E+06	-	-	5.24E+04	8.40E+05	1.00E+06	9.64E+04	6.92E+04
132648	1.07E+06	-	-	7.05E+04	1.07E+06	1.00E+06	1.08E+05	5.59E+04
135725	1.21E+06	-	-	5.89E+04	1.30E+06	1.00E+06	1.00E+05	6.88E+04
161098	1.09E+06	-	-	5.17E+04	1.46E+06	1.00E+06	-	6.00E+04
175073	1.26E+06	-	-	6.80E+04	1.21E+06	1.00E+06	9.94E+04	6.65E+04
181010	1.21E+06	-	-	6.18E+04	1.20E+06	1.00E+06	1.11E+05	6.49E+04
187154	1.16E+06	-	-	5.69E+04	1.17E+06	1.00E+06	1.06E+05	6.44E+04
216054	1.15E+06	-	-	4.88E+04	1.49E+06	1.00E+06	1.14E+05	6.58E+04
221275	1.15E+06	-	-	5.26E+04	1.35E+06	1.00E+06	1.04E+05	5.92E+04
157798	1.15E+06	6.34E+06	2.34E+07	-	1.36E+06	1.00E+06	8.59E+04	5.77E+04
147018	1.26E+06	-	4.32E+07	-	1.22E+06	1.00E+06	1.14E+05	5.76E+04
143120	1.12E+06	6.92E+06	-	-	1.20E+06	1.00E+06	1.07E+05	4.82E+04
1926	8.93E+05	5.95E+06	1.98E+07	3.53E+04	-	1.00E+06	8.56E+04	5.69E+04
42044	1.10E+06	8.39E+06	3.50E+07	4.56E+04	-	1.00E+06	6.82E+04	6.41E+04
43470	1.18E+06	5.93E+06	2.73E+07	4.58E+04	-	1.00E+06	7.78E+04	5.99E+04
46435	1.32E+06	1.01E+07	2.39E+07	4.50E+04	-	1.00E+06	8.68E+04	6.57E+04
58556	1.10E+06	6.09E+06	2.41E+07	3.90E+04	-	1.00E+06	6.94E+04	5.64E+04
84652	1.07E+06	6.70E+06	4.13E+07	4.97E+04	-	1.00E+06	6.63E+04	5.02E+04
94482	1.06E+06	7.68E+06	2.88E+07	5.23E+04	-	1.00E+06	8.20E+04	5.54E+04
96276	1.11E+06	8.48E+06	2.43E+07	5.19E+04	-	1.00E+06	9.12E+04	5.46E+04
106869	1.05E+06	6.57E+06	2.80E+07	4.65E+04	-	1.00E+06	8.86E+04	5.13E+04
119119	1.09E+06	8.36E+06	1.98E+07	3.32E+04	-	1.00E+06	7.78E+04	5.70E+04
126653	1.18E+06	8.27E+06	4.05E+07	4.70E+04	-	1.00E+06	5.22E+04	6.13E+04
128760	1.15E+06	5.82E+06	1.55E+07	5.14E+04	-	1.00E+06	6.86E+04	4.95E+04
136894	1.17E+06	6.49E+06	1.21E+07	6.71E+04	-	1.00E+06	1.21E+05	6.49E+04
137214	1.05E+06	7.07E+06	2.12E+07	3.86E+04	-	1.00E+06	7.43E+04	5.50E+04
141514	1.13E+06	7.61E+06	4.22E+07	4.62E+04	-	1.00E+06	8.91E+04	6.60E+04

Continued on next page

Table A.7 – *Continued from previous page*

Star	Fe	C	O	Na	Mg	Si	Al	Ca
143137	1.04E+06	6.38E+06	3.56E+07	4.64E+04	-	1.00E+06	8.84E+04	4.82E+04
148628	1.15E+06	1.01E+07	5.59E+07	3.61E+04	-	1.00E+06	8.66E+04	6.40E+04
151450	1.06E+06	5.78E+06	2.39E+07	5.17E+04	-	1.00E+06	8.20E+04	5.41E+04
158469	1.10E+06	7.16E+06	4.52E+07	4.12E+04	-	1.00E+06	9.66E+04	5.85E+04
165011	1.05E+06	7.92E+06	2.81E+07	4.06E+04	-	1.00E+06	8.01E+04	4.97E+04
165385	1.02E+06	8.05E+06	3.41E+07	5.66E+04	-	1.00E+06	6.80E+04	5.18E+04
169303	9.52E+05	8.67E+06	2.46E+07	3.60E+04	-	1.00E+06	9.15E+04	4.36E+04
177122	1.08E+06	9.22E+06	2.30E+07	4.33E+04	-	1.00E+06	7.97E+04	5.61E+04
186651	1.11E+06	6.46E+06	1.53E+07	4.25E+04	-	1.00E+06	7.92E+04	6.30E+04
206025	1.01E+06	7.46E+06	2.01E+07	3.78E+04	-	1.00E+06	7.90E+04	5.16E+04
220426	1.07E+06	5.65E+06	2.11E+07	5.13E+04	-	1.00E+06	6.24E+04	5.53E+04
6790	1.27E+06	-	1.42E+07	4.39E+04	-	1.00E+06	1.13E+05	6.98E+04
56662	1.10E+06	-	4.40E+07	4.56E+04	-	1.00E+06	9.41E+04	5.57E+04
7134	9.64E+05	6.53E+06	-	-	-	1.00E+06	8.51E+04	5.43E+04
10519	5.71E+05	8.41E+06	-	3.89E+04	-	1.00E+06	1.16E+05	5.19E+04
12951	9.61E+05	7.76E+06	-	5.08E+04	-	1.00E+06	8.44E+04	5.14E+04
20407	8.26E+05	7.82E+06	-	5.31E+04	-	1.00E+06	7.59E+04	4.34E+04
73744	9.50E+05	6.67E+06	-	4.14E+04	-	1.00E+06	8.86E+04	5.20E+04
86226	1.18E+06	7.87E+06	-	5.45E+04	-	1.00E+06	9.57E+04	5.92E+04
95521	1.08E+06	5.84E+06	-	-	-	1.00E+06	1.01E+05	5.54E+04
95542	1.23E+06	5.60E+06	-	4.57E+04	-	1.00E+06	7.24E+04	6.65E+04
101093	1.12E+06	6.05E+06	-	4.94E+04	-	1.00E+06	8.10E+04	5.96E+04
104982	1.79E+13	1.01E+14	-	-	-	1.00E+06	8.83E+05	1.36E+06
113027	1.08E+06	8.55E+06	-	5.52E+04	-	1.00E+06	7.53E+04	4.95E+04
114432	4.28E+13	1.96E+14	-	-	-	1.00E+06	9.60E+05	1.41E+06
115674	1.10E+06	6.61E+06	-	5.50E+04	-	1.00E+06	1.00E+05	5.28E+04
146835	1.06E+06	7.91E+06	-	6.33E+04	-	1.00E+06	6.78E+04	5.32E+04
154682	1.10E+06	1.02E+07	-	4.44E+04	-	1.00E+06	8.37E+04	5.91E+04
182498	1.09E+06	6.99E+06	-	3.92E+04	-	1.00E+06	9.51E+04	6.20E+04
186160	1.02E+06	5.85E+06	-	4.93E+04	-	1.00E+06	-	6.01E+04
361	1.11E+06	-	-	4.83E+04	-	1.00E+06	8.68E+04	6.06E+04
89418	9.95E+05	-	-	4.88E+04	-	1.00E+06	7.48E+04	5.06E+04
158630	1.06E+06	-	-	4.53E+04	-	1.00E+06	9.15E+04	5.91E+04
190613	1.09E+06	6.16E+06	1.54E+07	4.43E+04	1.40E+06	1.00E+06	-	5.58E+04
3359	1.15E+06	-	2.59E+07	7.99E+04	-	1.00E+06	-	5.01E+04
64114	1.26E+06	-	2.19E+07	4.37E+04	1.32E+06	1.00E+06	-	6.55E+04

A.3 Planet Host Abundance Study

Table A.8: Planet host parameters

Star HD	Temperature (K)	±	MtVel kms^{-1}	±	log(g)	[Fe/H]	±
10700	5387	53	1.30	0.23	4.55	-0.49	0.08
13808	5221	81	1.15	0.23	4.74	-0.07	0.13
20003	5605	55	1.06	0.12	4.56	0.13	0.08
100777	5575	41	1.11	0.06	4.5	0.32	0.07
101930	5247	77	0.95	0.16	4.55	0.23	0.11
111232	5504	40	1.23	0.18	4.49	-0.38	0.07
114386	5042	81	1.48	0.22	4.78	-0.07	0.11
126525	5671	40	1.08	0.1	4.65	-0.03	0.06
129445	5654	40	1.17	0.07	4.49	0.4	0.07
131664	5926	45	1.21	0.08	4.56	0.36	0.06
137388	5270	53	1.2	0.1	4.39	0.22	0.08
142022	5543	51	1.07	0.09	4.53	0.26	0.07
143361	5477	49	1.12	0.11	4.44	0.24	0.1
147018	5581	58	1.1	0.11	4.63	0.2	0.08
148156	6173	60	4.47	0.14	4.47	0.25	0.09
152079	5820	56	1.28	0.1	4.5	0.31	0.08
154672	5817	51	1.15	0.1	4.45	0.32	0.09
175167	5719	54	1.21	0.1	4.25	0.34	0.1
190647	5690	55	0.98	0.1	4.35	0.32	0.1
202206	5766	59	1.43	0.12	4.45	0.28	0.1
204313	5733	36	1.23	0.08	4.45	0.17	0.07
204941	5143	58	0.84	0.15	4.6	-0.09	0.08
205739	6273	65	1.24	0.18	4.42	0.23	0.1

Table A.9: Planet host abundances for Fe, C, O, Na, Mg, Al, Si, S and Ca.

Star	[Fe/H]	±	[C/H]	±	[O/H]	±	[Na/H]	±	[Mg/H]	±	[Al/H]	±	[Si/H]	±	[S/H]	±
10700	-0.49	0.08	-0.96	0.19	-0.54	0.08	-0.24	0.06	0.15	0.02	-0.07	0.01	-0.29	0.04	-0.49	0.11
13808	-0.07	0.13	0.07	0.15	9.42	0.27	0.31	0.09	0.32	0.02	0.3	0.01	-0.19	0.04	-0.56	*
20003	0.13	0.08	-0.28	0.15	0.38	0.04	0.24	0.04	0.15	0.11	0.2	0.02	0.01	0.04	-0.21	0.05
100777	0.32	0.07	-0.02	0.11	0.4	0.02	0.48	0.06	0.42	0.14	0.38	0.01	0.27	0.03	0.18	0.12
101930	0.23	0.11	-0.36	*	-	-	0.53	0.23	0.43	0.08	0.5	0.07	0.04	0.06	-0.2	0.18
111232	-0.38	0.07	-0.52	0.02	-0.31	0.18	-0.18	0.08	0.09	0.02	0.02	0.01	-0.19	0.04	-0.49	0.04
114386	-0.07	0.11	-0.2	0.19	1.17	*	0.51	0.06	0.44	0.06	0.53	0.01	-0.05	0.07	-0.69	0.48
126525	-0.03	0.06	-0.29	0.06	-0.04	*	-0.02	0.04	0.09	0.04	0.04	0.01	-0.04	0.03	-0.12	*
129445	0.4	0.07	0.23	0.07	0.37	0.04	0.56	0.04	0.46	0.14	0.49	0.03	0.35	0.02	0.1	0.28
131664	0.36	0.06	0.26	0.03	0.42	0.14	0.32	0.03	0.36	0.12	0.27	0.04	0.27	0.03	0.39	0.05
137388	0.22	0.08	-0.39	0.22	9.49	0.16	0.72	0.03	0.67	0.13	0.62	0.01	0.18	0.04	-0.08	0.25
142022	0.26	0.07	-0.11	0.05	-0.02	0.23	0.29	*	0.38	0.06	0.37	0.01	0.17	0.03	0.01	0.06
143361	0.24	0.1	0.13	0.46	0.2	0.07	0.38	0.01	0.43	0.06	0.42	0.02	0.24	0.05	0.03	0.29
147018	0.2	0.08	8.51	0.14	0.28	0.06	0.29	0.06	0.28	0.1	0.29	0.03	0.1	0.03	0.04	0.01
148156	0.25	0.09	0.46	0.12	0.53	*	0.13	0.08	0.15	0.04	0.02	0.1	0.18	0.06	0.23	0.08
152079	0.31	0.08	0.25	0.01	0.35	0.08	0.42	0.02	0.36	0.13	0.32	0.03	0.29	0.04	0.22	0.32
154672	0.32	0.09	0.25	0.02	0.39	0.16	0.2	0.08	0.25	0.1	0.29	0.01	0.18	0.05	0.18	0.06
175167	0.34	0.1	0.11	0.01	0.57	0.13	0.27	0.06	0.3	0.04	0.39	0.03	0.21	0.06	0.2	0.1
190647	0.32	0.1	0.16	0.06	0.49	0.12	0.3	0.09	0.32	*	0.36	0.01	0.21	0.05	0.33	0.13
202206	0.28	0.1	0.1	0.01	0.28	*	0.27	*	0.24	0.04	0.27	0.06	0.25	0.05	0.13	0.3
204313	0.17	0.07	0.13	0.05	0.26	0.04	0.22	0.1	0.29	0.12	0.2	0.03	0.12	0.08	0.2	0.07
204941	-0.09	0.08	-0.46	*	0.34	*	6.17	0.03	7.49	0.15	6.49	0.03	7.4	0.1	0	0
205739	0.23	0.1	0.34	0.17	0.55	*	-0.12	0.08	-0.1	0.11	-0.1	0.05	0	0.09	0.27	0.16

Table A.10: Planet host abundances for Ca, Sc, Ti, V, Cr, Mn an Co.

Star	[Ca/H]	±	[Sc/H]	±	[Ti/H]	±	[V/H]	±	[Cr/H]	±	[Mn/H]	±	[Co/H]	±
10700	0.04	0.1	-0.32	0.09	0.16	0.08	0.16	0.05	-0.33	0.22	-0.26	0.18	-0.21	0.04
13808	0.46	0.17	-0.24	0.18	0.65	0.11	0.87	0.14	0.13	0.36	0.63	0.25	0.27	0.27
20003	0.2	0.13	0	0.07	0.34	0.1	0.44	0.1	0.18	0.16	0.51	0.16	0.19	0.01
100777	0.42	0.11	0.2	0.09	0.51	0.07	0.62	0.09	0.33	0.14	0.75	0.22	0.56	0.24
101930	0.64	0.3	0.08	0.12	0.97	0.17	1.21	0.2	0.46	0.35	0.9	0.27	0.49	0.06
111232	0.01	0.09	-0.2	0.09	0.14	0.06	0.1	0.04	-0.24	0.11	-0.3	0.03	-0.11	0.02
114386	0.74	0.29	-0.2	0.22	1.04	0.2	1.2	0.28	0.29	0.43	0.84	0.25	0.17	0.05
121504	0	0.1	0.09	0.05	-0.11	0.06	-0.14	0.08	0	0.12	-0.13	0.21	-0.09	0.06
126525	0.07	0.07	-0.09	0.09	0.06	0.04	0.08	0.03	-0.02	0.02	0.08	0.11	-0.03	0.1
129445	0.42	0.09	0.3	0.07	0.46	0.12	0.59	0.06	0.37	0.12	0.86	0.21	0.54	0.1
131664	0.26	0.12	0.22	0.03	0.2	0.07	0.23	0.04	0.23	0.08	0.48	0.05	0.26	0.01
137388	0.66	0.2	0.11	0.12	0.82	0.11	1.08	0.21	0.46	0.32	1.03	0.26	0.5	0.12
142022	0.41	0.13	0.1	0.07	0.47	0.07	0.61	0.11	0.28	0.16	0.7	0.2	0.29	0.1
143361	0.42	0.1	0.22	0.15	0.56	0.25	0.61	0.31	0.29	0.17	0.45	0.5	0.68	0.45
147018	0.37	0.12	0.01	0.08	0.41	0.07	0.54	0.1	0.17	0.17	0.64	0.17	0.23	0.04
148156	0.05	0.2	0.19	0.08	-0.01	0.36	-0.15	0.07	0.04	0.22	-0.11	0.23	-0.04	0.06
152079	0.26	0.1	0.28	0.06	0.28	0.21	0.25	0.2	0.2	0.18	0.49	0.22	0.52	0.29
154672	0.21	0.13	0.31	0.04	0.31	0.1	0.34	0.06	0.24	0.11	0.51	0.15	0.32	0.04
175167	0.33	0.13	0.38	0.03	0.48	0.11	0.54	0.09	0.29	0.14	0.72	0.26	0.37	0.05
190647	0.28	0.15	0.35	0.05	0.45	0.16	0.54	0.13	0.29	0.12	0.57	0.23	0.4	0.1
202206	0.32	0.08	0.22	0.02	0.3	0.09	0.36	0.04	0.29	0.07	0.61	0.11	0.28	0.05
204313	0.18	0.11	0.13	0.08	0.16	0.06	0.2	0.02	0.12	0.08	0.44	0.12	0.18	0.03
205739	-0.12	0.17	0.18	0.05	-0.21	0.1	-0.24	0.08	-0.08	0.23	-0.42	0.34	-0.11	0.1

Table A.11: Planet host abundances for Ni, Cu, Zn, Y, Zr, Mo and Ba.

Star	[Ni/H]	±	[Cu/H]	±	[Zn/H]	±	[Y/H]	±	[Zr/H]	±	[Mo/H]	±	[Ba/H]	±
10700	-0.21	0.12	-0.20	0.15	-0.83	*	-0.26	0.30	-	*	-0.18	*	-0.44	0.02
13808	0.12	0.20	0.11	0.18	-0.12	*	0.00	0.46	-0.50	*	0.38	*	-0.12	0.09
20003	0.15	0.11	0.17	0.18	-0.86	*	0.09	0.16	-0.32	*	-0.22	*	-0.13	0.04
100777	0.40	0.13	0.44	0.14	0.08	*	0.07	0.13	-0.27	0.06	0.28	*	-0.01	0.07
101930	0.37	0.18	0.50	0.27	-0.95	*	0.35	0.42	0.54	*	0.10	*	-0.09	0.10
111232	-0.20	0.11	-0.15	0.12	-0.69	*	-0.24	0.23	-0.54	*	-0.24	*	-0.48	0.07
114386	0.13	0.22	0.16	0.42	-	-	0.09	0.63	-0.32	*	0.59	*	-0.06	0.07
121504	-0.02	0.12	-0.06	0.04	-0.66	*	0.21	0.03	0.24	*	-	-	0	0.13
126525	-0.02	0.06	0.03	0.08	-0.50	*	-0.13	0.10	-0.42	0.23	-0.02	*	-0.17	0.05
129445	0.46	0.12	0.55	0.14	0.22	*	0.18	0.21	0.05	0.13	0.34	*	0.01	0.10
131664	0.29	0.13	0.29	0.10	0.03	*	0.07	0.06	0.07	0.11	-0.14	*	0.01	0.07
137388	0.42	0.19	0.50	0.17	0.39	*	-0.18	0.62	-0.42	0.40	0.47	*	-0.11	0.09
142022	0.31	0.13	0.31	0.16	-0.04	*	0.13	0.20	-0.25	0.26	0.31	*	-0.05	0.08
143361	0.36	0.14	0.41	0.12	0.09	*	0.06	0.21	-0.10	0.25	0.38	*	0.00	0.09
147018	0.27	0.15	0.27	0.11	0.03	*	0.12	0.23	-0.26	0.32	0.42	*	-0.05	0.07
148156	0.03	0.18	0.09	0.05	0.05	*	0.19	0.01	-0.09	*	0.10	*	-0.03	0.17
152079	0.34	0.10	0.35	0.06	-0.01	*	0.13	0.15	-0.05	0.06	0.07	*	-0.03	0.09
154672	0.28	0.16	0.25	0.18	-0.62	*	0.20	0.06	0.17	0.34	-0.22	*	-0.03	0.10
175167	0.36	0.17	0.37	0.20	-0.66	*	0.43	0.29	0.23	*	-0.27	*	0.12	0.19
190647	0.36	0.18	0.36	0.14	-0.60	*	0.26	0.06	0.66	*	-0.26	*	0.00	0.14
202206	0.32	0.16	0.37	0.13	-0.74	*	0.25	0.10	0.19	0.40	-	-	0.05	0.08
204313	0.22	0.14	0.26	0.14	-0.16	*	0.03	0.12	-0.10	0.20	-0.06	*	-0.08	0.08
205739	-0.12	0.15	-0.19	0.05	-0.70	*	0.10	0.35	0.34	0.33	-	-	-0.01	0.15

Table A.12: Planet host abundances for La, Ce, Nd, Eu, Hf, Mg/Si ratio and C/O ratio

Star	[La/H]	±	[Ce/H]	±	[Nd/H]	±	[Eu/H]	±	[Hf/H]	±	Mg/Si	C/O
10700	-0.16	*	0.23	*	-0.03	0.38	-0.10	*	-	-	2.01	0.36
13808	0.03	0.07	-	0.00	0.03	0.00	0.14	*	-0.20	*	1.55	0.24
20003	0.18	0.01	-	0.00	-	0.00	-	-	-	-	1.18	0.58
100777	0.17	0.25	-	0.00	0.01	0.00	-0.03	*	0.31	*	1.13	0.66
101930	0.50	0.25	-	0.00	0.37	0.23	0.55	*	0.40	*	1.32	0.19
111232	-0.26	*	-0.03	*	-0.37	0.08	-0.18	*	-1.11	*	1.66	0.49
114386	0.12	0.06	-	0.00	0.06	*	-0.05	*	-0.52	*	1.08	0.53
121504	-	-	-	-	-0.04	*	0.21	*	0.21	*	1.06	0.57
126525	0.07	0.07	-0.25	*	-0.13	0.00	-0.04	*	-0.62	*	1.20	0.48
129445	0.40	0.15	-0.01	*	0.03	0.23	0.41	*	0.17	*	1.12	0.29
131664	0.19	0.01	-	0.00	-0.16	0.15	0.48	*	0.13	*	1.29	0.5
137388	0.40	0.06	-0.06	*	0.07	0.00	0.20	*	0.20	*	1.75	0.83
142022	0.43	0.11	-	0.00	-0.31	0.59	0.18	*	0.11	*	1.29	1.01
143361	0.22	0.25	-	0.00	0.09	*	-0.11	*	0.09	*	1.19	0.35
147018	0.20	0.47	-0.16	*	-0.39	0.56	0.28	*	-0.17	*	1.17	0.35
148156	-0.06	*	-0.54	*	0.84	0.06	0.21	*	0.40	*	1.15	0.48
152079	0.24	0.28	-	0.00	-0.07	0.21	0.33	*	-0.01	*	1.19	0.39
154672	0.35	0.12	-	0.00	0.37	0.19	0.55	*	0.56	*	1.22	0.2
175167	0.35	0.06	1.28	*	0.38	0.16	0.38	*	0.68	*	1.25	0.32
190647	0.48	0.20	-	0.00	0.31	0.06	0.61	*	0.52	*	1.28	0.2
202206	0.19	*	-	0.00	0.08	0.02	-	-	0.63	*	0.94	0.41
204313	0.01	0.30	-	0.00	-0.15	0.18	-0.05	*	-0.08	*	1.44	0.54
205739	-	*	-	0.00	-0.01	0.10	-	-	-	-	1.10	0.2

Table A.13: Absolute abundances normalized to 10^6 Si atoms

Star	Fe	C	O	Na	Mg	Si	Al	Ca
Solar	9.77E+05	8.32E+06	1.51E+07	5.37E+04	1.23E+06	1.00E+06	8.71E+04	6.76E+04
100777	9.34E+05	5.87E+06	1.62E+07	6.29E+04	1.13E+06	1.00E+06	8.59E+04	4.62E+04
101930	1.20E+06	8.15E+06	3.44E+07	6.78E+04	1.32E+06	1.00E+06	1.15E+05	6.63E+04
10700	7.51E+05	4.95E+06	8.61E+06	4.07E+04	2.04E+06	1.00E+06	1.16E+05	5.87E+04
111232	7.17E+05	7.81E+06	1.18E+07	4.64E+04	1.72E+06	1.00E+06	1.31E+05	5.66E+04
114386	7.14E+05	3.27E+07	1.70E+08	4.07E+04	1.08E+06	1.00E+06	1.06E+05	4.75E+04
121504	1.08E+06	7.38E+06	1.52E+07	3.60E+04	1.06E+06	1.00E+06	8.15E+04	5.70E+04
126525	9.57E+05	7.11E+06	1.33E+07	3.72E+04	1.20E+06	1.00E+06	9.77E+04	4.91E+04
129445	9.37E+05	8.06E+06	1.42E+07	6.86E+04	1.10E+06	1.00E+06	1.06E+05	4.08E+04
131664	9.93E+05	6.83E+06	1.43E+07	6.09E+04	1.26E+06	1.00E+06	9.11E+04	4.87E+04
137388	9.05E+05	4.70E+06	1.63E+07	8.27E+04	1.75E+06	1.00E+06	1.20E+05	5.36E+04
13808	1.21E+06	5.97E+07	2.17E+07	6.86E+04	1.55E+06	1.00E+06	1.28E+05	6.67E+04
142022	1.07E+06	6.41E+06	7.76E+06	4.90E+04	1.29E+06	1.00E+06	1.01E+05	5.54E+04
143361	9.55E+05	1.16E+07	1.15E+07	-	1.19E+06	1.00E+06	9.76E+04	4.64E+04
147018	1.09E+06	6.35E+06	1.80E+07	5.89E+04	1.17E+06	1.00E+06	1.02E+05	5.95E+04
148156	1.01E+06	6.24E+06	1.80E+07	4.79E+04	1.15E+06	1.00E+06	7.16E+04	5.32E+04
152079	9.34E+05	6.76E+06	1.40E+07	7.11E+04	1.19E+06	1.00E+06	9.48E+04	4.57E+04
154672	1.15E+06	7.52E+06	1.93E+07	5.45E+04	1.22E+06	1.00E+06	1.09E+05	5.33E+04
175167	1.22E+06	5.70E+06	2.83E+07	5.64E+04	1.25E+06	1.00E+06	1.23E+05	6.11E+04
190647	1.12E+06	7.49E+06	2.32E+07	5.64E+04	1.28E+06	1.00E+06	1.09E+05	5.44E+04
20003	1.20E+06	5.91E+06	2.96E+07	7.10E+04	1.18E+06	1.00E+06	1.14E+05	5.73E+04
202206	9.84E+05	5.52E+06	1.33E+07	4.03E+04	9.44E+05	1.00E+06	8.61E+04	5.08E+04
204313	1.03E+06	9.41E+06	1.75E+07	6.29E+04	1.44E+06	1.00E+06	-	5.14E+04
205739	1.14E+06	6.62E+06	3.37E+07	3.96E+04	1.10E+06	1.00E+06	8.86E+04	6.32E+04